UNIVERSITY OF HAWAII LIBRARY AUG 29 '61

Geochimica et Cosmochimica Acta

JOURNAL OF THE GEOCHEMICAL SOCIETY

Executive Editors

C. W. CORRENS, *Göttingen.* E. INGERSON, *Austin, Texas.* L. R. WAGER, *Oxford.*

Editors

L. H. AHRENS, *Capetown.* S. R. NOCKOLDS, *Cambridge.* H. C. UREY, *La Jolla, Calif.*
JOHN VERHOOGEN, *Berkeley, Calif.* A. P. VINOGRADOV, *Moscow.*

CONTENTS VOLUME 24, Nos. 3/4 JULY 1961

A. E. RINGWOOD: Chemical and genetic relationships among meteorites . . 159

E. R. DUFRESNE and S. K. ROY: A new phosphate mineral from the Springwater pallasite 198

NG SIEW KEE and C. BLOOMFIELD: The solution of some minor element oxides by decomposing plant materials 206

JAMES C. COBB and J. LAURENCE KULP: Isotopic geochemistry of uranium and lead in the Swedish kolm and its associated shale 226

H. G. F. WINKLER und H. VON PLATEN: Experimentelle Gesteinsmetamorphose-V 250

S. K. El WAKEEL and J. P. RILEY: Chemical and mineralogical studies of fossil red clays from Timor 260

M. A. TAMERS, J. J. STIPP and J. COLLIER: High sensitivity detection of naturally occurring radiocarbon—I 266

CHARLES D. KEELING: The concentration and isotopic abundances of carbon dioxide in rural and marine air 277

CHARLES D. KEELING: A mechanism for cyclic enrichment of carbon-12 by terrestrial plants 299

Geochemical Notes:

W. M. TUPPER and D. H. LORING: On the relative abundance of rubidium and strontium in vitrain ashes from coals in Nova Scotia 314

B. ZASLOW and L. M. KELLOGG: An analysis of metallic spheroids from Meteor Crater, Arizona 315

Letter to the Editors:

J. JEDWAB: Beryllium in river water 317

Book Review: 318

PERGAMON PRESS OXFORD • LONDON • NEW YORK • PARIS

GEOCHIMICA ET COSMOCHIMICA ACTA

EXECUTIVE EDITORS

PROF. C. W. CORRENS *Sedimentpetrographisches Institut der Universität, Lotzestr.* 13, *Göttingen, Germany*
PROF. E. INGERSON *Department of Geology, University of Texas, Austin* 12, *Texas, U.S.A.*
PROF. L. WAGER, F.R.S. *Department of Geology and Mineralogy, The University Museum, Oxford, England*

EDITORS

PROF. L. H. AHRENS *Department of Chemistry, University of Capetown, Rondebosch, Cape Province, South Africa*
Dr. S. R. NOCKOLDS *Department of Mineralogy and Petrology, The University, Cambridge, England*
PROF. H. C. UREY, For. Mem. R. S. *University of California, La Jolla, California, U.S.A.*
Dr. JOHN VERHOOGEN *Department of Geology, University of California, Berkeley, California, U.S.A.*
PROF. A. P. VINOGRADOV *Vernadsky Institute, Moscow, U.S.S.R.*

EDITORIAL ADVISORY BOARD

EUROPE

T. F. W. BARTH, *Oslo*
L. CAPDECOMME, *Toulouse*
E. J. CONWAY, *Dublin*
P. ESKOLA, *Helsinki*
P. GALLITELLI, *Modena*
A. HADDING, *Lund*
O. HAHN, *Göttingen*
H. W. HARVEY, *Plymouth*
F. HEIDE, *Jena*
A. HOLMES, *Edinburgh*
W. Q. KENNEDY, *Leeds*
PH. H. KUENEN, *Gröningen*
S. LANDERGREN, *Stockholm*
F. MASHATSCHKI, *Vienna*
A. MUIR, *Harpenden*
J. ORCEL, *Paris*
E. RAGUIN, *Paris*
E. REINHARD, *Basle*
TH. G. SAHAMA, *Helsinki*
C. E. TILLEY, *Cambridge*
T. VOGT, *Trondheim*

AMERICAN CONTINENT

A. F. BUDDINGTON, *Princeton*
D. GUIMÃRAES, *Belo Horizonte*
G. E. HUTCHINSON, *New Haven*
B. H. MASON, *New York*
F. WHIPPLE, *Cambridge*
R. WILDT, *New Haven*
H. S. YODER, *Washington*

FAR EAST

T. WATANABE, *Tokyo*

AUSTRALIA

D. J. SWAINE, *Sydney*

Publishing Offices: Pergamon Press Ltd., Headington Hill Hall, Oxford

Four issues per volume, three volumes per year

Subscription *per annum* (including postage) (A) £21 (U.S.A. $60.00); (B) For individual subscribers who write directly to the publisher certifying that the Journal is for their private use, £7.7s. (U.S.A. $21.50). Members of the Geochemical Society, or non-members who occasionally publish papers in the Journal, £3. 11s. 6d. (U.S.A. $10.00) *per annum.*

Back numbers, £10 (U.S.A. $28.00) per volume

Single issues, £2. 10s. (U.S.A. $7.00) each

Copyright © 1961 Pergamon Press Ltd.

PERGAMON PRESS LTD.

HEADINGTON HILL HALL, OXFORD 122 EAST 55TH STREET, NEW YORK 22, N.Y.

PRINTED IN NORTHERN IRELAND AT THE UNIVERSITIES PRESS, BELFAST

A Technical Writing Service for Industry

Do you need the services of professional technical writers, highly competent illustrators and compilers of modern, effective technical literature? A technical writing service is available to industrial companies and research organizations to prepare, illustrate, print and disseminate instruction manuals, parts lists, user handbooks, sales brochures, internal reports, etc.

The Technical Writing Division is staffed with experienced and highly qualified technical writers, engineers and illustrators and at their disposal are all the very extensive resources and connections of the Pergamon Press.

For further information please write to:

The Manager,
Pergamon Press Technical Writing Division,
566 Cable Street,
London, E.1

POTASSIUM – ARGON AGE DETERMINATIONS

GEOCHRON now offers complete determinations of geological age by potassium-argon isotope analysis.

Our Technical Director welcomes the opportunity to correspond with scientists concerning particular problems, or applications of interest to them.

For general details, send for our pamphlet, *Potassium-Argon Isotope Analysis*

GEOCHRON LABORATORIES, Inc.
Department O
24 Blackstone Street
Cambridge 39
Massachusetts
U.S.A.

PERGAMON PRESS

specialized journals for *specialized advertising!*

Advertise in GEOCHIMICA ET COSMOCHIMICA ACTA—

Space is available to all manufacturers of suitable products—the range which will appeal to readers of this journal is extensive and includes spectrometers, seismographs, seismic amplifiers and detectors, hydrometers, humidity instruments, monometers, galvanometers, radiation detectors and pyrometers, colorimeters, fluorometers, petrographic and other microscopes, flame photometers, surveying instruments, voltmeters, lenses and optical elements, mine ventilation instruments, X-ray microanalysers, pumps, pipe-lines, gas detection and measurement apparatus, microphotometers, X-ray films, plates and equipment, samplers of airborne dust and bacteria, telecommunications equipment, gyroscopic instruments, petroleum testing equipment, thermometers of all types, chemicals, oil boring equipment, electronic equipment . . . this list could easily be trebled!

We shall be happy to provide impartial advice as to the suitability of products not listed.

THIS IS ONE OF MORE THAN 70 INTERNATIONAL SCIENTIFIC JOURNALS. SPECIAL REDUCED "COMBINED RATES" ARE OFFERED TO MANUFACTURERS ADVERTISING IN MORE THAN ONE JOURNAL.

For details WRITE OR PHONE to

R. D. MILLER
Advertisement Manager

PERGAMON PRESS LIMITED
Pergamon House,
4 Fitzroy Square,
London W.1
Phone: EUSton 4455

PERGAMON PRESS INC.
122 East 55th Street,
New York 22, N.Y.,
U.S.A.
Phone: Plaza 3-9651

THE INTERNATIONAL SPECIALISTS FOR BACK FILES AND VOLUMES OF

Research Journals

I. R. MAXWELL & CO. LTD.
Headington Hill Hall, Oxford/England

MAXWELL, MEIER & HOLMES, INC.
103 Fifth Avenue, New York 3, N.Y.

- We SUPPLY complete sets, short runs, single volumes and odd issues.
- Our policy is to pay immediate attention to inquiries and orders, large or small.
- We invite you to send us your desiderata lists, indicating gaps in your holdings.
- We BUY sets, runs and odd lots of periodicals in all fields and should like to receive lists of material available for sale.
- We frequently issue catalogues and acquisitions bulletins, and should like to hear from librarians and research scientists who do not receive them regularly.

Representative offices:

LONDON · PARIS · LOS ANGELES · FRANKFURT
BUENOS AIRES

An invitation to subscribe to
this Important New Pergamon International Research Journal

INFRARED PHYSICS

This journal is being established as an international research journal for the publication of scientific papers concerning infrared physics and its applications. It is concerned with infrared theory, experiment, and instrumentation as applied to infrared detection and transmission and to problems of atmospheric, meteorological, geophysical, astrophysical and space research. Except as they pertain directly to infrared studies of planetary and stellar atmospheres, papers on molecular spectroscopy or spectrochemical analysis are considered outside the scope of INFRARED PHYSICS. The journal will contain Research Papers, specially invited Critical Surveys, quickly published Research Notes, and Book Reviews. The language preferred is English, but papers will be published occasionally in French and German. Manuscripts for editorial consideration should be sent to the Member of the Board of Editors most conveniently located.

CONTENTS OF VOLUME 1 NUMBER 1—JUST PUBLISHED

E. SCOTT BARR: The infrared pioneers—I. Sir William Herschel; N. C. BEESE: Light sources for optical communication; D. F. EDWARDS and M. MERCADO: Ultimate sensitivity and practical performance of the tellurium photoconductive detector; S. NEILSEN, W. D. LAWSON and A. F. FRAY: Some infrared transmitting glasses containing germanium dioxide; P. BRATT, W. ENGELER, H. LEVINSTEIN, A. MACRAE and J. PEHEK: A status report on infrared detectors; H. HAPP and L. GENZEL: Interferenz-Modulation mit monochromatischen Millimeter-Wellen; P. A. LAPP and H. S. KERR: Sunseeker for high-altitude infrared solar spectra; H. KALLMANN, J. RENNERT and M. SIDRAN: Infrared photography using persistent internal polarization in phosphor plates; C. HILSUM and G. R. HARDING: The theory of thermal imaging, and its application to the absorption-edge image-tube; R. BEER and J. RING: A high-pressure scanning Fabry-Perot interferometer for the infrared; T. S. MOSS and A. G. PEACOCK: Infrared optical properties of lead halides (Research Note).

Published Quarterly

BOARD OF EDITORS

N. MIGEOTTE	Université de Liège, Institut d'Astrophysique, Cointe Solessin, Belgium
T. S. MOSS	Royal Aircraft Establishment, Radio Department, Ambarrow Court, Lower Sandhurst Road, near Camberley, Surrey, England.
S. PASSMAN	The RAND Corporation, 1700 Main Street, Santa Monica, California, U.S.A.
W. K. WEIHE	U.S. Army, Engineer Research and Development Laboratories, Fort Belvoir, Virginia, U.S.A.

Assisted by an International Honorary Editorial Advisory Board

A copy of the journal and details of subscription rates gladly sent on application

PERGAMON PRESS

OXFORD · LONDON · NEW YORK

Headington Hill Hall, Oxford 4 & 5 *Fitzroy Square, London W.*1

122 *East 55th Street, New York* 22, *N.Y.*

Geochimica et Cosmochimica Acta, 1961, Vol. 24, pp. 159 to 197. Pergamon Press Ltd. Printed in Northern Ireland

Chemical and genetic relationships among meteorites

A. E. Ringwood
Department of Geophysics, Australian National University, Canberra

(*Received* 10 June 1960)

Abstract—Optical and X-ray studies have been made on the olivines, pyroxenes and metal phases from thirty-four chondrites for which chemical analyses exist. These data enable a selection of reliable analyses to be made, and confirm a conclusion first expressed by Prior—namely, that chondrites are samples of a homogeneous parental material which varied widely in its state of oxidation. There is an almost continuous range in oxidation states from carbonaceous chondrites, in which all the iron and nickel is oxidized, through to enstatite chondrites, in which all the iron is reduced, and which contain, in addition, reduced Si, Cr, Ca and P. The mineralogy and chemistry of silicate and metal phases in chondrites are dominated by this oxidation–reduction equilibrium.

The original state of the parental chondritic material probably resembled that displayed by carbonaceous chondrites. This material was cold and oxidized, containing up to 5 per cent carbon, and 20 per cent water, together with obscure compounds of carbon, hydrogen, nitrogen, sulphur and other volatiles. Subsequently it was subjected to higher temperatures under such conditions that the carbon (and hydrogen) reacted with oxidized iron and nickel to form a metal phase *in situ*, whilst volatiles (principally water and CO_2) were lost.

Mineralogical and textural evidence shows that the silicates in most chondrites crystallized from the liquid state at a temperature below 1000°C. A high pressure of volatiles (H_2O and CO_2) must have been present to produce the observed melting point depression of the silicates.

Primary chondritic textures are tuffaceous in nature and therefore of volcanic origin. They have formed by the rapid liberation of H_2O and CO_2 from the chondritic magma. Sudden loss of volatiles has caused rapid crystallization and chondrule formation. The principal difference between formation of chondrites and terrestrial tuffs is due to the relatively low viscosity of chondritic magma, which has facilitated chondrule formation.

Chondrites have subsequently been exposed to varying degrees of metamorphism, which has caused compaction and recrystallization. The range of pressures indicated is such that at least one of the parent bodies of chrondrites was of lunar size.

The genesis of other groups of meteorites can be understood in terms of melting and differentiation of a small amount of parental chondritic material. Several lines of evidence indicate that the irons have crystallized under high pressures,—probably exceeding 30,000 atm. It therefore seems probable that melting and differentiation occurred near the centre of a parent meteoritic planet, and that the metal partially segregated to form a small core.

Melting and differentiation of the parent meteoritic planet (or planets) occurred about 4.5×10^9 years ago. Subsequent cooling below 450°C occurred within approximately 10^8 years. Cooling of the small molten core occurred by adiabatic heat exchange with the outer chondritic mantle, which had been rapidly cooled to about 300°C, during the endothermic volcanic phase of evolution.

The meteoritic planet(s) broke up less than 10^9 years after melting and differentiation, and the fragments have since been colliding and becoming further reduced in size, thus forming the asteroids. Some suggestions regarding the cause of the initial break-up are hazarded.

1. Introduction

The assumption that elemental abundances in meteorites are similar to those in the earth has provided a fruitful basis for the construction of earth models. It is most important that the justification for this assumption should be examined, and if possible, confirmed. Detailed studies of the physics, chemistry and petrography of meteorites are therefore required. These may be expected to provide information on the relationships between silicate and metallic phases, and the manner of formation of the latter. It appears likely that these relationships will have an important bearing upon problems connected with the origin of the solar system.

In this paper, a detailed study is made of the oxidation–reduction relationships in meteorites, first described by Prior (1916). The data derived from this study

provide the foundation for a general hypothesis on meteorite genesis, which has been briefly described in a previous publication (Ringwood, 1959).

It is widely believed that meteorites are derived from the region of the solar system between Mars and Jupiter, where thousands of asteroids are known to occur. These asteroids range in diameter from 370 km downwards. Some are observed to possess irregular shapes, suggesting an origin by fragmentation of a larger body. It is of interest that, according to Bode's law, a planet should exist in this region of the solar system.

Opik and Singer (1957) have pointed out that the asteroids have high mutual collision probabilities, and that collisions will perturb the orbits of some of these bodies so that they intersect that of the earth, falling as meteorites. Since the collision processes are random, one may plausibly assume that the meteorites falling upon the earth provide a representative cross-section of the solid non-volatile material in the asteroidal belt. There are complications, however, since friable meteorites stand less chance of survival through the earth's atmosphere than tough, coherent types.

Many classifications for meteorites have been devised, and they usually have much in common. Perhaps the most satisfactory is that of Prior (1920). The principal groups together with their major constituents are as follows:

Irons (*siderites*)

Iron containing from 4 to 35 per cent of nickel, together with small amounts of S, P, C and Co.

Stony irons (*siderolites*)

(a) Pallasites—nickel–iron, olivine.
(b) Mesosiderites—Nickel–iron, hypersthene, anorthite, olivine.

Stones (*aerolites*)

(a) Chondrites—olivine, orthopyroxene, nickel–iron, oligoclase. Possess a characteristic spheroidal texture.

(b) Achondrites—Do not possess the spheroidal texture. Poor in metal. Subdivided into:

(i) calcium poor, or chondritic type achondrites; these are similar mineralogically to chondrites;
(ii) calcium rich, or basaltic-type achondrites. Composed of clinohypersthene, hypersthene, calcic plagioclase.

The above classification is incomplete. However, it includes 99 per cent of known falls. Further details of subgroups will be given in the following specific sections.

Observed falls of meteorites on the earth's surface are as follows (Prior, 1953):

Irons, 42.
Stony irons, 12 incl. pallasites (2) and mesosiderites (7).
Chondrites, 523.
Chondritic-type achondrites, 24.
Basaltic type achondrites, 31.

It is obvious from this distribution, that chondrites are by far the most abundant and important class of meteorites. Accordingly, the present study will commence upon them.

2. The Chondrites

(a) *Chemical composition*

Early workers on chondrites noticed their uniformity of chemical composition. Prior (1913) laid particular emphasis on this point and suggested that most of the observed scatter could be attributed to errors in chemical analysis. Urey and Craig (1953), using various reliability criteria, selected ninety-four "superior" analyses from 350 available, and found that dispersions were considerably reduced, thus supporting the above conclusions (Table 1). More recently, Wiik (1956), has

Table 1. Average composition of chondrites.
(Urey and Craig, 1953)

SiO_2	38·04
MgO	28·84
FeO	12·45
Al_2O_3	2·50
CaO	1·95
Na_2O	0·98
K_2O	0·09
Cr_2O_3	0·36
MnO	0·25
TiO_2	0·11
P_2O_5	0·21
Fe	11·76
Ni	1·34
Co	0·08
FeS	5·73

carefully analysed a suite of twenty-one chondrites, including eleven carbonaceous varieties, and demonstrated that the uniformity was even greater than previously supposed. This is in agreement with spectrographic work by Pinson (1954), who determined a series of abundance ratios for pairs of major components of twenty-one chondrites. He found that corresponding ratios were similar in all chondrites within the experimental error.

Uniformity in composition extends also to many trace elements (Ahrens, 1957). Pinson *et al.* (1953) found relative deviations of only 15–25 per cent for Li, K, Rb, Sc, Sr, Ba and Zr in twenty-one chondrites. Similar results have been obtained for Mo (Kuroda and Sandell, 1954), Na and K (Edwards and Urey, 1955; Edwards, 1955), and Ti and Mn (Pinson, 1954). Pinson (1954) pointed out that these results contrasted strongly with the wide scatter observed in genetically related igneous rocks and concluded that chondrites could not be the products of a magmatic differentiation process.

In contrast to the above results, Reed *et al.* (1960) have found that certain trace elements (Pb, Bi and Tl) are up to a hundred times more abundant in carbonaceous chondrites than in ordinary chondrites. They are also relatively abundant in enstatite chondrites.

It therefore appears that two distinct classes of elements, displaying radically different abundance patterns, are present in chondrites. In subsequent discussion, when reference is made to "the uniformity in chemical composition of chondrites", the author will be considering class I elements only. These display relative deviations less than 50 per cent and include all the common elements, and, perhaps, most trace elements. The elements of class II are present in chondrites in highly variable amounts. Present indications suggest that they are quantitatively insignificant. Nevertheless, they are of considerable genetic importance and will be considered subsequently.

(b) *Prior's rules in chondrites*

It was realized quite early (Wahl, 1910) that the relative amounts of metallic and oxidized iron in chondrites were widely variable, despite the fact that total iron was approximately constant. Prior (1916) made a critical study of the chemistry of chondrites and concluded: "*The less the amount of nickel–iron in chondritic stones, the richer it is in nickel, and the richer in iron are the magnesium silicates*". This generalization has become known as "Prior's rule" or rather, "rules", since there are two relations expressed—one between total metal present and its Ni/Fe ratio, and the other between total metal and the MgO/FeO ratio of the silicates.

These rules appear to have been accepted by most subsequent investigators and have been supported by further data (Brown and Patterson, 1947a, b, 1948). Recently, however, Urey and Craig (1953) in their detailed study of chondrite compositions have expressed a somewhat sceptical conclusion: "It seems therefore, that Prior's law relative to the amount of iron in the metal phase as compared to the oxide phase is only partly true, and considering the lack of precision of many of the older analyses, it may be largely a matter of error of analysis".

During recent years, it has become clear that the correctness (or otherwise) of Prior's rules will have an important bearing on understanding not only the genesis of chondrites, but also the broader genetic relationships between metals and silicates in other planets. Accordingly, it appeared desirable to make a further study of the validity and consequences of these rules.

A large number of chemical analyses of chondrites exist. Many, if not most of these, are unreliable. Thus the principal problem arises in the selection of reliable chemical analyses on which to form a judgement. The major uncertainty in meteorite analysis is the determination of iron as metal, sulphide and silicate. Metallic iron is often determined separately. Sulphur is then determined and the amount of iron required to form troilite is calculated. Finally, the total iron in the meteorite is determined and metallic and sulphide iron are subtracted, thus yielding the oxidized iron occurring in silicates. Maximum errors are likely to arise in the FeO estimation, since this is found by subtraction after three separate analyses. In order to select a satisfactory chemical analysis, an independent method of checking the FeO determination is therefore required.

Oxidized iron occurs almost exclusively in the olivine and pyroxene. The compositions of these minerals can be determined from optical data, thus allowing calculation of an independent FeO/(FeO + MgO) ratio for the whole meteorite. This can then be compared with the same ratio found from chemical analysis. If

the two agree within some satisfactory arbitrary limits, say 5 mol per cent FeO, we may accept the chemical analysis as trustworthy.

The composition of olivines and/or pyroxenes from thirty-four analysed chondrites were determined by measuring their α and γ refractive indices. In addition, refractive index data for nine meteorites (incl. three chondritic-type achondrites) were found in the literature. Optic axial angle data were not considered sufficiently reliable for composition determination. Due possibly to stress, they showed a poor correlation with compositions of pyroxenes determined by other methods. Most meteoritic olivines have $2V$'s close to 90° and in this region, accurate composition determination is often difficult.

In addition, lattice parameters for the kamacite and taenite metallic phases were determined, using Co radiation and a silicon internal standard.

Results of this study are presented in Table 2. They enable a selection to be made of reliable analyses.

An additional criterion has also been used in the selection of superior analyses. All available analyses by Prior, Borgstrom and Wiik have been regarded as superior and plotted in Figs. 1 and 2, whether or not optical properties had been measured. This procedure may appear somewhat arbitrary. However, these workers are well known to be experienced and able meteorite analysts, and the author believes that confidence in their results is justified. An attempt has been made to obtain as many meteorites analysed by these authors as possible, for optical examination. Of twenty-two analyses by Wiik, twelve by Prior, and four by Borgstrom, the author has made optical and X-ray determinations on twelve, six and two, respectively. In all cases, agreement between optical and chemical determinations has been good.* This should justify the procedure adopted.

The meteorites analysed by these authors, but not optically examined by the present author, and which are included in Figs. 1 and 2, are as follows:

Wiik (1956): Ivuna, Cold Bokkeveldt, Mighei, Nawapali, Haripura, Santa Cruz, Murray, Oakley, Tromoy, Monte des Fortes, Linum, Varpaisjarvi.

Prior (Urey and Craig, 1953): Baroti, Cronstad, Crumlin, Khairpur, Launton, Wittekranz.

Borgstrom (Urey and Craig, 1953): Shelburne, St. Michel.

In Fig. 1, the weight per cent metallic iron has been plotted against weight per cent oxidized iron for fifty-five chondrites covered by superior analyses within the terms of the above definitions. Iron occurring in troilite has been included with metallic iron. This procedure was adapted because troilite is an intermetallic compound in which iron forms covalent–metallic bonds with sulphur. The iron thus occurs essentially in the atomic, or reduced, state. In carbonaceous chondrites, which contain Fe_3O_4 and NiO, there is no evidence that the sulphur present is combined with iron as FeS. Some occurs as organic sulphur, some native, and some as sulphate (Mueller, 1953). In these chondrites, therefore, no FeS, and hence no metallic iron, is tabulated. All the iron is apparently oxidized.

* Optical studies on some of the meteorites analysed by Wiik showed that the olivines and pyroxenes were not uniform in composition. Thus, direct comparisons of FeO/(FeO + MgO) ratios from the optical and chemical results were not possible. However, the meteorites concerned were rather extreme in composition (highly oxidized) and the author's results, based upon average compositions of ferromagnesians, agree, at least qualitatively, with Wiik's.

Table 2

A	B	C			D			E	F	G	H	I	J		K	
		Olivine			Orthopyroxene								Kamacite		Taenite	
No.	meteorite	Refractive indices		FeO (FeO + MgO)	Refractive indices		FeO (FeO + MgO)	Average FeO (FeO + NgO)	FeO (FeO + MgO)	Oxidized iron	Metallic iron	Ni (Ni + Fe) Metal phase	Lattice parameter	Atoms % Ni	Lattice parameter	Atoms % Ni
		α	γ	(mol %)	α	γ	(mol %)	Optics (mol %)	Chem. anal. (mol %)	(wt. %)	(wt. %)	(atoms %)	(Å)		(Å)	
(1)	Adelie Land	1·678	1·718	23	1·678	1·688	22	23	27	12·4	6·6	17·5	d.		3·581	54
(2)	Allegan	1·671	1·705	18	1·672	1·682	18	18	17·6	6·6	24·3	7·6	d.		3·582	53
(3)	Bjurbole	1·682	1·722	25	1·676	1·690	22	24	22·3	10·2	10·3	9·7	d.		3·581	54
(4)	Blithfield	Not present			1·652	1·661	1	1	0·6	0·2	18·5	6·4	2·8659		Not present	
(5)	Chicora	1·695	1·735	32	1·683	1·697	28	31	30	15	5·5	26·2				
(6)	Collescipoli	1·668	1·703	17	1·681	1·670	16	16	13	4·8	22·3	7·5	d.			
(7)	Daniels Kuil				1·650	1·660	0	0	0·5	0·15	28·9	6·2	2·8655		d.	
(8)	Elsinora	1·671	1·713	20	1·672	1·682	17	18	17	6·8	21·3	6·4	d.		Not present	
(9)	Felix	1·64 → 1·77		3 → 50				3 → 50	35	17·8	8·2	21	2·8682	5	d.	
(10)	Forest City	1·671	1·708	19	1·670	1·680	16	17	16	6·3	23·6	5·9	d.		3·580	54
(11)	Groenewald	1·668	1·710	20	1·665	1·685	18	19	19·3	7·6	20·9	8·5			3·581	54
(12)	Hainaut	1·662	1·710	20				20	21·3	8·7	18·4	8·8	d.			
(13)	Holbrook	1·684	1·723	27	1·680	1·690	24	25·5	21	9·3	12·3	12·6	d.		d.	
(14)	Homestead	1·676	1·715	22	1·676	1·685	20	21	22·2	9·7	13·7	10·4	2·8681	5	3·580	55
(15)	Hvittis				1·652	1·661	1	1	0·8	0·25	24·7	7·6	2·8655		3·582	53
(16)	Indarch	Not present			1·653	1·663	1	1	0	0	33·1	6·7	2·8619			
(17)	Karoonda	1·696	1·735	32	Magnetite present			>32	38	21·5	(Sulphide)	—	Not present		Not present	
(18)	Jelica	1·693	1·735	31							2·5				Not present	
(19)	Knyahinya	1·682	1·719	24	1·676	1·685	21	31	32	16·6	6·1	50			3·580	54
(21)	Lance	1·642 → 1·765		4 → 47				23	28			20	2·8687	6·3	3·590	46
(22)	Limerick	1·670	1·707	18	1·670	1·680	16	4 → 47	37·6	19·4	6·3	39·3	2·8682	5	3·579	55
(23)	Mackinney	1·681	1·722	25	1·680	1·690	24	17	16	6·2	22·1	7·9	d.		3·582	51
(24)	Manbhoom	1·691	1·733	31				25	23·1	10	11·9	8·8	d.		d.	
(25)	Mauerkirchen	1·682	1·723	26				31	29·5	15·5	5·3	50			3·580	55
(26)	Mt. Browne	1·666	1·704	17	1·670	1·682	17	26	40	20·1	5·9	<17			3·581	54
(27)	Mokoia	1·640 → 1·740		3 → 35	Magnetite present			17	23	8·8	19·3	9·6	d.		3·579	55
				Av. 10				>10	40·5	23·1	0		Not present		Not present	
(28)	Norton County	1·645	1·683	6			0	<1	0	0		5·6				
(29)	Ochansk	1·670	1·708	19	1·672	1·682	17	18	14	5·4	22·5	7·3	d.		3·580	55
(30)	Olivenza	1·690	1·730	30				30	32·1	16·3	4·6	33·5			3·578	56
(31)	Orgueil	Serpentine and magnetite							41·9	26·4	0	—				
(32)	Ornans	1·64 → 1·78		3 → 54				3 → 54	36	19·5	4·4	65	Not present		3·567	65
(33)	Pena Blenca Spring	1·635	1·670	0	1·650	1·658	0	0	<1	0·3		4·0				
(34)	Pillistfer	Not present			1·651	1·660	0	0	3	1·2	25·7	8·4	2·8652		Not present	
(35)	Plantersville		1·707	19		1·678	14	17	22·2	8·5	19·5	9·7				
(36)	Saint Marks				1·650	1·659	0	0		0	31·4	5·5	2·8630		Not present	
(37)	Saint Sauveur				1·650	1·659	0	0	0·6	0·2	34·9	4·4	2·8632		Not present	
(38)	Shallowater	1·635	1·670	0	1·650	1·659	0	0	1·1			6·4				
(39)	Sinnai	1·685	1·718	25	1·673	1·685	19	22	20	7·8	21·8	6·9				
(40)	Soko-Banja	1·686	1·730	29	1·682	1·692	26	28	28	13·8	6·3	24·1			3·578	56
(41)	Tenham	1·682	1·722	25				25	24·1	11·0	10·6	14·4	d.		d.	
(42)	Utzensdorf	$\beta = 1·685$		16	β1·670	1·676	12	15	26	11	15·9	10·4				
(43)	Vengeroo	1·676	1·710	21	1·657	1·668	6	15	17·6	8	14·2	10·3				
(44)	Warrenton	1·710	1·754	40				<40	37	18·9	7·3	25·2	2·8676	3·5	3·579	55
(45)	Yonozu	1·705	1·745	37	1·703	1·718	44	39	38·3	19	10·6	8·4				

Notes on Table 2

References
(1) Bayley P. G. W. and Stillwell F. L. (1923) *Aust. Ant. Exp.* 1911–16 *Sci. Rept.* Ser. A Geol., Part I.
(4) Johnston R. A. A. and Connor M. F. (1922) *Trans. Roy. Soc. Canad.* Ser. III **16**, 187.
(5) Preston F. W. *et al.* (1941) *Proc. U.S. Nat. Mus.* **90**, 387.
(11) Gevers T. W. and Mendelssohn E. (1946) *Trans. Geol. Soc. S. Afr.* **48**, 83.
(13) Mason B. and Wiik H. B. (1960) *Geochim. et Cosmochim. Acta.* In press.
(17) Mawson D. (1934) *Trans. Roy. Soc. S. Aust.* **58**, 1.
(19) von Baumhauer E. H. (1872) *Arch. Neerland. Sci. Nat. Haarlem* **7**, 146.
(32) Pisani M. F. (1868) *C.R. Acad. Sci., Paris* **67**, 663.
(33) Lonsdale J. T. (1947) *Amer. Min.* **32**, 354.
(35) Lonsdale J. T. (1937) *Amer. Min.* **22**, 877.
(38) Foshag W. F. (1940) *Amer. Min.* **25**, 779.
(39) Rossetti V. and Sitzia R. (1957) *Periodico Min. Rome* **27**, 179.
(42) Huttenlocher H. and Hügi Th. (1952) *Mitt. Naturf. Ges. Bern.* **9**, 67.
(43) Yudin I. A. (1954) *Meteoritica. Acad. Sci. USSR.* **11**, 89.
(45) Beck C. W. and Stevenson R. G. (1951) *Amer. J. Sci.* **249**, 815.

Chemical data for meteorites not referred to above are to be found in the compilations by Urey, H. C. and Craig H. (1953) *Geochim. et Cosmochim. Acta* **4**, 36, and Wilk H. B. (1956) *Geochim. et Cosmochim. Acta* **9**, 279.

Optical data for minerals from meteorites nos. 5, 11, 28, 33, 35, 38, 39, 42, 43 and 45 were obtained by the authors cited above. The remainder were obtained by the present author.

Column B. Meteorites are all chondrites, except nos. 28, 33 and 38, which are chondritic-type achondrites.

Column C. Alpha and γ-refractive indices of olivines were determined using immersion liquids and are probably correct to $\pm 0{\cdot}003$. The curves relating indices to molar composition are those of Bowen and Schairer (1935). Olivine compositions thus determined should be correct to ± 2 mol per cent. Where indices are not given for either pyroxene or olivine, it means that either the particular mineral was extremely scarce, or else accurate refractive index determination was impossible due to imperfect crystallization difficulty of identification, large numbers of inclusions, etc. These problems were frequently encountered with the pyroxenes.

Column D. Alpha and γ-refractive indices of orthopyroxenes are probably correct to $\pm 0{\cdot}003$ in most cases, which correspond to an error of ± 3 mol per cent in composition determination. The determinative curves are, based upon α- and γ-indices of 1·650 and 1·659 for $MgSiO_3$ (Shallowater meteorite) and 1·768 and 1·790 for $FeSiO_3$ (extrapolated from Kuno's (1954) data). The values near the magnesian end are somewhat lower than terrestrial enstatites since the latter usually contain significant quantities of Ca and Al in solid solution (Kuno, 1954). Chondrites are poorer in these components and the lower values are probably more correct In some cases, however, it is possible that chondritic orthopyroxenes may carry some Ca and Al in solid solution. This could make the determined value slightly high. It is noticeable that in two chondrites rich in orthopyroxene (Ochansk and Collescipoli), analysed by Wiik, the optically determined FeO/(FeO + MgO) ratio is higher than the corresponding chemical ratio by 3–4 mol per cent. This is possibly due to the same cause.

Column E. The overall FeO/(FeO + MgO) ratio for the meteorite is found by weighting the corresponding values for olivine and pyroxene according to the relative proportions of these minerals which are present.

Columns F,G,H,I. These values are calculated from the chemical analysis.

Column J. The lattice parameter of kamacite was determined on the minus 150-mesh magnetic fraction of the meteorite, using an 11-cm powder camera and cobalt radiation. The data relating nickel content to lattice parameter, given by Owen (1940), were used to estimate the nickel content of the kamacite. The symbol *d* indicates that the back diffraction lines were too diffuse for precise measurement, probably indicating the presence of α_2-phase.

Column K. The lattice parameter of taenite was estimated from the 311 reflection, using the 422 and 333 reflections of silicon as an internal standard. The relationship between nickel content and lattice parameter of taenite, for the range Ni_{100} to Ni_{38}, is taken from Owen and Sully (1941). Between Ni_{40} and Ni_0, the lattice parameters of synthetic taenites behave in a most complicated way, with two maxima and one minimum. Owen and Sully (1941) showed that this was caused by nucleation effects and consequent disequilibrium between the two phases in the α–γ region. The behaviour is not displayed above 500°C, where equilibrium is readily attained (Owen *et al.*, 1937). The anomalous behaviour tends to disappear at temperatures between 500°C and 300°C, under conditions of long annealing (up to a year). Estimation of the composition of taenite in meteorites thus involves the plausible assumption that the metal phase has been subjected to temperatures between 500°C and 300°C for more than a year. (The observed textures and phase segregation practically ensure this.)

(4) *Blithfield.* Johnston and Connor (1922) give the refractive indices of the enstatite as $\alpha = 1{\cdot}657$ and $\gamma = 1{\cdot}667$. The values determined by the author are $\alpha = 1{\cdot}652$ and $\gamma = 1{\cdot}661$. The latter give an FeO/(FeO + MgO) ratio in excellent agreement with the chemical analysis.

(7) *Daniels Kuil, also* (4) *Blithfield,* (15) *Hvittis,* (16) *Indarch,* (34) *Pillistfer,* (36) *Saint Marks and* (37) *Saint Sauveur.* Anomalous lattice parameters of kamacite from these enstatite chondrites are due to presence of silicon in solid solution (Ringwood, 1960a).

(9) *Felix, also* (21) *Lance,* (27) *Mokoia, and* (32) *Ornans.* Olivines display an extreme range in composition.

(12) *Hainaut.* Most olivines have the composition given, but a few extend up to $\alpha \sim 1{\cdot}720$, equivalent to 24 mol per cent FeO.

(18) *Jelica.* Nickel content of metal phase was determined from lattice parameters and relative X-ray intensities of kamacite and taenite lines. Taenite/kamacite ~ 20.

(19) *Knyahinya.* A polymict chondrite (Wahl, 1952) and two very different analyses exist. These probably apply to different fragments of the breccia. The analysis which agrees better with the optical and X-ray data has been quoted in Table 2.

(24) *Manbhoom.* Composition of metal phase was determined by X-ray (cf. Jelica). Taenite/kamacite ~ 20.

(25) *Mauerkirchen.* Optical and X-ray data disagree markedly with chemical analysis.

(36) *Saint Marks.* The chemical analysis gives 6·5 per cent FeO. Optical examination shows that this has been formed by terrestrial oxidation of metallic phase. The oxidized iron has therefore been included with metallic iron.

(41) *Tenham.* The chemical analysis quoted is that of Warbreccan which belongs to the same fall (Prior, 1953).

(44) *Warrenton.* Most olivines have the stated composition. However, a small proportion range down to $\alpha = 1{\cdot}670$, equivalent to 18 mol per cent FeO.

From Fig. 1, it is observed that as the amount of oxidized iron increases from 0 to 26 per cent, the metallic iron decreases from about 30 to 0 per cent. A complete range of oxidation states exists, whilst the total iron content remains approximately constant. Much of the small scatter can be attributed to experimental error. *Fig.* 1 *thus demonstrates most decisively, the validity of Prior's rule.*

Bearing in mind the uniform compositions of chondrites, the obvious conclusion from Prior's rule is that *chondrites are derived from a common parental material*

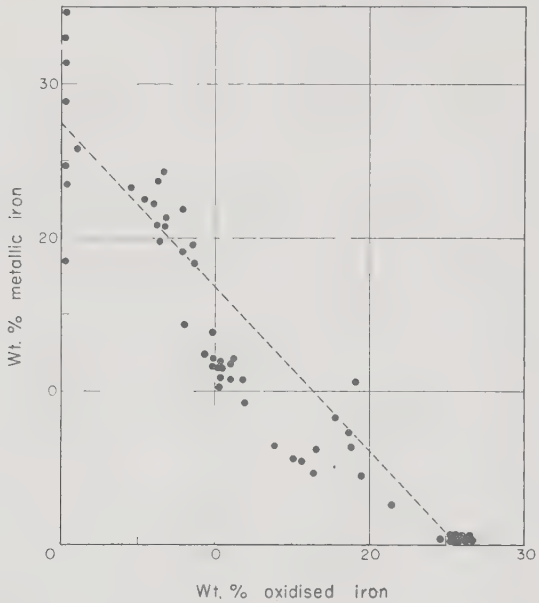

Fig. 1. Relationship between metallic and oxidized iron in fifty-five chondrites covered by superior chemical analyses. Dotted line is a line of constant total iron composition.

possessing widely varying states of oxidation. This, indeed, is the interpretation which Prior placed on his rule. The second part of Prior's rule, relating to the nickel content of the metal, may be considered in the light of this conclusion.

In Fig. 2, this rule has been tested by plotting the nickel content of the metal phase against the FeO/(FeO + MgO) ratio of the silicates, for all meteorites which were examined optically, together with the remaining ones analysed by Prior, Wiik and Borgstrom. The FeO/(FeO + MgO) ratio is usually reliable; however, rather large errors are likely in the estimation of the nickel content of the metal, since often, only small quantities of material are procurable for this analysis. Fig. 2 nevertheless displays well the trend observed and formulated by Prior, although, as might be expected, there is a rather large scatter, due largely to the analytical uncertainty in the nickel determination.

Interpretation of this relationship is simple. Nickel is more noble than iron. Accordingly, in chondrites rich in oxidized iron and containing only a small amount of metal phase, all the nickel occurs in the metal, giving it a high Ni/(Ni + Fe) ratio. As the amount of oxidised iron falls, reduced iron enters the metal phase, thereby increasing its abundance and decreasing the Ni/(Ni + Fe) ratio. This

behaviour is thus a consequence of Prior's first rule and provides an independent confirmation.

The data in Figs. 1 and 2 show that the metal phase in a chondrite is genetically related to the silicate phase. This conclusion, together with the data described in Section (d), shows quite definitely that chondrites are *not* random mixtures of iron and silicate fragments, as suggested by Urey (1956, 1957a, b, 1958, 1959).

In Fig. 2, it is observed that a complete sequence of FeO/(FeO + MgO) ratios between 40 and 15 (perhaps 13) per cent exist, but a gap occurs between 15 and the

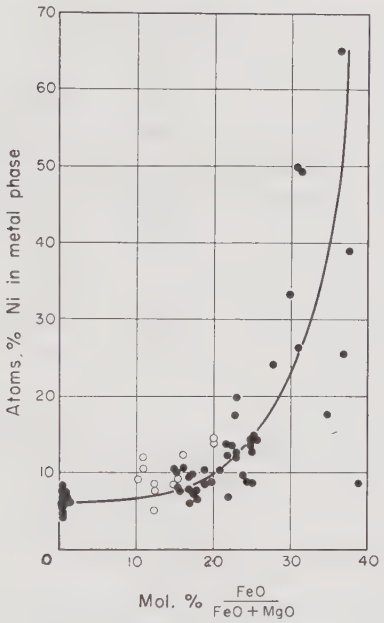

Fig. 2. Relationship between the FeO/(FeO + MgO) ratios of silicates and the nickel contents of coexisting metal phases for fifty-five chondrites and three achondrites covered by superior chemical analyses. Corresponding chemical data for eleven pallasites (open circles) are also plotted.

group of enstatite chondrites with FeO/(FeO + MgO) between 0–2. It is possible that chondrites falling in this gap exist, but they are very rare compared with the great bulk, which fall between 15 and 25. The corresponding ratios for pallasites have been plotted on Fig. 2 (open circles) and it is interesting that they tend partially to close this gap. This aspect will be commented upon subsequently.

(c) *Group concepts among chondrites*

Urey and Craig (1953) observed a tendency towards bimodal distribution when they plotted the iron contents of chondrites. This led them to classify chondrites into "high iron" and "low iron" groups.

Conclusions which can reasonably be drawn from Urey and Craig's data are as follows:

(a) The amounts of oxidized and reduced iron vary over a wide range and obey Prior's rule, in the quantitative sense expressed by that author.

(b) The distribution of iron within the observed range of oxidation states is not uniform. A pronounced frequency maximum occurs around 12 per cent metallic iron. A second region of high concentration occurs around 20–22 per cent metallic iron.

(c) The total iron in the 12 per cent (low) group is about 5 per cent less than in the remainder (high group) to which the 20 per cent group belong.

Subsequent analyses by Wiik supported this high-low grouping, and the effect can be seen in Fig. 2. This shows that the low-iron group fall 5 per cent below the principal high-iron curve, directly opposite a region in which there are no high-iron representatives. This suggests that the low-iron group are essentially members of the parental high-iron group from which a small proportion of iron has been removed. The analyses show that the low group are relatively deficient in nickel, indicating that the loss has been of metallic nickel–iron rather than oxidized iron.

Loss of nickel–iron from the low group could possibly have been due to some iron sinking and segregating in the parent body. Many of the high iron group are substantially richer in iron and nickel than the average of this group (dotted line in Fig. 2). Thus the low group and the 20 per cent region of the high group might be regarded as complementary differentiates. This aspect is discussed further in Section 7(c). Another possibility is that some iron and nickel might have been lost as volatile compounds (chlorides or carbonyls?) during the reduction process which occurred (also to be discussed subsequently).

Urey and Craig also discuss the existence of other groups —enstatite chondrites, amphoteric chondrites* and carbonaceous chondrites. Whilst these names may be convenient for discussion, they do not necessarily imply any genetic individuality. These meteorites fall directly on the oxidation–reduction curves (Figs. 2 and 3) and possess similar chemical compositions to other chondrites, apart from volatile components and Class II trace elements. Furthermore, they display complete minerological transitions with other chondrites. Enstatite chondrites are an exception to this latter point, due to a hiatus in FeO/(FeO + MgO) ratios.

(d) *The chemical evolution of chondrites*

We have noted previously that chondrites constitute about 90 per cent of all known meteorite falls. Furthermore, the average composition of chondrites enables a useful geochemical model of the earth to be constructed. Finally, the relative abundances of most elements in chondrites are very uniform and similar within a factor of two to those in the sun† (MacDonald, 1959). These considerations strongly suggest that chondrites are the most fundamental and primitive group of meteorites. It is possible to understand the genesis of other groups of meteorites in terms of differentiation processes operating on primary chondritic material.

In Section 2(b), evidence confirming Prior's conclusion—that chondrites are samples of a uniform parental material which varied widely in its oxidation state—was cited. It is plausible to assume that this parental material originally possessed

* Some authors have classified these as achondrites, principally because of their low metallic iron content. However, they usually contain some chondrules, and are mineralogically and chemically indistinguishable from ordinary chondrites with which they should be classified.

† However, recent work by Aller *et al.* (1960) indicates that a large discrepancy may exist between the solar and chondritic abundances of iron.

a uniform oxidation state, and that the variations displayed by chondrites are of later derivation. Only two original states appear likely in the light of astronomical theory—completely reduced and completely oxidized. Prior (1916) suggested that the primitive state was that of a completely reduced, metallic magma, and that chondrites were formed when oxygen (source unspecified) was allowed access to this magma, causing varying degrees of oxidation. This hypothesis was probably influenced by contemporary theories on the origin of the solar system, which regarded

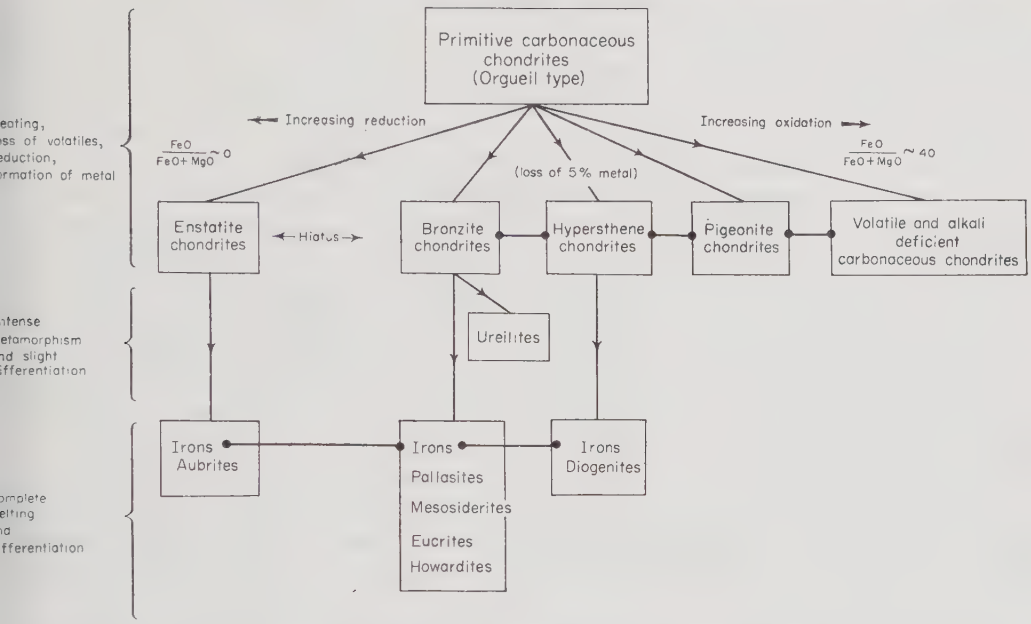

Fig. 3. Genetic relationships between principal groups of meteorites. Based upon Prior (1920), Wiik (1956), and the present paper. Establishment of new group of pigeonite chondrites is based upon unpublished work by Mason (personal communication).

the planets as being torn out of the sun, due to some unusual cosmic event. In this case, the initial state of the raw material of meteorites and planets would have been extremely hot, and therefore, highly reduced. We shall see subsequently that this hypothesis does not satisfactorily account for many of the detailed chemical and mineralogical features displayed by chondrites.

In recent years, many astronomers have favoured the view that stars and planets have formed from low-temperature gas-dust clouds. Latimer (1950) and Urey (1952) have shown that under these conditions, with the solar abundances of elements present, the metals, including iron, would be completely oxidized. These authors (also Brown, 1952) have furthermore shown that the low-temperature origin is the only one consistent with the known composition of the earth and meteorites.

We therefore assume that chondrites are derived from parental material which was cold ($<0°C$) and highly oxidized. This material has subsequently been subjected to reduction processes, such that the varying amounts of metal found in chondrites have been produced. Urey (1953) has pointed out that the carbonaceous chondrites

closely approximate to the aggregate of oxidized dust and volatiles which would be expected when a dust cloud accreted at low temperatures, and that these bodies may represent the nearest approach to the primitive dust which we possess.* Although only nineteen are known out of 523 chondrites seen to fall, he points out that they are probably more abundant cosmically than this ratio would suggest. Carbonaceous chondrites are extremely fragile and few would be expected to survive collision processes and passage through the earth's atmosphere. Nine of these chondrites have been analysed by Wiik and have been plotted (on a volatile free basis) on Fig. 1. Some consist dominantly of serpentine and magnetite, together with carbon, hydrogen, sulphur, chlorine and nitrogen, the latter elements being partly combined in obscure organic compounds (Mueller, 1953). Others consist mainly of olivine, pyroxene, magnetite and some carbon. These have evidently been subjected to temperatures sufficiently high to cause escape of some of the volatiles.

We previously inferred that the metal in chondrites was formed by a reduction process. Cosmically, the two most abundant reducing agents are hydrogen and carbon. Both are present in carbonaceous chondrites, but the latter is in excess. Mineralogical evidence, shortly to be described, shows that carbon has been the dominant reducing agent. If hydrogen had been the chief reducing agent, it would be difficult to understand the ubiquitous occurrence of FeS in chondrites, together with reduced P, Si and C in enstatite chondrites. A reduction process in the presence of a high concentration of hydrogen would have removed these elements as the gases H_2S, PH_3, SiH_4 and CH_4.

As one passes from carbonaceous chondrites to highly reduced types, an interesting and continuous series of mineralogical and chemical changes occur. Attention has been drawn to some of these changes by Wiik (1956). They may be illustrated by examples taken at various stages. The examples are mostly those studied by the author (Table 2).

(i) Orgueil, Cold Bokeveldt (Mueller, 1953), Mighei (Kvasha, 1948). Dominantly composed of serpentine and magnetite. Metal absent. Up to 20 per cent water, 6·5 per cent sulphur and 4 per cent carbon. A small amount of SO_4^{2-} and CO_3^{2-} may be present, together with some H, Cl and N. Chondritic structure

* Edwards and Urey (1955) later found that sodium and potassium occur in variable amounts in carbonaceous chondrites, and are, on the average, about 30 per cent less abundant than in ordinary chondrites. Accordingly they rejected Urey's original suggestion that carbonaceous chondrites are of primitive origin.

In the opinion of the present author, this rejection was premature. Most carbonaceous chondrites appear to have been subjected to a very low grade of metamorphism, resulting in slight compaction, and differential loss of volatiles—particularly water. If the sodium and potassium originally occurred as water-soluble compounds, which seems quite possible, then varying amounts of these elements would have accompanied the volatiles, and would thus have become lost. In this respect, it is highly significant that in two of the most primitive and volatile-rich types of carbonaceous condrites—Orgueil and Ivuna, the amounts of sodium and potassium present are similar to those in ordinary chondrites.

In the latter, sodium and potassium are fixed in stable and insoluble feldspars. According to the hypothesis developed in this paper, ordinary chondrites are formed when primitive carbonaceous chondrite material (containing normal amounts of Na and K) is subjected to much higher temperatures, resulting in complete melting. Subsequently, a rapid loss of volatiles occurs, resulting in a *nuée ardente* type of eruption. Under these conditions, Na and K are not lost with the volatiles but remain fixed in the feldspars.

The recent discovery by Reed *et al.* (1960) of possible primordial abundances of Pb, Bi and Tl in carbonaceous chondrites, and the finding by Reynolds (1960b) of large amounts of primordial rare gases in a carbonaceous chondrite, provide powerful support for the view that these meteorites are of primitive origin.

absent, or poorly developed. Highly friable, unmetamorphosed. Contain large amounts of Pb, Tl and Bi, compared to other chondrites.

(ii) Mokoia. Composed dominantly of magnesian olivine with varying composition (Fa_3–Fa_{35}) but averaging Fa_{10}, together with magnetite and some pyroxene. One half per cent carbon present. Metal absent. Much of the S, H, N and Cl present in group (i) appears to have been lost. Chondritic texture poorly developed. Friable, unmetamorphosed.

(iii) Karoonda. Composed of olivine, hypersthene and magnetite. Olivine $\geqslant$ hypersthene. Metal, carbon, water absent. Sulphur normal (1·5 per cent). Olivine uniform in composition (Fa_{32}). Karoonda shows a higher degree of reduction than Mokoia, since more of the Fe^3 from magnetite is entering olivine and pyroxene as Fe^2. Friable, unmetamorphosed.

(iv) Lance, Ornans, Felix, Warrenton. Composed of olivine, hypersthene, with up to 6 per cent metal, rich in nickel. Olivine $\geqslant$ hypersthene. Up to $\frac{1}{2}$ per cent carbon present. Sulphur normal ($\sim$2 per cent). Olivine and pyroxene are highly variable in composition (Fa_4–Fa_{54}). FeO/(FeO + MgO) averages between 30 and 40. Chondritic texture poorly developed. Friable and unmetamorphosed.

(v) Olivenza, Soko Banja, Jelica, Manbhoom. Similar to group (iv). However, the olivine and pyroxene are uniform in composition. FeO/(FeO + MgO) ranges between 28 and 31. Carbon is absent.

(vi) Bjurbole, Adelieland, Holbrook, Tenham, Homestead, Mackinney. These possess between 6 and 15 per cent metal, with from 10 to 20 per cent oxidized iron. Magnetite, carbon and volatiles are absent. Sulphur $\sim$2 per cent. Olivine usually $\geqslant$ pyroxene. Minerals are uniform in composition. FeO/(FeO + MgO) ranges between 20 and 26. Chondritic textures usually well developed. Sometimes coherent and metamorphosed, but more frequently friable. Members of this group are about 5 per cent poorer in iron than their neighbours.

(vii) Forest City, Mt. Browne, Allegan, Collescipoli, Elsinora, Hainaut, Ochansk, Limerick. These possess between 15 and 23 per cent of nickel-poor metal, with FeO/(FeO + MgO) between 20 and 13. Sulphur $\sim$2 per cent. Olivine usually $\leqslant$ pyroxene. Minerals are generally uniform in composition –except when meteorite is polymict (e.g. Hainaut). Frequently coherent and metamorphosed. Ca, Si and Cr occur as oxides but some P occurs as schreibersite (Forest City, Urey and Mayeda, 1959). The great majority of chondrites belong to groups (vi) and (vii).*

(viii) Indarch, Pillistfer, Daniels Kuil, Hvittis, Blithfield, Khairpur, Saint Marks, Saint Sauveur. Metallic iron between 15 and 30 per cent. Nickel poor. Enstatite $\ggg$ olivine. FeO/(FeO + MgO) < 1. Carbon present between 0 and $\frac{1}{2}$ per cent. Sulphur is higher than usual—up to 5 per cent. Kamacite only is present. Minerals are uniform in composition. Chondritic texture often partly obscured by metamorphism and recrystallization. Some Ca and Cr occur as sulphides, P as schreibersite, whilst several per cent of Si may occur in solid solution in the kamacite (Ringwood, 1960a).

The mineralogical and chemical changes observed as we pass from carbonaceous

* The chondrites studies by the author include a larger proportion of those very rich or very poor in metal, than would occur in a random sampling. The object of this selection was to study in detail the transitional relationships along the oxidation–reduction sequence.

chondrites towards chondrites which are increasingly rich in iron have been noted above. We will now discuss some of these trends separately, and note some correlations.

(*1*) *Passing from carbonaceous to enstatite chondrites through the stages* (*i*) *to* (*vii*) *above, a most important trend is the loss of carbon and oxygen, together with the formation of metal:* This suggests the possibility that the metal in chondrites has been formed by a process of carbon reduction from the original low-temperature oxidized state. Such an origin was suggested by Daubree (1879). The amount of carbon occurring in carbonaceous chondrites (up to 5 per cent) is adequate to reduce all the iron found in the most metal-rich varieties. It seems likely, too, that a limited contribution to the reduction may have been made by the hydrogen present in the carbonaceous chondrites. The reactions principally concerned are:

$$C + 2FeO \rightarrow 2Fe + CO_2 \quad (I)$$

$$C + FeO \rightarrow Fe + CO \quad (II)$$

From the known equilibria, we may expect reaction (I) to dominate throughout most of the reduction sequence. However, in the enstatite chondrites containing no FeO, and containing reduced Si, Ca, Cr and P, reaction (II) would be most important.

Strong support for this view is provided by the mineralogy of chondrites.

In chondrites which contain an appreciable amount of oxidized iron, all the silicon, calcium, chromium and phosphorus occur as oxides. However, in the highly reduced enstatite chondrites, the minerals oldhamite CaS, schreibersite $(FeNi)_3P$, and daubreelite ($Fe\ Cr_2\ S_4$) are characteristic, whilst silicon occurs in solid solution in the kamacite phase. These minerals and relationships are characteristic of blast furnace assemblages, which are formed when iron ores are strongly reduced by carbon. Iron meteorites contain a similar assemblage (except for oldhamite), together with additional minerals characteristic of blast furnace products, e.g. cohenite $(FeNi)_3C$. Graphite occurs in meteoritic irons, as well as blast furnace irons.

A comparison of gases found in meteoritic irons and steels is most instructive (Nash and Baxter, 1947):

(mm^3/g)	CO_2	CO	H_2	N_2
Average eight meteorites	12·2	1·4	1·9	0·6
Average three steels	13·3	5·7	2·4	0·3

The compositions of the gases from the two sources are very similar. It is notable that the CO_2/CO ratio is higher in the meteorites than in the steels. This indicates that meteoritic irons have not been formed under such intense reducing conditions as occur during cast iron and steel manufacture.

The common occurrence of this group of minerals and gases in both environments suggests that the chemical processes which produced meteoritic iron and blast furnace iron have been similar, i.e. that the iron in meteorites has been produced by reduction in the presence of carbon.

(2) *Other variations noticeable in the reduction sequence of chondrites are the ratios of olivine to pyroxene and taenite to kamacite:*

In chondrites rich in oxidized iron, and containing less than 6 per cent metal, olivine is much more common than pyroxene. In the varieties containing intermediate amounts of metal (from 6 to 18 per cent), olivine and pyroxene are approximately equal, whereas in the most reduced varieties (metal >18 per cent) pyroxene dominates and olivine may be absent. This effect is directly caused by the oxidation-reduction relationships mentioned above. As FeO is reduced to metal, less divalent cations remain to form olivine, and hence pyroxenes must form. This trend was first suggested by WAHL (1910).

The compositions of taenite and kamacite from the metal phases of chondrites are fairly constant, but the relative proportions of these phases, as estimated from the intensities of X-ray powder patterns,* vary widely. This is a consequence of Prior's rule. Thus Ornans contains less than 1 per cent of metal, which consists purely of taenite carrying 65 per cent Ni. In Manbhoom and Jelica (about 3 per cent metal) the ratios of taenite to kamacite are about 20. In more metal-rich meteorites, kamacite becomes more abundant, and finally, in the enstatite chondrites, it is present exclusively. Thus the mineralogy is consistent with the chemical data, on which Prior's rule is based.

(3) *Homogeneity and equilibrium of major phases;* In some of the chondrites with low or zero metal content, e.g. Lance, Warrenton, Mokoia, Ornans, the ferromagnesian minerals display a wide variation in composition. Thus in Ornans, the olivines range from Fa_3 to Fa_{54}. These chondrites are clearly in a state of internal disequilibrium. However, in nearly all others studied, the olivines and pyroxenes are approximately uniform in composition. This is shown by the refractive index variation and by the sharp lines on X-ray powder photographs (MASON (personal communication) has reached a similar conclusion on identical grounds). The pyroxenes usually possess a slightly lower FeO/(FeO + MgO) ratio than the coexisting olivines. It appears that most chondrites, excepting the more primitive, slightly reduced varieties, closely approach a state of chemical equilibrium.† A minor exception to this generalization is the frequent occurrence of clinopyroxene in association with orthopyroxene, which is discussed in Section 2(e). Coexisting

---

* In most cases these proportions can only be estimated qualitatively. The samples X-rayed were the —150-mesh magnetic fractions. If the metal phase is coarse, one tends to find a disproportionate amount of taenite in the fines. This is apparently due to the tendency of taenite to form fine rims around large kamacite particles. Crushing breaks these off and they go through the screen, whereas the residual kamacite may be too coarse to go through. Despite this effect, however, qualitative conclusions can be drawn. In some chondrites which contain small amounts of metal, this is sufficiently fine to pass —150-mesh quantitatively. The relative amount of kamacite and taenite can be estimated quite accurately in these, e.g. Manbhoom, Jelica.

† In most cases, the author's study has been restricted to samples smaller than 1 g, which nevertheless contain many thousands of individual crystals. Thus, the data cited really refer to the existence of *local* equilibrium in chondrites. In several cases, however, specimens of the same fall from different museums have been examined with identical results, suggesting that the "local" equilibrium is applicable throughout much greater masses than 1 g. This view is supported by the good agreement between the author's optical results and the chemical results obtained upon identical meteorites with different origins, by PRIOR, BORGSTROM and WIIK.

In Hainaut, some compositional inhomogeniety was apparent. The specimen studied was a crushed sample from a large amount of this meteorite, donated by H. B. WIIK. The inhomogeniety is apparently caused by the fact that Hainaut is polymict (WAHL, 1952) and the sample examined contains crystals from more than one kind of chondrite.

clinopyroxene and orthopyroxene are observed to possess similar FeO/(FeO + MgO) ratios.

X-ray data on the metal phase lead to a similar conclusion. Compositional inhomogeneity in the taenite phase of any individual chondrite is less than ± 4 per cent Ni. Furthermore, the average nickel content of taenite in all chondrites* except Knyahinya (46 per cent) and Ornans (65 per cent) is constant and equal to 54 ± 2 per cent. It is interesting that this result is considerably higher than the values found for the taenite from iron meteorites ($\sim$30 per cent Ni).

Some complications arise in the determination of the composition of kamacite. Most of the powder patterns yielded diffuse high angle lines. This is probably due to the presence of α_2-phase. The measurable lattice parameters from relatively well defined back diffraction lines yielded values between 3·5 and 6·3 per cent nickel, averaging 5 per cent. Although the X-ray determinative method is being used at the limits of accuracy in these cases, it appears that the nickel content of kamacite from chondrites is significantly lower than kamacite from irons, which averages 6·2 per cent Ni and is very uniform (Owen, 1940).

(4) *Correlation between loss of volatiles, amount of metal and development of chondritic textures:* Primitive dust collecting at low temperature would contain substantial amounts of volatiles—particularly water. Carbonaceous chondrites contain up to 20 per cent water, mainly bound as the OH group in serpentine minerals. As heating and reduction occur, the water is driven off, together with other volatiles, e.g. CO_2 and Class II trace elements, so that the vast majority of chondrites are poor in these constituents.

At the same time it is noticeable that the highly oxidized chondrites, containing little or no metal, usually possess poorly developed chondritic structures. However, where a reasonable amount of metal is present, chondritic structures are observed to be well developed —unless they have been obscured by subsequent metamorphism.

It will be suggested in Section 2(f) that there is a genetic relationship between loss of water and other volatiles from the primitive carbonaceous chondrites and the development of chondritic textures.

(5) *Coherence and metamorphism:* A further correlation is evident from the data in the introduction of Section 3(d). Chondrites containing less than 6 per cent of metal are extremely friable and porous. They do not appear to have suffered any substantial metamorphism or recrystallization. On the other hand, the metal-rich enstatite chondrites are tough, coherent stones, with low porosity. Frequently they display substantial recrystallization and metamorphism, leading to partial obscuring of the original chondritic textures. The common group of chondrites, with metal between 6 and 18 per cent, display wide variations in their degree of coherence metamorphism, and porosity. Among the meteorites of this group examined by the author, there appears a tendency for the metal-rich stones to be more coherent and metamorphosed, although there are numerous exceptions.

Summarizing, there appears to be a distinct correlation between the degree of reduction and the intensity of metamorphism in chondrites.

* Perhaps some bias is possible here, since nearly all the taenites measured were from friable, relatively unmetamorphosed meteorites. There is a suggestion that taenite from tougher, recrystallized chondrites may be lower in Ni, eg. Knyahinya. However, the composition of taenite separated from such specimens was usually indeterminate, since distortion during crushing tended to yield a diffuse X-ray pattern.

(6) *Loss of volatile metals during reduction:* Reed *et al.* (1960) have found that lead, thallium and bismuth are from ten to a hundred times as abundant in carbonaceous chondrites as in ordinary chondrites. These elements are readily reduced from their oxide compounds by carbon at elevated temperatures, and would tend to be lost with other volatile components during the reduction stage. Reed *et al.* have also found high abundances of these elements in enstatite chondrites. This is difficult to explain. Perhaps it may be related to the high sulphur content of enstatite chondrites and the chalcophilic nature of these elements. The equilibria governing reduction and volatilization of these elements from chondritic melts, in the presence of carbon and sulphur, and at varying oxygen pressures, are likely to be extremely complex, and simple explanations of anomalies may not be possible at the present stage.

(e) *Temperatures of formation of chondrites*

The shapes of metal and sulphide grains in chondrites provide an important clue to the temperature of crystallization.* These are characteristically rough and irregular. *Obviously, they have not been melted.* If they had been, they would occur as spheroids similar to those found in slags. This point has been emphasized by Merrill (1928), who pointed out that the textures of metal in chondrites resembles sponge iron, formed by reduction of iron ores at low temperatures (~700°–800°C). Troilite melts at 1193°C and the troilite–iron eutectic is at 981°C. Thus the maximum temperature at which the carbon reduction process could have operated was about 1000°C.

The chondrules within chondrites (Section 2f) have clearly crystallized from a molten state. These chondrules frequently contain small irregular crystals of troilite and metal, which have not been melted. However, the melting point of the silicates which constitute the chondrules ranges between 1200°C and 1500°C. It is clear that these temperatures have not been reached, otherwise the metal and sulphide would occur as spheroids, owing to the high surface tensions of their melts. *It follows that some volatile component must have been present during the reduction process, which lowered the melting temperature of the silicates below* 1000°C, *but did not affect the melting points of the metal and sulphide.* The trend of previous discussion, combined with geologic evidence, suggests rather strongly that water vapour and carbon dioxide are the volatiles most likely to be involved. Crystallization of chondrites under high partial pressures of these components therefore seems likely.

Evidence that the silicates in chondrites have crystallized at temperatures below 1075°C is provided by the pyroxenes. By far the most common type present is orthopyroxene. Smaller amounts of clinopyroxene usually occur associated with the orthopyroxene. The relevant phase relationships among Mg–Fe pyroxenes have been studied by Bowen and Schairer (1935), Atlas (1952), and Schairer and Boyd (1956–1957). The stable form of pyroxene below 1075°C is orthopyroxene. Pyroxenes formed above that temperature crystallize as clinopyroxene or protoenstatite—a high-temperature form which readily inverts to clinoenstatite at low

* This argument applies most strongly to friable, unmetamorphosed chondrites. In the case of compact, metamorphosed varieties, some re-crystallization and migration of metal may have occurred, and this could cause a degree of irregularity in grain shape.

temperatures. The transition between clinoenstatite and enstatite is extremely sluggish and has occurred only in very slowly cooled plutonic and deep-seated metamorphic rocks. It seems unlikely that this transition would have occurred in friable and unmetamorphosed chondrites –hence the orthopyroxene in these chondrites is probably of primary origin, indicating crystallization below 1075°C.

Clinopyroxene frequently occurs in small amounts in chondrites, sometimes intergrown with orthopyroxene possessing the same FeO/(FeO + MgO) ratio. This association is observed when glasses of pyroxene composition are devitrified (Bowen and Schairer, 1935). Clinopyroxene forms readily as a metastable phase in the field of orthopyroxene stability*, but the reverse relationship is not observed.

Relationships between Mg Fe pyroxenes and diopsidic pyroxenes also provide data on crystallization temperatures. Occasionally, a small amount of individual diopside crystals is observed in chondrites, e.g. Jeremine and Sandrei (1953), Roy and Wyant (1951). If the chondrite had formed above 1075°C, the small amount of observed diopside would have entered into solid solution in clinopyroxene —Atlas (1952), Schairer and Boyd (1956–1957). If, subsequently, the pyroxene had cooled and inverted to orthopyroxene, the diopside would be exsolved as an intergrowth. It would not segregate into separate crystals except under conditions of extremely slow cooling, which have not been realized in most chondrites. Thus the association of separate orthopyroxene and diopside crystals provides further evidence of crystallization below 1075°C.

Diopsidic intergrowths are sometimes observed in the orthopyroxenes of chondrites, e.g. Mt. Browne. These are parallel to the 100 plane. This orientation is characteristic of diopside exsolving from primary orthopyroxene. If exsolution had occurred in clinopyroxene which subsequently inverted to orthopyroxene, the exsolved laminae would be parallel to 001 (Poldervaart and Hess, 1951). The author has never observed this orientation in chondrites, nor seen it recorded elsewhere.

The preceding evidence from metal phase, sulphides and pyroxenes points strongly to a maximum temperature of formation of chondrites below 1000°C. A minimum value is given by the temperature required for the carbon reduction processes which produced the metal. A rough estimate is 650°C. The temperature must also have been high enough to produce a melt. It seems unlikely that even very high partial pressures of H_2O and CO_2 could lower the liquidus temperature of a chondritic melt below 700°C. Thus the temperature range of chondrite formation is quite restricted.

The data in Table 2 show that the taenite in most chondrites is uniform in composition, averaging 54 per cent Ni. From the Ni–Fe phase diagram (Fig. 4), the temperature at which the metal from chondrites finally reached equilibrium was about 320°C. A considerable amount of cooling is therefore indicated.

(f) *The textures of chondrites*

No single feature of meteorites has caused as much confusion in interpretation as the textures of chondrites. If, however, these unique textures could be

* At the International Geological Congress (Copenhagen, 1960), Turner described the synthesis of clinopyroxene by shearing orthopyroxeneat 700° C. Mason (personal communication) suggests that the clinopyroxene in chondrites map have an analogous origin.

understood, they would provide invaluable evidence, since they must be indicative of highly specialized conditions of formation.

A number of different factors have contributed to produce the textures observed. The most important of these are:

(i) Chondrule formation.
(ii) Processes leading to polymict structures.
(iii) Metamorphism and recrystallization.
(iv) Fragmentation and veining.

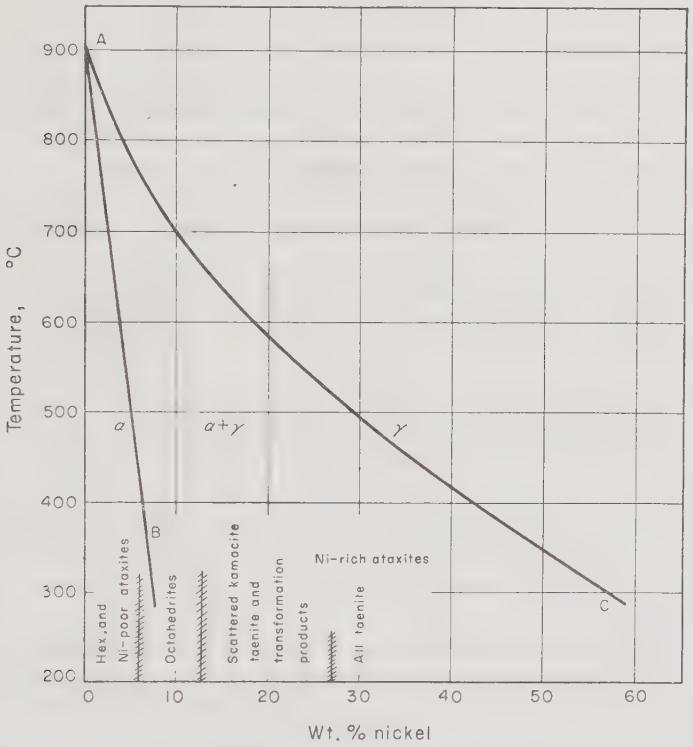

Fig. 4. Iron-nickel phase diagram at zero pressure combined with iron meteorite classification (from Uhlig, 1954).

Although some of these factors are interconnected, it will be convenient to consider them separately.

(i) *Origin of the primary chondritic textures.* These textures are characteristic of chondrites and are responsible for the name of this class of meteorite.

A typical chondrite consists of an aggregate of spherules ranging in size from 5 mm downwards, set in a fine grained, fragmental matrix. The spherules (chondrules) consist dominantly of olivine, pyroxene and oligoclase (originally a glass) and sometimes contain small amounts of metal and troilite. The matrix in which they occur is composed of the same minerals, but contains, in addition, most of the metal and troilite. Structures of individual chondrules display a bewildering variety

of forms, all in close proximity. Shapes of chondrules range from almost perfectly spherical, through spheroidal, to irregularly shaped sub-spheroidal fragments.

The textures and internal structures of chondrules show clearly that they have crystallized very rapidly. The widespread presence of formerly glassy* material is one indication of this, as are the complex intergrowths displayed by olivines and pyroxenes. Synthetic melts rich in olivine and pyroxene possess low viscosities and crystallize very readily into well formed crystals. The imperfection and irregularity of crystallization of these minerals within chondrules is indicative of crystallization times of the order of minutes rather than hours. Detailed microscopical examination of individual crystals reveal that they are crowded with bubbles and inclusions – quite unlike similar crystals from terrestrial rocks. It is most important to note that olivines and pyroxenes from the matrix, between chondrules, display similar features, and hence must also have crystallized rapidly. Occurrence of coexisting and intergrown ortho- and clinopyroxene is also indicative of this.

Despite the wide variety of crystallization forms of chondrules, the compositions of olivines and pyroxenes are uniform in the great majority of chondrites, and similar to those in the matrix. Clearly, the chondrules and groundmass must have formed in close proximity, by rapid crystallization of some locally homogeneous parent material which had never been subjected to processes of fractional crystallization (Section 2a).

Most investigators consider that chondrites are of tuffaceous and volcanic origin. This view, based upon extensive petrological study, is held by Tschermak (1875, 1878), Merrill (1920, 1921, 1928), Wahl (1952) and many others. Evidence leading to this conclusion has been the obviously fragmental nature of chondrites, their textural and structural resemblence to tuffs, occurrence of polymict structures (next section), rapidity of crystallization, and the igneous nature of the constituent minerals.

Terrestrial tuffaceous rocks are formed when magmas containing water and other volatiles ascend into shallow regions of the earth's crust, where the confining pressure is insufficient to keep the volatiles in solution. Under these conditions the gas phase escapes, often violently, and the magma is disintegrated into a mass of crystals and quickly cooled fragments, which may be erupted high into the atmosphere, descending to form tuffs. Alternatively, the eruption may form a very mobile gas–solid system, as an ignimbrite or *nuée ardente*.

Recognition that chondrites are of tuffaceous origin therefore implies that they have undergone a melting process in the presence of volatiles—probably water and carbon dioxide. Subsequently the confining pressure has been lowered and the volatiles have suddenly escaped, causing fragmentation and dispersion of the magma, and formation of tuffs. We shall attempt to follow the consequences of this basic model as far as possible and shall find that it provides a satisfactory explanation for many important features such as:

* Optical isotropy of this material has frequently lead to its identification as glass. No doubt it was, initially. It has probably since devitrified in most cases. Fredriksson (personal communication) has X-rayed a typical "black glass" and found it to consist of very finely crystallized soda-rich plagioclase.

(1) The silicates in chondrites have crystallized rapidly below 1000°C (Section 2e), whereas the dry melting points are between 1200°C and 1400°C. Volatiles must have been present to lower the melting temperatures.

(2) Rapid loss of volatiles from the parental chondritic magma below 1000°C must cause rapid crystallization. It is impossible to account for the rapid crystallization inferred in chondrites by any *cooling* process known to the author. It will be shown later that chondrites are derived from a large parental body, and the cooling of such an object by conduction in a few minutes seems impossible.

(3) The uniformity of local chemical composition in chondrites and lack of crystal fractionation, could be due to the fact that loss of volatiles makes the homogeneous parental magma crystallize immediately, without differentiation. The situation is analogous to the devitrification of a homogeneous glass.

(4) We have previously noted that as one proceeds from carbonaceous chondrites, through metal-poor chondrites, to chondrites containing more than 5 per cent of metal, the abundance of chondrules increases. At the same time, water and CO_2 are lost. This is consistent with the model.

The crucial test for this model lies in its capacity to account for the formation of chondrules. Sorby (1877) suggested that chondrules are, in effect, "drops of fiery rain". He pointed out the similarity of radiating pyroxene chondrules to blowpipe beads, which cooled to a glass and crystallized from a surface nucleus. This interpretation has become widely accepted and may well apply to the majority of chondrules. However, it is uncertain whether it can account for chondrules which are apparently monomineralic, such as the radiating bronzite and the monosomatic olivine chondrules. It is difficult to see how these pure minerals could form when a complex chondritic magma is disrupted into drops.

Brezina, quoted by Farrington (1915), suggested that chondrules originate by spherulitic crystallization within a homogeneous magma. Ringwood (1959) has supported this suggestion. Spherulite formation is a common mode of crystallization in a wide variety of rapidly cooled and supersaturated liquids, including silicate melts. It is possible that many chondrules, not readily accounted for by the Sorby mechanism, may be formed by spherulitic crystallization.

The volcanic model adopted above can account rather simply, both for the formation of rapidly crystallized drops, and for spherulitic crystallization. We have already noted that melts of chondritic composition possess low viscosities and crystallize very readily into well formed crystals. For spherulite formation to occur in melts of this type, it is necessary that they should either be suddenly chilled, or should become suddenly supersaturated. A state of supersaturation would rapidly be reached if volatiles (H_2O and CO_2) in solution in the melt should suddenly escape. This explanation for chondrule formation is therefore consistent with the mechanism proposed for the formation of chondritic tuffs.

Chondrules of the chilled drop variety may be simultaneously formed by cavitation (Ringwood, 1959). As the volatiles are released from the magma, intense cavitation, fragmentation and formation of new surfaces occurs. Since chondritic melts possess low viscosities and high surface tensions, the loss of volatiles may well cause the chondritic liquid to disintegrate into an aggregate of spheroidal drops. Loss of volatiles will also cause simultaneous crystallization of these drops,

which we now recognize as chondrules.* Thus, this process is analogous with that suggested by Sorby, although the cause envisaged is rather different.

The similarity between the formation of terrestrial tuffs, *nuées ardentes*, and ignimbrites, on the one hand, and chondritic structures on the other, has been maintained throughout this section. The basic phenomenon is the rapid loss of volatiles from solution in a melt. In tuffs formed from terrestrial magmas, small lapilli, fragments and threads of glass, are very common. These are caused by the disruption as volatiles escape from the magma, and owe their form and structure largely to the relatively high viscosity of the parent magma. If, however, the terrestrial magmas had possessed much lower viscosities, these threads, glassy fragments, and lapilli, would have contracted into spheres, which we may have called "chondrules". It is concluded that the principal structural difference between tuffs and chondrites is due to the lower viscosity of the parent chondritic magma which facilitated the abundant development of chondrules.

(ii) *Polymict structure in chondrites.* Wahl (1952) has pointed out that large numbers of chondrites are polymict in structure. Such chondrites are found to be brecciated and to contain fragmental inclusions of other meteorites which are foreign to their host. Wahl concludes: "All the various kinds of meteorites must have had their origin on the same cosmic body or on cosmic bodies of exactly similar composition, since they contain fragments of nearly all other kinds of meteorities." It is thus evident that many meteorites have been intermingled to some extent. This process, however, has occurred *after* the primary chondrule forming processes discussed in the previous section.

Foreign inclusions are common in volcanic rocks, tuffs, and ignimbrites. It is possible that analogous processes have been responsible for the incorporation of the polymict inclusions in many chondrites. Brecciation can be caused by explosive evolution of volatiles, whilst an ascending chondritic magma may engulf and enclose fragments of earlier formed chondrites.

(iii) *Metamorphism in chondrites.* Chondrites vary widely in their strength and coherence. There is a complete sequence between highly porous, fragile types and dense, tough, crystalline types. Microscopic examination shows that this sequence is paralleled by recrystallization and grain growth within the meteorite. Merrill (1921) points out that chondrites, although originally of tuffaceous origin, have subsequently been subjected to varying degrees of metamorphism. One of the first effects is to recrystallize the glass of chondrules into oligoclase feldspar. Recrystallization may proceed to the ferromagnesians and may continue so far as to obscure the original chondritic texture.

In Section 2(d5) a very rough correlation between the intensity of metamorphism and the amount of metal present in a chondrite, was pointed out. It appears likely that this correlation is of genetic significance and it will be discussed subsequently.

* Since this paper was submitted for publication I have been privileged to see some most important unpublished work on the structures and compositions of large numbers of individual chondrules, carried out by Dr. K. Fredriksson of the Swedish Geological Survey. This work indicates that chondrules may be far more uniform in structure and composition than is suggested from random thin sections, upon which most of our conceptions are based. Fredriksson's data have persuaded me that the vast majority of chondrules may be of "liquid drop" rather than of spherulitic origin. Fredriksson has independently remarked upon the fundamental resemblence between chondrites and terrestrial ignimbrites.

The varying degrees of metamorphism reflect a wide range of pressures to which chondrites have been subjected. An upper limit to the pressures which chondrites have undergone is indicated by the widespread presence of oligoclase or sodic andesine. It is known that feldspars break down to denser phases such as jadeite under high pressures (Robertson *et al* 1957.) The pressure at which chondritic feldspars would break down depends to some extent on the effect of the anorthite component in solid solution, the temperature involved, and whether or not equilibrium was reached. These uncertainties make it impossible to be too specific; nevertheless, the available evidence strongly suggests that chondrites which contain feldspars have not been subjected to pressures greater than 50,000 atm.

The ureilites Goalpara (Urey *et al.*, 1958) and Novo Urei (Jerofejeff and Latschinoff, 1888; Ringwood, 1960c) contain diamond. These meteorites are composed of olivine, clinopyroxene and nickel–iron, i.e. the essential minerals of chondrites, but they do not contain chondrules. The textures of these meteorites indicate that they have never been thoroughly molten, although a small amount of fractional melting and differentiation is possible. It appears likely that these meteorites are essentially intensely metamorphosed chondrites in which complete recrystallization has obscured the original chondritic textures (Ringwood, 1960c).

The presence of diamond in these stones shows that they have been subjected to pressures probably greater than 35,000 atm. (Urey, 1956; Berman and Simon, 1955). Such pressures would be attained deep within a parent body which was at least of lunar size. It appears plausible to correlate the varying degrees of metamorphism displayed by chondrites with the depth at which they were derived within this parent body.

(iv) *Fragmentation and brecciation in chondrites.* A large number of chondrites are brecciated and veined. Some of these effects have previously been mentioned in the section on polymict chondrites, in which the origin of brecciation was attributed to primary explosive vulcanicity associated with loss of volatiles, and subsequent flowage of ignimbritic aggregates. The distortion of metal particles, and the separation sometimes observed between kamacite and taenite (Urey, 1959; Urey and Mayeda, 1959) could also be caused during the flowing and deformation of these aggregates of fragmental solids.

Another type of brecciation with a different origin exists. Many of the brecciated chondrites possess black veins very similar to slickensides (Farrington, 1915). The material in these veins is chemically similar to the remainder of the chondrite. However, they are glassy and contain rounded blebs of metal and sulphides which have obviously been melted. These black veins show all degrees of gradation into minor cracks along which only slight relative displacement has occurred.

Astronomers believe that meteorites are derived from the asteroidal belt, in which asteroids are continually colliding and perturbing each other's orbits. A plausible explanation of this type of veining would be that it is formed by the stresses and shock waves resulting from these collisions. It is, therefore, of secondary origin.

Within some of the veins, metallic iron is observed to form a most complex system of interlaced, minute threads (Merrill 1928; Fredriksson, personal

communication). Apparently during the brecciation process, iron must have been highly mobile within the meteorite. Possibly it has migrated as a flash-melted liquid. The fineness of the threads suggested to Merrill that it must have migrated through a gas phase. Merrill suggested iron chloride as a transport medium. Another possibility is iron carbonyl.

3. Differentiation of Chondrites and the Formation of Irons, Stony Irons and Achondrites

We have previously inferred that chondrites are the parental group of meteorites. It should, therefore, be possible to understand the genesis of other groups of meteorites in terms of the differentiation of primary chondritic material. It will be convenient to consider the differentiation of two groups separately, although they are doubtless in part interconnected.

(a) *The pallasite–mesosiderite–eucrite association*

A commonly discussed terrestrial differentiation process is the fractional melting of chondritic material to produce residual dunite and peridotite on the one hand and a segregated basaltic magma on the other. The complementary differentiation sequence has a close analogue among meteoritic assemblages.

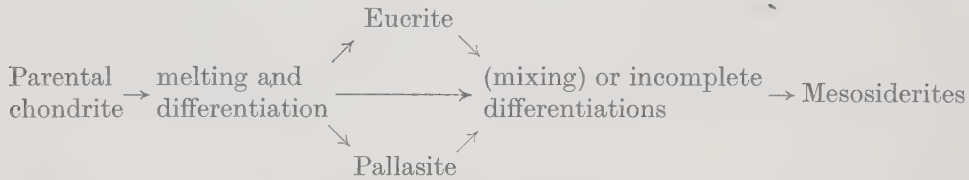

Eucrites (and howardites) are the meteoritic equivalents of basalts, consisting of calcium-rich plagioclase and clinopyroxene. Pallasities consist of olivine and nickel–iron, and are essentially free of calcium and aluminium. They contain from 10 to 60 per cent nickel–iron, which has clearly been melted. Rough calculations based mainly on Ca and Al partition show that one part of eucrite could be derived from six parts of parental chondrite, leaving five parts of residual pallasite. The pallasite would contain about 25 per cent of metal.

Transitional between the eucrites and pallasites are the mesosiderites, which consist of nickel–iron, pyroxene, calcium-rich plagioclase and olivine. Prior (1918) has made a study of this group and pointed out that the Ni/(Ni + Fe) and FeO/(FeO + MgO) ratios of the metal and olivine, respectively, are very similar to those of pallasites, whereas the FeO/(FeO + MgO) ratio of the pyroxene is much higher and is similar to that of the pyroxenes from eucrites. Prior emphasized the transitional mineralogical relationships between pallasites, mesosiderites and eucrites. From the textures of mesosiderites he concluded that they were essentially mixtures, formed by pallasitic magma invading eucritic material.

The Ni/(Ni + Fe) and FeO/(FeO + MgO) ratios of the metal and olivine from pallasites (data from Prior (1953), and Lovering, personal communication) have been plotted on the chondrite diagram, Fig. 2. It is notable that they fall directly upon the main chondrite curve, thus strongly suggesting a genetic relationship.

Furthermore they fill in part of the "gap" on the chondrite curve between FeO/(FeO + MgO) ratios of 15 to 0. This suggests that pallasites formed by the melting and differentiation of parent chondrites with a very restricted range of FeO/(FeO + MgO) and Ni/(Ni + Fe) values, namely, those rich in metal and poor in oxidized iron. Further notice will be taken of this point subsequently.

Two further pieces of data on eucrites are worthy of mention. Firstly, they sometimes contain tridymite (Hess and Henderson, 1949) and must therefore have crystallized under high-temperature–low-pressure conditions. Secondly they are deficient in potassium, rubidium and sodium, compared to chondrites. Urey (1957a) suggests that these elements have been removed from the eucrite magma by volatilization.

Falls and finds of meteorites in the above groups are as follows:

	Falls	Finds
Pallasites	2	37
Mesosiderites	7	10
Eucrites and howardites	28	5

The suggestion that these groups are complementary differentiates from a parent chondritic magma implies that pallasites should be more abundant than eucrites. This is not so, as far as falls are concerned, but it is difficult to be sure of the significance of the statistics on these relatively rare varieties. (For example, many more pallasites are finds than mesosiderites, whereas the opposite relationship holds for falls.) Pallasites are sometimes very large and this would have some statistical weight. It must be admitted, however, that the suggested relationships between the groups are based essentially on chemical, mineralogical and textural evidence, rather than on observed falls. Whether the latter data are significant is not yet clear.

(b) *Irons and chondritic-type achondrites as complementary differentiates*

Reliably determined nickel contents of meteoritic irons range from 5 to 35 per cent. Recent work by Lovering *et al.* (1957) gives 8·3 mol per cent Ni as the average for eighty-eight irons.

The aubrites and diogenites (achondrites) are probable complementary differentiates with the irons. The former consist of enstatite, small amounts of olivine, with minor metal, troilite and oligoclase. Prior (1916) has pointed out that these are mineralogically equivalent to enstatite chondrites and would be formed if enstatite chondritic material had melted, allowing the iron to sink and segregate. The textures of aubrites show clearly that they have been melted, thus supporting the above conclusions. The diogenites are closely related to hypersthene chondrites and could be formed in an analogous manner. The average nickel content of irons is intermediate between those of the metal phases of enstatite and hypersthene chondrites, suggesting a mixing of metal from these two sources.

Although this scheme of complementary differentiation is satisfactory from mineralogical, chemical and textural viewpoints, it may not be complete. Forty-two irons have been observed to fall compared to only six aubrites and five diogenites. There is a marked discrepancy here and no satisfactory explanation can be advanced at present.

It may be significant that the average nickel content of irons (8·3 per cent) corresponds to that which would be expected from chondrites filling the "gap" in Fig. 2. If all chondrites in this composition range had melted and allowed the iron to separate, an explanation would be provided both for the existence of the gap and of iron meteorites. Unfortunately, however, no complementary achondrites with the relevant compositions are known. Perhaps the discrepancy is due to the relative abundance of irons being grossly overestimated, due to their superior ability, compared to stones, to withstand collisions and passage through the atmosphere.

(c) *Relationships between irons and pallasites*

The average metal from pallasites contains about 10 per cent nickel, compared to 8 per cent nickel in irons. According to Fig. 2, this means that the irons have differentiated from parent chondrites which were, on the average, more reduced than the parent chondrites of pallasites. This inference is supported by the mineralogy. Irons contain daubreelite as an accessory mineral, which does not, however, occur in pallasites. Daubreelite is known only in the most strongly reduced (enstatite) chondrites.

The textures of the metal in pallasites and octahedral iron meteorites are very similar, both displaying Widmanstatten textures. Sometimes the metal in pallasites is observed to grade into segregations which consist exclusively of metal (Brenham). If such a portion had been detached during an asteroidal collision, it would be regarded as a normal iron meteorite.

The complete gradation in texture, chemistry and mineralogy between all the major classes of meteorites argues very strongly for a cogenetic origin. A genetically based classification of meteorites, based upon the previous discussion, is suggested in Fig. 3.

4. The Iron Meteorites

(a) *Introductory*

Although minor in abundance compared to chondrites, the irons have received a great deal of study, and much progress has been made in the interpretation of their origin. In this section a few specialized features of genetic importance will be discussed. Before proceeding, some introductory data will be mentioned.

The principal phases in irons are kamacite (α-phase, Ni — from 4 to 6 per cent), taenite (γ-phase, from 25 to 50% Ni) and the martensitic α_2 phase, consisting of a distorted kamacitic solid solution supersaturated with nickel. Phase relationships in this system have been worked out by Owen and Sully (1939), and Owen and Liu (1949) (Fig. 4). Superimposed upon Fig. 4 is the major structural classification of irons—hexahedrites (from 4 to 6·2 per cent Ni), octahedrites (from 6·2 to 13 per cent Ni) and nickel-rich ataxites with more than 13 per cent Ni.

Octahedrites are the most abundant irons and consist of an intergrowth in which taenite lies along the octahedral planes of kamacite. To a first approximation, the structures and phase compositions can be understood in terms of the phase diagram (Fig. 4). The intergrowths, called Widmanstatten patterns, are often very coarse. Continuous patterns extending for more than 10 ft indicate that the initial taenite crystals which transformed were at least this large. Crystals of this size could be formed only by very slow cooling. Furthermore, the coarse Widmanstatten textures imply that the irons have passed through the α–γ transition very slowly. Estimates of the cooling rate based upon diffusion constants of nickel and iron in the kamacite and taenite have been made by Uhlig (1954) and Urey (1956). They are in conflict owing to the different assumptions made on the temperature at which equilibrium was finally reached. The times required are estimated to be between 10^7 and 10^{11} years.

These slow cooling rates suggest that the irons have been insulated within a fairly large parent body.

(b) *Crystallization pressures of iron meteorites*

This topic is of key importance in the study of meteorite genesis. Recent investigations have produced conflicting results; hence, a rather detailed discussion of relevant data will be made.

In octahedrites, the kamacite contains about 6 per cent nickel (Owen, 1940) whilst the coexisting taenite, although very variable, appears to average 30 per cent Ni (Farrington, 1915; Uhlig, 1954; Nichiporuk, 1958; Parry (personal communication). Much of the variation is doubtless due to experimental error. These compositions indicate that equilibrium has been reached around 450°C if the diagram of Owen and Liu, Fig. 4, is applied.

Uhlig (1954) points out that the Widmanstatten texture is not found in irons containing more than 13 per cent nickel. The textures of these irons (nickel-rich ataxites) show that they have passed through the α–γ transition quickly and at relatively low temperatures. Restriction of the Widmanstatten texture to irons ranging from 6 to 13 per cent nickel implies that the transformation stopped at 665°C. But this disagrees with the compositions of taenite and kamacite from octahedrites, which indicate a temperature of 450°C. It is apparent that the phase and compositional relationships in irons do not obey Owen and Liu's diagram. Uhlig's explanation is that both the equilibria and kinetics of the phase changes within the Fe–Ni system have been substantially altered by the high pressure under which meteoritic irons have crystallized. He shows that *qualitatively* this could provide an adequate answer for the anomaly.*

* An alternative explanation occasionally suggested is that "impurities" present in the irons in small amount could significantly alter the equilibria. To effect this they must be substantially soluble in either the kamacite or taenite. Cobalt, phosphorus and carbon are possibilities. Sulphur is not. In most irons, carbon is not present in amounts sufficient to modify the equilibria. Phosphorus occurs widely, averaging 0.2 per cent. Some of this is associated with troilite as an immiscible phase. In addition many irons are poorer than average in this component. It appears improbable that such small amounts will significantly alter the equilibria. Cobalt averages 0.5 per cent in irons. It is, however, soluble in both phases without any clearly defined preferences, and will therefore not displace the equilibria substantially. Strong evidence that impurities are irrelevant is provided by the experiments of Owen and Burns (1939) on meteoritic irons, who found that they behaved similarly to pure artificial Ni–Fe alloys during heat treatment. Finally, it can be demonstrated that phosphorus would alter the equilibria in the opposite direction to that required.

A second argument advanced by Uhlig concerns the occurrence of the α_2-phase in nickel-rich ataxites. Owen and Burns (1939) observed that the ataxites Babbs Mill (17·3 per cent Ni), Klondyke (18·2 per cent Ni) and San Cristobel (25·6 per cent Ni) consisted only of the martensitic α_2-kamacite phase which forms when alloys in this range are suddenly quenched. Owen and Burns observed that the α_2-phase broke down to normal α- and γ-phases when annealed for 56 days at250 °C or 8 days at 300°C. The required annealing times at 350°C were very much shorter. Uhlig points out that preservation of the α_2-phase requires rapid cooling from a high temperature. Since it is not possible to cool large bodies rapidly, the α_2-phase is more readily accounted for by sudden displacement of the phase boundaries in the Ni–Fe system due to reduction of the pressure when the parent meteorite body broke up. A large number of irons contain plessite which was probably formed by sub-zero transformation of this α_2-phase.

The qualitative arguments of Uhlig are persuasive. It does not appear likely that the constitution of iron meteorites can be understood satisfactorily on the basis of the zero pressure Fe–Ni phase diagram. The discrepancies may vanish if one assumes that irons crystallized under high pressure, which altered the phase boundaries. General thermodynamic reasoning suggests that pressures greater than 10^4 bars would be required to charge the phase boundaries significantly.

Uhlig suggested that high pressure (10^5 bars) would uniformly displace the Ni–Fe diagram downwards by 200°C, without altering its shape. This assumption is doubtful. Pressure is likely to alter not only the relative positions of the phase boundaries but also their shapes. This occurs because of the rather complex behaviour of the partial molar volumes of Ni and Fe in kamacite and taenite solid solutions. At present, no conclusions can be drawn about the shapes and positions of the high-pressure phase boundaries.*

Urey (1956, 1958) has criticized Uhlig's conclusion that meteoritic irons crystallized under high pressure, but his criticism hinges principally upon the consequence of Uhlig's high-pressure diagram. Since this diagram may be incorrect, the criticisms are perhaps premature.

There is another qualitative indication that iron meteorites crystallized under high pressure. Troilite, iron and nickel are miscible in the liquid state. However, the appearance of spheroidal segregations of troilite in meteoritic irons strongly suggests that the sulphide phase has separated as an immiscible liquid. The Fe–FeS phase diagram shows incipient immiscibility, which is usually characterized by positive deviations from volume additivity in the melt. Vogel (1945) has pointed out that high pressure would therefore tend to produce immiscibility.

Ringwood (1960b) has studied the stability of cohenite in irons. He has shown that under the crystallization conditions to which irons have been subjected, cohenite would not be formed unless the pressure was above 25,000 atm. Cohenite is known in at least nine irons and is probably considerably more abundant, since it is likely to be confused with schreibersite (Perry, 1944). It therefore provides a most useful pressure indicator.

* Kaufman and Ringwood (manuscript) have recently computed the phase boundaries in the Fe–Ni system at high pressures. Their results support the view that iron meteorites cooled slowly under high pressure, as suggested by Uhlig.

The preceding observations indicate that irons as a group have formed under high pressures, whereas stones have formed under a very wide range of pressures, perhaps from 0 to 35,000 atm. This would suggest that irons occupied the core of the meteoritic parent body, whilst the stones formed the mantle, as in the earth. Support for this view has been provided by Stacey and Lovering (1959, and personal communication) who have shown that chondrites possess remnant magnetizations of pre-terrestrial origin. These are most plausibly interpreted as having formed in the parent body by the action of magnetic fields generated by the convecting core.*

5. Age Relationships among Meteorites

Patterson (1956) has determined the isotope ratios of leads extracted from two irons, two chondrites and one basaltic-type achondrite. He was able to show that the age of this array was 4·55 aeons.† Subsequently, some doubts arose on the validity of the chondrites ages due to possible contamination. However, Marshall and Hess (1958) have since analysed lead from two chondrites (Richardson and Holbrook) and obtained an age of 4·7 aeons. The ages calculated refer to the time when an iron phase separated from silicates in the parent body, and also when differentiation of the silicate phase occurred to produce the differing U/Pb ratios found in chondrites and in Nuevo Laredo—the basaltic-type achondrite.

The rubidium–strontium method has been applied to the basaltic-type achondrite, Pasamonte, the chondritic-type achondrite, Bustee, and the chondrites, Forest City and Homestead (Schumacher, 1956; Herzog and Pinson, 1956). Within the limits of error imposed by uncertainty in the half life of Rb^{87}, these results agree with the lead ages. The calculated ages refer to the time when differentiation of silicates occurred in the primary body, causing variation in Rb/Sr ratios between chondrites and achondrites.

A large number of potassium–argon ages have now been determined. Early work (Gerling and Rik, 1955) indicated chondrite ages between 2·3 and 4·5 aeons. Later, and probably more accurate, work has shown that the ages of eight chondrites range between 4·0 and 4·4 aeons (Wasserburg and Hayden, 1955a, b; Geiss and Hess, 1958). These results are most significant since they refer to the time at which the meteorite was sufficiently cool to retain its argon. Since some of the argon may have been lost by subsequent diffusion at low temperature, these are minimum ages.

Geiss and Hess also report an age of 4·4 aeons for Norton Country (chondritic type achondrite) and ages between 3·23 and 3·8 aeons for three basaltic type achondrites.

Uranium–helium ages have recently been estimated for a number of stones by Reed and Turkevich (1957). Upper limits of 4·3 aeons are again found.

The above data permits the following conclusions. Parent meteoritic material underwent a major chemical differentiation about 4·5 aeons ago during which

* Urey (1959) has argued that the irons in the parent body occur as scattered small bodies, as in "raisin bread". This would not explain the above data. Urey's arguments are nowhere inconsistent with the hypothesis of a metallic core surrounded by a stony-iron zone in which varying degrees of segregation of metals and silicates have occurred (Section 3). Urey's "raisin bread" arguments would apply to this stony-iron zone.

† The term "aeon" is defined as 10^9 years (Urey, 1957b).

chondrites, achondrites and irons possessing different U/Pb and Rb/Sr ratios were formed. This differentiation involved a melting process. The maximum K-A and U-He ages show that after melting and differentiation, chondrites and chondritic-type achondrites must have cooled below 300°C within times of the order of 10^8 years.

6. Recapitulation

The principal conclusions which emerged during the preceding enquiry will now be summarized. These conclusions are based as closely as possible on empirical data provided by the direct study of meteorites, and may be regarded as boundary conditions to be satisfied by any general hypothesis of meteorite genesis. An attempt to set up such a hypothesis will be made in the next section.

(1) The chemical, mineralogical, textural and age relationships existing between all major classes of meteorites strongly suggest a cogenetic origin.

(2) Some evidence suggests that meteorites are derived from the asteroidal belt. The relatively high probabilities of collisions between asteroids, together with the observed irregular shapes of some asteroids, suggest that the parental asteroidal (or meteorite) bodies were much larger than present asteroidal dimensions.

(3) Chondrites are by far the most abundant meteorites, representing about 90 per cent of all known falls.

(4) Apart from certain volatile components and trace elements, chondrites are extremely uniform in chemical composition. This average composition provides the basis for a satisfactory geochemical model of the earth, and, with the exception of iron, is in reasonable agreement with the solar elemental abundances. The genesis of other classes of meteorites can be satisfactorily understood in terms of melting and differentiation of chondritic material. These considerations are strongly indicative of the primitive and parental nature of chondrites.

(5) The original state of the parental chondritic material probably resembled that displayed by carbonaceous chondrites. The material was cold and oxidized, containing up to 5 per cent carbon and 20 per cent of water, together with obscure compounds of carbon with hydrogen, nitrogen, sulphur, chlorine and other volatiles.

This material has been subjected to higher temperatures under such conditions that the carbon (and hydrogen) reacted with oxidized iron and nickel to form a metal phase *in situ*, whilst volatiles (principally water, CO_2 and certain trace elements) were lost.

(6) The oxidation states of chondrites extend over a very wide range because of the varying degrees to which the reduction process has operated. There is an almost continuous range from carbonaceous chondrites containing Fe^3 and no metal, to enstatite chondrites in which all the iron is reduced, and which contain, in addition, reduced Si, Cr, Ca and P compounds. The mineralogy and chemistry of chondrites is largely controlled by the oxidation reduction equilibria. This applies particularly to the amount and nickel contents of the metal phase (Prior's rules).

(7) FeO/(FeO + MgO) ratios of the silicates vary continuously from about 40 per cent (in carbonaceous chondrites) to 15 per cent. There is a hiatus between FeO/(FeO + MgO) ratios of 15 per cent and the ratios of 0-1 per cent which are characteristic of enstatite chondrites.

(8) A common group of chondrites containing about 12 per cent metallic iron appears to have lost about 5 per cent of metal compared with their neighbours in the oxidation–reduction sequence.

(9) Most chondrites closely approach a state of internal chemical equilibrium.

(10) The silicate phase of most chondrites has crystallized at a temperature below 1000°C. The presence of chondrules shows that crystallization occurred from the liquid state. In order to produce silicate liquid of chondritic composition at this temperature, melting must have occurred under a high pressure of volatile components, e.g. water and carbon dioxide.

(11) The composition of the accompanying metal phases indicates that chondrites subsequently cooled to temperatures in the neighbourhood of 300°C. Conclusion (22) indicates that the time required for cooling was of the order of 10^8 years.

(12) Primary chondritic textures are tuffaceous in nature and therefore of volcanic origin. They have probably formed by the rapid liberation of water and carbon dioxide from a chondritic magma below 1000°C. Sudden loss of volatiles has caused rapid crystallization and chondrule formation. The principal difference between formation of chondrites and terrestrial tuffs is due to the relatively low viscosity of chondritic magma which has facilitated chondrule formation.

(13) The volcanic activity leading to chondrite formation has also resulted in the formation of brecciated and polymict structures.

(14) Chondrites have subsequently been subjected to varying degrees of metamorphism, which is manifested by compaction and recrystallization. In some cases these may destroy the former chondritic textures. It seems likely that diamond containing ureilites are essentially intensely metamorphosed chondrites. This would imply that at least one of the parent bodies of chondrites was of lunar size.

(15) There is a correlation between intensity of metamorphism and the amount of metal in a chondrite. Intensity of metamorphism may be associated with depth of origin in the parent body. The correlation therefore suggests that the degree of reduction of chondritic material increases with depth in the parent body. This generalization has many exceptions, however.

(16) Portion of the parent chondritic material has melted and differentiated. Two related series of complementary differentiation products have been formed:

(i) the pallasite–mesosiderite–eucrite association;

(ii) the chondritic-type achondrite–iron association.

The chondritic material parental to these associations was relatively reduced and would occupy part of the hiatus observed in the oxidation-reduction series (conclusion 7). Association (ii) above appears to have formed from more reduced parental material than (i).

(17) Conclusions (15) and (16) suggest that melting and differentiation occurred deep within the parent body and that association (ii) is of deeper origin than (i).

(18) Nevertheless, eucrites have finally crystallised under low-pressure–high-temperature conditions.

(19) Iron meteorites have crystallized very slowly under high pressures, probably exceeding 30,000 atm. This suggests that they formed a core in the parent body.

(20) Chondrites possess remnant magnetizations of pre-terrestrial origin, suggesting that a convecting metallic core was present in the parent body.

(21) Conclusions (14) to (20) suggest that a typical parent body may have consisted of a chondritic mantle, grading downwards into pallasites and mesosiderites and then into irons. Such a sequence would be anticipated during gravitational segregation. Low crystallization pressures and high crystallization temperatures of eucrites could perhaps be explained if eucritic magma had migrated or stopped its way to the surface of the parent body, subsequent to its formation by differentiation near the core.

(22) All the major classes of meteorites appear to possess the same age. This age refers to the time when melting and differentiation of chondrules, achondrites and irons occurred. Subsequent cooling of chondrites to temperatures in the vicinity of 300°C occurred within a relatively short time interval, of the order of 10^8 years.

7. The Evolution of Meteorites

An attempt will now be made to set up a model for meteorite genesis, which is consistent with the conclusions drawn in the previous section. It is not claimed that the suggested model is satisfactory in all respects, or that it is the only model which will satisfy the boundary conditions in Section 6. Doubtless there are numerous possible variants, but it seems likely that they will have much in common. One advantage of the proposed model is that certain critical aspects can be subjected to experimental investigation. Preparations are being made towards this end.

Several aspects of the model have been discussed in previous papers (Ringwood, 1959, 1960c).

It is assumed that the parent body or bodies of meteorites formed by accretion from a cold dust cloud of solar composition. The accretion process was part of the series of events which led to the formation of the solar system about 4·5 aeons ago. Meteorites may be derived from one or more parent bodies, at least one of which was of approximate lunar size. In subsequent discussion, we will consider the evolution of a typical parent body—which may, with some justification, be called a meteoritic planet.

After the accretion stage, it is assumed that the meteoritic planet possessed a composition similar to that of carbonaceous chondrites, but perhaps containing a higher concentration of volatiles. Such a composition would be expected for a low-temperature accumulation of dust of solar composition. The planet was then subjected to internal heating, which caused melting to occur in the deep interior. When the molten region became sufficiently extensive, convection set in. The molten chondritic material, containing water and carbon under confining pressure, rose to the surface regions of the planet, where the confining pressure was released. Under these conditions, volatiles (including class II metals) rapidly escaped, and the surface of the planet was subjected to volcanism on a grand scale. The rapid loss of volatiles caused rapid crystallization and resulted in the formation of the tuffaceous and chondritic structures of chondrites. During the same heating process, the carbon (and hydrogen) reacted with the oxidized iron and nickel to produce a metallic phase, whilst the resultant carbon dioxide was lost with the volatiles. It is suggested that nearly all the material in the meteoritic planet passed through this melting-convection-volcanism stage, thus producing the familiar chondritic meteorite parental material.

The temperature at which melting occurred was around 900°C, but after the convection–reduction–volcanism stage, it fell to 300°C. However, in a relatively small region in the deep interior, temperatures substantially higher than 900C were reached, which caused complete melting and differentiation of the chondritic material. As a result, the metal phase sank to the centre to form a small core, separated from the relatively cool chondritic mantle by a zone of mixed iron and silicates, the pallasites and mesosiderites. The complementary eucritic and howarditic silicate differentiates possessed a lower density than surrounding stony iron and chondritic material, and hence, rose to the surface of the planet in much the same manner as basalts on the earth. Because of their relatively high temperature and the presence of volatiles, they lost much of their rubidium and potassium by volatilization and gas streaming.

The molten inner zone of irons and stony irons cooled to a temperature below 500°C by heat transfer with the surrounding cool chondritic mantle. At the same time, a certain amount of metamorphism and recrystallization occurred in the mantle.

Subsequently the meteoritic planet was disrupted into fragments, which have since been colliding among themselves, thus further reducing their sizes. The remnants of these collisions are the asteroids and meteorites.

Certain aspects of this model require further discussion.

(a) *The heating process*

Mineralogical and textural evidence show that the meteoritic planet warmed up and melted about 4·5 aeons ago.

The only satisfactory heat sources suggested so far are the disintegration of unstable nuclides with short half lives (Urey, 1956; Fish *et al.*, 1960) and chemical heating (Urey, 1956; Ringwood, 1959). Heating by unstable long-lived nuclides of potassium, uranium and thorium is unsatisfactory (Ringwood, 1960c).

If radioelements with short half-lives are to provide an adequate source of heat, it is necessary that the time interval between nucleogenesis and accretion into the meteoritic planet should be small, of the order of 10^8 years. Recent discovery of radiogenic xenon in meteorites by Reynolds (1960a) has indicated that the time interval was at least as small as $3{\cdot}5 \times 10^8$ years (Wasserburg *et al.*, 1960)*. There is no doubt that this heat source, if available, would provide a satisfactory solution to the heating problem.

Other interesting possibilities are also raised. If accretion occurred over the same time-scale as the decay of short lived radioactivities (i.e. about 10^8 years), then the earliest material accreting in a parent body would be raised to the highest temperature, and could therefore become melted, differentiated, and strongly reduced. The outer regions in such a parent body would not have been heated so strongly, since they accreted later. Hence they would not have become as strongly reduced. Thus, the correlation previously inferred, between depth in the parent body and the intensity of reduction, might be rather simply explained.

If chondrites have been derived from more than one parent body, it is possible that they might have accreted at different times over the interval of 10^8 years.

* Recent data obtained by Anders (personal communication) imply that the time interval was around 100—120 million years.

Accordingly, overall differences in thermal histories and the degrees of reduction might well be caused between different bodies. Further speculations must await more decisive evidence on the role of radiogenic heating by short-lived nuclides.

Chemical heat sources arise from the fact that the primitive dust which condenses from interstellar gas at extremely low temperatures and pressures is unlikely to be in chemical equilibrium, the nature of the precipitate being governed largely by kinetic factors. If chemically unstable dust is trapped in a planet during accretion, subsequent annealing processes leading to equilibrium will provide a heat source, which, under favourable conditions, may be very substantial. Urey (1956) suggests that free radicals (as found in interstellar gas) may condense in the dust and be trapped in the accreting planet.

There are, in addition, innumerable saturated but unstable molecular assemblages which may precipitate. These may well provide a more satisfactory heat source than free radicals since they can be trapped at higher accretion temperatures. Other sources include stored radiation damage in the dust grains, and surface energy. In the case of graphite, the former can amount to 500 cal/g, whilst in finely divided oxides, the latter can provide 100 cal/g.

Chemical energy of this type is essentially an unknown quantity and provides wide fields for further study. There are, however, grounds for believing that it could provide the 350 cal/g necessary for melting and reduction of the primitive dust.

(b) *Reduction*

The principal equilibrium involved in the reduction is

$$2FeO + C \rightleftharpoons 2Fe + CO_2\nearrow$$

Two factors which greatly affect this equilibrium are the amount of carbon available and the temperature. Since these factors may be expected to vary widely during the complex early evolution of chondrites, we might expect widely variable amounts of metal to be produced in different regions of the parent body. A third factor of basic importance is the pressure of CO_2. If iron oxide and carbon are held at high temperature under a high confining pressure, so that CO_2 is unable to escape, reduction will not occur. For the reaction above to proceed from left to right, it is necessary that the partial pressure, or fugacity, of the CO_2 should be kept low. This may be accomplished in a number of ways.

(i) After melting occurs in the interior, the chondritic magma rises convectively to the surface where confining pressure is lowered. Under these conditions, CO_2 and other volatiles can escape, and the reduction process continues until the carbon, or the energy source, is exhausted.

(ii) When melting occurs in the interior of the planet it is possible that CO_2 may be able to dissolve in quantity, in the hydrous silicate melt. This will lower its fugacity and allow the reduction reaction to proceed, despite the high confining pressure.

(iii) It is also possible that the mantle of the planet may not be impervious to volatile components such as H_2O and CO_2. Under these conditions, reduction could occur in the deep interior before any melting took place, whilst much of the volatile CO_2 and H_2O was gradually squeezed or otherwise migrated to the surface.

In the previous section it was concluded that some fractionation of metal had occurred among chondrites. Furthermore, a tendency was noted for the intensity of reduction to increase with depth in the parent planet. This suggests that at least some reduction occurred by mechanisms (ii) and (iii), deep within the planet, where sinking and fractionation of solid metal particles would be possible before the melt rose to the surface. Furthermore, since increasing depth in the planet can be associated with increasing temperature, it is possible that the tendency towards stronger reduction with depth may be explained on this basis.

(c) *Cooling of the meteoritic planet*

Mineralogical and dating evidence shows that the whole of the meteoritic planet passed through a melting stage about 4·5 aeons ago. For the chondritic mantle, which comprised most of the planet, a temperature in the neighbourhood of 900°C is required. Subsequently, however, the planet cooled to 300–450°C in times of the order of 10^8 years. Urey (1956, 1957a, b, 1958) has commented on the difficulties implied by this history, if the cooling is assumed to be by conduction throughout a lunar sized body. In order to avoid these difficulties (and also to explain his own interpretation of chondritic textures) Urey proposed a hypothesis involving "primary and secondary objects". This postulated collisions between primary differentiated silicate–metal bodies, followed by complete fragmentation, and then random collection into "secondary bodies" from which chondrites are derived. This hypothesis is inconsistent with most of the detailed chemical, mineralogical and textural data on meteorites, which have been discussed in previous sections. It also meets with grave difficulties on other grounds. The author believes that the cooling problem, which has been rightly emphasized by Urey, is not insuperable on the present model.

The chondritic material in the meteoritic planet has been assumed to melt in the interior around 900°C, under a high pressure of CO_2 and H_2O. The melt rises to the surface, where a volcanic cycle occurs during which the volatiles are lost. It seems likely that the overall effect of this volcanic cycle will be highly endothermic and rapid cooling will result. The following factors are involved:

(i) Water and carbon dioxide dissolve in the silicate melt with the evolution of heat. Accordingly, when they leave the melt, they will cause a corresponding amount of cooling.

(ii) The volatiles are under high confining pressure initially. When they escape from the magma, they undergo rapid adiabatic expansion, which will cause cooling.

(iii) The reduction processes during which metal is produced are endothermic and will cause cooling.

(iv) During the volcanic phase, the rising magma is intimately fragmented in a turbulent gas–solid, or *nuée ardente* type of eruption, during which a large surface area is exposed to space. This allows direct radiative cooling to occur. Further convective movements extend this process so that the whole of the chondritic mantle has been exposed to radiative surface cooling. Because of the low gravitational acceleration on the parent meteoritic planet, a *nuée ardente* eruption will be rather different than on the earth. The gas–dust cloud will arise far higher and become much more dispersed before it finally settles down. Thus the cooling of the dust and

fragments will be much greater than is the case for terrestrial eruptions. The inferred cooling from molten chondritic material at 900°C to solid chondritic material at 300°C involves the loss of about 200 cal/g (including the latent heat of melting). It seems quite possible that the above factors could account for this amount of heat loss.

Textures of the irons and pallasites show that they have cooled very slowly from the melting temperature to below 500°C, and it has been inferred that this cooling took place whilst they occupied the core of the meteoritic planet. These meteorites are very small in amount, compared with the surrounding chondritic mantle, which has been cooled by the volcanic processes previously outlined to a temperature of about 300°C. Thus, cooling of the core can be simply due to conductive transport and thermal equilibrization between the small hot core and the outer cool mantle. This would not require an extensive period of time.

(d) *Fragmentation of the meteoritic planet*

Following the processes which were responsible for producing meteorites as we know them, the parent meteoritic planet has been shattered by some event. It is only necessary that it should have broken initially into a few, or perhaps only two fragments. Subsequent collisions among fragments would greatly multiply the numbers and reduce the sizes.

It seems likely that disruption occurred less than one aeon after the planet was formed. If a longer time was allowed, the K–U–Th series of long-lived nuclides would have caused sufficient heating to cause more extensive recrystallization and loss of argon among the minerals of the chondritic mantle than is observed.

Only the vaguest suggestions can be advanced regarding the cause of disruption. If meteorites are derived from a single parent planet it is possible that:

(i) Fragmentation could be due to the development of intense water vapour pressure near the differentiated core, as silicates crystallized from a magma containing volatiles (the Goransen effect).

(ii) The model for the evolution of the meteoritic planet previously described, involves a substantial reduction in moment of inertia, compared with the original, unreduced state. If the original body had been rotating anywhere near the instability limit, the decrease in moment of inertia may have caused an increase in rotation velocity, leading to instability and disruption.

(iii) If, on the other hand, meteorites are derived from more than one parental planet, which have been subjected to similar evolutionary histories, it is possible that disruption may have been caused by a collision between these bodies.

The history outlined above for the meteoritic planet may also be applicable to other bodies of similar size in the solar system, e.g. Io, Europa, the Moon, Ganymide, Callisto and Titan. The lower densities of the latter four, compared to the meteoritic averages, may be due to a higher content of oxidized, water bearing, carbonaceous chondritic material.

Acknowledgements—The author is greatly indebted to the following individuals and institutions for donations of meteorite specimens used in this study. Mr. R. O. Chalmers, Australian Museum; Dr. K. Fredriksson, Geological Survey of Sweden; Dr. H. B. Wiik, Geological Survey

of Finland; Dr. B. Mason, American Museum of Natural History; Dr. C. Frondel, Department of Mineralogy, Harvard University; Dr. J. F. Lovering, Australian National University; Dr. E. P. Henderson, U.S. National Museum; Dr. E. Jeremine, Museum d'Histoire Naturelle, Paris; Mr. J. M. Harrison, Geological Survey of Canada; Dr. M. Hey, British Museum; Dr. E. Vincent, Oxford University, The Director, South African Museum; and the Director, Geological Survey of India. The author is also greatly indebted to numerous workers for stimulating discussions and constructive critism—in particular, Dr. Kurt Fredriksson, Dr. Brian Mason, Dr. M. Hey, Dr. J. Lovering, Prof. J. C. Jaeger and Dr. E. C. Anders. Thanks are also due to Prof. H. C. Urey, whose detailed consideration of an early (1959) draft of the manuscript stimulated the author to obtain further empirical data.

References

Ahrens L. H. (1957) A survey of the quality of some of the principal abundance data of geochemistry. *Physics and Chemistry of the Earth.* Vol. 2, pp. 30–45. Pergamon Press, London.

Aller L. H., Goldberg L. and Müller E., (1960) Primordial composition of the solar system. *Sky and Telescope* **19,** 338–339.

Atlas L. (1952) The polymorphism of $MgSiO_3$ and solid-state equilibria in the system $MgSiO_3$–$CaMgSi_2O_6$. *J. Geol.* **60,** 125–147.

Berman R. and Simon F. (1955) On the graphite–diamond equilibrium. *Z. Electrochem.* **59,** 333–338.

Bowen N. L. and Schairer J. F. (1935) The system MgO—FeO—SiO_2. *Amer. J. Sci.* **229,** 151–217.

Brown H. (1952) Rare gases and the formation of the earth's atmosphere. *The Atmospheres of the Earth and Planets.* (Edited by G. P. Kuiper) pp. 258–266.

Brown H. and Patterson C. (1947a) The composition of meteoritic matter—I. The composition of the silicate phase of stony meteorites. *J. Geol.* **55,** 405–411.

Brown H. and Patterson C. (1947b) The composition of meteoritic matter—II. The composition of iron meteorites and of the metal phase of stony meteorites. *J. Geol.* **55,** 508–510.

Brown H. and Patterson C. (1948) The composition of meteoritic matter—III. Phase equilibria, genetic relationships and planet structure. *J. Geol.* **56,** 85–111.

Daubree G. (1879) *Geologie Experimentale, Paris* 517–523, 580, 596.

Edwards G. (1955) Sodium and potassium in meteorites. *Geochim. et Cosmochim. Acta* **8,** 285–294.

Edwards G. and Urey H. C. (1955) Determination of alkali metals in meteorites by a distillation process. *Geochim. et Cosmochim. Acta* **7,** 154–168.

Farrington O. C. (1915) *Meteorites* p. 108. Chicago.

Fish A. R., Goles G. G. and Anders E. (1960) The record in the meteorites—III. On the development of meteorites in asteroidal bodies. *Astrophys. J.* In press.

Geiss J. and Hess D. C. (1958) Argon-potassium ages and the isotopic composition of argon from meteorites. *Astrophys. J.* **127,** 224–236.

Gerling E. K. and Rik K. G. (1955) Determination of the ages of meteoritic stones by the Argon method. *Dokl., Akad. Nauk SSSR* **101,** 433–435.

Herzog L. F. and Pinson W. H. (1956) Rb/Sr age, elemental and isotopic abundance studies of stony meteorites. *Amer. J. Sci.* **254,** 555–566.

Hess H. H. and Henderson E. P. (1949) The Moore County meteorite—A further study with comment on its primordial environment. *Amer. Min.* **34,** 494–507.

Jeremine E. and Sandrea A. (1953) Sur la meteorite de Guidder. *Geochim. et Cosmochim. Acta* **4,** 83–88.

Jerofejeff M. and Latschinoff P. (1888) Meteorite diamantifere tombe (1886) en Russie, a Nowo-Urei. *Verh. Russ. Min. Ges. St Petersburg* **24,** 263–294.

Kuno H. (1954) Study of orthopyroxenes from volcanic rocks. *Amer. Min.* **39,** 30–46.

Kuroda P. K. and Sandell E. B. (1954) Geochemistry of molybdenum. *Geochim. et Cosmochim. Acta* **6,** 35–63.

Kvasha L. G. (1948) Investigation of the stony meteorite Staroye Boriskino. *Meteoritica, Acad. Sci. U.S.S.R.* **4,** 83–96.

Latimer W. M. (1950) Astrochemical problems in the formation of the earth. *Science* **112,** 101–104.

Lovering J. F., Nichiporuk W., Chodos R. and Brown H. (1957) The distribution of gallium, germanium, cobalt, chromium and copper in iron and stony-iron meteorites in relation to nickel content and structure. *Geochim. et Cosmochim. Acta* **11,** 263–278.

MacDonald G. J. F. (1959) Chondrites and the chemical composition of the earth. *Researches in Geochemistry.* (Edited by P. Abelson) pp. 476–494, John Wiley, New York.

Marshall R. R. and Hess D. C. (1958) Lead from some stone meteorites. *J. Chem. Phys.* **28,** 1258–1259.

Merrill G. P. (1920) On chondrules and chondritic structure in meteorites. *Proc. Nat. Acad. Sci., Wash.* **6,** 449–472.

Merrill G. P. (1921) On metamorphism in meteorites. *Bull. Geol. Soc. Amer.* **32,** 395–414.

Merrill G. P. (1928) Concerning the origin of the metal in meteorites. *Proc. U.S. Nat. Mus.* **73,** art. 21.

Mueller G. (1953) The properties and theory of genesis of the carbonaceous complex within the Cold Bokevelt meteorite. *Geochim. et Cosmochim. Acta* **4,** 1–10.

Nash L. K. and Baxter G. P. (1947) The determination of the gases in meteoritic and terrestrial iron and steels. *J. Amer. Chem. Soc.* **69,** 2534–2544.

Nichiporuk W. (1958) Variations in the content of nickel, gallium, germanium, cobalt, copper and chromium in the kamacite and taenite phases of iron meteorites. *Geochim. et Cosmochim. Acta* **13,** 233–247.

Opik E. J. and Singer L. F. (1957) Reinterpretation of the uranium-helium ages of iron meteorites. *Trans. Amer. Geophys. Un.* **38,** 566–568.

Owen E. A. (1940) The structure of meteoritic iron. *Phil. Mag.* **29,** 553–567.

Owen E. A., Yates E. L. and Sully A. H. (1937) An X-ray investigation of pure iron-nickel alloys—IV. The variation of lattice-parameter with composition. *Proc. Phys. Soc., Lond.* **49,** 315–322.

Owen E. A. and Burns B. D. (1939) X-ray study of some meteoric irons. *Phil. Mag.* **28,** 497–519.

Owen E. A. and Liu Y. H. (1949) Further X-ray study of the equilibrium diagram of the iron-nickel system. *J. Iron and Steel Inst.* **163,** 132–137.

Owen E. A. and Sully A. H. (1939) The equilibrium diagram of iron-nickel alloys. *Phil. Mag.* **27,** 614–636.

Owen. E. A. and Sully A. H. (1941) On the migration of atoms in iron–nickel alloys. *Phil. Mag.* **31,** 314–338.

Patterson C. (1956) Age of meteorites and the earth. *Nuclear Processes in Geologic Settings.* pp. 157–159. N.R.C. Pub. 400, Washington D.C.

Perry S. H. (1944) The metallography of meteoric iron. *Bull. U.S. Nat. Mus.* **184,** 21.

Pinson W. H. (1954) *The Chemical Composition of Meteorites and the Shattered Planet Hypothesis.* Ann. Prog. Rept. M.I.T. Dept. of Geol. and Geophys. D.I.C. Project 7033, Part IIIe.

Pinson W. H., Ahrens L. H. and Franck M. L. (1953) The abundances of Li, Sc, Sr, Ba and Zr in chondrites and some ultramafic rocks. *Geochim. et Cosmochim. Acta* **4,** 251–260.

Poldervaart A. and Hess H. H. (1951) Pyroxenes in the crystallization of basaltic magma. *J. Geol.* **59,** 472–489.

Prior G. T. (1913) On the remarkable similarity in chemical and mineral composition of chondritic meteoritic stones. *Min. Mag.* **17,** 33–38.

Prior G. T. (1916) On the genetic relationship and classification of meteorites. *Min. Mag.* **18,** 26–44.

Prior G. T. (1918) On the Mesosiderite-Grahamite group of meteorites. *Min. Mag.* **18,** 151–172.

Prior G. T. (1920) Classification of meteorites. *Min. Mag.* **19,** 51–63.

Prior G. T. (1953) *Catalogue of Meteorites* (2nd Ed.). British Museum, London.

Reed G. W., Kigoshi K. and Turkevich A. (1960) *Geochim. et Cosmochim. Acta.* In press.

Reed G. W. and Turkevich (1957) Uranium, helium and the age of meteorites. *Nature, Lond.* **180,** 594–596.

Reynolds J. H. (1960a) Determination of the age of the elements. *Phys. Rev. Letters* **4,** 8–10.

Reynolds J. H. (1960b) Isotopic composition of primordial xenon. *Phys. Rev. Letters* **4,** 351–354.

Ringwood A. E. (1959) On the chemical evolution and densities of the planets. *Geochim. et Cosmochim. Acta* **15,** 257–283.

Ringwood A. E. (1960a) Silicon in the metal phase of enstatite chondrites. *Nature, Lond.* **186,** 465.

Ringwood A. E. (1960b) Cohenite as a pressure indicator in iron meteorites. *Geochim. et Cosmochim. Acta.* **20,** 155–158.

Ringwood A. E. (1960c) The Novo Urei meteorite. *Geochim. et Cosmochim. Acta.* **20,** 1–4.

Robertson E. C., Birch F. and MacDonald G. J. F. (1957) Experimental determination of jadeite stability relations to 25,000 bars. *Amer. J. Sci.* **255,** 115–137.

Roy S. K. and Wyant R. K. (1951) The Benld meteorite. *Geol. Ser. Field Mus. Nat. Hist., Chicago,* **7,** 145–157.

Schairer J. F. and Boyd F. R. (1956–1957) Pyroxenes. *Annual Report of the Director of the Geophysical Laboratory, Washington,* pp. 223–225.

Schumacher E. (1956) Age of meteorites by the Rb^{87}–Sr^{87} method. *Nuclear Processes in Geologic Settings,* pp. 90–96. N.R.C. Pub. 400, Washington, D.C.

Sorby H. C. (1877) On the structure and origin of meteorites. *Nature, Lond.* **15,** 495–498.

Stacey F. and Lovering J. F. (1959) Natural magnetic moments of chondritic meteorites. *Nature, Lond.* **183,** 529–530.

Tschermak G. (1875) Der Bildung der Meteoriten und der Vulcanismus. *Sitzber. Akad. Wiss. Wien* **71,** 381–392.

Tschermak and Makowsky (1878) Bericht uber den Meteoritenfall bei Trischitz in Mabren. *Denksch. Wien, Akad.* **39,** 187–202.

Uhlig H. H. (1954) Contribution of metallurgy to the origin of meteorites—I. Structure of metallic meteorites, their composition and the effect of pressure. *Geochim. et Cosmochim. Acta* **6,** 282–301.

Urey H. C. (1952) *The Planets.* Yale University Press, New Haven.

Urey H. C. (1953) Discussion. *Nuclear Processes in Geologic Settings,* p. 49. N.R.C. Pub. 400, Washington, D.C.

Urey H. C. (1956) Diamonds, meteorites and the origin of the solar system. *Astrophys. J.* **124,** 623–637.

Urey H. C. (1957a) Boundary conditions for theories of the origin of the solar system—The evidence given by meteorites. *Physics and Chemistry of the Earth.* Vol. 2, pp. 60–68. Pergamon Press, London.

Urey H. C. (1957b) Meteorites and the origin of the solar system. *Year Book of the Physical Society,* pp. 14–29. Physical Society, London.

Urey H. C. (1958) The early history of the solar system as indicated by the meteorites. *Proc. Chem. Soc.* 67–78.

Urey H. C. (1959) Primary and secondary objects. *J. Geophys. Res.* **64,** 1721–1737.

Urey H. C. and Craig H. (1953) The composition of the stone meteorites and the origin of the meteorites. *Geochim. et Cosmochim. Acta* **4,** 36–82.

Urey H. C. and Mayeda T. (1959) The metallic particles of some chondrites. *Geochim. et Cosmochim. Acta* **17,** 113–124.

Urey H. C., Mele H. and Mayeda T. (1958) Diamonds in stone meteorites. *Geochim. et Cosmochim. Acta* **13,** 1–4.

Vogel R. (1945) Description of the iron sulfide found in meteorites and known as troilite. *Chem. Erde* **15,** 371–387.

Wahl W. (1910) Beitrage zur Chemie der Meteoriten. *Z. Anorg. Chem.* **69,** 52–96.

Wahl W. (1952) The brecciated stony meteorites and meteorites containing foreign fragments. *Geochim. et Cosmochim. Acta* **2,** 91–117.

Wasserburg G. J., Fowler W. A. and Hoyle F. (1960) Duration of nucleosynthesis. *Phys. Rev. Letters* **4,** 112–114.

Wasserburg G. J. and Hayden R. J. (1955a) Age of meteorites by the A^{40}–K^{40} method. *Phys. Rev.* **97,** 86–87.

Wasserburg G. J. and Hayden R. J. (1955b) A^{40}–K^{40} dating. *Geochim. et Cosmochim. Acta* **7,** 51–60.

Wiik H. B. (1956) The chemical composition of some stony meteorites. *Geochim. et Cosmochim. Acta* **9,** 279–289.

Geochimica et Cosmochimica Acta, 1961, Vol. 24, pp. 198 to 205. Pergamon Press Ltd. Printed in Northern Ireland

A new phosphate mineral from the Springwater pallasite*

E. R. DuFresne** and S. K. Roy†

(*Received* 28 *November* 1960)

Abstract—Springwater contains substantial amounts of anhydrous magnesium phosphate, a new mineral. The phosphate is in contact with the iron and was in contact with it at the time of solidification of the meteorite. From the physical properties and chemical reactions of the two phases it can be inferred that the cooling through the freezing range was rapid.

The optical properties and physical description of the mineral are presented, together with chemical analyses and the X-ray diffraction pattern. The discussion of the analyses permits the conclusion that SiO_2, FeO and excess MgO can be contained in solid solution by the phosphate mineral.

I. Introduction

Several fragments of the Springwater meteorite, a pallasite, were found in 1931 in a field near Springwater, about 100 miles west of Saskatoon, Saskatchewan, Canada. The meteorite was described by Nininger (1932), with an analysis of the metallic portion by F. G. Hawley. The silicate portion was not analysed, perhaps because of its similarity to that of the Brenham pallasite, in which the silicate portion is olivine. But Springwater, unlike Brenham, displays what seems to be a second silicate phase which can be distinguished from olivine, despite occasional superficial resemblances, because it does not form nodules and shows a recognizable interface at the contact with the nodules of olivine. The great diversity of colour and texture of this material restricts the areas in which confusion with olivine is possible; in addition, its occurrence is confined to a single type of location. It has never been observed in the interior of the olivine nodules, but is always peripheral, nor has any olivine been observed occupying the peripheral region of the strange material. The association is apparently only mechanical: the new phase serves as a sort of mortar cementing together clumps of olivine nodules.

Figs. 1 and 2 illustrate these statements, and lead one to expect that if the strange material is a silicate, it was produced by igneous differentiation from the same melt that was the source of the olivine. This is not the case. The intruding mineral is rich in phosphorus and consists of an anhydrous magnesium phosphate, which seems to have been unobserved in nature up to the present time. If this mineral did indeed arise from the same melt as the olivine, as well it may, the melt itself must have been quite unlike terrestrial ultrabasic melts: anhydrous phosphates are extremely rare in igneous rocks of dunitic composition (Rankama and Sahama, 1950). The presence of metallic iron adds to the difficulty of accounting for this phosphate: first, there is a great difference in the densities of these substances, iron, olivine and phosphate, as well as in their melting points (see Table 1); second, the phosphate is unstable in the presence of metallic iron at temperatures near its melting point. These problems will be considered in greater detail in a later section, for while the ultimate origin of the phosphate remains a puzzle, its mere

* This work was supported in part by the U.S. Atomic Energy Commission.

** Enrico Fermi Institute for Nuclear Studies.

† Chicago Natural History Museum, Chicago, Illinois.

presence permits certain inferences about the conditions of solidification of the meteorite as a whole.

The new mineral has been named farringtonite in honour of the distinguished student of meteoritics, the late Dr. Oliver Cummings Farrington (1864–1933). Farrington, for 39 years Curator of Geology in the Field Museum (now Chicago Natural History Museum), established and built that museum's meteorite collection till it included specimens of nearly 700 falls. His numerous publications were important in the growth of interest in meteoritics.

II. Experimental

The slice of Springwater in Fig. 1 has been sampled by taking 0·1 mg portions for X-ray diffraction analysis at some dozens of recorded loci on its surfaces, the loci being chosen for their diversity and unfamiliar appearance. A large number of the films so obtained show the same new pattern, thus establishing that the new mineral varies widely in appearance: in places transparent amber and reticulated with cracks, in others, darker, ruddier, and opaque, with a rugulose texture after polishing and etching, while in still other places it becomes waxy-white and may be shot through with tiny rust-coloured veins. The common feature of all these forms is the parallel parting invariably shown by farringtonite.

Fig. 4(a) displays the powder pattern as taken in a North American Philips camera of Straumanis arrangement and 180 mm circumference, using FeK_α radiation. The more prominent lines are laid out in Table 2.

Spectrographic analyses are recorded in Table 3. The material for analysis was quarried out of the slice at various points and delivered to the analyst as two samples of roughly 25 mg each. The first sample was cut out with some care and cleaned up magnetically to remove small buttons of magnetic troilite, etc., but in spite of the precautions against chipping olivine from neighbouring nodules, this sample has a high silica content corresponding to at least 25 per cent olivine. With this experience, the second sample was treated more exhaustively, being ground and subjected to gravity-separation by centrifuging in di-iodomethane. This removed a substantial fraction of olivine as well as troilite and metal.

III. Discussion

The analysis of Sample II agrees closely with anhydrous magnesium orthophosphate, and the X-ray identification is likewise good, with a few provisos. There is a difficulty in preparing fused magnesium orthophosphate from hydrated starting material in that the substance tends to lose a high-boiling volatile (possibly H_3PO_4 or perhaps P_4O_{10}) at the white heat necessary for fusion; also, there is a side-reaction leading to pyrophosphate. Thus, three synthetic samples prepared for comparison purposes showed wide variation in average refractive index (1·55, $1{\cdot}60_5$, $1{\cdot}58_5$) as determined on polycrystalline material, the latter two samples proving subsequently to be rich in a pyrophosphate phase. But the orthophosphate phase itself shows a minor variation in diffraction pattern. The variation in pattern was first observed by Klement (1936), who was able to present evidence that the orthophosphate can contain MgO in solid solution, the limit being a composition expressible as $MgO{\cdot}3Mg_3(PO_4)_2$. With this borne in mind, the agreement between the

Table 1

	Density at room temp.	Melting range (°C)
Nickel–iron	7·8	1490–1535
Olivine	3·26–3·40	1600–1890
Magnesium orthophosphate	2·80	1180

Table 2. Prominent lines in the X-ray powder pattern of the phosphate mineral (Radiation: FeK_α unfiltered; checked against filtered CuK_α)

*I**	*d*	*I*	*d*	*I*	*d*
mw	4·30	mw	2·48	mw	1·532
mw+	4·04	ms (3)	2·39	w, d	1·345
vs, d (1)	3·83	w, d	2·32	w, d	1·323
w	3·62	m	2·11	mw	1·247
w	3·45	w	2·05	m	1·074
vs (2)	3·41	w	2·03	m	1·071
m, d	2·77	w	1·770	m, d	1·013
w, d	2·64	w	1·715	m	1·002
mw	2·51	mw	1·687	m	0·984
				w, d	0·980

* Intensities are as estimated visually, and expressed in the following symbols: w = weak, mw = weak to medium, m = medium, s = strong, vs = very strong, d = diffuse. The three strongest lines are given rank numbers, 1 for the strongest and so on.

Table 3. Spectrographic analyses of phosphate mineral with comparison data

Constituent	Sample		Synthetic (hydrate)	Theoretical $Mg_3(PO_4)_2$
	I	II		
P_2O_5	37·6 ± 0·6†	49·7 ± 1·0	34·8 ± 1·1	54·0
MgO	49·2 ± 0·2	41·6 ± 1·3	32·9 ± 0·9	46·0
SiO_2	11·1 ± 0·2	2·9 ± 0·1	Trace	
Fe^0*	5·4 ± 0·1	3·7 ± 0·2	Trace	
No. of Replicates‡	4	5	2	
Base/acid ratio§	1·13	0·96	1·11	1·00
Base/acid ratio ("olivine" subtracted)	1·19	0·95		

* It is to be understood that this conventional form of reporting analyses makes no commitment whatever concerning the actual valence state of an element within the mineral itself.

† Standard deviations of the individual data, not standard errors.

‡ Number of spectra taken on the same sample.

§ Ratio of equivalents of acid and base present, calculated on the basis of Fe^0 or FeO = 2. Ratio corrected for "olivine" made by subtracting SiO_2 from the sum of the bases and dividing by P_2O_5.

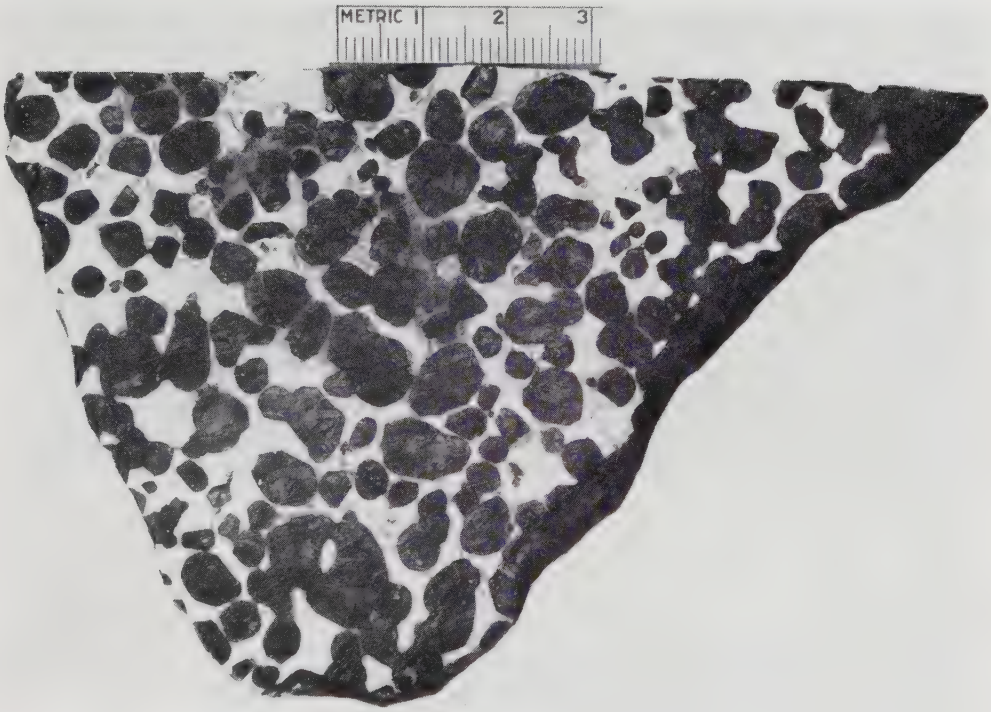

Fig. 1. Polished slab of Springwater from which specimens were taken. At least three phosphate areas are quite prominent, the largest (shown magnified in Fig. 2a) being below the "1" on the metric scale and 2 or 3 cm from it. The contrast in shade between the phosphate and the neighbouring olivine nodules is quite clear. Small areas at the borders of other olivine nodules may be seen, but not all of these are phosphate, some are troilite.

A rough measurement of this slab shows phosphate = 2·4 per cent, schreibersite = 0·8 per cent (by area). This cannot be regarded as typical, but rather should be thought of as an estimate on a rather rich sample.

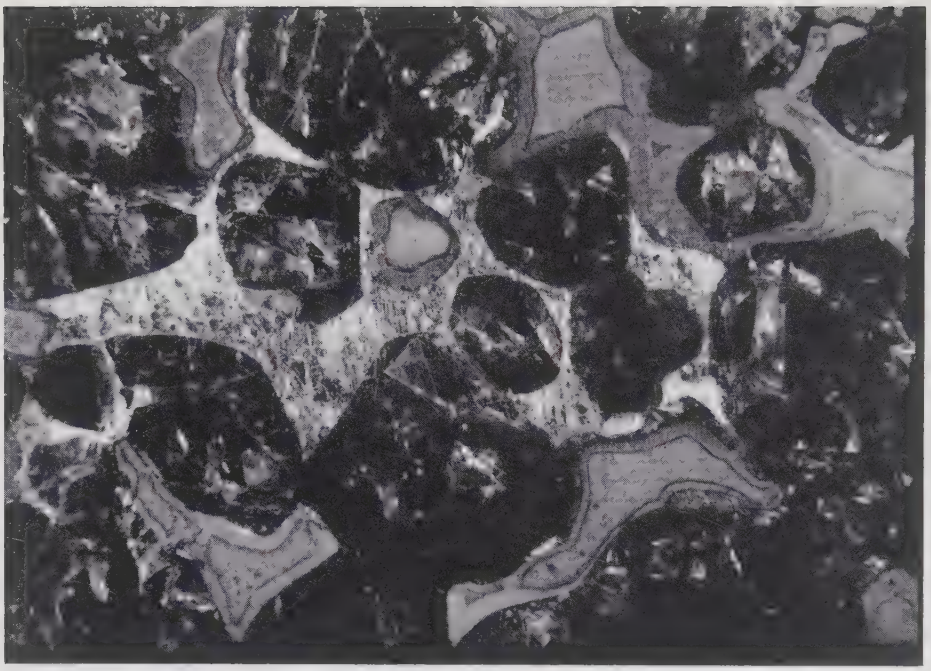

Fig. 2(a). A closer look at the largest phosphate area. The farringtonite owes its straw-like appearance to its parallel parting. Both types of iron are shown in grey, the olivine dark. ×6 (approx.).

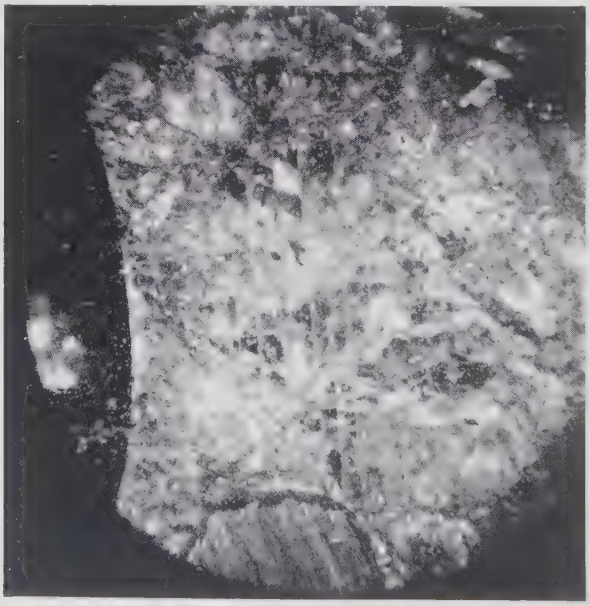

Fig. 2(b). Farringtonite from another slab. ×45 (approx.).

pattern of Table 2, the patterns of the synthetics, and the patterns published by KLEMENT is seen to be quite good. (The pattern of the synthetic of index 1·55 is shown in Fig. 4(b)). Confirmation is provided by the fact that there is no match between the farringtonite pattern and those of the hydrated magnesium phosphates, pyrophosphates, or other likely choices.

In addition, farringtonite is virtually insoluble in water, is attacked only slowly by the dilute nitric acid used to etch the metal phase, and gives a positive reaction in the molybdate test for orthophosphate. The suite of optical properties, density, etc., which characterize the mineral are set forth in Table 4.

Table 4. Optical properties and other characteristics

$Mg_3(PO_4)_2$	$n_\alpha = 1{\cdot}540 \pm 0{\cdot}002$ $n_\beta = 1{\cdot}544 \pm 0{\cdot}002$ $n_\gamma = 1{\cdot}559 \pm 0{\cdot}002$ $2V = 54$–55; opt. (+) Optic plane parallel with 010. Colour: colourless to pale yellow. Form: subhedral to euhedral Cleavage: fair to good (100) and (010). Relief: $n >$ balsam. Birefringence low: 0·010–0·014. Extinction: $Z_X C = 16$–$17°$ in β obtuse Density: approximately 2·80. Distinguishing features: parallel partings along 100. Occurrence: found associated with olivine. One possible independent nodule of farringtonite observed.	Monoclinic

The silica and iron reported in the analyses deserve some comment. The technique of preparing the samples was such that the final content of metallic iron was quite negligible: the iron thus must be present in the 2+ or 3+ state or both. Magnetite (which occurs in association with goethite in deep cracks, and is evidently a weathering product) would have been removed with the metal. The possibility of rust contamination exists, but is unlikely in Sample II. During the gravity separation leading to the production of this sample, two phosphate fractions were obtained, both with the same X-ray pattern. The heavier fraction was homogeneous in density and microscopic appearance, while the lighter fraction varied considerably in density from particle to particle, many of which particles were seen at high magnification to be encrusted with dark, cryptocrystalline material. Only the heavy, uniform material was retained for analysis. Since the Fe^{2+} ion occurs in many minerals as a replacement for Mg^{2+}, such substitution in solid solution must account for most of the reported iron.

Unfortunately the chemistry of this mineral is such that it is not possible to discuss the impurities without considering the stoichiometry of the substance as well as the accuracy of the analytical method. The standard deviations in Table 3 show the within-sample reproducibility of the analytical method to be remarkably good, while the agreement between samples is rather bad, and actually is worsened by allowing for the possible contamination by olivine. Since the whole of each sample

was fused with Li_2CO_3 and internal standard, etc., at the same time, the standard deviations found do not theoretically represent all the possible sources of error, but only those consequent to burning. As a check on the possibility that a strong component of error was introduced in the weighing-out and fusion steps, an analysed sample was run through the process at the same time as the unknowns. This was U.S. Bureau of Standards Sample 56-B (Phosphate Rock), with a published analysis giving $P_2O_5 = 31{\cdot}5$ per cent, $SiO_2 = 10{\cdot}1$ per cent. The check analyses gave $P_2O_5 = 31{\cdot}0 \pm 0{\cdot}71$, and $SiO_2 = 9{\cdot}85 \pm 0{\cdot}07$, with two replicates; this is rather better than consideration of Table 3 would lead one to expect. From Klement's results alone the base/acid ratio should be confined between the limits of 1·00 for pure orthophosphate and 1·11 for the MgO-rich end of the solid-solution range. Both farringtonite samples lie outside these limits and the synthetic, hydrated sample shows a ratio of 1·11 instead of the expected 1·00. Further, the farringtonite samples deviate from the expected range in opposite directions, so that a simple, directed error is ruled out. Without a lengthy study of the analytical method combined with further analyses of the mineral, it is impossible to be certain whether these deviations represent errors or real variations in composition.

There is good evidence that the system contains an extra degree of freedom, in that some silica may be held in solid solution also, as opposed to entrained olivine. Sample II, with its special purification, may be entirely free from olivine. Microscopic search at magnifications up to 500 diameters has failed to reveal olivine intergrown or occluded with the phosphate. Unless the olivine as such exists as a very fine precipitate, it is not present at all. If all the silica in Sample II is recalculated as wt.% of olivine, the figure obtained is between 6·5 and 9·5. To check the ability of X-ray diffraction to detect this amount, an artifical mechanical mixture was prepared, containing 6 per cent forsterite and the remainder being fused synthetic phosphate: this gave an X-ray pattern with a good many overlaps, but the principal lines of forsterite were visible, though not particularly clear. Conceivably, conditions might exist such that as much as 10 per cent olivine might be missed, and 3 per cent is unlikely to be seen except under favourable conditions.

Since even microscopic examination of farringtonite thin sections fails to reveal any traces of occluded olivine, any secondary olivine present must exist as a submicroscopic precipitate if the silica is not taken up in solid solution. Such a precipitate would have a fixed (but unknown) crystallographic relationship with the parent farringtonite. A diffraction film made of a farringtonite single crystal containing such a precipitate should therefore display additional spots corresponding to the oriented olivine. The number of discrete olivine orientations would not only be finite, but small; no more than six. Indeed, since farringtonite is monoclinic, it is likely that the number is less; thus the multitude of small precipitated crystals should behave like a few larger ones. By preparing the film in the same camera, with the same radiation, as powder films of olivine and synthetic magnesium phosphate, it becomes possible to distinguish between spot sets for spacings that are sufficiently separated by using film overlay or blink techniques: this method provides a much better image-to-background ratio and separates the spots of one mineral from those of the other in a second dimension, i.e. while adjacent lines may overlap, the spots will not, in general, do so. An advantage of employing the

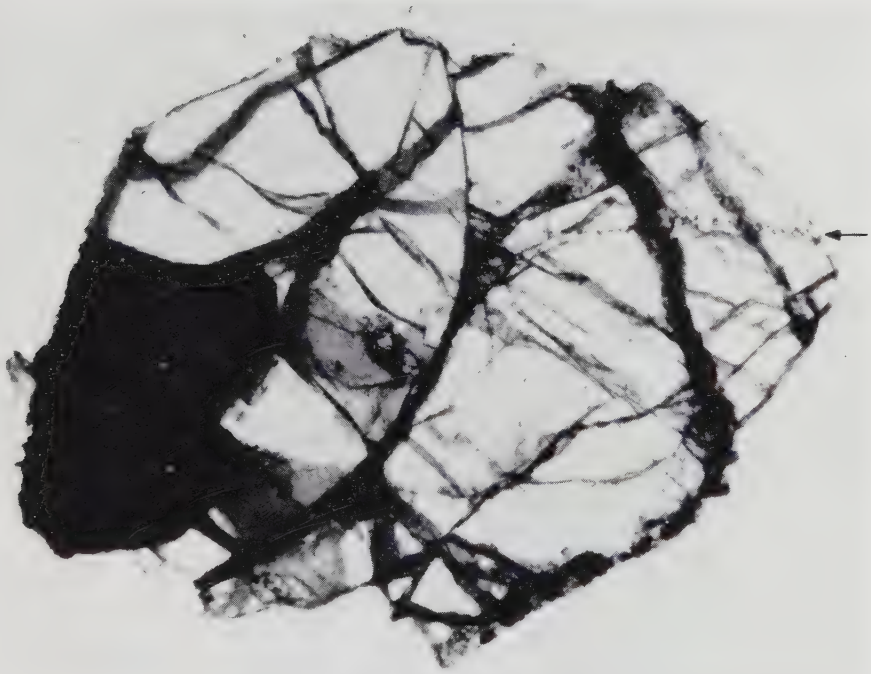

Fig. 3. Thin section at 44 diameters magnification. Black zone is metal, convex grey area olivine, the farringtonite recognizable by its partings. Arrow indicates the line of blobs mentioned in the text; another line of blobs, very short, is also to be found. Note that some of the partings cut right across the line of blobs without change of course.

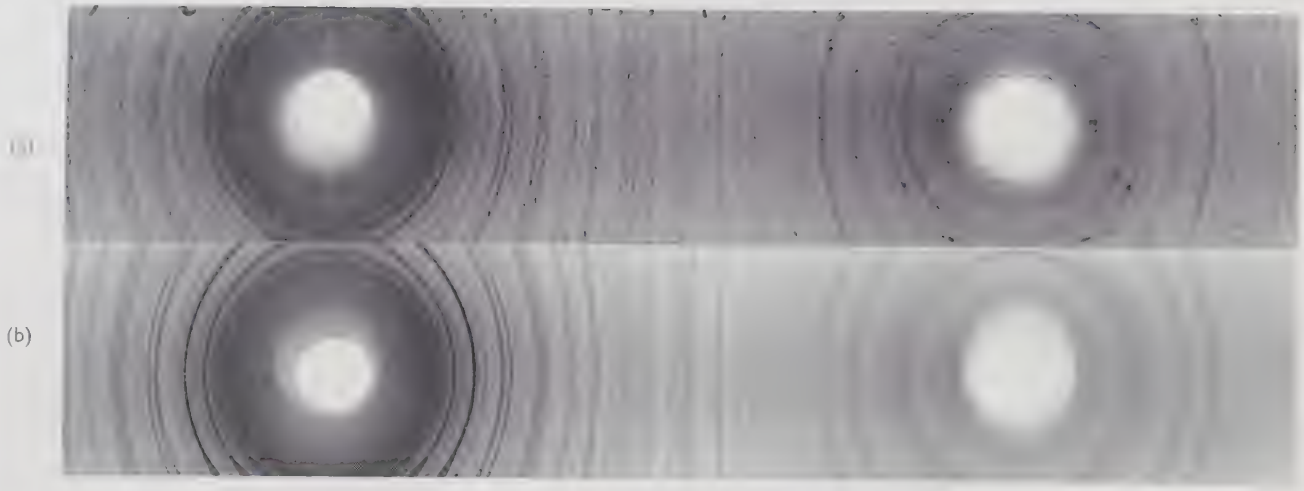

Fig. 4(a). Diffraction film of farringtonite.

Fig. 4(b). Film of synthetic magnesium phosphate (impure). FeK_α radiation.

method in this way is that our ignorance regarding the exact crystallographic relation postulated between farringtonite and olivine is of no importance. Further, the orientation of the farringtonite single crystal is of no importance. And lastly, should the basic assumption of a *fixed* relationship be incorrect, our mistake will make itself known in the form of a faint line-pattern of olivine appearing with the spot-pattern of farringtonite.

The experiment was performed as described, with rotation of the specimen, and no spots that could be uniquely ascribed to olivine were found. The case of the 1·748 Å spacing of olivine was particularly convincing. This reflection does not overlap with any of those of farringtonite, and it is rather intense (60 per cent of the most intense line for pure forsterite with CuK_α radiation; Swanson and Tatge (1953). The planes with this spacing are a 222 set in an orthorhombic crystal, and because of this multiple degeneracy should give rise to spots on the film regardless of the orientation of the olivine (more than forty experiments with submicrogram olivine single crystals substantiate these deductions). It is difficult to estimate the increase in sensitivity provided by this method, but a conservative minimum would be a factor of 10.

We may thus conclude that most or all of the silica in the analysis of Sample II is held in solid solution. A replacement of PO_4 tetrahedra by SiO_4 tetrahedra seems reasonable as the reverse is known to take place (Rankama and Sahama, 1950).

IV. Boundary Conditions for the Solidification of the Meteorite

Both the morphology of the meteorite and the knowledge of the melting ranges involved make it clear that the iron and the phosphate must both have been liquid at a time and temperature at which the olivine was already solid (see Table 1). Considering firstly only the difference in density between the iron and the other phases, it seems rather odd that the buoyant olivine nodules did not rise in the liquid iron to form a close-packed aggregate at the "top" of the body of liquid iron (Fish *et al.*, 1960a). It may be argued that the structures shown in Figs. 1 and 2 need not be close-packed if they originated in a quiescent pool of iron; that the olivine nodules may have risen gently to form a mechanically metastable network of spheres in contact which would have collapsed to the stable close-packed array if subjected to shock or vibration. This argument is not inconsistent with the arrangement of olivine in Figs. 1 and 2, perhaps, but neglects the liquid phosphate present with the iron melt. Considering the buoyancy of the phosphate, it is strange that the two liquids did not separate: even if the gravitational field was very low, the time-scale for cooling through the freezing interval must have been very short, i.e. on the order of a few days (Fish *et al.*, 1960b). Wetting of the olivine by the phosphate liquid would delay, but not prevent, upward motion of the phosphate.

This line of attack on the problem of the time-scale may be coupled with the information gained from artificial samples. When magnesium phosphate is melted in a thick-walled iron crucible, it is rapidly destroyed by reduction with the iron. This reaction results in the formation of appreciable amounts of the Fe–Fe_3P eutectic in less than a quarter of an hour, even though it is competing with the evaporation of the phosphate and other reactions. The reduction takes place even in the presence of air. Far from possessing a convenient oxidizing agent to reverse

the reduction, the meteorite itself evidently contains free carbon as graphite (visible as oriented leaves and lenses in some of the troilite zones). The general impression gained from these exploratory experiments is that the meteoritic phosphate cannot have been molten in the presence of the iron for times of the order of a day without being wholly reduced to schreibersite.

Added to this there seems to be some evidence for turbulent motion during the solidification of the meteorite. Fig. 3 shows a line of small blobs extending across what is now a single crystal of phosphate. These blobs are presumably troilite, since similar blobs, dug from the phosphate-olivine interface, are found to be troilite on X-ray diffraction analysis. The interfacial troilite could perhaps be accounted for by some injection or exsolution process taking place after the solidification of the phosphate, but these processes will not explain the line in single-crystal material.*

In sum, the evidence seems very difficult to reconcile with the often-presented picture of the pallasite as a sample of a quiescent boundary layer between the massive core and the mantle of a slowly cooling planetary object (Lovering, 1957). Everything points the other way, to suggest that substances from at least two separate and wholly distinct environments were brought together, agitated and mixed, and then cooled rapidly before they could react completely with one another. This is at least not inconsistent with the view of Fish *et al.* (1960a) that the pallasites were formed in some violent mixing process immediately preceding the freezing of the core of an asteroidal object, possibly in a caldera collapse caused by the contraction of the core. Of course, schemes alternative to caldera collapse are suggested, such as some sort of volcanic activity. But it nevertheless seems that ideas involving a deep-seated environment within a planet (properly so called) must be ruled out because of the requirement that cooling be rapid. For, unless all our notions about the temperature distribution within a planet are incorrect, the materials of Springwater would have had to travel hundreds of kilometres from the core boundary to a zone cooler than the freezing interval in the space of a day or so: a hypothetical scheme that is nearly impossible to defend.

Yet, apart from the presence of farringtonite, Springwater does not seem to be qualitatively different from other pallasites, and indeed has passed muster among them for some years. The origins of the various pallasites thus need not be different in kind, although they may be different in locality.

V. Conclusions

Farringtonite is best characterized as a series of solid solutions into which FeO and SiO_2 can enter, as well as an excess of MgO, the basis compound being $Mg_3(PO_4)_2$.

* Apart from the troilite mentioned above, which exists both as small blobs and as more extensive regions, the zones with a metallic appearance may be summarized as follows (see Fig. 1): (a) Peripheral kamacite and acicular kamacite (shown quite white in Fig. 1). (b) Grey areas, which diffraction reveals to be principally alpha-phase with a much smaller amount of retained γ-phase, to which the catchall name of "plessite" might be applied. (c) Hackly areas of schreibersite, visible particularly near the lower bight of the slab. (d) Pocket-lining and vein material, such as that shown next the 1·7 cm mark on the scale, where an olivine nodule has fallen out of its pocket. This last material consists of oxides, chiefly magnetite and goethite, and must be a product of weathering. Another variety of goethite has been found veining the schreibersite, while rust veins have been seen in the phosphate areas near the crust of the meteorite.

Farringtonite, like the artificial compound, should be unstable to reduction of phosphorus in the presence of metallic iron in the range of temperature near its melting point. From its continued existence it is thus possible to conclude that the freezing of the Springwater pallasite was rapid.

Acknowledgements—We wish to thank Dr. Ann DuFresne, then of the Department of Geology, University of Chicago, for providing the spectrographic analyses; Mrs. Betty Nielson for some of the photographic work, and Dr. Bertram Woodland of the Chicago Natural History Museum for assistance in the petrographic analysis. Our thanks also to Dr. Edward Anders, of the Enrico Fermi Institute for Nuclear Studies, who originally pointed out that there was an extra "silicate" phase in Springwater, and whose criticisms and encouragement furthered the work substantially.

One of us (E. R. D.) wishes to thank the National Science Foundation and the United States Rubber Company for fellowships during a part of the period when this and related work was being done.

References

Fish R. A., Goles G. G. and Anders E. (1960a) The record in the meteorites—III. On the development of meteorites in asteroidal bodies. Preprint EFINS 59–43, Enrico Fermi Institute for Nuclear Studies.

Fish R. A., Goles G. G. and Anders E. (1960b) The record in the meteorites—III. On the development of meteorites in asteroidal bodies. *Astrophys. J.* **132**, 243–58.

Klement R. (1936) Basische Phosphate zweiwertiger Metalle. *Z. anorg. Chem.* **228**, 232–9.

Lovering J. F. (1957) Pressures and temperatures within a typical parent meteorite body. *Geochim. et Cosmochim. Acta* **12**, 253–61.

Nininger H. H. (1932) The Springwater Meteorite. *Amer. Min.* **17**, 396–400.

Rankama K. and Sahama T. G. (1950) *Geochemistry.* University of Chicago Press.

Swanson H. E. and Tatge E. (1953) Standard x-ray diffraction powder patterns. *Nat. Bur. Stand.*, Circular 539.

Geochimica et Cosmochimica Acta, 1961, Vol. 24, pp. 206 to 225. Pergamon Press Ltd. Printed in Northern Ireland

The solution of some minor element oxides by decomposing plant materials

Ng Siew Kee* and C. Bloomfield
Rothamsted Experimental Station

(*Received* 11 *November* 1960)

Abstract—Oxides of several trace elements are dissolved by the action of anaerobically fermenting plant material and, less effectively, by sterile aqueous extracts of undecomposed plant material. The dissolved metals seem to be in complex form and in true solution, not colloidally dispersed. The solutions are stable to atmospheric oxidation, but in the presence of ferrous iron aeration causes coprecipitation of the trace elements with ferric oxide. The order of ease of coprecipitation appears to be Mo, V > Zn > Cu > Co > Ni. Sorption on ferric oxide is appreciable under certain conditions. Copper and nickel are irreversibly sorbed from fermentation solutions by plant fibres.

Laboratory studies on waterlogged soils have established that iron, manganese and phosphate are readily mobilized by the action of anaerobically decomposing plant residues (Bloomfield, 1951; Bétrémieux, 1951; Gasser and Bloomfield, 1955). In recent years it has become apparent that the extractability of a number of minor elements is increased when a soil is flooded. Thus Mitchell (1955) found that in a gleyed soil the concentrations of extractable Co, Ni, Fe, V, Cu and Mn were from ten to twenty times as great as in a corresponding well-drained soil. In soils of a hydromorphic series, Walsh *et al.* (1956) found a higher cobalt content in the surface layer of the freely drained member than in the wettest member of the series, although the acetic acid-soluble cobalt was highest in the poorly drained soil.

The present study was made to investigate the effect of anaerobically decomposing plant material on a number of minor element oxides, and to obtain some information about the nature and properties of the reaction products.

Materials and Methods

Two plant materials were used: cocksfoot (*Dactylis glomerata*) and lucerne (*Medicago sativa*). The lucerne was collected in mid-summer, the cocksfoot in late autumn. After washing, the plant material was dried at 105° C and ground in a stainless steel mill.

The following metal oxides were used: CuO, ZnO, CoO-Co_2O_3, NiO, MnO_2, PbO_2, Cr_2O_3, TiO_2 and Ga_2O_3. $CaMoO_4$ and molybdenum and vanadium hydrous ferric oxide coprecipitates were also studied, the oxides of these elements being too soluble in water to permit their use in these experiments.

The CuO was prepared by precipitation from copper sulphate solution with sodium hydroxide. After boiling, the precipitate was filtered and washed successively with hot water, alcohol, and benzene, dried at 105°C and ground to a fine powder. X-ray analysis established its composition as CuO.

The hydroxides of cobalt and nickel were precipitated from aqueous solutions

* Present address: Division of Soils, Department of Agriculture, Kuala Lumpur, Federation of Malaya.

of their salts with sodium hydroxide and washed and dried in the same way as the CuO. After air-drying the two preparations were heated at 250°C for 3 hr. The nickel preparation proved to be rather refractory, and consequently a second batch was prepared, the drying being limited to heating at 105°C after the alcohol and benzene treatments. X-ray examinations showed that the cobalt oxide was a mixture of CoO and Co_2O_3, and that the first nickel preparation consisted of NiO containing a small amount of $Ni(OH)_2$. The second preparation consisted entirely of $Ni(OH)_2$.

Cr_2O_3 was prepared by boiling a solution of chromic sulphate to which sodium hydroxide was added. Washing and drying were as with cobalt. The green product consisted of Cr_2O_3 containing some water of hydration.

Calcium molybdate was precipitated by the addition of a solution of calcium chloride to a solution of ammonium molybdate. The precipitate was washed as before and dried at 105°C. X-ray analysis showed its composition to be $CaMoO_4$.

Molybdenum and vanadium ferric oxide coprecipitates were prepared by the addition of ammonia solution to solutions of ferric chloride containing 10 per cent of Mo or V relative to the equivalent Fe_2O_3 contents. The preparations were washed with water to remove soluble Mo and V compounds and then washed with alcohol and benzene and finally dried at 105° C. The preparations contained approximately 1 and 2 per cent V and Mo respectively.

The other compounds were laboratory supplies.

Fermentation experiments were done as described by Bloomfield (1950). The reaction mixtures consisted of 5 g of the dry plant material, 0·1 g of the oxide and 200 ml of distilled water: a few drops of a soil suspension were added as inoculant to each. With sterile plant extracts the reaction mixture consisted of 200 ml of an aqueous extract of 5 g of the plant material and 0·1 g of the oxide, with 1–2 ml of toluene. In both cases the reaction vessels were flushed with nitrogen to remove oxygen, and incubated at 27°C. The use of toluene to prevent microbial growth was adopted after a number of other compounds had been investigated. Chloroform was rejected as it caused a fall of 1·2 units in the pH of the mixture after a few days incubation—presumably the result of the formation of hydrochloric acid. Although not ideal for the purpose, toluene has been used successfully in experiments of this type for some years: in long-term experiments the toluene may be completely removed by repeated flushing with nitrogen, and microbial action is then apparent within 24 hr or so. As this is invariably accompanied by a very rapid rise in the concentration of dissolved material, there is no difficulty in detecting the disappearance of sterility. Enzymes would have been inactivated during the original drying of the plant material at 105°C.

Samples were expelled from the flasks by a stream of nitrogen and centrifuged; aliquots of the solutions were evaporated with redistilled nitric acid and then heated to fuming with a few drops of a 1:1 mixture of sulphuric and perchloric acids. Manganese and lead residues were redissolved in nitric acid, hydrochloric acid being used in all other cases.

Blank determinations on water/oxide, and water/plant material mixtures were made under the same conditions; allowance for these values has been made in the results reported below.

Copper was determined colorimetrically with bis-cyclohexanoneoxalyldihydrazone (Williams and Morgan, 1954), zinc with Zincon (Rush and Yoe, 1954), cobalt with 2-nitroso-1-naphthol-4-sulphonic acid (Wise and Brandt, 1954), nickel with dimethylglyoxime (Forster, 1953), manganese by periodate oxidation, iron with 2:2′-dipyridyl (Piper, 1950), and lead with dithizone (Holmes, 1945). Gallium, titanium, molybdenum and chromium were determined spectro-chemically, employing the concentration procedure of Mitchell (1948), with palladium as the internal standard.

In the experiments on the molybdenum– and vanadium–ferric oxide preparations, molybdenum was determined with dithiol (Williams, 1955). Vanadium was determined spectrographically; the sample was evaporated on to spectrographically pure alumina which was arced after ignition at 450° C.

Results

Gallium, titanium, molybdenum and chromium

No gallium was detected in the lucerne fermentation solution, but trace amounts were mobilized by fermenting cocksfoot. However, as there is some doubt as to the completeness of precipitation of gallium in the concentrating process employed (Mitchell, 1948), slightly more may have been mobilized than shown in Table 1.

Calcium molybdate did not appear to be affected by either fermenting cocksfoot or lucerne: with either, over a period of 22 days, the dissolved molybdenum did not vary significantly from the very small zero time values.

Table 1. Solution of Ga_2O_3, TiO_2, Cr_2O_3 and $CaMoO_4$ by fermenting lucerne and cocksfoot (mg/l.)

Days	Lucerne				Cocksfoot			
	Ga	Ti	Cr	Mo	Ga	Ti	Cr	Mo
0	Not detected	0·34	0·54	0·36	Not detected	0·50	0·74	0·18
22	Not detected	0·44	0·74	0·34	Trace	0·86	0·80	0·20

Slight mobilization of titanium and chromium was observed in fermentation experiments (Table 1).

Zinc

Fig. 1 shows the behaviour of zinc in fermentation and sterile experiments. More zinc was mobilized during fermentation, and there was little difference between the final concentrations obtained with lucerne or cocksfoot, although the latter caused a quicker initial rise in the concentration of dissolved zinc.

The sterile extracts caused appreciable solution, lucerne being the more effective of the species.

Manganese

Bétrémieux (1951) showed that manganese is readily mobilized by the fermentation of various forms of organic matter. Similar results, summarized in Table 2, were obtained in our work.

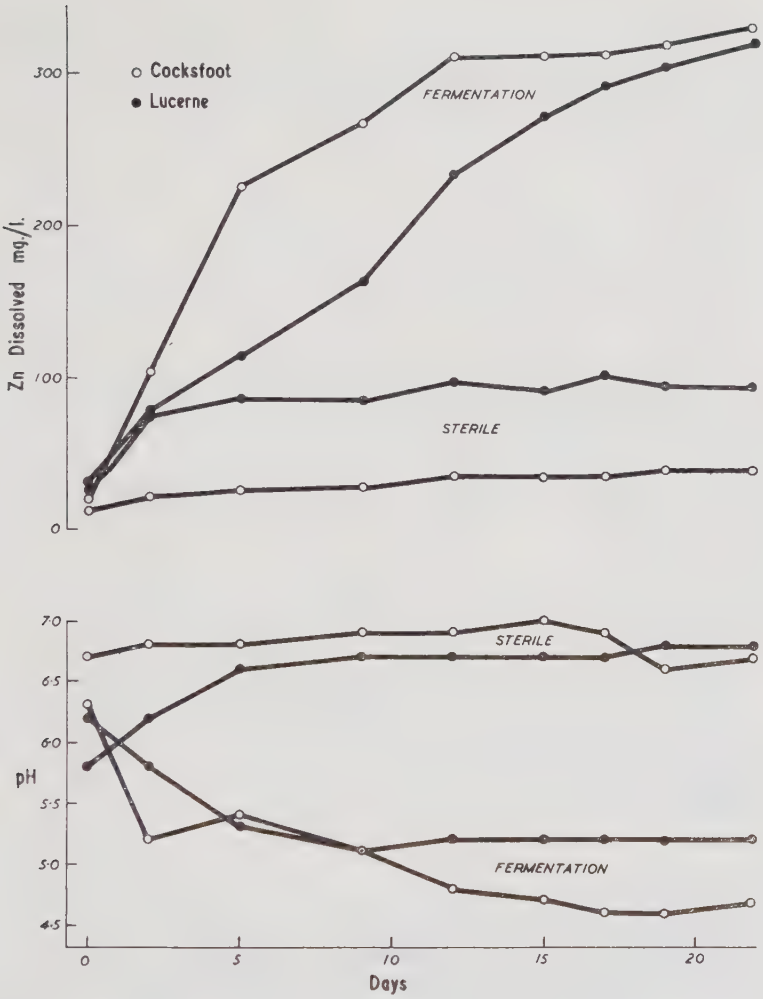

Fig. 1. Solution of ZnO by fermenting and sterile lucerne and cocksfoot.

Table 2. Solution of MnO_2 by fermenting and sterile lucerne and cocksfoot

Days	Fermentation				Sterile			
	Lucerne		Cocksfoot		Lucerne		Cocksfoot	
	mg Mn/l.	pH	mg Mn/l.	pH	mg Mn/l.	pH	mg Mn/l.	pH
0	10	5·6	5·4	6·6	2·4	5·6	7·0	6·4
22	248	5·3	230	4·5	74·4	6·6	45	6·8

Lead

Appreciable amounts of lead were dissolved (Fig. 2). Despite the much lower pH that developed during the fermentation, lucerne was equally effective under sterile and non-sterile conditions. Under sterile conditions, the pH of the cocksfoot system remained at about 6, although the concentration of lead rose to nearly 35 mg/l. in 9 days.

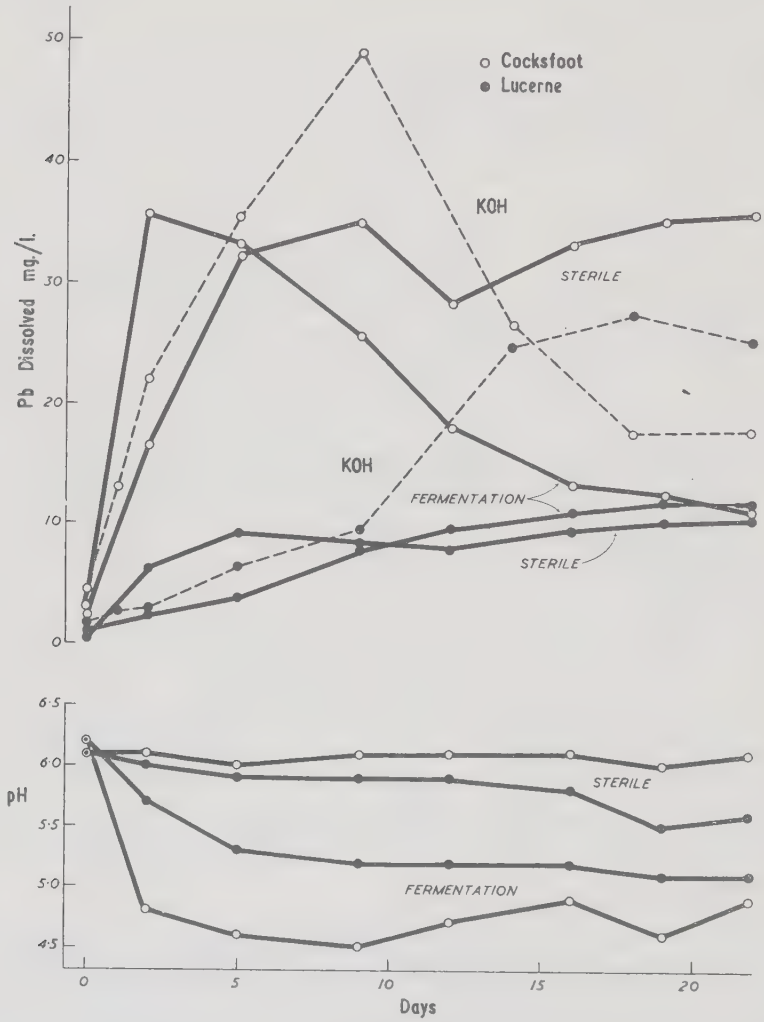

Fig. 2. Solution of PbO_2 by fermenting and sterile lucerne and cocksfoot.

Fermenting cocksfoot gave a rapid initial solution of lead, reaching its maximum by the second day. The pH of the mixture fell from 6·2 to 4·8 during this initial period, and then remained fairly constant, although the concentration of lead decreased to a final value very close to the lucerne values. This decrease could have been caused by the precipitation of lead carbonate by carbon dioxide formed during

the fermentation. The absence of such a decrease in the sterile cocksfoot curve lends support to this suggestion. Fig. 2 shows the effect of limiting the accumulation of carbon dioxide by including tubes containing potassium hydroxide in the reaction vessels. In both cases greater amounts of lead were dissolved, and although the decrease still occurred, in the cocksfoot fermentation its onset was retarded from 2 to 9 days. Comparison of the two lucerne fermentation curves shows that ultimately more lead was dissolved in the presence of potassium hydroxide. It seems therefore, that for both lucerne and cocksfoot fermentation, the presence of carbon dioxide limits the solution of lead, and that the lucerne fermentation and sterile curves are so alike because the net result of solution and reprecipitation of lead in the formentation approximated to the amount of lead dissolved by the sterile extract.

The cocksfoot– and lucerne–lead solutions obtained in the last experiment were saturated with carbon dioxide, after treatment with toluene to inhibit microbial growth. In 3 days the lead content of the lucerne solution fell from 24·8 to 12·6 mg/l., and that of the cocksfoot solution from 17·5 to 16·8 mg/l. Presumably the cocksfoot solution had already lost most of the lead that was precipitatable by carbon dioxide.

Table 3. Solution of CoO–Co_2O_3 by fermenting and sterile lucerne and cocksfoot

Days	Fermentation				Sterile			
	Lucerne		Cocksfoot		Lucerne		Cocksfoot	
	mg Co/l.	pH	mg Co/l.	pH	mg Co/l.	pH	mg Co/l.	pH
0	1·0	5·6	0·8	5·9	0·0	5·5	0·6	6·3
22	30·2	5·0	52·6	4·7	15·4	5·6	13·2	6·4

It is possible that inorganic phosphate derived from the plant material, by precipitating lead phosphate, may have limited the net solution of lead in these experiments. Appreciable amounts of soluble phosphorus compounds are liberated from anaerobically fermenting grass (Gasser and Bloomfield, 1955), but it is not known what proportion of the soluble phosphorus is in the form of inorganic phosphate; it is therefore not possible to assess the importance of this factor. As the amount of phosphorus liberated does not increase greatly during fermentation, it is unlikely that the sharp decrease observed in the cocksfoot fermentation curve is related to this aspect of the fermentation process.

It is also possible that lead may have been immobilized by sulphate present in the plant materials, but in this case, under the reducing conditions of the fermentation, precipitation of sulphide rather than sulphate would probably result.

Cobalt

In fermentation experiments cocksfoot was considerably more active than lucerne, although under sterile conditions there was little difference between the two (Table 3).

Nickel

The nickel oxide used was very much more refractory than the cobalt preparation. In later work a sample of nickel hydroxide which had been dried at 105°C gave a final concentration of 216 mg Ni/l. in a lucerne fermentation. The ease of solution thus depends on the history of the metal oxide; this has previously been observed with ferric oxides, and no doubt is also true for such elements as gallium and aluminium.

More nickel was dissolved by the sterile extracts, although lower pH values developed in the fermenting mixtures (Table 4).

Table 4. Solution of NiO by fermenting and sterile lucerne and cocksfoot

Days	Fermentation				Sterile			
	Lucerne		Cocksfoot		Lucerne		Cocksfoot	
	mg Ni/l.	pH	mg Ni/l.	pH	mg Ni/l.	pH	mg Ni/l.	pH
0	1·9	5·7	1·6	6·0	1·2	5·5	1·6	6·4
22	4·3	5·2	3·7	4·9	5·4	5·2	4·7	6·8

Copper

Much copper dissolved in both the fermentation and sterile experiments (Fig. 3) and, as with nickel, both species dissolved more copper under sterile than under non-sterile conditions, although with copper the difference was much greater. This behaviour cannot be attributed to an intrinsic characteristic of either the sterile or non-sterile systems, because fermentation in the latter ceased after about 2 days. Presumably microbial action was only possible in the early stages, before the concentration of dissolved copper reached a toxic level. The fundamental difference between the two systems is that in the fermentation the whole plant material was present, whereas the sterile system contained only the water-soluble constituents. The fibrous grass material became vivid green during the course of the fermentation, so it seemed probable that fermentation was apparently less active because dissolved copper was sorbed on the fibrous plant material. It has been shown that both copper and nickel are irreversibly sorbed from fermentation solutions by plant fibre, which explains the inversion of the usual order of effectiveness of the two processes. This subject is being studied in more detail, and will be reported later.

The effect of the presence of excess ferric oxide on the mobilization of minor elements

Ferric oxide is readily mobilized by the action of anaerobically fermenting plant material (Bloomfield, 1951). As a normal soil contains so much more ferric oxide than minor elements, mobilization of the latter might be limited by competition with excess ferric oxide.

To investigate this possibility lucerne fermentations were done in the presence of both hydrous ferric oxide and the minor element oxides; ferric oxide/minor element ratios of 1:1 and 50:1 were studied. Before determining the trace metals,

iron was removed from the digests by extraction with isopropyl ether (Dodson *et al.*, 1936). Table 5 shows that except for nickel, solution of the minor elements was depressed by ferric oxide, although significant amounts of the elements were dissolved under the least favourable conditions. A more easily soluble nickel oxide sample would probably have behaved similarly to the other elements.

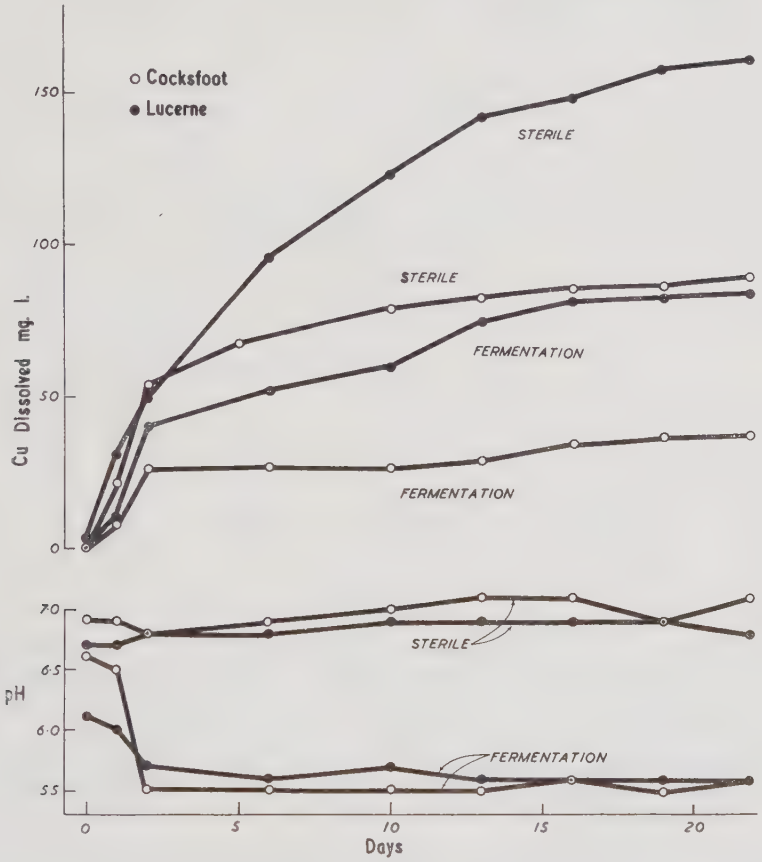

Fig. 3. Solution of CuO by fermenting and sterile lucerne and cocksfoot.

Manganese dioxide is clearly more readily attacked than ferric oxide; under comparable conditions the difference in reactivity between ferric oxide and manganese dioxide would probably be even greater than these figures indicate, because the manganese dioxide used was a commercial sample, whereas the ferric oxide was a laboratory preparation of relatively great reactivity.

Table 5 shows that the amount of iron dissolved in fermentation experiments is very largely influenced by the amount of ferric oxide present initially. This characteristic of these systems, together with the extent to which the reactivity of the metal oxides may be modified by ageing, shows that the assessment of relative reactivities of different elements from such experiments as these is not a straightforward matter.

Solution of molybdenum and vanadium

Because of the solubility of their oxides, the behaviour of molybdenum and vanadium was investigated using hydrous ferric oxide, precipitated in the presence of molybdate or vanadate, as the source of these elements.

Figs. 4 and 5 illustrate the results obtained when 5 g of lucerne was fermented anaerobically, in 200 ml of water, in the presence of 1 g of the ferric oxide coprecipitates.

Molybdenum was mobilized with iron, but the molybdenum concentration did not increase appreciably until after the sixth day; from this point the molybdenum

Table 5. Solution of mixtures of minor element and ferric oxides by fermenting lucerne (mg/l. dissolved in 22 days)

Element	Fe_2O_3: minor element oxide			
	1:1 (0·1 g:0·1 g)		50:1 (2·5 g:0·05 g)	
	Fe	Minor element	Fe	Minor element
Cu	6·0	59·6	52	23·0
Zn	33·7	244	470	60·0
Co	158	24·0	675	4·4
Ni	146	4·0	667	3·0
Mn	88·0	236	394	113

curve rises and is virtually parallel to the pH curve, which rises from pH 5 to 6 during this period. As ferric molybdate is least soluble in the region of pH 3 (Jones, 1957), it is not possible, on the evidence provided by this experiment, to decide whether the mobilization of molybdenum was anything other than the result of the increase in pH brought about by the solution and reduction of ferric iron. However, the possibility of molybdenum being sorbed on undissolved ferric oxide or lucerne fibre, thus giving rise to the minimum in the solution curve, cannot be excluded.

Such a mechanism seems more probable, however, as an explanation of the decrease in the concentration of dissolved vanadium, as the maximum solution of vanadium during fermentation corresponds with the minimum pH; moreover, much of the subsequent decrease in the vanadium concentration occurred while the pH was almost constant.

Stability of minor element–fermentation solutions to atmospheric oxidation

Highly reducing conditions develop during anaerobic fermentation, and ferric iron is reduced when ferric oxide is dissolved by this process; exposure of ferrous-fermentation solutions to atmospheric oxidation results in the precipitation, as ferric oxide, of a large proportion of the dissolved iron.

Polynov (1937) compared the composition of the country rock with the composition of river water draining the area, and on this basis proposed a mobility sequence for the common soil constituents. More recently Jackson *et al.* (1948)

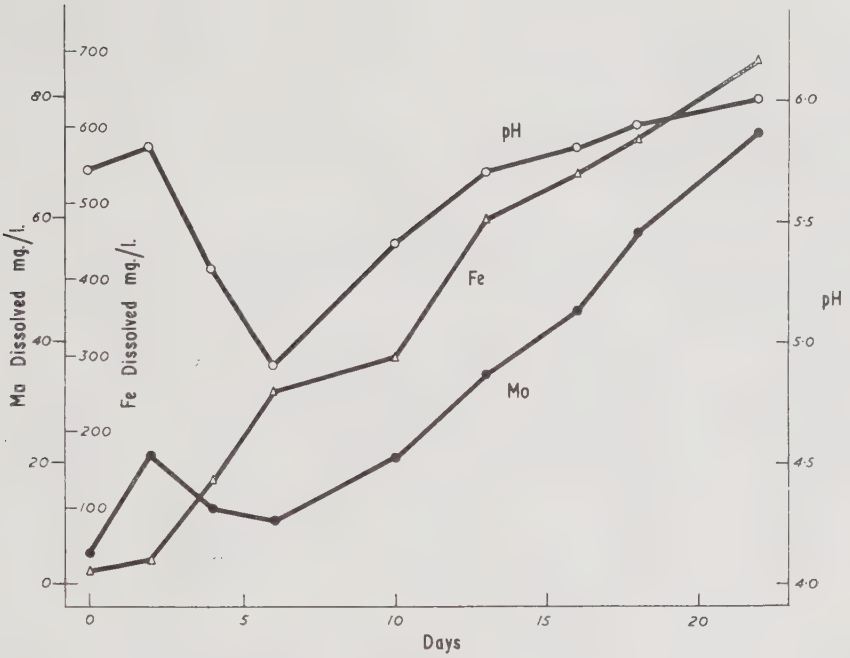

Fig. 4. Solution of Fe and Mo by fermenting lucerne.

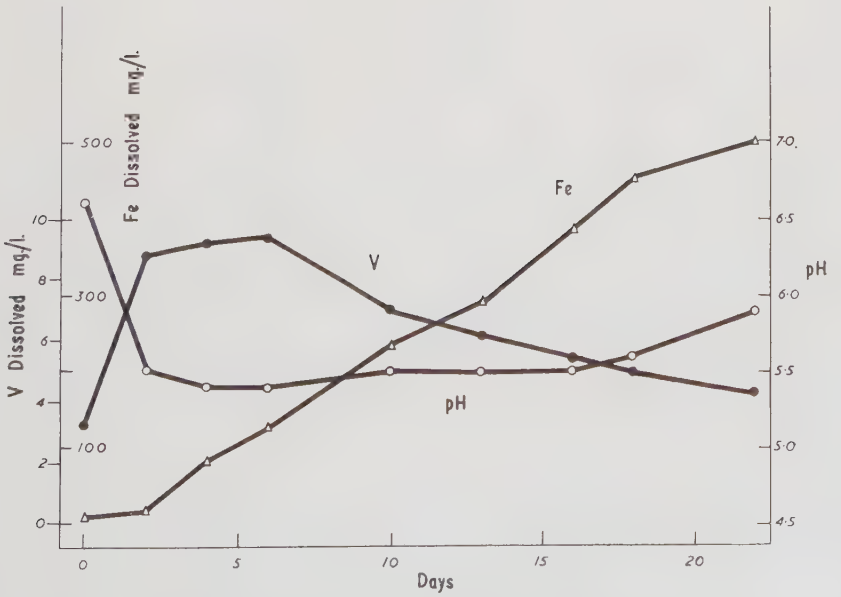

Fig. 5. Solution of Fe and V by fermenting lucerne.

have proposed a corresponding weathering sequence. In both these classifications iron oxides are included among the least readily mobilized minerals. Laboratory investigations indicate that in fact iron is very readily mobilized, but the ease with which ferric oxides are reprecipitated, once oxidizing conditions supervene, often causes this to be obscured in the field.

As Greene observed (1954), the sesquioxides may move over relatively small distances, producing results of considerable importance, without necessarily contributing much to the material dissolved in river water.

The ease with which a minor element is reprecipitated on exposure to atmospheric oxidation may thus be an important factor in determining its availability to plants, as well as the probability of its retention in, or loss from, the soil. With this in mind the stability of the minor element fermentation solutions on exposure to atmospheric oxidation was investigated. The solutions were centrifuged and 100 ml portions were transferred to 250 ml reagent bottles and treated with toluene. The bottles were kept at room temperature for 3 weeks and shaken frequently; samples were withdrawn periodically and the concentrations of the elements determined. Table 6 shows that losses from all the solutions were slight.

Table 6. Stability of minor element fermentation solutions to atmospheric oxidation (amount retained in solution after 21 days)

Element	Lucerne		Cocksfoot	
	mg/l.	Percentage of initial content	mg/l.	Percentage of initial content
Cu	80·0	94·1	52·5	99·1
Zn	161	94·7	181	95·3
Co	31·5	96·6	56·8	97·9
Ni	5·9	93·9	6·2	95·1
Mn	262	99·6	318	99·4

Under similar conditions some 80 per cent of the iron is precipitated from a ferrous–fermentation solution, and, in view of the well-known scavenging action of precipitated ferric hydroxide, the minor elements might be coprecipitated when the fermentation solution contains appreciable amounts of ferrous iron.

To test this assumption the reoxidation experiment was repeated using solutions obtained by fermenting lucerne in the presence of ferric oxide and the oxides of the minor elements considered. To obtain a reasonable excess of iron over copper, the proportion of iron in the solution was increased by adding a separately prepared iron fermentation solution.

As the relative concentrations of iron and minor element differed widely for each element, the results of this experiment provide no quantitative basis for comparison of the tendencies of the various elements to be copredipitated. However, one may reasonably infer from Table 7 that Cu, Zn, Mo and V tend to be concentrated in the precipitated ferric oxide: with Co, Ni and Mn the tendency is very slight.

Table 8 gives the results of a similar experiment in which equal volumes of a lucerne iron fermentation solution were allowed to reoxidize in the presence of

20 μg of each of the various trace elements which were added as inorganic salts. Here the conditions were more nearly comparable for each element, and the results agree with those of Table 7; Cu, Zn, Mo and V, as well as Pb and Sn, were coprecipitated to a considerable extent; as before Co and Ni were only slightly affected.

These results are of interest in view of the fact that trace metals may be concentrated in ironstone and lateritic concretions. Thus Simpson (1916) and Lindgren

Table 7. Coprecipitation with ferric oxide of minor elements from lucerne fermentation solutions (14 days aeration)

Element	Initial concentration (mg/l.)		Minor element coprecipitated	
	Iron	Minor element	mg/g Fe_2O_3	%
Mo	696	74·8	82·5	98·9
Zn	540	60·0	35·3	43·3
Cu	540	33·3	16·8	72·4
V	512	4·3	7·1	96·1
Mn	664	123	4·7	3·3
Co	675	4·4	0·25	4·6
Ni	667	2·4	0·17	5·9

Table 8. Coprecipitation of minor elements, present in ionic form, on aeration of lucerne–iron fermentation solutions

Element	Present as	μg coprecipitated	% coprecipitated
Pb	acetate	20·0	100
Sn	chloride	20·0	100
Mo	molybdate	20·0	100
V	vanadate	20·0	100
Zn	sulphate	13·3	66·5
Cu	sulphate	6·4	32·0
Ni	nitrate	1·9	9·5
Co	nitrate	0·8	4·0

(1923) reported concentration of vanadium in ironstone concretions; Turton (unpublished) found that an ironstone gravel from Western Australia contained 23 per cent Fe, 22 ppm Mo and 1120 ppm V. Oertel and Prescott (1944) studied the trace metals in hydrochloric acid extracts of ironstone concretions, and deduced from their results that Co, Cu, Mn and Ni were probably not concentrated with iron, but that Ga, Mo, Pb, V and Zn appeared to be so concentrated. There is thus a fair measure of agreement between the field and laboratory evidence.

Sorption of minor elements from fermentation solutions by hydrous ferric oxide

The extent to which sorption on ferric oxide is involved in the coprecipitation process was next investigated.

Fermentation solutions of the trace metals were prepared as before; portions of these were adjusted to pH values 7, 6, 5 and 4, and centrifuged. Volumes of 20 ml

of these were shaken for 90 min with 0·1 g of hydrous ferric oxide and again centrifuged. Determination of the concentrations of the unsorbed elements gave the results given in Table 9. As would be expected, sorption is more pronounced at the higher pH values, and the relative order of sorption is the same as the order of coprecipitation obtained in the previous experiments, i.e. Zn, Cu > Co, Ni.

Table 10 shows that under suitable conditions sorption may be important in preventing loss of trace elements from a soil. These results were obtained by percolating measured volumes of fermentation solutions through columns of ferric oxide-coated quartz sand. After thorough washing with water, the unsorbed trace metals were determined in the combined effluents and washings.

Table 9. Sorption of minor elements from lucerne fermentation solutions by hydrous ferric oxide (mg sorbed/g ferric oxide)

pH	Cu		Zn		Co		Ni	
	Added	Sorbed	Added	Sorbed	Added	Sorbed	Added	Sorbed
4	15·9	3·1	37·5	4·2	8·2	0·4	1·5	0·3
5	16·4	3·3	37·5	5·0	8·5	1·0	1·5	0·4
6	13·7	3·8	40·0	13·0	8·1	2·6	1·5	0·6
7	13·7	4·6	32·0	16·6	8·0	4·8	1·5	0·6

Table 10. Sorption of minor elements from fermentation solutions by ferruginous sand (mg)

pH	Zn		Cu		Co		Ni		Mn	
	Added	Sorbed	Added	Sorbed	Added	Sorbed	Added	Sorbed	Added	Sorbed
4	6·26	0·03	2·00	0·08	1·85	0·22	0·20	0·01	5·67	0·07
5	6·71	1·95	2·03	0·25	1·95	0·37	0·20	0·02	5·82	0·27
6	3·54	1·80	2·03	0·60	1·93	0·77	0·19	0·05	5·46	1·53
7	3·91	3·14	1·93	0·74	1·93	1·45	—	—	3·98	1·27

Dialysis of fermentation trace metal solutions

The ultimate fate of metals mobilized in the soil will be strongly influenced by the state, whether colloidal, ionic or complex, in which they occur in the soil solution. Accordingly fermentation solutions were dialysed to establish whether the trace metals were in true solution or in colloidal form.

Volumes of 10 ml of the fermentation solutions were pipetted into Cellophane containers which were then immersed in 20 ml of deionized water. Carbon dioxide-free water was used with lead, and all the dialyses were done under an atmosphere of nitrogen. Dialysis for 72 hr, with three changes of water, gave the results in Table 11. Although the dialysis was by no means exhaustive, almost all the trace metal passed through the Cellophane, and therefore must have been in true solution.

pH–stability relationships of trace metals in fermentation solutions

Having established the non-colloidal nature of the dissolved metals, the stabilities of the solutions at increasingly alkaline reaction were investigated in an attempt

to establish whether the trace metals were in complex or ionic form. Volumes of 100 ml of the solutions were titrated with 5 N sodium hydroxide solution to definite pH values; after centrifuging, the concentration of metal remaining in solution was determined. Fig. 6 gives the results obtained with lucerne solutions; cocksfoot solutions behaved similarly.

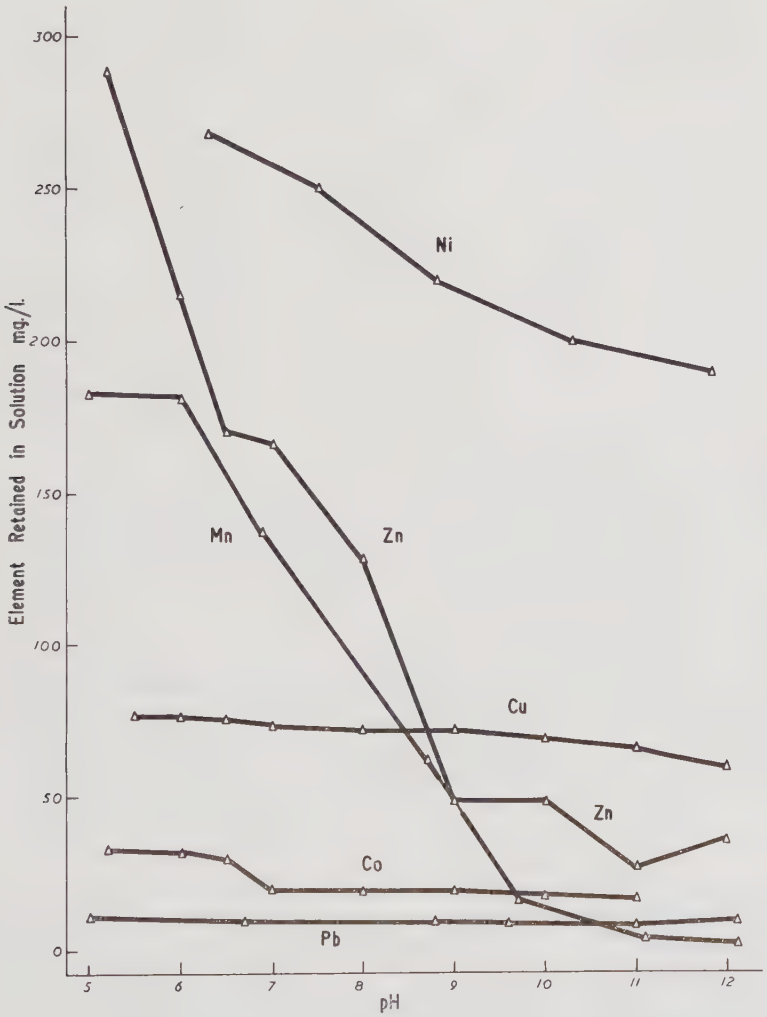

Fig. 6. pH–stability relationship of lucerne fermentation solutions.

The pH values at which the metal concentrations would fall to 1 mg/l in ionic systems may be calculated from the solubility products of the hydroxides. For Mn and Cu the values are 9·7 and 6·8, respectively; for the other elements the values vary from 8·3 to 8·7. Although the solubility product concept can be only a rough guide, the differences between the calculated and experimental values are large enough to establish the complex nature of the metal–fermentation solutions.

Dialysis experiments showed that retention of the trace metals in solution at high pH values was not associated with the development of colloidal properties. For example, 81·1 per cent of the copper in a fermentation solution at pH 10·5 was removed when the solution was dialysed, as described above, against three changes of distilled water.

Table 11. Dialysis of trace metal-fermentation solutions

Element	Lucerne		Cocksfoot	
	Initial content (μg)	% dialysed	Initial content (μg)	% dialysed
Mn	2500	93·2	2320	96·6
Zn	2470	93·0	3000	87·9
Cu	867	86·2	540	72·9
Co	324	99·0	415	95·7
Pb	143	80·1	112	79·5
Ni	59	84·3	78	67·3

Ion exchange from fermentation solutions

The distribution of a cation between the solid and aqueous phases in a cation exchange system is a function of the total cation concentration. Although a metal complex may sometimes be absorbed more strongly than the uncomplexed cation, in general a complexing agent increases the equilibrium concentration of the metal in the aqueous phase.

To obtain some idea of the stabilites of the fermentation complex compounds under acid conditions, measurement was made of the extent to which the various metals were taken up by a cation exchange resin from fermentation and inorganic solutions of equivalent concentrations. Fig. 7 shows that, except for cobalt, all the elements were taken up more extensively from the inorganic control solutions by the resin, indicating the complex state of the metals dissolved in the fermentation process.

Discussion

Halvorson and Starkey (1927) who seem to have been first to study the microbiological solution and reduction of ferric oxide, found that mixed soil inocula, *Escherichia coli* or *Clostridium sporogenes* have this activity. Roberts (1947) examined a large number of micro-organisms isolated from soils and found that only freshly isolated strains of *Bacillus polymyxa* gave extensive solution and reduction, but Bromfield (1954a) showed that *Bacillus circulans* is also active, and that in certain media bacteria of the genera *Escherichia* and *Aerobacter* will dissolve ferric oxide to a limited extent.

Broomfield found iron-reducing bacteria only in the surface horizons of a gleyed soil, and not in strongly gleyed material at a depth of 10 ft in the same profile. This indicates that reduction of iron at this depth might be a purely chemical and not a bacterial effect—a possibility suggested by Bloomfield (1951), and

which suggests a parallel with the action of sterile plant extracts on minor element oxides.

Bromfield (1954b) found that the culture fluid of *Bacillus circulans* does not reduce ferric compounds unless cells are present; he concluded that the reduction of

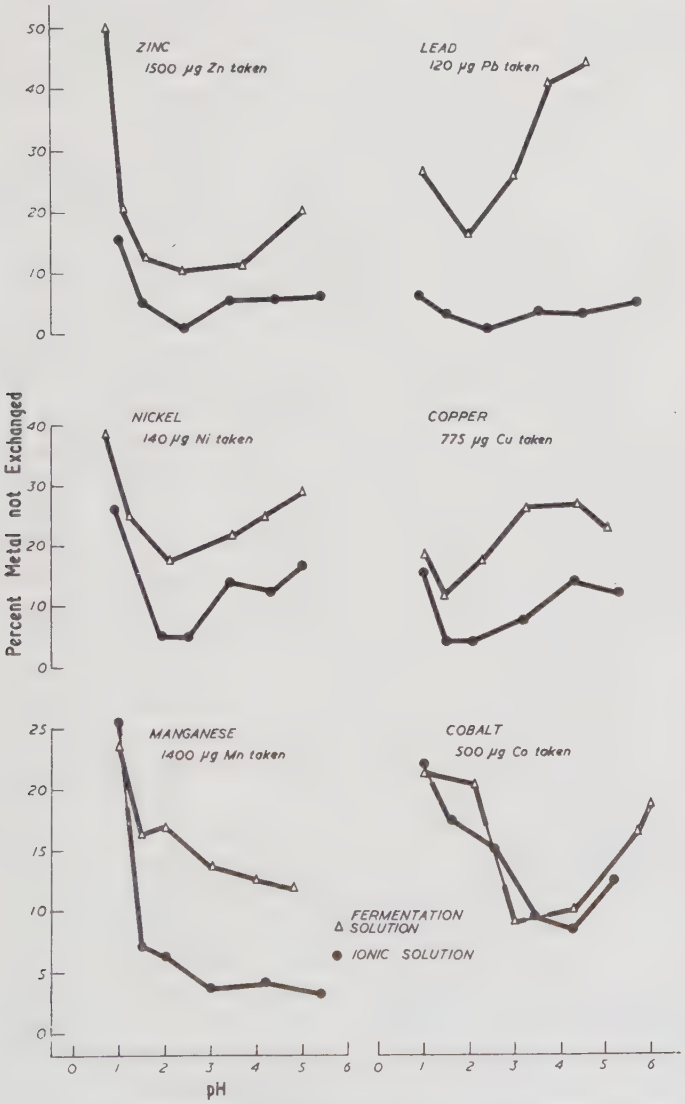

Fig. 7. Exchange of minor elements on a cation exchange resin.

ferric iron is associated with dehydrogenase activity, but that this alone does not induce reduction of ferric hydroxide, because ferric iron is reduced by such a system only when the iron is already in solution, or when complex-forming substances, such as 2:2′-dipyridyl, are present. Complex formation thus appears to be a necessary stage in the reduction of ferric oxide by soil bacteria, which fulfil a double function

in the mobilization process—first in producing complex-forming compounds by the breakdown of plant material, and secondly in being directly responsible for the reduction.

Sterile water extracts of plant material will dissolve ferric oxide (Bloomfield, 1951, 1953, 1954, 1955, 1957) and we have shown that such extracts also dissolve some trace metal oxides. This suggests that complex-forming compounds need not necessarily be produced by soil micro-organisms for solution to take place, because complex-forming constituents of undecomposed plant material will apparently fulfil the function of the 2:2′-dipyridyl used by Bromfield.

Sap expressed from the leaves of runner beans will dissolve considerable amounts of copper from Bordeaux mixture residues (Wain and Wilkinson, 1943): Arman and Wain (1958) showed that exudates from apple and dwarf bean leaves possess the same property, and that the solution of copper is not associated with bacterial decomposition of these substances. Bromfield (1958) showed that plants grown under sterile conditions can obtain manganese from oxides of this element, and that root washings of oat plants contain substances able to dissolve manganese oxides. There is thus abundant evidence that undecomposed plant material contains compounds which will mobilize some elements.

Reduction is certainly involved in the solution of ferric oxide by fermenting plant material, and reduction is probably equally important in the solution of manganese; with zinc, and in these experiments nickel also, reduction cannot have been involved in the solution process. Reduction might have been involved in the solution of molybdenum and vanadium, but these elements are most readily mobilized in anionic form, and in consequence the process would be favoured by oxidizing conditions. By analogy with the behaviour of phosphate (Gasser and Bloomfield, 1955), however, if molybdenum or vanadium were "fixed" on ferric oxide, reduction processes promoting solution of the ferric oxide would also mobilize the associated minor elements. The completeness with which molybdenum and vanadium were coprecipitated with ferric oxide on aeration of fermentation solutions suggests that these elements persisted in their original anionic forms throughout the fermentation process.

The extent of sorption of trace metals on pre-formed ferric oxide (Tables 9 and 10) is surprisingly high in comparison with the extent of coprecipitation (Table 7). In this connexion it is perhaps significant that the appearance of precipitates formed by aeration of iron-fermentation solutions is conditioned by the amount of plant material present in the original fermentation mixture. At low organic contents the precipitate has the usual red-brown colour of hydrous ferric oxides, but precipitates formed from solutions of higher organic contents are dark green-black in colour, and presumably contain appreciable amounts of organic matter. Possibly organic matter is taken up preferentially by the ferric oxide under the conditions of the coprecipitation experiments, and sorption of trace metals is thus inhibited. If this reasoning be correct it is possible that, under normal soil conditions, where relatively smaller amounts of organic matter are involved, coprecipitation effects are likely to be more pronounced than would appear from these results.

In the coprecipitation experiments Mo, V, Pb, Sn and Zn were concentrated in the ferric oxide. Copper showed some tendency to be so precipitated, but Co, Ni

and Mn were only slightly affected. According to GOLDSCHMIDT (1954) molybdenum is noticeably concentrated in oxidate sediments, the tendency being most pronounced in manganiferous minerals. Considerable coprecipitation of vanadium with ferric oxide takes place under soil conditions (SIMPSON, 1916; LINDGREN, 1923; SLATER *et al.*, 1937; OERTEL and PRESCOTT, 1944). GOLDSCHMIDT (1954) considers that lead is probably concentrated with ferric oxides, possibly as a hydrated ferrite, although he does not exclude the possibility that lead may be bound primarily to clay minerals in marine muds and clays.

Tin does not appear to be concentrated in ferruginous soil material; this probably reflects the difficulty with which tin minerals are mobilized, as tin was readily coprecipitated in these experiments (Table 8).

WHITE (1957) studied several soil samples from Tennessee. He concluded that 30–60 per cent of the total zinc of these soils is associated with iron oxides, that 20–45 per cent is held in lattice positions of clay minerals, and that from 1–7 per cent is base exchanged in the clay minerals.

GOLDSCHMIDT considers it proved that copper is concentrated in marine oxidate sediments, and that the contents of nickel and cobalt in oxidate sediments are usually less than the average proportions of these elements in the lithosphere, although RANKAMA and SAHAMA (1950) consider that these elements are concentrated in oxidates, cobalt being taken up more readily than nickel. LANDERGREN (1948) has found evidence of concentration of cobalt in Finnish bog iron ores.

KUBOTA (1958) found a similar distribution pattern for the total cobalt and iron contents of a number of soils, which agrees with the observations made in this study.

It is apparent from the foregoing that there is a considerable measure of agreement between field observations and the results of these experiments; this affords some justification for assuming that the essential features of the natural processes were duplicated in the laboratory experiments, despite the necessarily simplified systems that were studied.

The irreversible sorption of copper and nickel on plant fibre suggests an analogy with the copper deficiency, "reclamation disease", which is often found in highly organic soils. The fact that undecomposed plant residues possess the same copper-fixing properties as peat raises the question: how far is the ability of peat to fix copper, for example, a property dependent upon the process of peat formation, and how far is it a property of the original plant material that has remained unaffected throughout humification?

In preliminary experiments it has been found that cobalt and manganese are not fixed by plant fibre, and it seems significant that while GOLDSCHMIDT found that copper and nickel are amongst those elements that accumulate in forest humus, cobalt and manganese do not appear to be immobilized in this manner, although DUCHAUFOUR and ROUSSEAU (1959) showed that large amounts of exchangeable manganese may occur in forest litter.

Acknowledgements –We thank Drs. A. MUIR and H. GREENE for their helpful criticism and advice and Mr. G. BROWN for the X-ray analyses. One of us (N. S. K.) is indebted to the Government of the Federation of Malaya for the grant of a post-graduate scholarship. The material presented in this paper was submitted by N. S. K. to the University of London in partial fulfillment of the requirements for the Ph.D. degree.

References

Arman P. N. and Wain R. L. (1958) The role of leaf exudates in the solution of copper from Bordeaux mixture. *Ann. Appl. Biol.* **46,** 366–374.

Bétrémieux R. (1951) Étude expérimental de l'évolution du fer et du manganèse dans les sols. *Ann. Agron.* **2,** 193–195.

Bloomfield C. (1950) Some observations on gleying. *J. Soil Sci.* **1,** 205–211.

Bloomfield C. (1951) Experiments on the mechanism of gley formation. *J. Soil Sci.* **2,** 196–211.

Bloomfield C. (1953) A study of podzolization. *J. Soil Sci.* **4,** 5, 17–23.

Bloomfield C. (1954) A study of podzolization. *J. Soil Sci.* **5,** 39, 46, 50–56.

Bloomfield C. (1955) A study of podzolization. *J. Soil. Sci.* **6,** 284–292.

Bloomfield C. (1957) The possible significance of polyphenols in soil formation. *J. Sci. Food Agric.* **8,** 389–392.

Bromfield S. M. (1954a) The reduction of iron oxide by bacteria. *J. Soil Sci.* **5,** 129–139.

Bromfield S. M. (1954b) Reduction of ferric compounds by soil bacteria. *J. Gen. Microbiol.* **11,** 1–6.

Bromfield S. M. (1958) The solution of γ-MnO_2 by substances released from soil and from the roots of oats and vetch in relation to manganese availability. *Plant and Soil* **10,** 147–160.

Dodson R. W., Ferney G. J. and Swift E. H. (1936) The extraction of ferric chloride from hydrochloric acid solutions by isopropyl ether. *J. Amer. Chem. Soc.* **58,** 2573–2577.

Duchaufour Ph. and Rousseau L. Z. (1959) Les phénomènes d'intoxication des plantules de résineux par le manganèse dans les humus forestiers. *Rev. for franç.* No. 12, 835–847.

Forster W. A. (1953) The determination of nickel in plant materials in the presence of other metals. *Analyst* **78,** 560–562.

Gasser J. K. R. and Bloomfield C. (1955) The mobilisation of phosphate in waterlogged soils. *J. Soil Sci.* **6,** 219–232.

Goldschmidt V. M. (1954) *Geochemistry* (Edited by Muir A.). Clarendon Press, Oxford.

Greene H. (1954) Tropical soils. *J. Sci. Food Agric.* **5,** 65–69.

Halvorson H. O. and Starkey R. L. (1927) Studies on the transformation of iron in nature—II. Concerning the importance of micro-organisms in the solution and precipitation of iron. *Soil Sci.* **24,** 381–402.

Holmes R. S. (1945) Determination of total copper, zinc, cobalt and lead in soils and soil solutions. *Soil Sci.* **59,** 77–84.

Jackson M. L., Tyler S. A., Willis A. L., Sourbeau C. A. and Pennington R. P. (1948) Weathering sequence of clay size minerals in soils and sediments. *J. Phys. Chem.* **52,** 1237–1260.

Jones L. H. P. (1957) The solubility of molybdenum in simplified systems and aqueous soil suspensions. *J. Soil Sci.* **8,** 313–327.

Kubota J. (1958) Cobalt status of soils of south eastern United States—I. Cobalt, its distribution and relationship to iron and clays in five selected soils. *Soil Sci.* **85,** 130–140.

Landergreen S. (1948). On the geochemistry of Swedish iron ores and associated rocks. *Sveriges Geol. Undersökn. C.*, **42,** No. 5.

Lindgren W. (1923) Concentration and circulation of the elements from the standpoint of economic geology. *Econ. Geol.* **18,** 419–442.

Mitchell R. L. (1948) *The Spectrographic Analysis of Soils, Plants and Related Materials* Commonwealth Bur. Soil Sci. Tech. Comm. No. 44.

Mitchell R. L. (1955) *Trace elements. Chemistry of the Soil* (Edited by Bear F.) Reinhold, New York.

Oertel A. C. and Prescott J. A. (1944) A spectrochemical examination of some ironstone gravels from Australian soils. *Trans. Roy. Soc. S. Aust.* **68,** 173–176.

Piper C. S. (1950) *Soil and Plant Analysis.* University of Adelaide.

Polynov S. S. (1937) *The Cycle of Weathering* (Translated by Muir A.). T. Murby, London.

Rankama K. and Sahama T. G. (1950) *Geochemistry.* University of Chicago Press.

Roberts J. L. (1947) Reduction of ferric hydroxide by strains of *Bacillus polymyxa*. *Soil Sci.* **63,** 135–140.

Rush R. M. and Yoe J. H. (1954) Colorimetric determination of zinc and copper with "Zincon". *Analyt. Chem.* **26,** 1345–1347.

Slater C. S., Holmes R. S. and Byers H. G. (1937) Trace elements in the soils from the Erosion Experiment Stations, with supplementary data on other soils. *U.S. Dept. Agric. Tech. Bull.* No. 552.

Simpson E. S. (1916) Analyses of Western Australian rocks, meteorites and natural waters. *W. Aust. Geol. Surv. Bull.* **67,** 118–119.

Wain R. L. and Wilkinson E. H. (1943) Studies upon copper fungicides—4. The solution of copper from Bordeaux and Burgundy mixtures. *Ann. Appl. Biol.* **30,** 379–391.

Walsh T., Ryan P., and Fleming G. A. (1956) Cobalt deficiency in relation to weathering processes in soils. *Proc. VIth Int. Congr. Soil Sci.* Vol B, 771–779.

White M. L. (1957) The occurrence of zinc in soil. *Econ. Geol.* **52,** 645–51.

Williams C. H. (1955) A colorimetric method for the determination of molybdenum in soils. *J. Sci. Food Agric.* **6,** 104–110.

Williams T. R. and Morgan R. R. T. (1954) A rapid method for the determination of copper in plant material. *Chem. & Ind.* 461.

Wise W. M. and Brandt W. W. (1954) Spectrophotometric determination of cobalt with 2-nitroso-1-naphthol-4-sulphonic acid. *Analyt. Chem.* **26,** 693–697.

Geochimica et Cosmochimica Acta, 1961, Vol. 24, pp. 226 to 249. Pergamon Press Ltd. Printed in Northern Ireland

Isotopic geochemistry of uranium and lead in the Swedish kolm and its associated shale*

James C. Cobb† and J. Laurence Kulp
Lamont Geological Observatory, Columbia University, Palisades, New York

(*Received* 15 *January* 1960)

Abstract—The uranium and lead concentration and isotopic composition in a variety of samples of kolm and associated black shale from the Peltura beds (Franconian stage) of the Upper Cambrian of Sweden have been determined by isotope dilution techniques. In addition Th^{230}, Ra^{226}, Pb^{210} and radon leakage values have been determined on certain samples. All samples show discordant U–Pb isotopic ages. It appears that two processes have been at work; selective removal of Pb^{206}, resulting from the movement of an intermediate member of the U^{238}–Pb^{206} series, and removal of bulk radiogenic lead. The absolute age of the formation is concluded to be greater than 500 million years with the most probable age near this lower limit. This is in good agreement with the latest results on the absolute geologic time scale. The stratigraphically well-dated kolm cannot, however, be considered a calibration point in the absolute time scale. It does show that uranium–lead dating on bituminous shales will lead to minimum ages for these formations.

Introduction

The establishment of an absolute geologic time scale for Paleozoic and younger eras requires the age determination of rocks which are closely defined by faunal assemblages. The ideal technique would be to date directly a formation containing suitable index fossils. One possibility for such an approach is the application of the U–Pb method to marine black shale. This rock type occurs in all of the geologic periods. It is intimately associated with fossils, so that the place in the stratigraphic sequence may be precisely defined and, most important, it contains unusually high amounts of uranium. Before isotopic data on such formations can provide quantitative age data, the following conditions are necessary:

(1) Uranium and its radiogenic daughter, lead, should be sufficiently abundant to be measurable with the necessary precision.

(2) The common lead abundance should be low enough so that a correction can be applied with reasonable accuracy.

(3) No alteration in the chemical composition has occurred during the geological history of the material, or the alteration is simple enough to be easily corrected.

(4) The uranium is accumulated during the sedimentation or diagenetic process.

The middle Upper Cambrian Swedish alum shales contain the highest amounts of uranium reported for any black shale. The uranium concentration is as high as 6500 p.p.m. in small organic-rich pods called "kolm" and is about 200 p.p.m. for the shale itself. This formation was therefore chosen for an investigation of the isotopic geochemistry of uranium and lead in the black shale environment with a view to its possible use in geochronometry. The relatively high uranium concentration in the kolm makes it possible to measure ages based on three isotopic

* Lamont Geological Observatory Contribution No. 485.
† Present address: Chemistry Department, Brookhaven National Laboratory, Upton, N.Y.

ratios: Pb^{206}/U^{238}, Pb^{207}/U^{235} and Pb^{207}/Pb^{206}. Agreement among the three ages is a strong indication that a true age for the formation has been obtained. If the ages disagree, a closed system has not been maintained since deposition of the formation and the pattern of disagreement may give an indication of the factors causing the discrepancies.

The first measurements on the Swedish kolm were made in 1926 by R. C. Wells (1930) who obtained a Pb/U ratio of 0·0563 which corresponds to an apparent age of 400 million years. Nier (1939) made the first isotopic measurements on a sample of the kolm and obtained the following isotopic ages: U^{238}–Pb^{206} = 375 million years; U^{235}–Pb^{207} = 430 million years; and Pb^{207}–Pb^{206} = 800 million years. This severe discordance was interpreted by Wickman (1942) as due to radon leakage which results in loss of Pb^{206} and an erroneously low Pb^{206}/U^{238} ratio and a high Pb^{207}/Pb^{206} ratio. Holmes (1947), therefore, adopted the 430 million year U^{235}–Pb^{207} age as the middle of the Upper Cambrian for his proposed geologic time scale.

In recent years isotopic studies of uranium minerals have shown that such discordances are fairly common and result most frequently from lead loss (Kulp and Eckelmann, 1957; Tilton *et al.*, 1957). The potential importance of marine black shales in quantitative geochronometry and the geochemical processes involved in producing these discordances indicated that a detailed study of the Swedish Cambrian black shale would be rewarding.

Geologic Setting

The Lower Paleozoic sedimentary sequence occurs in only a few scattered places in southern Sweden (Fig. 1). These rocks, which now lie platelike upon the Pre-cambrian complex of the Fennoscandian Shield, represent the remnants of rocks which at one time covered the entire area. In the Billingen region of Vastergotland, the basal Lower Cambrian sandstone rests uncomformably on gneisses and schists which were finally metamorphosed about 1800 million years ago (F. Wickman, personal communication) (Fig. 2). Above the Lower Cambrian lies the Middle Cambrian green shale which is superseded by the Upper Cambrian black shale. A disconformity, generally not discernible in the outcrop, exists at the very top of the Upper Cambrian and some zones representing the upper Upper Cambrian are missing. Deposition of a glauconitic limestone with fossils indicative of the lowest Ordovician (Tremadocian) followed this hiatus. In some localities, however, graptolites have been found in black shale below this limestone. The sequence in this region is capped by a diabase sill supposed to have been intruded in Permian time.

The post-depositional history of the formations is not well known but it seems unlikely that deposition continued beyond the Silurian and since the Caledonian orogeny to the north and west appears to have no effect on southern Sweden, the sedimentary sequence has probably been undisturbed and lying near the surface since Devonian time (B. Dahlman, private communication).

The black shale in which the kolm is incorporated represents a fairly complete record of deposition in the Upper Cambrian. Although the formation is only 17·6 m thick on the average, it has been possible to divide it into ten distinct faunal zones

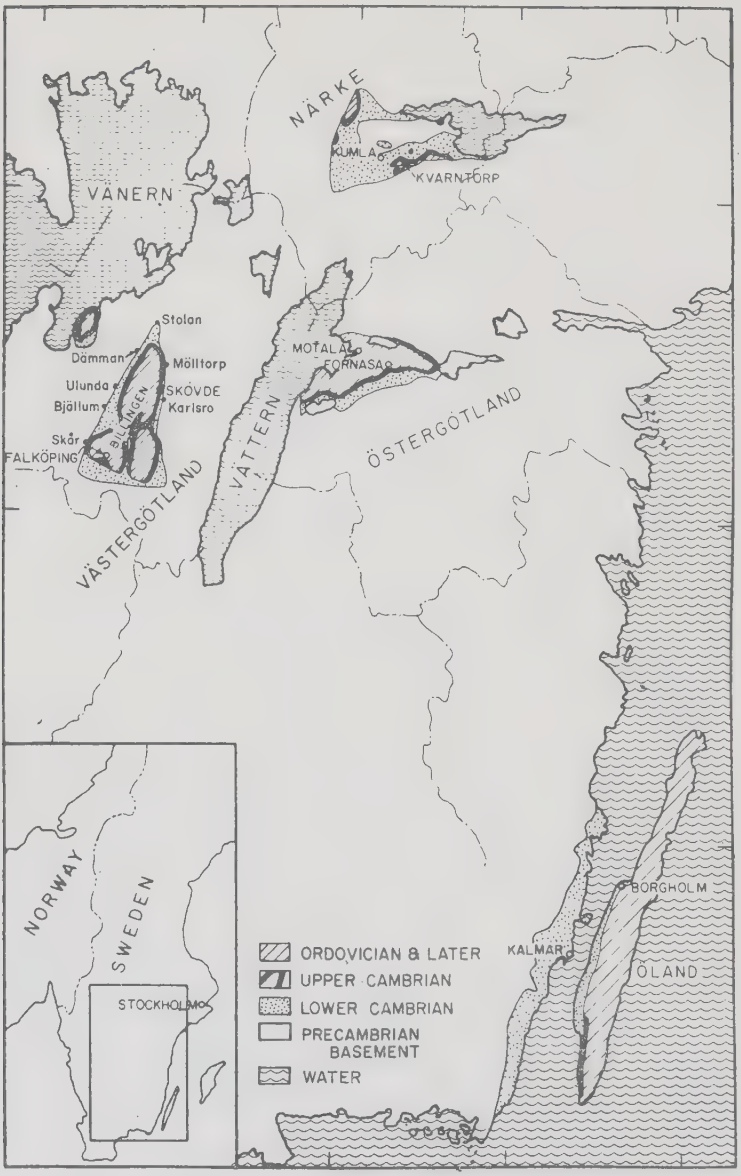

Fig. 1. Geologic map of Southern Sweden (after B. Dahlman).

(Westergard, 1922). The kolm lenses lie consistently within the zone containing Peltura *scarabaeoides*. Correlation of these zones with the faunal assemblages throughout most of North America is difficult, but it is the opinion of Howell *et al.* (1944) that the Peltura zone corresponds to the Prosaukia–Ptychaspis zone of the Mississippi Valley which covers the middle of the Franconian Stage of the Upper Cambrian. It appears most unlikely that Peltura *scarabaeoides* extended beyond the Franconian Stage (B. F. Howell, private communication).

The development of the kolm lenses is a phenomenon which is peculiar to this formation. It has its best development in the Billingen region where the black shale is thickest, and which represents the probable axis of the depositional basin (B. DAHLMAN, personal communication). East of this region, in Östergotland and Öland, the Peltura zone which carries the kolm is either missing or represented by a very thin layer.

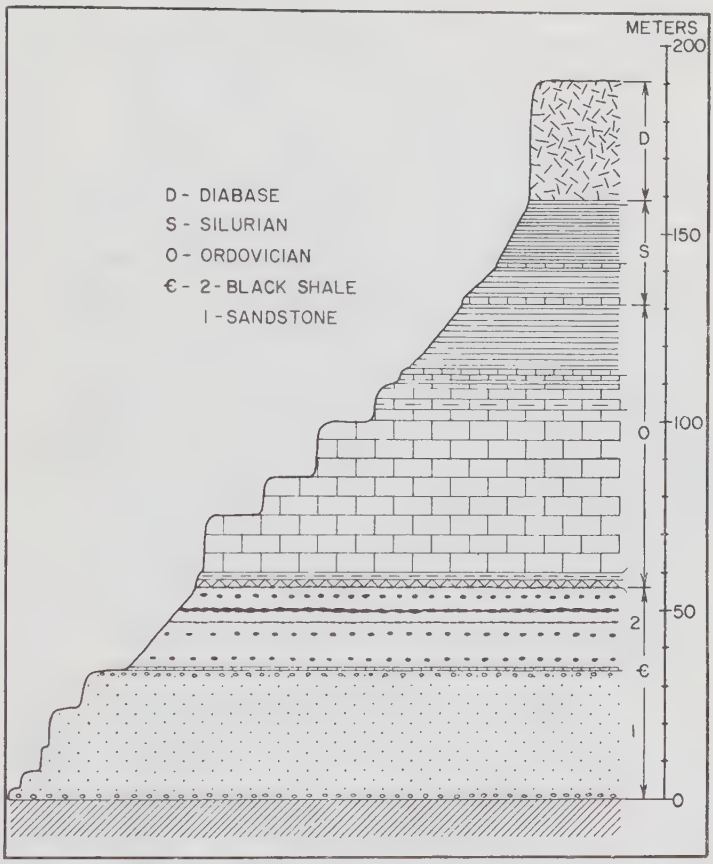

Fig. 2. Generalized geologic cross-section in Billingen region (MUNTHE *et al.*, 1928)

The kolm is characterized chiefly by its very high organic content which ranges up to 80 per cent as opposed to 30 per cent for shale. WETZEL (1947) considers that the formation was formed in shallow water and that sluggish, swirling currents acted so as to collect organic matter into small depressions in the sediment. Later, during lithification, the organic material compacted together and flattened out into the lens-like form seen today (Fig. 3). In its maximum development, these lenses can be as much as 12 cm thick in the centre. They are always arranged with the long dimension parallel to the bedding.

Fig. 4 is a schematic drawing of a quarry face near Stolan in the Billingen region. The kolm lenses occur in two zones, the upper and lower horizons, about 1 m apart. The organic content varies progressively from the edge to a maximum

in the centre. The uranium content varies directly with this parameter (Wetzel, 1947) and with the other trace metals such as vanadium, zinc and copper, is believed to have been precipitated along with the sediment. The association of these elements with a reducing environment as exemplified by the organic content, is a common geologic occurrence (Colorado Plateau, Mansfeld Kupferschiefer, etc.).

Bates and Strahl (1957, 1958) have done by far the most detailed work on the uranium occurrence in black shales. Most of the work was done on the Chattanooga shale, but numerous samples of the Swedish alum shale were run. Both

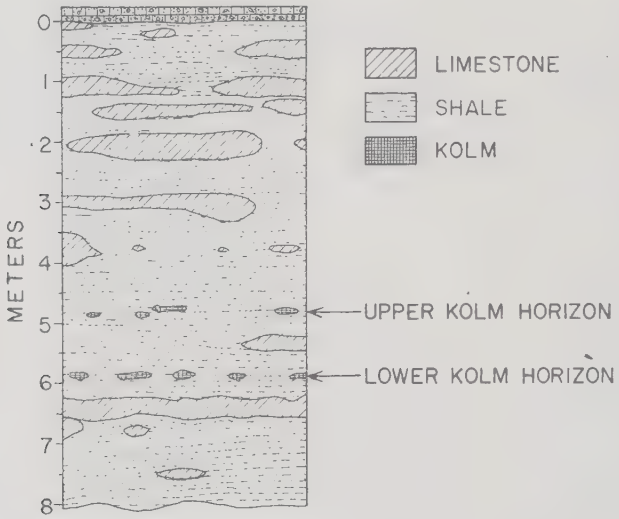

Fig. 4. Sketch of Upper Cambrian shale near Stolan (Lundqvist *et al.*, 1931)

these formations are examples of bituminous black shales. Organic matter occurs largely as coatings on mineral grains. They find a positive correlation of uranium with the organic material and, to a lesser extent, with pyrite. Uranium is evenly dispersed in the fine-grained matrix of the rock. Autoradiographic studies show no track clusters indicating absence of uranium-bearing minerals and veins. Most of the uranium is readily leached with acid, showing that it is held on the surfaces of the organic and inorganic grains.

Rynninger (1957) has made some experiments on the Swedish alum shale and finds uranium to be at present associated with the inorganic fraction of the rock. He postulates original precipitation of uranium with humic material, with the humus being destroyed later by bacterial action.

Table 1 presents the chemical analysis of the ash from two typical samples of kolm. The major element concentrations are more or less representative of the average shale (Clarke, 1924). The high iron content is a consequence of the presence of pyrite. The potassium/sodium ratio is high, suggesting an authigenic origin for at least part of the sediment. The Th/U ratio in the shale is about 0·01 (Koczy, 1949) as compared with 3–4 in igneous rocks. Adams and Weaver (1958)

Fig. 3. Photograph of kolm lens

have used this quantity as an indication of the environment of deposition of sediments. A very low Th/U ratio is considered to be due to precipitation of these elements from sea water.

These observations point to the deposition of the kolm-bearing black shale from a shallow epicontinental sea. Reducing conditions at the bottom of the sea permitted the precipitation of uranium; and an extremely slow sedimentation rate

Table 1. Chemical analysis of kolm samples

(1)		(2)
Sample as Received		
S	3·60	
CO_2	0·58	
Ash	27·83	27–31%
Analysis of Ash		*Analysis of Ash*
SiO_2	54·44	48·68
Al_2O_3	18·23	20·34
Fe_2O_3	12·62	20·00
TiO_2	0·95	0·20
MnO	0·07	
MgO	1·14	1·40
CaO	2·75	0·90
Na_2O	0·27	0·60
K_2O	5·90	5·84
P_2O_5	0·31	0·15
V_2O_5	0·24	
U_3O_8	0·73	
SO_3	2·31	0·62
Undetermined		1·27

(1) Kolm from Bjallum Quarry, University of Minnesota Rock Analysis Laboratory, C. O. Ingamells, Analyst.
(2) Kolm from Gullhogen, Wells and Stevens (1931).

permitted the concentration of uranium to build up. It is the opinion of both Wetzel (1947) and Bates and Strahl (1957) that uranium was introduced during the sedimentation or diagenetic process.

Experimental Techniques

The conventional procedures for determining microquantities of material suffer from the fact that measurements rarely can be made with an accuracy of better than 5–10 per cent. In many cases it is much worse than this. The problem to be investigated here requires much greater accuracy so that the stable isotope dilution method (Inghram, 1954) was indicated. Uranium and lead were determined by this method using procedures modified after those described by Tilton *et al.* (1955). The detailed steps of the chemical procedures are given elsewhere (Cobb, 1959). The mass spectrometric technique is described by Miller (1960). Radium and radon were determined by the radon emanation technique (Bate *et al.*, 1954).

Chemical procedures

1. *Uranium.* An aliquot of the unknown containing roughly 50 μg uranium was mixed with the same amount of spike. The spike was enriched U^{235} (>99·5 per cent) obtained from the U.S. Atomic Energy Commission. The natural uranium isotopic composition was assumed to be invariant at 99·27 per cent U^{238}. After equilibration of the mixture, the uranium was purified by successive hexone extractions from saturated solutions of aluminium nitrate and ammonium nitrate (Tilton, 1951). Uranium was prepared for mass spectrometric analysis by dissolving it in dilute nitric acid and evaporating it on to a tantalum filament.

2. *Lead.* Two aliquots were necessary for lead analysis. One, containing about 60 μg of lead, was processed alone to obtain the isotopic composition. To the other, a spike with a Pb^{208} concentration of 95·8 per cent was added. The samples were purified by the dithizone extraction technique (Sandell, 1950). Briefly, the method involves extraction of lead from a basic solution using dithizone in chloroform in the presence of citrate and cyanide ions to complex interfering cations. Lead is removed from chloroform by shaking with 0·1 N nitric acid. About 20 μg lead is mounted on a tantalum filament, preparatory to mass spectrometric analysis.

3. Th^{230} *and* Pb^{210}. These analyses were done at Brookhaven National Laboratory. Th^{230} was determined directly by α-counting using a pulse-height analyser coupled to a 100-channel analyser. A known amount of Th^{228} was added to the sample to determine yield. Pb^{210} was measured by counting its Po^{210} daughter using the α-pulse-height analysis system. A known amount of Po^{209} was used as tracer. Analytical errors were probably less than 5 per cent.

The contamination problem

In this work the danger of introduction of lead via reagents, glassware, or fall-in from the air is particularly acute. Much experience concerning purification of reagents and the shielding from dust during evaporation on the hot plate has been accumulated by Patterson (1951) and Tilton *et al.* (1955). All acids used were doubly distilled. Water was prepared by running singly distilled water through an ion-exchange column and then redistilling from a quartz still. Blanks were frequently run, both on individual reagents and during a complete analysis. The amount of contaminating lead introduced was monitored by the isotope dilution method using a spike lead with a Pb^{206}/Pb^{208} ratio of 507 and assuming the contaminant to be modern common lead (Pb^{206}/Pb^{208} ~0·5). Results indicate a level of from 0·3 to 0·8 μg of contaminating lead per run.

Reproducibility

Replicate analyses were made on five samples, four having been run in duplicate and one in quadruplicate. In almost every case, the results agree within the standard deviation of the isotope ratio measurements on the mass spectrometer, so that the mass spectrometer runs appear to be the limiting factor in determining precision and all previous steps, such as dissolving the sample, taking aliquots and adding spike contribute no significant error.

On the basis of these replicate analyses, it can be stated that the U/Pb ratio is reproducible to at least 2 per cent. Results on spike standardization indicate that

the spike concentrations are known to better than 1 per cent. Therefore, the absolute accuracy of these analyses should be ±3 per cent. The errors quoted on the isotopic ages include errors on the uranium, lead and lead isotopic mass spectrometer runs.

Common lead correction

Of the four stable lead isotopes, only Pb^{204} is not produced by radioactive transformations, so that in any uranium-rich mineral, this isotope is a measure of the concentration of original lead. In the case of the Swedish kolm and shale, Pb^{208} can also be used in this way since there are negligible quantities of thorium present (Koczy, 1949). The Pb^{208}/Pb^{204} ratio of 37·0 as found in samples S–9K and S–12S is taken to represent the value of the ratio at the time of precipitation of the shale. Studies on the isotopic compositions of common leads of different ages have shown that if any two of the ratios Pb^{208}/Pb^{204}, Pb^{207}/Pb^{204} and Pb^{206}/Pb^{204} are plotted against each other a smooth curve results which represents the increase of the radiogenic isotopes with time. Using such plots, the observed Pb^{208}/Pb^{204} ratio can be used to derive the original Pb^{206}/Pb^{204} and Pb^{207}/Pb^{204}. From the data compiled by Bate (1955), the ratios are $Pb^{206}/Pb^{204} = 17{\cdot}1$, $Pb^{207}/Pb^{204} = 15{\cdot}5$, $Pb^{208}/Pb^{204} = 37{\cdot}0$. These isotopic ratios were used to compute the common lead correction for all samples analysed in this study.

Some mention should be made of the possibility that the original lead is a mixture of common lead and radiogenic lead. That is, an appreciable fraction of the radiogenic lead formed from uranium is depositing along with uranium in the sediment. In such a case a plot of U/Pb^{208} vs. Pb^{206}/Pb^{208} should be instructive in assessing the amount of radiogenic lead originally present. Such a plot is shown in Fig. 5. Extrapolation to a U/Pb^{208} of zero yields a Pb^{206}/Pb^{208} roughly 50 per cent higher than the value expected for a common lead. Later in this paper attempts will be made to show that the Pb^{206}/Pb^{208} of the shales is high because of addition of unaccompanied Pb^{206} into the shale from the kolm. This accounts for the high Pb^{206}/Pb^{208} derived from Fig. 5.

In any case, the Pb^{206}/Pb^{208} of 0·7 represents the maximum correction for original lead. This correction is still only a second-order one for the kolm (the U^{238}/Pb^{206} and U^{235}/Pb^{206} ages will be lowered by about 1 per cent) but the apparent isotopic ages for the shales will be considerably lowered (the U^{238}/Pb^{206} age will be reduced by from 10 to 40 per cent).

If uranium, lead and other elements found in the kolm are directly precipitated from sea water, the lead isotopic composition must almost certainly be normal. Any lead of an anomalous composition dissolved in the ocean would be swamped by rock lead of a normal isotopic composition.

Results

The samples analysed in this study are listed in Table 2. The quarry and stratigraphic location, the uranium and lead concentrations and the lead isotopic compositions are given, and a map showing the individual quarries is given in Fig. 6. It should be noted that all samples were collected from outcrops except for one kolm (S–19K) and three shales (S–17S, S–18S and S–20S) which were taken

from a drill core. It is evident that there are no systematic variations with geographical location. The common lead content of the kolm is uniformly low and independent of geographical location or stratigraphic position. The shale samples show a uranium concentration about twenty times less than the kolm and slightly more variation in uranium and common lead content.

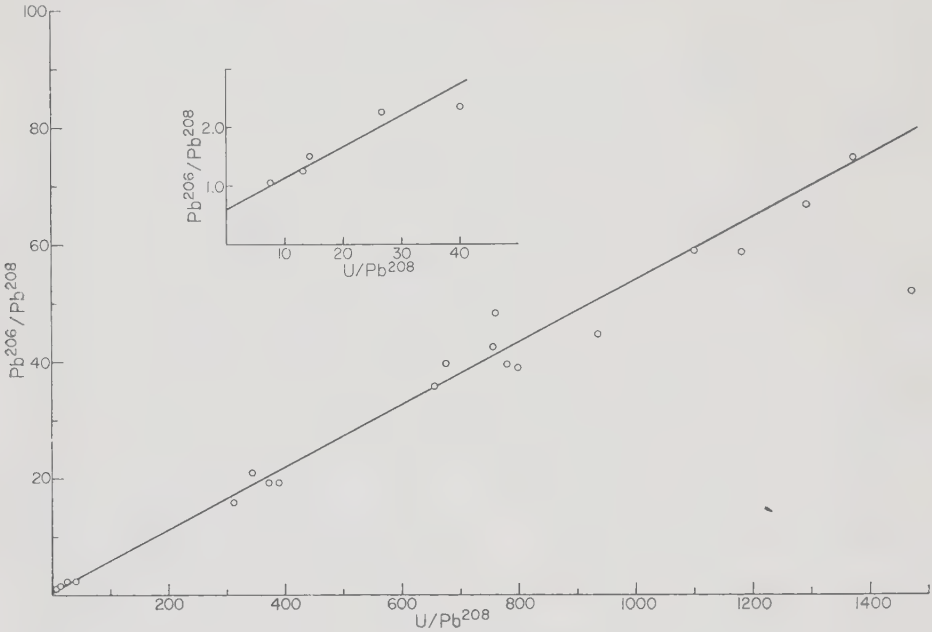

Fig. 5. Pb^{206}/Pb^{208} vs. U/Pb^{208}.

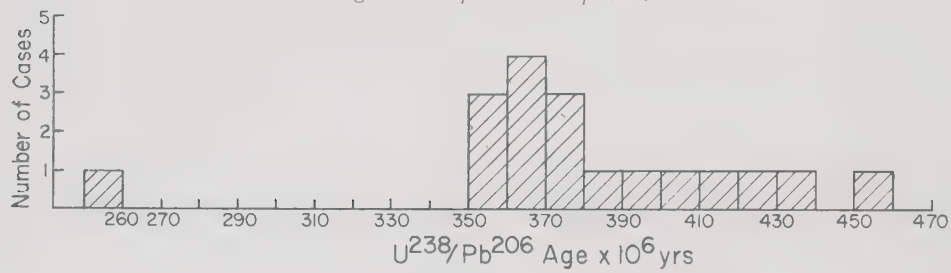

Fig. 6. Histogram of U^{238}/Pb^{206} ages for Swedish kolm.

The apparent isotopic ages for the kolm are given in Table 3. The errors are analytical only and do not include the uncertainty introduced from the common lead correction.

All specimens except the one from Kvarntorp are from the Billingen area (Fig. 1) where the quarries represent a north–south section of 35 km and an east–west section of 10 km.

Discussion

All the samples of the Swedish kolm that have been analysed have shown a discordance in the isotopic ages, with the consistent pattern U^{238}–$Pb^{206} < U^{235}$–$Pb^{207} < Pb^{207}$–Pb^{206}. This discordance is not due to analytical errors or

Table 2. Analytical data on black shale and kolm samples

Number	Location	U (p.p.m.)	Pb (p.p.m.)	Isotopic composition of lead		
				Pb^{204}/Pb^{206}	Pb^{207}/Pb^{206}	Pb^{208}/Pb^{206}
	Bjallum					
	Kolm lens 6·1 cm thick					
S–9K	edge of lens (0·0 to 0·5 cm)	4240 ± 40	235 ± 2	0·000690 ± 0·000010	0·0786 ± 0·00075	0·0254 ± 0·0004
S–10K	centre (3·0 to 3·75 cm)	6400 ± 60	351 ± 3	—	0·0690 ± 0·00075	0·0106 ± 0·0003
S–11K	edge (5·5 to 6·1 cm)	4260 ± 60	240 ± 5	—	0·0898 ± 0·00070	0·0520 ± 0·0010
	Stolan					
	Kolm lens 5·4 cm thick					
S–14K	centre	5590 ± 120	301 ± 3	0·0005	0·0740 ± 0·0006	0·0171 ± 0·0003
S–15K	edge	5020 ± 80	270 ± 2·6	—	0·0765 ± 0·0003	0·0257 ± 0·0007
	Kolm lens 6·0 cm thick					
S–22K	centre	5070 ± 70	278 ± 3·5	—	0·0698 ± 0·00068	0·0117 ± 0·00015
S–23K	edge	4600 ± 40	261 ± 2	—	0·0757 ± 0·0008	0·0224 ± 0·00035
	Different lenses					
S–1K		4700 ± 50	324 ± 4	—	0·0816 ± 0·0008	0·0477 ± 0·0018
S–4K		4760 ± 70	328 ± 5	0·0006	0·0688 ± 0·00055	0·0208 ± 0·00025
S–5K		4910 ± 100	301 ± 10	0·0007	0·0710 ± 0·00045	0·0236 ± 0·00025

Table 2—(contd.)

Number	Location	U (p.p.m.)	Pb (p.p.m.)	Isotopic composition of lead		
				Pb^{204}/Pb^{206}	Pb^{207}/Pb^{206}	Pb^{208}/Pb^{207}
	Ulunda					
	Kolm Lens 6 cm thick (lower zone)					
S–24K	centre	6120 ± 60	363 ± 1	—	0·0708 ± 0·0014	0·0134 ± 0·0008
S–25K	edge	5700 ± 85	220 ± 2	—	0·0769 ± 0·0008	0·0193 ± 0·00035
S–6K	upper zone lens	4560 ± 120	294 ± 5	0·0008	0·0746 ± 0·0006	0·0253 ± 0·0003
S–8K	upper zone lens	6000 ± 70	322 ± 2	—	0·0758 ± 0·0007	0·0170 ± 0·0005
S–7K	Skär	3250 ± 30	190 ± 1	—	0·0890 ± 0·0016	0·0524 ± 0·0011
S–26K	Kvarntorp	2980 ± 120	177 ± 2	—	0·0957 ± 0·0009	0·0628 ± 0·00085
	Karlsro					
S–2K	drill core:	5020 ± 250	302 ± 7	—	0·0731 ± 0·0021	0·0279 ± 0·0014
S–19K	5·97 m	6120 ± 60	344 ± 1·5	—	0·0691 ± 0·0007	0·0150 ± 0·00035
S–17S	6·01 m	306 ± 3	29·4 ± 0·3	0·0110 ± 0·00007	0·216 ± 0·0014	0·432 ± 0·003
S–20S	6·05 m	318 ± 3	44·9 ± 0·4	0·0114 ± 0·00018	0·221 ± 0·0013	0·446 ± 0·006
S–18S	5·21 m	170 ± 1·2	35·7 ± 0·3	—	0·306 ± 0·0045	0·664 ± 0·0075
S–12S	along bedding plane ~6 in. from kolm lens	113 ± 2	36·8 ± 0·37	0·0258 ± 0·0005	0·416 ± 0·003	0·954 ± 0·013
	Dammän					
S–13S	along bedding plane ~6 in. from kolm lens	136 ± 3	27·8 ± 0·6	—	0·363 ± 0·010	0·809 ± 0·013

Letter K after sample denotes kolm sample.
Letter S denotes shale sample.

Table 3. Apparent isotopic ages of Swedish kolm samples
(age in million years)

Number	Location	U (p.p.m.)	Pb (p.p.m.)	U^{238}–Pb^{206}	U^{235}–Pb^{207}	Pb^{207}–Pb^{206}
	Bjallum					
S–9K	edge	4240 ± 45	235 ± 2	365 ± 5	435 ± 10	920 ± 15
S–10K	centre	6400 ± 60	351 ± 3	370 ± 8	425 ± 10	770 ± 25
S–11K	edge	4260 ± 60	240 ± 5	355 ± 7	435 ± 15	945 ± 20
	Stolan					
S–14K	centre	5590 ± 120	301 ± 3	360 ± 7	430 ± 10	865 ± 20
S–15K	edge	5020 ± 80	270 ± 2·6	355 ± 7	420 ± 8	840 ± 10
S–22K	centre	5070 ± 70	278 ± 3·5	370 ± 8	425 ± 8	785 ± 20
S–23K	edge	4600 ± 40	261 ± 2	350 ± 5	415 ± 7	840 ± 30
S– 1K		4700 ± 50	324 ± 4	435 ± 8	480 ± 10	730 ± 25
S– 4K		4760 ± 70	328 ± 5	455 ± 10	480 ± 10	650 ± 25
S– 5K		4910 ± 100	301 ± 10	410 ± 10	440 ± 10	680 ± 15
	Ulunda					
S–24K	centre	6120 ± 60	363 ± 1	400 ± 5	455 ± 10	800 ± 40
S–25K	edge	5700 ± 85	220 ± 2	255 ± 10	330 ± 8	920 ± 30
S– 6K	upper zone	4560 ± 120	294 ± 5	425 ± 13	480 ± 10	785 ± 30
S– 8K	upper zone	6000 ± 70	322 ± 2	360 ± 5	430 ± 8	905 ± 30
	Skär					
S– 7K		3250 ± 30	190 ± 1	365 ± 8	445 ± 10	915 ± 60
	Kvarntorp					
S–26K		2980 ± 120	177 ± 2	370 ± 15	455 ± 17	970 ± 40
	Karlsro					
S– 2K		5020 ± 250	307 ± 7	395 ± 20	435 ± 25	700 ± 80
S–19K	Karlsro drill core	6120 ± 60	344 ± 1·5	380 ± 5	420 ± 10	720 ± 30

assumptions concerning the common lead correction. The explanation lies in the differential movement of parent or daughter elements due to chemical alteration. The kolm has not satisfied the basic assumption of a closed chemical system since the mineral was first formed. If the nature and extent of alteration can be understood, some further information on the actual age of this and similar formations may be obtained from the isotopic ages. The isotopic ages are remarkably uniform and are independent of geographical locality or stratigraphic position. The histogram of U^{238}/Pb^{206} ages given in Fig. 6 illustrates this uniformity. The isotopic ages, U^{238}/Pb^{206} = 370 million years, U^{235}/Pb^{207} = 430 million years and Pb^{207}/Pb^{206} = 860 million years, are representative of this formation, with two groups of samples varying from this by minor but significant amounts. One group comprises three samples from Stolan and possibly one from Ulunda where the U^{238}/Pb^{206} age averages 440 million years and the Pb^{207}/Pb^{206} age 720 million years. This suggests a higher Pb^{206} content relative to the other lead isotopes in this group than the average. The other group comprises two samples taken from a single kolm lens from Ulunda. Here, one sample has a U^{238}/Pb^{206} of 255 million years, by far the largest variation from the average noted while another sample just 2 cm away has a U^{238}/Pb^{206} of 400 million years. In both samples the Pb^{207}/Pb^{206} age is within the average of most of the samples run. Variations of lead–uranium ages without a corresponding variation in the lead–lead age indicates geologically recent alteration.

The fact that the Kvarntorp specimen is as discordant as the average kolm from the Billingen area shows that the Permian (?) diabase sill which intruded the overlying Silurian strata in the Billingen area (Fig. 2), but which did not cover the Kvarntorp area, is not the cause of the discordance. Likewise the data from Ulunda show that there is no difference in the apparent age or degree of discordance of the upper and lower kolm horizons.

Table 4 presents the isotopic ages measured at the centre and edge of four different kolm lenses together with data on the present state of equilibrium for some selected samples. The analyses established several important facts. (1) The uranium content of the centre is consistently higher than the edge. This has been observed before (for example, Wetzel, 1947) and illustrates the correlation of uranium with organic content. (2) The U/Pb ratio is essentially constant except for the lens from Ulunda (S–24K, S–25K).

In the lens from Ulunda there is a definite correlation between the observed isotopic ages and the non-equilibrium condition of the uranium daughters. The 400 million year U^{238}/Pb^{206} age on S–24K reflects the loss of some uranium which occurred recently since Th^{230} is in excess by 15 per cent. Also, the low U/Pb ages of S–25K may be explained as due to recent lead loss as seen in the great deficiency in Pb^{210}. S–24K is the only sample where Th^{230} was found to be not in equilibrium with U^{238}. S–25K is the only sample where the activity of Pb^{210} varies greatly from the activity of its nearest long-lived parent, Ra^{226}.

In all cases, where Ra^{226} has been measured, its activity is deficient with respect to uranium. Where centre–edge pairs have been measured, the piece in the centre of the lens has lost less radium than the edge piece. This pattern, if prolonged over considerable portions of geologic time, would cause corresponding variations

Table 4. Swedish kolm, comparison of isotopic age with present alteration

Sample		Apparent age $\times 10^6$ years			Activity ratio: $U = 1{\cdot}00$		
		U^{238}–Pb^{206}	U^{235}–Pb^{207}	Pb^{207}–Pb^{206}	Th^{230} (80,000 years)	Ra^{226} (1620 years)	Pb^{210} (22 years)
S–10K	centre of lens	365	435	920	—	0·84	—
S–9K	edge of lens	370	425	770	—	0·64	—
S–14K	centre of lens	360	430	865	0·995 ± 0·025	0·82	0·736 ± 0·014
S–15K	edge of lens	355	420	840	1·02 ± 0·02	0·46	0·422 ± 0·010
S–24K	centre of lens	400	455	800	1·15 ± 0·04	0·85	0·794 ± 0·010
S–25K	edge of lens	255	330	920	0·995 ± 0·02	0·68	0·370 ± 0·015
S–26K	Kvarntorp	370	455	970	—	0·51	—
S–19K	Karlsro drill core	380	420	720	1·00 ± 0·02	0·93	—

in the U/Pb ages; since such variations are not observed, the radium loss pattern observed is geologically recent. It appears that there may be some loss of lead at the present time also, but the 10 per cent error on the radium determinations almost covers the discrepancies.

In summary therefore, the Swedish kolm samples are undergoing an accelerated leaching process, due probably to their present outcropping position. Radium is the most easily leached element followed by lead. It should be emphasized, however, that the isotopic ages U^{238}/Pb^{206} = 370 million years, U^{235}/Pb^{207} = 430 million years and Pb^{207}/Pb^{206} = 860 million years, were fixed by events occurring in the geologic past and that present-day alteration has not affected this except for the Ulunda lens (S–24K, S–25K).

The drill core sample (S–19K) shows less radium loss than other specimens which may indicate that it is more protected from surface leaching, but the isotopic ages on S–19K are not significantly different from those on outcrop samples.

The magnitude of alteration observed cannot be extrapolated back throughout the history of the formation. However, the fact that radium is readily leachable, and lead somewhat so, means that these elements are the most likely to have been leached in the geologic past.

The results of investigations as to the present state of equilibrium in the shale phase of the formation are presented in Table 5 together with the isotopic ages and the radiogenic Pb^{207}/Pb^{206} ratios.

In the case of the shales, there is no correlation at all between the isotopic ages and the present state of equilibrium. Indeed, the shales appear to be more nearly in equilibrium than the kolm lenses, although the U/Pb ages are much more variable than in the kolm. As with the kolm, the isotopic ages found in the shale are a consequence of processes occurring in the geologic past. Two points are worth noting concerning the isotopic ages:

(1) Three of the five shales analyzed give U^{238}/Pb^{206} ages greater then 500 million years, considerably greater than found in any kolm sample.

(2) The radiogenic Pb^{207}/Pb^{206} ratios in all shale samples are considerably lower than in any kolm sample. Indeed, in three cases, the radiogenic Pb^{207}/Pb^{206} ratio is less than 0·046, the present-day activity ratio of U^{235}/U^{238}.

Both these phenomena can be explained by the presence in the shale of excess Pb^{206} which originated in the nearby kolm lenses. Such a mechanism can also explain the presence on the histogram of Fig. 6 of the high group of samples which come from the Stolan quarry. These samples have, along with high U^{238}/Pb^{206} ages, low Pb^{207}/Pb^{206} ages. This phenomenon can be produced by selective loss of Pb^{206} from the kolm. This point will be elaborated on later.

Data on the leakage of radon from samples of kolm and shale under laboratory conditions are presented in Table 6. The numbers were obtained by sealing a small chip (from 200 to 500 mg) in a vacuum for 3 days and then flowing the radon which had accumulated outside the chip into an ionization chamber for counting. Values for per cent radon loss were then calculated using the measured radium content of the sample.

It appears that under laboratory conditions the kolm and shale have similar radon leakage rates of 1–4 per cent. This increases significantly with temperature

Table 5. Swedish alum shale, comparison of isotopic age with present alteration

Sample	U^{238}–Pb^{206} ($\times 10^6$ years)	Pb^{207}/Pb^{206} ratio	Activity ratio: $U = 1{\cdot}00$		
			Th^{230} (80,000 years)	Ra^{226} (1620 years)	Pb^{210} (22 years)
S–12S Karlsro within 6 in. of kolm lens along bedding plane	550 ± 30	0·030 ± 0·012	—	—	—
S–13S Damman within 6 in. of kolm lens along bedding plane	435 ± 20	0·035 ± 0·018	—	1·0	—
Karlsro drill core*					
S–17S 6·01 m	345 ± 15	0·055 ± 0·004	1·01 ± 0·03	0·92	0·830 ± 0·024
S–18S 5·21 m	530 ± 15	0·040 ± 0·010	1·04 ± 0·03	1·0	0·814 ± 0·018
S–20S 6·05 m	505 ± 15	0·056 ± 0·005	—	0·55	—
S–21S 6·10 m	—	—	—	0·88	—

* Kolm lens intercepted at 5·97 m.

so that at 150°C the apparent leakage is 10–50 per cent. No major structural change occurs as can be seen by the reproducibility at 25°C as measured after each experiment at elevated temperature. The cause of this increase with temperature is probably the increased rate of diffusion of the radon in the microfissures of the kolm. Thus these experiments show that at room temperature a large percentage of the radon is released into microfissures but does not reach the surface of the kolm. It must decay in this position to Pb^{206} which may then be potentially more available to leaching solutions than radiogenic Pb^{206} in the bulk mineral lattice.

Table 6. Radon leakage on kolm and shale (%)

Temp. (°C)	R–9 (near S–9K edge of lens)	R–10 (near S–10K centre of lens)	R–17 (shale near S–17S)	R–18 (shale near S–18S)	R–24 (centre of kolm near S–24K)	R–25 (edge near S–25K)
25	1·5	0·82	1·3	2·7	5·0	2·9
50	2·3	1·2	2·5	4·8	7·6	4·4
25	1·4	0·82	1·2	3·1	4·8	2·8
100	1·3	3·9	32	14	13	12
25	1·9	0·82	1·0	2·2	4·2	2·6
150	24	12	36	56	14	15
25	1·3	0·79	1·0	1·7	4·1	2·4
200	72	27	88			
25	1·2					

The paleogeography of the region, as discussed above, makes it unlikely that the horizon has ever been at a significantly higher temperature than it is now. Furthermore, under conditions of compaction and burial, even at shallow depths, the radon leakage *in situ* must be less than in the free space of the laboratory vessel. Finally, it is noted that there is no correlation between the degree of discordance of the isotopic ages in a kolm lens and the apparent radon leakage as measured in the laboratory.

It is therefore concluded that radon leakage from the bulk kolm lattice is not a direct cause of the age discordance but it may contribute to the alteration process by putting some of the Pb^{206} in more readily leachable positions, i.e. in the microfissures of the kolm.

Interpretation of isotopic relations in the Swedish kolm–shale system

A rigorous formulation of the effects of loss (or gain) of parent or daughter isotopes in the U–Pb system has been given by Wetherill (1956). In principle, Wetherill has shown that an array of minerals showing discordant uranium–lead ages can lead to a solution of the true age provided only one process was responsible for the discordance and also provided that the discordant process occurred only once or has been occurring continuously. For example, if lead loss happened at

one distinct time, a true age can be deduced from the pattern of the isotopic ages. Lead loss at two or more distinct periods, however, so complicates the apparent isotopic ages that no unique solution for a true age can be made.

It is of interest to determine on this basis whether a single mechanism of discordance occurring at a single time or continuously can explain the pattern of ages obtained. If this situation prevails, a true age for the kolm can be deduced. If this situation does not prevail, it should be possible, by using other geological and chemical considerations, to deduce what multiple processes of discordance have occurred.

All Swedish kolm samples assume the age pattern $U^{238}/Pb^{206} < U^{235}/Pb^{207} < Pb^{207}/Pb^{206}$. Three processes occurring alone, can cause such a pattern: lead loss, uranium introduction and loss of an intermediate in the U^{238} decay chain. The latter possibility is a result of the finding in disequilibrium studies that Ra^{226} is deficient in these samples. An atom of Ra^{226} in the U^{238} chain has a mean life of 2340 years, while the corresponding radium isotope in the U^{235} chain has a mean life of only 16·2 days.

Therefore, if slow leaching of radium occurs, there should be a great fractionation of these two isotopes. Such fractionation would eventually result in loss by the sample of Pb^{206}. Thus the U^{238}/Pb^{206} age would be lowered and the Pb^{207}/Pb^{206} raised, while the U^{235}/Pb^{207} ratio would be unaffected and yield the true age of the sediment.

The same kind of argument can be applied to the radon isotopes in the decay chain Rn^{222} ($t_{1/2} = 3{\cdot}82$ days, U^{238} chain) and Rn^{219} ($t_{1/2} = 3{\cdot}9$ sec, U^{235} chain). Slow leakage of radon could result in preferential loss of Rn^{222} and its daughter Pb^{206}.

It should be noted that preferential leaching of Ra^{226} or Rn^{222} would have to be continuous throughout geologic time if there is to be any effect on the isotopic ages. Detailed analysis of the magnitude of the individual apparent ages shows that none of the three processes alone can cause the observed discordance in the isotopic ages.

First, if leaching of a radioactive daughter of U^{238} alone occurred, the U^{235}–Pb^{207} age should be constant. The data show that this quantity varies in apparent age from 480 million years (S–1K, S–4K, S–6K) down to 330 million years (S–25K). Actually, the variation, except for S–25K, is much smaller than this, say from 420 to 480 million years, but well outside the experimental error.

The other possibilities involving lead loss or its equivalent, uranium gain, also cannot explain the data completely. This is true whether it is assumed that the lead loss occurred only recently, continuously over the life of the mineral, or at a single event in the past. This conclusion can perhaps be most easily seen in the two samples which give the most extreme ages, S–4 and S–25K. Lead loss is an essentially simple process in that the greater the lead loss, the lower all three isotopic ages become. S–25K has the lowest U–Pb ages, yet the Pb^{207}–Pb^{206} age of 920 million years is one of the highest found. Similarly S–4K has the highest U–Pb ages, but the lowest Pb^{207}–Pb^{206} age. This behaviour is incompatible with bulk lead loss being the only process.

The above conclusions can be illustrated further by use of the plot of the Pb^{206}/U^{238} vs. Pb^{207}/Pb^{206} ratios which is essentially similar to the Wetherill

(1956) plot of Pb^{206}/U^{238} vs. Pb^{207}/U^{235}, except that it emphasizes variations in the Pb^{206} content. Fig. 7 is such a graph with all the Swedish kolm points plotted. The insert of this figure depicts where the points would fall if only a single mechanism was responsible for the discordance. It is seen that the points spread out in a manner indicative of loss of an intermediate U^{238} daughter or Pb^{206}, but that they do not fall along one curve which they should do if this mechanism were the sole

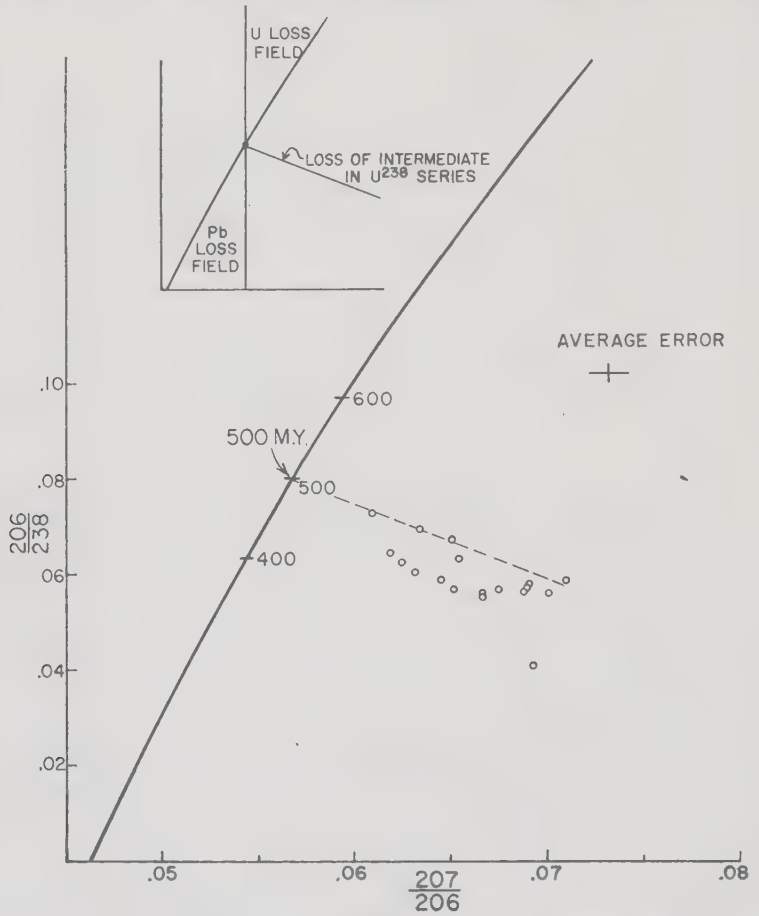

Fig. 7. Plot of Pb^{206}/U^{238} vs. Pb^{207}/Pb^{206} ratios for Swedish kolm samples.

factor causing discordance. If a true age of about 1000 million years is assumed, all the points will lie within the lead loss field, but the spread of points is such that each sample would have had to lose lead or pick up uranium at a time different from all the others, a possibility which is very unlikely.

An explanation involving lead loss is that of two or more discrete periods of lead leaching. This can explain the observed spread in points but it necessitates assuming a true age for this Upper Cambrian formation of at least 970 million years. Such an assumption is contradictory to a large body of evidence for the geological time scale which has been accumulating (Kulp, 1961).

Several lines of reasoning indicate that selective Pb^{206} loss has an important role in causing discordance:

(1) In the concordia plot (Fig. 7) the points spread out in a manner indicating Pb^{206} loss.
(2) The disequilibrium data which shows that Ra^{226} is readily leachable.
(3) The anomalous isotopic data on the shales which can readily be explained by loss of Pb^{206} from the kolm "hot spots" to the shale.
(4) The isotopic ages on certain kolm samples (S–1K, S–4K, S–5K) which have high U^{238}–Pb^{206} ages but low Pb^{207}–Pb^{206} ages.

Isotopic variations of radium, probably resulting from preferential leaching of Ra^{226}, were observed in several uraninites by Kuroda (1955). He measured Ra^{223}/Ra^{226} ratio and found that it was often significantly greater than the expected value of 0·046. He ascribed this as possibly due to variations in the U^{235}/U^{238} ratio, but this was found to be in error (Senftle *et al.*, 1957; Hamer and Robbins, 1960). Rosholt (1958) has investigated uranium disequilibrium in some highly oxidized environments. He found several cases, for example, where the Ac^{227}/Ra^{226} was abnormally low. If this behaviour is continued long enough to build up the stable end products, Pb^{207} and Pb^{206}, these deposits would have abnormally high amounts of Pb^{206} in them, just like the samples of Swedish alum shale measured in this study.

Selective loss of Pb^{206} resulting from migration of Ra^{226} or Rn^{222} makes the points spread out from upper left to lower right on the plot in Fig. 7. The scatter of points off the smooth curve depicting removal of a member of the U^{238} decay chain can be caused by loss of lead or gain of uranium. Lead loss is regarded as the likely process. Pb^{210} is more deficient than Ra^{226} in all samples analysed (Tables 4 and 5). Thus lead loss is known to be occurring at the present time. Further, the postulate of lead loss (meaning loss of Pb^{206} and Pb^{207} in the proportion that they are present in the sample) plus selective Pb^{206} loss leads to a reasonable estimate of the absolute age of this formation. This can be seen with the aid of Fig. 7. Lead loss means all U–Pb ages are minimum, therefore, a line drawn parallel to the theoretical selective Pb^{206} loss line and through the uppermost points will intersect concordia at 500 million years. This is a minimum age since the absolute amount of lead loss is not known. There is still some uncertainty in the absolute age of the Upper Cambrian, but an age of 500 million years or a little greater is quite consistent with the best lines of evidence on the Paleozoic time scale (Kulp, 1961).

The postulate that uranium loss occurs along with selective Pb^{206} loss to cause the discrepant isotopic ages in the Swedish kolm can be ruled out by inspection of Fig. 7. In this case, an approximation to the absolute age of the formation can be made by drawing a line parallel to the theoretical selective Pb^{206} loss and through the lowermost points on the diagram. The intersection with concordia yields a maximum age of 380 million years. This is far lower than any reasonable estimate of the absolute age of the Upper Cambrian. According to the present estimates (Kulp, 1961), an age of 380 million years would correspond to the Lower–Middle Devonian. Also, disequilibrium studies (Tables 4 and 5) show U^{238} to be in equilibrium with Th^{230} except for S–24K which may be taken to be a special case in view of the large amount of lead loss found for a neighbouring sample (S–25K).

Disequilibrium studies also rule out the possibility that the kolm pods have acquired their uranium gradually over geologic time. If this were the case, there is no reason why it should not be occurring at the present time, but there is no evidence of this in the U^{238}/Th^{230} ratios. Also, if the high concentrations of organic material in the kolm localize precipitation of uranium, the greatest amount of uranium should be found at the points of abrupt change in organic content, which are at the edges of the kolm pods. Table 4 shows that this is not the case and that uranium is concentrated in the centre of the lens and varies with the change in organic content of the kolm itself. These arguments support the conclusion of Wetzel (1947), and Bates and Strahl (1957) that uranium (and inferentially, other elements present in abnormal concentrations such as V, Cu, Zn) were accumulated in bituminous shales during the sedimentation or diagenetic process.

Extent of alteration

The conclusion has been reached that loss of pure Pb^{206} and lead loss (which means loss of both Pb^{206} and Pb^{207} in the same proportion in which they are present in the sample) are responsible for the isotopic ages seen in the kolm. It is of interest now to consider how much of this loss has occurred for each sample. This can be done by assuming certain true ages and calculating the amount of lead loss and Pb^{206} loss needed to correct the observed ages. The calculations can be done using the following formulae:

$$Q = \text{lead loss} = \frac{(Pb^{207}/U^{235})_{true} - (Pb^{207}/U^{235})_{observed}}{(Pb^{207}/U^{235})true}$$

$$X = Pb^{206}\ \text{loss} = \frac{1 - Q - (Pb^{206}/U^{238})_{observed}/(Pb^{206}/U^{238})_{true}}{1 - Q}$$

Assuming that 500 million years is a reasonable approximation to the true age of the formation, it can be calculated from the above equations that the average kolm sample (represented by the peak in the histogram of Fig. 6) would have lost a total of 16 per cent bulk lead plus another 13 per cent pure Pb^{206}. The most discordant sample, S–25K lost 40 per cent lead and 14 per cent Pb^{206}. The least discordant samples (S–1, S–4, S–5) lost as little as 5 per cent total lead and 5 per cent pure Pb^{206}.

Mechanism and time of alteration

Alteration may have occurred continuously over the life of the kolm or only recently. A thermal pulse in the geologic past might conceivably have produced the bulk lead loss but not the Pb^{206} loss. Such a thermal pulse appears unlikely, however, for a number of reasons. The presence of petroleum in the shale, the thin stratigraphic load, the undisturbed sedimentary structure and the absence of major intrusives in the area all argue against such an event. The only potential source of heat in the geologic past is the presence of the thin Permian (?) diabase sill in the Silurian rocks about 110 m above the kolm horizon. This sill could not have had any appreciable effect on the isotopic ages because S–26K from Kvarntorp, where there is no diabase sill, has apparent ages similar to the rest of the samples.

Therefore the alternatives are that alteration has been taking place continuously, or it has all taken place recently.

The losses of radium and lead which the kolm is at present experiencing are probably due to ground water action. Such action, if continuous throughout the history of the formation would result in the isotopic ages seen today. Ground water could remove radium and lead from the kolm lens and transfer it via cracks and fissures or bedding planes into the shale or entirely out of the area. Thus, it is to be expected that increments of radium and lead from the kolm would be deposited rather spottily in the shale and would account for the variations in isotopic ratios seen in the shale (Table 5). Certainly, a continuous halo of excess Pb^{207} and Pb^{206} in shale around kolm lens is not found as can be seen from the drill core samples in Table 5. Since both radium and lead are migrating, they will presumably deposit in different proportions in different shale samples. Thus, it is theoretically possible to find any lead ratio in the introduced lead from pure Pb^{206} to a Pb^{207}/Pb^{206} representative of the bulk ratio in the kolm.

The isotopic ages can also be explained if it is assumed that the formation was a closed system during most of geologic time and has become subject to ground water action since it has been at the surface for the last few million years. Lead loss is straightforward, but in order to account for excess Pb^{206} loss, it must be postulated that this isotope was introduced into positions more readily leachable by slight migration of Ra^{226} and/or Rn^{222}. Then recent ground water can remove both pure Pb^{206} and bulk lead (Pb^{206} and Pb^{207}). Deposition of these isotopes in the shale need not be uniform since Pb^{206} would be removed before the bulk lead.

One method of deciding between the alternatives of continuous vs. recent ground water action would be to run a sample from a deep drill core. If the isotopic ages showed little or no discordance, recent surface ground water leaching is indicated. If the isotopic ages show little change from those already run, continuous ground water action is the probable mechanism.

Summary and Conclusions

The results and analysis above lead to the following conclusions:

(1) Techniques have been developed for performing lead, uranium and lead isotopic analysis of samples of black shale. The analytical accuracy is at least ± 3 per cent. In addition, measurements of Th^{230}, Ra^{226}, Pb^{210} and radon leakage have been made to further elucidate the history of uranium and lead in black shales.

(2) In the Upper Cambrian Swedish kolm, the isotopic age discordance, U^{238}–$Pb^{206} < U^{235}$–$Pb^{207} < Pb^{207}$–Pb^{206} is invariably present. It can be shown that at least two processes of discordance are responsible for these apparent ages.

(3) Inspection of the isotopic ages shows that preferential removal of Pb^{206} must have been an important cause of the discordance.

(4) Experimental confirmation of point (3) is seen in the isotopic data on the shale surrounding the kolm. The age pattern U^{238}–$Pb^{206} > U^{235}$–$Pb^{207} > Pb^{207}$–Pb^{206} and the very low Pb^{207}/Pb^{206} ratios must have been caused by removal of Pb^{206} from the kolm and deposition in the shale.

(5) Both radium and radon are found to be mobile in the kolm under suitable conditions. Since the half-lives of radium and radon in the U^{238} decay chain are

considerably longer than their respective isotopes in the U^{235} chain, this provides a mechanism which can result in loss of pure Pb^{206}. The exact mechanism involves either direct loss of Ra^{226} or movement of Ra^{226} and Rn^{222} into intergranular spaces in the kolm, followed by decay to Pb^{206} and then preferential removal of this isotope by ground water action.

(6) Disequilibrium studies show that the radium isotopes are the most readily leachable of the daughters of the uranium series followed by the lead isotopes.

(7) A minimum of 500 million years can be deduced for the age of the Swedish kolm assuming that discordance is due to loss of Pb^{206} due to movement of Ra^{226} and/or Rn^{222} and bulk lead loss. The 500 million years minimum date for the Upper Cambrian is in excellent agreement with the latest results on the absolute geologic time scale.

(8) Studies on the disequilibrium condition of uranium and its daughters in bituminous shales can lead to valuable conclusions concerning the interpretation of measured isotopic ages.

Acknowledgements—The results of this investigation were submitted in partial fulfillment of the requirements for the Ph.D. dissertation at Columbia University. The authors wish to thank B. Dahlman of the Swedish Geological Survey for his help in collecting the samples and his invaluable information on the geological relationships. B. F. Howell provided a comprehensive evaluation of the present status of the Swedish Peltura zone in world-wide paleontologic correlation. T. F. Bates of Pennsylvania State University kindly provided drill core samples. Discussions of these problems with many of our scientific colleagues were helpful in planning and interpreting the measurements; these included W. S. Broecker, J. Eklund, R. J. Holmes, M. Kay, L. E. Long, R. Rynninger, E. O. Strahl, G. R. Tilton, G. W. Wetherill and F. E. Wickman.

D. S. Miller was responsible for the development of the mass spectrometer techniques and supervised its maintenance. R. Kologrivov ably performed most of the radon leakage and radium measurements. M. Rippey and J. Sonderburg typed the manuscript and J. Brokaw prepared the illustrations.

Financial assistance, without which this study could not have been made, was provided by the United States Atomic Energy Commission under Contract AT (30-1)-1114.

References

Adams J. A. S. and Weaver C. E. (1958) Thorium to uranium ratios as indicators of sedimentary processes: example of concept of geochemical facies. *Bull. Amer. Ass. Pet. Geol.* **42,** 387–430.

Bate G. L. (1955) Variations in the isotopic composition of common lead and the history of the crust of the earth. Ph.D. thesis, Columbia University.

Bate G. L., Volchok H. L. and Kulp J. L. (1954) A low level radon counting system. *Rev. Sci. Instrum.* **25,** 153–157.

Bates T. F. and Strahl E. D. (1957) Mineralogy, petrography and radioactivity of representative samples of Chattanooga shale. *Bull. Geol. Soc. Amer.* **68,** 1305–1314.

Bates T. F. and Strahl E. D. (1958) Mineralogy and chemistry of uranium shales. *Proceedings of the Second International Conference on Peaceful Uses of Atomic Energy* Vol. 2, p. 407–411. United Nations, New York.

Clarke F. W. (1924) The data of geochemistry. *U.S. Geol. Surv. Bull.* 770, 841.

Cobb J. C. (1959) Isotopic geochemistry of uranium and lead in the Swedish kolm and its associated shale. Ph.D. thesis, Columbia University.

Hamer A. N. and Robbins E. J. (1960) A search for variations in the natural abundance of U-235. *Geochim. et Cosmochim. Acta* **19,** 143–145.

Holmes A. (1947) The construction of a geological time scale. *Trans. Geol. Soc. Glasgow* **21,** 117–152.

Howell B. F. and Committee (1944) Correlation of the Cambrian formations of North America. *Bull. Geol. Soc. Amer.* **56,** 993–1003.

Inghram M. (1954) Stable isotope dilution as an analytical tool. *Ann. Rev. Nucl. Sci.* **4,** 81–91.

Koczy F. F. (1949) The thorium content of the Cambrian alum shales of Sweden. *Sver. Geol. Undersok.* C, No. 509.

Kulp J. L. (1961) The geological time scale. *Science,* In press.

Kulp J. L. and Eckelmann W. R. (1957) Discordant U-Pb ages and mineral types. *Amer. Min.* **42,** 154–164.

Kuroda P. K. (1955) On the isotopic constitution of radium in uranium minerals and recent problems of geochronology. *Ann. N.Y. Acad. Sci.* **62,** No. 8, 177–208.

Lundqvist G., Hogbom A. and Westergard A. H. (1931) Beskrivning till Kartbladet Lugnas. *Sver. Geol. Undersok.* Aa, No. 172.

Miller D. S. (1960) isotopic geochemistry of uranium, lead and sulfur in Colorado Plateau ores. Ph.D. Thesis, Columbia University.

Munthe H., Westergard A. H. and Lundqvist G. (1928) Beskrivning till Kartbladet Skovde. *Sver. Geol. Undersok.* Aa, No. 121.

Nier A. O. (1939) The isotopic constitution of radiogenic leads and the measurement of geological time—II. *Phys. Rev.* **55,** 153–163.

Patterson C. C. (1951) *The Isotopic Composition of Trace Quantities of Lead and Calcium.* Atomic Energy Commission Report AECD 3180.

Rosholt J. N. (1958) Radioactive disequilibrium studies as an aid in understanding the natural migration of uranium and its decay products. *Proceedings of the Second International Conference on the Peaceful Uses of Atomic Energy, Geneva,* 1958, Paper 772, pp. 230–236. United Nations, New York (1958).

Rynninger R. (1957) Mode of occurrence of uranium in Swedish black shales preliminary investigations. *Geol. Foren. Stockholm Forh.* **79,** 88–90.

Sandell E. B. (1950) *Colorimetric Analysis of Traces of Metals.* Interscience, New York.

Senftle F. E., Stieff L., Cuttitta F. and Kuroda P. K. (1957) Comparison of the isotopic abundance of U^{235} and U^{238} and the radium activity ratios in Colorado Plateau uranium ores. *Geochim. et Cosmochim. Acta* **11,** 189–193.

Tilton G. R. (1951) *The Distribution of Trace Quantities of Uranium in Nature.* Atomic Energy Commission Report AECD 3182.

Tilton G. R., Patterson C., Brown H., Inghram M., Hayden R., Hess D. and Larsen E. S., Jr. (1955) Isotopic composition and distribution of lead, uranium and thorium in a Pre-Cambrian granite. *Bull. Geol. Soc. Amer.* **66,** 1131–1148.

Tilton G. R., Davis G. L., Wetherill G. W. and Aldrich L. T. (1957) Isotopic ages of zircons from granites and pegmatites. *Trans. Amer. Geophys. Un.* **38,** 360–371.

Wells R. C. (1930) *Report of Committee on Measurement of Geological Time* p. 4.

Wells R. C. and Stevens R. E. (1931) Further studies on kolm. *J. Wash. Acad. Sci.* **21,** 409–414.

Westergard A. H. (1922) Sveriges olenidskiffer. *Sver. Geol. Undersok.* Ca, No. 18.

Wetherill G. W. (1956) Discordant uranium-lead ages—I. *Trans. Amer. Geophys. Un.* **37,** 320–326.

Wetzel W. (1947) Sedimentpetrographische studien an den Kambro-Silurischen Ablagerungen des Billingen. *Z. dent. geol. Ges.* **99,** 139–149.

Wickman F. E. (1942) On the emanating power and the measurement of geologic time. *Geol. Foren. Stockholm Forh.* **64,** 465–476.

Geochimica et Cosmochimica Acta, 1961, Vol. 24, pp. 250 to 259. Pergamon Press Ltd. Printed in Northern Ireland

Experimentelle Gesteinsmetamorphose—V

Experimentelle anatektische Schmelzen und ihre petrogenetische Bedeutung

H. G. F. Winkler und H. von Platen
Mineralogisches Institut der Universität, Marburg/Lahn, Germany

(*Received* 25 *November* 1960)

Abstract -In high-grade metamorphic rocks a partial anatectic melt is formed at a temperature of 700 ± 40 C and 2000 atm of H_2O-pressure whenever quartz and alkali-feldspar are constituents of the rock. If only plagioclase and quartz are the leucocratic minerals that temperature is a little higher, whereas higher pressures lowers it. Formation of a *liquid* portion in a high-grade regional metamorphic complex must be reckoned upon, thus giving rise to migmatites and palingenetic granitic rocks.

Anatexis always starts with the formation of an aplitic quartz–alkali-feldspar melt; with small rise in temperature, this changes continually to granitic, granodioritic and tonalitic. But it depends on the ratio of the components of albite to potassium-feldspar in the metamorphic rock which of those compositions is attained by the melt in the final anatectic stage. Metamorphosed greywackes with often an extremely high ratio give tonalitic melts; those clays with extremely low ratio give aplitic melts, and rocks with intermediate ratios give granitic or granodioritic melts, as, per example, most shales.

Melts formed by anatexis of metamorphosed greywackes and different lime-free and lime-bearing clays (partly with increased Na-content) are represented in Fig. 1 and compared with the frequency of distribution of magmatic rocks which contain quartz as a main constituent. Fig. 2. These are the "granitoid" or granitic rocks in the wider sense. The compositions of the anatectic melts lie well in the field of the granitoid rocks, except the aplitic melts which are not abundant and cannot be expected to be so.

Regarding the formation of migmatites, a sedimentary complex of different greywackes only is visualised as an example. By metamorphism a complex of banded gneiss will be formed; when this reaches the stage of anatexis this complex will show that at a same temperature some beds are partially liquified, but the amount of melt is very different, whereas other beds are still completely solid. This has the consequence of a very different mechanical behaviour of the different beds within the complex. This might be one of the principal causes for the very different structures which migmatites display. If the temperature of anatexis has risen further so that more than about 50% of *each* of the beds are liquid, then a mingling and an obliteration of the previous boundaries between different beds will take place, thus giving rise to nebulites and even to rather homogenous rocks.

In unseren Arbeiten über experimentelle Gesteinsmetamorphose wurde festgestellt, dass es nur einer geringen Temperaturerhöhung bedarf, um eine Anatexis, d.h. eine partielle Verflüssigung eines hochgradigen Metamorphits zu erreichen. Die Anatexis schliesst sich unmittelbar an die hochgradige Metamorphose an und beginnt bereits bei Temperaturen um 700 ± 40°C (bei 2000 atm H_2O-Druck) vorausgesetzt, dass der Metamorphit Quarz und Alkalifeldspat enthält. Wenn kein Alkalifeldspat, sondern nur Plagioklas und Quarz als leukokrate Minerale vorhanden sind, dann liegt die Temperatur des Beginns der Anatexis etwas höher; bei höherem H_2O-Druck etwas niedriger. Man muss daher in einem hochmetamorphen Grundgebirgskomplex mit der Entstehung partieller *Schmelzen* und mit der Möglichkeit ihrer mehr bzw. weniger weiten Abtrennung und Verselbständigung rechnen, was zur Palingenese "granitoider" Magmatite bzw. zur Bildung von Migmatiten führt.

Es soll ein zusammenfassender Überblick über alle anatektischen Schmelzen gegeben werden, welche in unseren bisherigen Versuchen entstanden sind. Ausser der Anatexis hochgradig metamorphisierter Grauwacken (Winkler und von Platen, 1961) wurde die Anatexis von metamorphisierten kalkfreien und kalkführenden Tonen, deren Na_2O-Gehalt zum Teil dem Mittelwert von Schiefertonen

angeglichen worden ist, untersucht (WINKLER, 1957; WINKLER und VON PLATEN, 1958, 1960).

Alle Experimente wurden isochemisch unter 2000 atm H_2O-Druck und bei Temperaturen bis zu 810°C ausgeführt. H_2O war immer in ausreichender Menge zugegen, so dass die entstandene Schmelzphase stets an H_2O gesättigt war. Es wurde sorgfältig darauf geachtet, dass sich immer das Reaktionsgleichgewicht eingestellt hat und ferner, dass beim Abschrecken der Versuchsproben keine der schon in der Schmelze gelösten Komponenten auskristallisierten (siehe WINKLER und VON PLATEN, 1961).

Die Untersuchungen ergaben, dass sich *aplitische, granitische, granodioritische und tonalitische Schmelzen* bilden können. In jedem Fall beginnt die Anatexis bei Temperaturen zwischen 670°C und 740°C bei 2000 atm H_2O-Druck mit der Bildung von aplitischen Alkalifeldspat–Quarz–Schmelzen, aus denen sich mit steigender Temperatur durch fraktionierte Aufschmelzung vor allem von Plagioklas *kontinuierlich* granitische, granodioritische und tonalitische Schmelzen entwickeln, welche dann auch einige Prozente an Mafiten gelöst enthalten.

Die Zusammensetzung des hochgradig metamorphen Gesteins bestimmt, welche Schmelze jener kontinuierlichen Reihe im Endstadium erreicht wird. Bei sechs der acht untersuchten Grauwacken werden anatektische Schmelzen tonalitischen Charakters gebildet, so dass alle vorhergehenden Stadien der kontinuierlichen Reihe, nämlich aplitisch, granitisch und granodioritisch, als Zwischenstadien in einem engen Temperaturbereich von insgesamt nur 40–60°C durchschritten werden. Das Endstadium, welches in diesen Fällen tonalitische Zusammensetzung hat, bleibt dagegen auch bei Temperatursteigerung um mehrere hundert Grad erhalten. Es ist daher vor allem das Endstadium, welchem eine besondere petrogenetische Bedeutung für die Palingenese zukommt. Bei zwei der acht metamorphen Grauwacken und bei den in Abb. 1* (Feld III) vermerkten Ausgangsgesteinen wird im Laufe der Anatexis keine tonalitische sondern eine granodioritische Schmelze als Endstadium erreicht. Andere Ausgangsgesteine bilden bei der Anatexis eine granitische Schmelze als Endstadium (Abb. 1, Feld II), und wiederum andere Gesteine, welche besonders wenig Na_2O enthalten, liefern nur aplitische Schmelzen (Feld I in Abb. 1).

Entscheidend für den *petrochemischen Charakter der anatektischen Schmelzen im Endstadium* ist in erster Linie das modale, aus dem quantitativen Mineralbestand des hochgradigen Metamorphits feststellbare Verhältnis der Komponenten Albit zu Kalifeldspat, was völlig einleuchtend ist. Wenn dieses Verhältnis kleiner als etwa 0,4 ist, dann entstehen nur aplitische Schmelzen; granitische Schmelzen bilden das Endstadium, wenn das Verhältnis Albit zu Kalifeldspat zwischen 0,4 und 1,5 liegt; für granodioritische Schmelzen liegt es zwischen 1,5 und 3,5, und für tonalitische Schmelzen ist es grösser als etwa 3,5. Dies bedeutet, dass in der Regel mit steigendem Verhältnis der Gew-% Na_2O/K_2O der Metamorphite die anatektischen Schmelzen in der Reihe aplitisch bis tonalitisch voranschreiten. Aber dieses

* In Abb. 1 konnte nur das kritische Komponentenverhältnis von normativem Quarz zu Albit zu Kalifeldspat dargestellt werden. Es sei aber darauf hingewiesen, dass in allen granitischen, granodioritischen und tonalitischen Schmelzen sich neben Albit-stets auch Anorthit-Komponente befindet, so dass die Schmelzen kalkalkalischen Charakter haben; siehe die zitierten Arbeiten.

Verhältnis der Gew-% erlaubt nur eine angenäherte Aussage, weil Glimmer K_2O bindet und dadurch das entscheidende modale Komponentenverhältnis Albit zu Kalifeldspat nur angenähert wiedergegeben ist.

Die anatektischen Schmelzen müssen, wenn sie von ihrem jeweiligen kristallinen Rest, speziell vom An-reichen Plagioklas und grösseren Mengen von Cordierit (soweit diese vorhanden) mehr oder weniger weit separiert sind, als Mineralgemenge von Apliten, Graniten, Granodioriten bzw. Tonaliten auskristallisieren. Grössere Komplexe von Apliten sind nicht häufig zu erwarten, weil es nur wenige metamorphe Gesteine gibt, die ein so kleines Albit- zu Kalifeldspatverhältnis von $<0{,}4$ haben, um ein aplitisches Endstadium zu bilden. Wenn auch alle Gesteine, deren Verhältnis Albit zu Kalifeldspat grösser ist, stets aplitische Schmelzen im *Anfangs*stadium der Anatexis bilden, so werden diese keine grosse Bedeutung haben, weil (a) die Schmelzmenge noch recht gering ist, und weil (b) schon eine sehr geringe Temperatursteigerung von meistens 10–20°C, bisweilen 40°C, die aplitische Schmelze in eine granitische verändert. Dagegen werden granitische, granodioritische und auch tonalitische Schmelzen wesentlich häufiger entstehen, weil das für ihre anatektische Bildung notwendige Verhältnis von Albit zu Kalifeldspat ($>0{,}4$) wesentlich häufiger in metamorphen Gesteinen anzutreffen ist. Insbesondere müssen sich, entsprechend der geochemischen Häufigkeit von Schiefertonen und ihrer mittleren Zusammensetzung vor allem granitische Schmelzen häufig bilden.

Es ist erforderlich, noch einmal darauf hinzuweisen, dass alle unsere Ausgangsgesteine so quarzreich waren, dass während der Anatexis noch Quarz als kristalliner Rest übrig bleibt; bei fast allen Ausgangsgesteinen lag von Natur aus eine ausreichende Quarzmenge vor, nur bei zwei Calcit-führenden Tonen musste Quarz zugegeben werden. Es hatten sich also bei der Anatexis stets Schmelzen bilden können, die an Quarzkomponente gesättigt waren, was auf Grund unserer Versuche bei der Anatexis von metamorphisierten Sedimenten in der Natur ebenfalls die Regel sein muss. Quarz ist also ein Hauptbestandteil der anatektisch gebildeten Schmelzen.

Die Anatexis beginnt natürlich mit der Bildung einer geringen Schmelzmenge, die sich schnell mit steigender Temperatur vergrössert; siehe Tabelle 1. Eine über einen grossen Temperaturbereich fast unveränderte, nahezu maximale Schmelzmenge wird dann in dem vorher gekennzeichneten Endstadium der Anatexis erreicht. Diese Mengen hängen von der mineralogischen Zusammensetzung des hochgradigen Metamorphits ab. Sie sind umso grösser, je grösser die Mineralmengen an Alkalifeldspat und An-ärmerem Plagioklas (bis etwa An 30) sind, und je vollkommener die Menge des Quarzes das jeweilige kotektische Verhältnis erfüllt; dies ist der Fall, wenn die Menge des Quarzes etwa halb so gross ist (50–60%) wie die Menge aller Feldspäte. Liegt mehr Quarz vor, dann bleibt ein nichtaufgeschmolzener Rest übrig. Ist An-reicherer Plagioklas vorhanden, dann wird nur ein Ab-reicher Anteil aufgeschmolzen; sehr An-reiche Plagioklase bleiben als kristalliner Rest erhalten. Die Menge der Schmelze ist umso geringer, je grösser die Menge an Mafiten ist; denn nur wenige Prozente von Biotit, Cordierit (wahrscheinlich auch Granat) und Sillimanit werden in den anatektischen Schmelzen gelöst, während Hämatit überhaupt nicht von der Schmelzphase aufgenommen wird.

Die bei der Anatexis verschiedener Ausgangsgesteine gebildeten maximalen

Mengen der Schmelzen sind aus Tabelle 1 ersichtlich, wo ebenfalls ihr petrochemischer Charakter angegeben ist. In fast allen Fällen ist mehr als die Hälfte des Metamorphits im Endstadium der Anatexis verflüssigt worden; sehr oft macht die Schmelzmenge mehr als 2/3 und bisweilen über 80% aus.

Tabelle 1. Anatektische Schmelzmengen in Gew-% bei verschiedenen Temperaturen und Ausgangsgesteinen

Lfd. Nr.	Ausgangsgestein	690°C	710°C	730°C	745°C	750°C	780°C	810°C	
1	Ton A (40/42)	—	37	40	40	40	40	40	aplitisch
2	Ton B (Fithian)	—	—	15	65	65	65	65	
3	Ton C (Bl. Ton)	—	—	52	52	52	52	52	
4	Bl. Ton + 1,8% NaCl	—	—	52	55	56	56	56	granitisch
5	Bl. Ton + 5% $CaCO_3$ + 3% NaCl	—	—	—	6	(28)	32	48	
6	Bl. Ton + 8% $CaCO_3$ + 3% NaCl	—	—	—	6	(24)	23	39	
7	Bl. Ton + 15% $CaCO_3$ + 3% NaCl	—	—	—	4	(34)	34	53	
8	Bl. Ton + 3,2% NaCl	48	54	56	58	58	60	60	grano-dioritisch
9	Bl. Ton + 5% $CaCO_3$ + 6% NaCl	—	—	—	4	(28)	50	81	
10	Bl. Ton + 8% $CaCO_3$ + 6% NaCl	—	—	—	8	(24)	43	63	
11	Bl. Ton + 15% $CaCO_3$ + 6% NaCl	—	—	—	4	(34)	47	71	
12	Strassbg. 1d	—	—	25		43	67	67	
13	Schmittloth.	19	31	43		74	83	83	
14	Gr. St. IV/25	23	48	59		68	73	73	tonalitisch
15	Bicken	24	47	94		96	96	96	
16	OK I/33	19	35	50		74	82	82	
17	Gr. St. IV/29	10	20	49		68	68	68	
18	Gr. St. IV/16	—	10	31		48	63	63	
19	Strassbg. 7b	—	15	38		73	86	86	

Die *Temperatur*, bei der das *Endstadium der Anatexis* erreicht ist, hängt ebenfalls von der mineralogischen Zusammensetzung des hochgradigen Metamorphits ab. Vor allem scheinen zwei Faktoren von Einfluss zu sein: (1) Das modale Verhältnis Albit- zu Kalifeldspatkomponente, welches den petrochemischen Charakter des Endstadiums der Reihe aplitisch–granitisch-granodioritisch-tonalitisch bestimmt; denn je weiter die Zusammensetzung vom aplitischen Anfangsstadium wegrücken kann, umso grösser ist die hierfür notwendige Temperaturerhöhung. (2) Je grösser der An-Gehalt der Plagioklase ist, umso höher ist die Temperatur, bei der das Endstadium erreicht ist. Folgende Beispiele mögen Punkt (2) erläutern: In lfd. Nr. 4 der Tabelle 1 hat sich bei der Metamorphose u.a. Plagioklas der Zusammensetzung An 33 gebildet; bei der Anatexis dieses Metamorphits liegt ein granitisches

Endstadium der Schmelze bereits bei 730°C vor. Die Gesteine der lfd. Nr. 5–7 dagegen enthalten im Metamorphit einen Plagioklas von An 55–60; und daher hat sich die granitische Schmelze erst bei 810°C gebildet. Ein weiteres Beispiel: Die lfd. Nr. 8 bis 11 liefern granodioritische Schmelzen im anatektischen Endstadium und zwar, wenn An 26 (Nr. 8) vorliegt, bei 750°C, und wenn die Zusammensetzung des Plagioklases im Metamorphit An 40–45 (Nr. 9–11) betragen hat, erst bei 810°C.

Die *Temperatur des Beginns der Anatexis* ist, da sich zuerst stets eine Alkalifeldspat–Quarz-Schmelze bildet, von der Zusammensetzung des Alkalifeldspats abhängig. Liegt reiner K-Feldspat vor, dann beginnt die Schmelzbildung bei 740°C; ein zunehmender Ab-Gehalt im Alkalifeldspat (bis etwa Ab 20/Or 80) erniedrigt jene Temperatur bis auf 670°C, wenn 2000 atm H_2O-Druck herrscht.

Wenn nun die Trennung der anatektischen Schmelzen von dem kristallinen Rest die Grössenordnung von Zentimetern bis Metern nicht überschritten hat, dann haben sich migmatitische Gesteine gebildet, auf die später näher eingegangen wird; wenn dagegen eine grossräumige Trennung stattfinden konnte, dann sind *palingene Magmen* entstanden, die auch in kältere Krustenteile *intrudieren* können, weil sie oft überhitzt sein werden. Dies ist für granitische Schmelzen bereits nachgewiesen worden (Winkler und von Platen, 1960) und für tonalitische Schmelzen durch folgendes Beispiel leicht zu belegen: Der hochgradige Metamorphit, der aus der Grauwacke von Bicken gebildet worden ist, ist bei 730°C bereits zu 94% aufgeschmolzen. Bei weiterer Temperatursteigerung wird die Zusammensetzung der Schmelze nicht mehr verändert; Tabelle 1, lfd. Nr. 15. Da bei der natürlichen Anatexis die Temperaturerhöhung nicht gerade bei 730°C aufgehört haben wird, muss die tonalitische Schmelze überhitzt sein.

Es soll nun geprüft werden, ob solche palingenen Schmelzen, wie sie in unseren Experimenten entstanden sind, auch in der Natur vorkommen. In Abb. 1 sind die Zusammensetzungen der verschiedenen Schmelzen dargestellt, die sich im Endstadium der Anatexis befinden, d.h. in dem Stadium, in dem sie über einen grossen Temperaturbereich fast unverändert bleiben. Zum Vergleich ist die Häufigkeitsverteilung aller magmatischen Gesteine, welche Quarz als einen Hauptbestandteil enthalten, aus den chemischen Analysen der Tabellen von Washington (1917) in Abb. 2 dargestellt worden. Die Auswahl der Gesteinsanalysen erfüllte folgende Bedingungen: (1) Die Summe der normativen Mengen an Quarz, Orthoklas, Albit und Anorthit ist $\geq 80\%$; (2) der normative Quarzgehalt ist $\geq 20\%$; (3) die Zusammensetzung der Plagioklase überschreitet An 30 nicht. Auf diese Weise werden alle Gesteine erfasst, welche Quarz als Hauptgemengteil ($\geq 20\%$) und nicht mehr als 20% an normativen Mafiten enthalten. Es sind also alle Gesteine erfasst, die man in der petrogenetischen Literatur mit granitisch im weiteren Sinne oder mit granitoid bezeichnet. Die in Abb. 2 gegebene Darstellung basiert auf 1190 Analysen magmatischer Gesteine und umfasst einen grösseren Bereich als er von Tuttle und Bowen (1958) in ähnlicher Weise dargestellt worden ist. Diese Autoren berücksichtigen mit ihrer Bedingung, dass Q + Or + Ab > 80%, im wesentlichen nur die Granite im engeren Sinne; denn bereits einige Adamellite, fast alle Granodiorite und alle Tonalite sind in ihrer Darstellung nicht mit erfasst worden.

Da bisweilen in granitoiden Gesteinen der Plagioklas die Zusammensetzung An 30 übersteigt, wurde ein zweites Diagramm konstruiert, in dem die vorher gegebene

Bedingung (3) auf An $\leq$ 50 erweitert worden ist. Es ergeben sich dann insgesamt 1500 zu berücksichtigende Analysen, die sich aber hinsichtlich ihrer Verteilung im Diagramm so wenig von Abb. 2 unterscheiden, dass eine Wiedergabe nicht nötig ist; d.h. die Abb. 2 umfasst praktisch auch die erweiterte Bedingung (3).

Vergleicht man das Diagramm von TUTTLE und BOWEN (1958) mit unserer Abb. 2, so stellt man als Gemeinsamkeit fest, dass der Bereich der grössten Häufigkeit sich in Lage und Form nahezu deckt. Der wesentliche Unterschied besteht

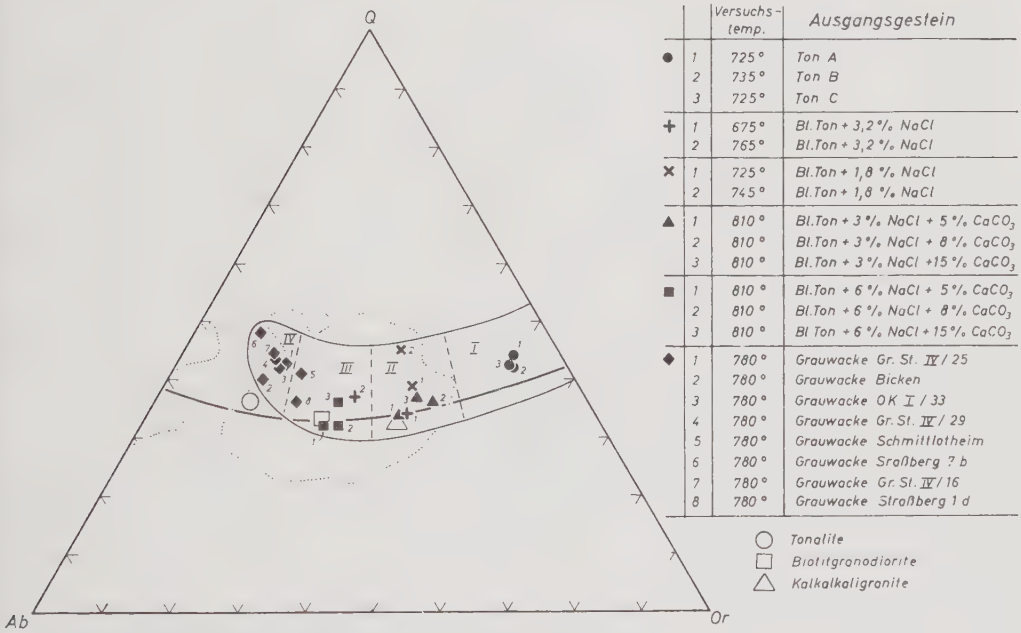

		Versuchs-temp.	Ausgangsgestein
●	1	725°	Ton A
	2	735°	Ton B
	3	725°	Ton C
+	1	675°	Bl.Ton + 3,2 % NaCl
	2	765°	Bl.Ton + 3,2 % NaCl
×	1	725°	Bl.Ton + 1,6 % NaCl
	2	745°	Bl.Ton + 1,6 % NaCl
▲	1	810°	Bl.Ton + 3 % NaCl + 5 % $CaCO_3$
	2	810°	Bl.Ton + 3 % NaCl + 8 % $CaCO_3$
	3	810°	Bl.Ton + 3 % NaCl +15 % $CaCO_3$
■	1	810°	Bl.Ton + 6 % NaCl + 5 % $CaCO_3$
	2	810°	Bl.Ton + 6 % NaCl + 8 % $CaCO_3$
	3	810°	Bl Ton + 6 % NaCl + 15 % $CaCO_3$
◆	1	780°	Grauwacke Gr. St. IV / 25
	2	780°	Grauwacke Bicken
	3	780°	Grauwacke OK I / 33
	4	780°	Grauwacke Gr. St. IV / 29
	5	780°	Grauwacke Schmittlotheim
	6	780°	Grauwacke Straßberg 7 b
	7	780°	Grauwacke Gr. St. IV / 16
	8	780°	Grauwacke Straßberg 1 d

○ Tonalite
□ Biotitgranodiorite
△ Kalkalkaligranite

Abb. 1. Normatives Komponentenverhältnis Q:Ab:Or aller bisherigen experimentellen anatektischen Schmelzen im Endstadium. Die Zusammensetzung dieser Schmelzen ändert sich bei Temperatursteigerung um mehrere Zehnergrade nur noch wenig (WINKLER, 1957; und VON PLATEN, 1958, 1960, 1961). Zum Vergleich sind jene Komponentenverhältnisse der mittleren Zusammensetzungen von Kalkalkaligraniten, Biotitgranodioriten und Tonaliten (nach NOCKOLDS, 1954) eingezeichnet. Die kotektische Linie für das System Q–Ab–Or–H_2O und 2000 atm H_2O-Druck ist ebenfalls angegeben. Die mit römischen Ziffern gekennzeichneten Felder geben an: I, aplitische; II, granitische; III, granodioritische; und IV, tonalitische Zusammensetzung. Der punktiert umgrenzte Bereich basiert auf Abb. 2.

darin, dass in unserem weitergefassten Diagramm der Abb. 2 die Konzentrationsbereiche sich in Richtung auf die Ab–Q-Seite hin vergrössern.

Wenn nun die Lage der in Abb. 1 dargestellten anatektischen Schmelzen mit der Häufigkeitsverteilung der in Abb. 2 dargestellten magmatischen Gesteine verglichen wird, dann erkennt man, dass fast alle anatektischen Schmelzen in demjenigen Bereich sich befinden, in dem 86% aller granitoid zusammengesetzen magmatischen Gesteine liegen. Da die Anzahl unserer Versuche die Häufigkeit der Sedimente in der Natur nicht berücksichtigt, kann aus der Verteilung der darstellenden Punkte der Abb. 1 natürlich nicht auf die Häufigkeitsverteilung der anatektischen Schmelzen geschlossen werden. Aber man erkennt aus den Abb. 1 und 2, dass diejenigen

magmatischen Schmelzen seltener sind, welche bei der Anatexis aus ursprünglich sedimentären Gesteinen entstehen, wenn in den Ausgangsgesteinen das Gewichts-Verhältnis Na_2O zu K_2O extrem gross oder klein ist. Dieses Verhältnis ist bei den metamorphisierten Grauwacken gross, und die Häufigkeit der aus ihnen gebildeten tonalitischen Schmelzen (Feld IV, Abb. 1) ist geringer als die der in den Feldern II und III liegenden granitischen und granodioritischen Schmelzen. Andererseits

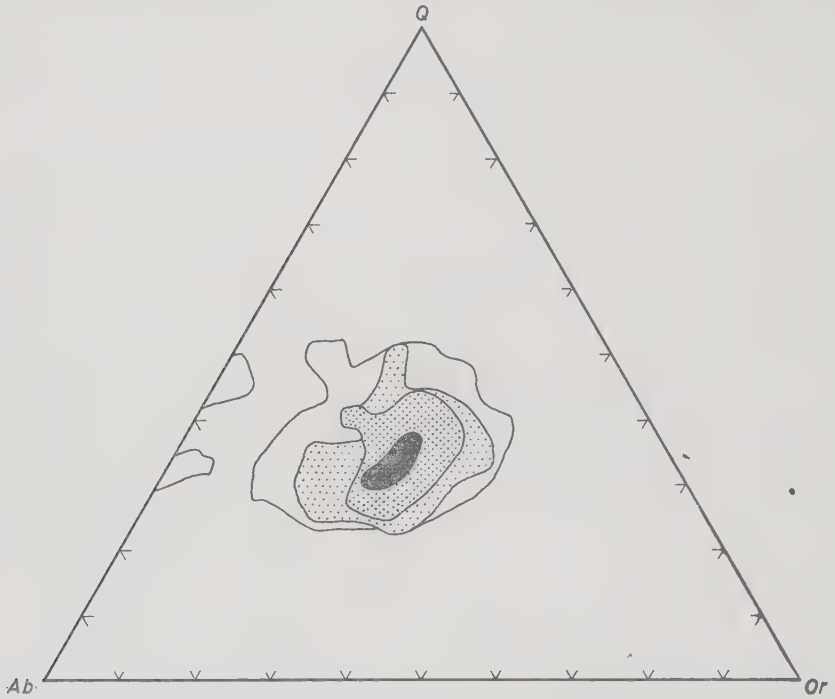

Abb. 2. Häufigkeitsverteilung des normativen Q–Ab–Or–Verhältnisses von 1190 magmatischen Gesteinen aus den Tabellen von Washington, welche die im Text angegebenen Bedingungen erfüllen. Das Diagramm ist auf folgende Weise konstruiert worden: Zuerst wurde die Konzentration der darstellenden Punkte in einer Flächeneinheit, die $\frac{1}{8}$% der gesamten Dreiecksfläche ausmacht, ausgezählt. Dann konnten durch Grenzlinien die Konzentrationsbereiche $>0{,}25$, $>0{,}5$, $>1{,}0$ und $>2{,}0$%, bezogen auf die Anzahl der berücksichtigten 1190 Gesteine = 100%, unterschieden werden. Daraufhin wurde ermittelt, wieviel Prozent der Gesteine in den einzelnen Konzentrationsbereichen liegen; es sind mit abnehmender Grösse der eingezeichneten Bereiche 86, 73, 53 und im schwarz gezeichneten, innersten und kleinsten Bereich 14 %. Ausserhalb der äussersten Kontur liegen die restlichen 14% ziemlich gleichmässig verstreut.

haben einige der von uns untersuchten Tone ein extrem kleines Na_2O/K_2O-Verhältnis; die bei ihrer Anatexis entstehenden aplitischen Schmelzen (Feld I, Abb. 1) sind sehr selten. Wenn jedoch das Na_2O/K_2O-Verhältnis zwischen den Extremen liegt und etwa Werte wie bei der mittleren Zusammensetzung von Schiefertonen, der häufigsten Gruppe sedimentärer Gesteine, besitzt, dann entstehen bei der Anatexis vor allem granitische Schmelzen. Bedenkt man, dass Wechsellagerungen von z.B. Schiefertonen und Grauwacken recht häufig sind, dann muss nach Metamorphose eines derartigen grossräumigen Komplexes bei einer Anatexis und Separierung

palingener Magmen eine Homogenisierung der Schmelzen stattfinden. Die resultierende Zusammensetzung wird granodioritisch–granitisch sein und sich im Bereich grösster Häufigkeit der Abb. 2 befinden.

Es soll nun dargelegt werden, welche Bedeutung anatektische Schmelzen für die Genese von *Migmatiten* haben können. Dazu betrachten wir zunächst sedimentäre Gesteinskomplexe. Diese sind in der Regel aus unterschiedlichen Sedimenten aufgebaut, wie Tonen oder Tonschiefern, die speziell einen variablen Quarz- und Calcitgehalt haben, Sandeinlagerungen aufweisen und z.B. ausserdem mit Grauwacken und noch anderen Gesteinen wechsellagern. Zum Beispiel besteht der von Mattiat (1960) untersuchte Grauwackenkomplex (Kulm) im Harz aus feinkörnigen, mittelkörnigen und grobkörnigen Grauwacken von unterschiedlicher Zusammensetzung und Mächtigkeit, denen dünne Tonlagen zwischengeschaltet sind; zum Teil aber wechseln auch mächtige Tonschiefer mit Grauwacken ab.

Wir haben aus einer der von Mattiat untersuchten Lokalitäten je eine typische Probe von feinkörniger, mittelkörniger und grobkörniger Grauwacke für unsere Untersuchungen zur Verfügung gehabt; diese drei Proben entstammen dem gleichen Bruch (Gr. St. IV, Grosses Steimkertal), in dem in der aufgeschlossenen Profilmächtigkeit von 29 m Mattiat 37 Grauwackenbänke kartiert hat, welche mit 11 Tonschieferlagen ein mächtiges, heterogenes Wechsellagerungspaket bilden. Die Dicke der Grauwackenlagen ist sehr variabel und liegt zwischen 6 und 380 cm, die der Tonschiefer zwischen 4 und 13 cm; in anderen Bereichen sind letztere jedoch wesentlich mächtiger.

Wir wollen uns nun vorstellen, dass ein derartiger sedimentärer Komplex der Metamorphose und Anatexis unterworfen wird. Leider sind die Tonschiefer jenes Aufschlusses von uns noch nicht untersucht worden, aber bereits die drei verschiedenkörnigen Grauwacken des Aufschlusses, die wir durch eine 5% Calcit-führende Grauwacke vom Südharz (Strassberg 1d) ergänzen, zeigen ein sehr interessantes unterschiedliches Verhalten bei der Metamorphose und Anatexis. Der hochmetamorphe Mineralbestand aller dieser vier Grauwacken ist der von Cordierit–Biotit–Plagioklas–Kalifeldspat–Quarz–Gneisen, deren quantitativer Mineralbestand jedoch recht unterschiedlich ist, speziell hinsichtlich der Menge an Biotit, Cordierit, Kalifeldspat und Quarz und der Zusammensetzung des Plagioklases (siehe Winkler und von Platen, 1961, Tabelle 3, S. 53) Bei der regionalen Metamorphose wird unter dem höheren Druck an Stelle von Cordierit Granat entstehen, so dass aus dem sedimentären Komplex granatführende gebänderte Gneise gebildet worden sind.

Wenn nun genügend H_2O vorhanden ist und die Temperatur der Metamorphose den Bereich der Anatexis erreicht, dann beginnt sich in zwei der Grauwackenbänke eine anatektische Schmelze zu bilden, die bei 690°C (und 2000 atm H_2O-Druck) in einem Falle bereits 23%, im anderen nur 10 Gew-% der betreffenden Gesteinspartie ausmacht; in den beiden anderen Grauwacken (IV/16 und Strassberg 1d) dagegen ist bei 690°C noch überhaupt keine flüssige Phase gebildet worden, siehe Tabelle 2, vertikale Spalte.

Bei 710°C liegen noch krassere Unterschiede vor; denn in der einen metamorphisierten Grauwackenlage ist bereits fast die Hälfte flüssig, in der zweiten sind 20% Schmelze, in der dritten sind es 10%, und die vierte Lage ist noch vollkommen fest. Wenn nun eine tektonische Beanspruchung stattfindet, dann ist das mechanische

Verhalten der vier metamorphisierten Grauwackenbänke sehr unterschiedlich. Die eine Lage ist als fester Körper sehr schwer deformierbar, so dass z.B. bei kurzfristigem gerichteten Druck diese zerbrechen kann, während die anderen Lagen, welche 10 bzw. 20% Schmelze enthalten, leicht bzw. sehr leicht plastisch deformierbar sind. Die vierte Lage schliesslich, in der fast 50% Schmelze vorhanden sind, benimmt sich bereits als Ganzes wie ein flüssiger Brei und wird z.B. in aufgebrochene Klüfte der festen Lagen eindringen.

Tabelle 2. Anatexis von Grauwacken. Unterschiedliche Schmelzmengen bei gleicher Temperatur

Ausgangsgestein	Beginn d. Schmelzbildung	Schmelzmengen bei den verschiedenen Versuchstemperaturen in Gew-%				
		690°C	710°C	730°C	750°C	780°C
Gr. St. IV/25	685°	23	48	59	68	73
Gr. St. IV/29	685°	10	20	49	68	68
Gr. St. IV/16	705°	—	10	31	48	63
Strassbg. 1d	725°	—	—	25	43	67

Wenn die Temperatur nur um weitere 20°C steigt, dann hat sich bei 730°C eine Schmelzphase in allen vier Bänderlagen gebildet; die schwer deformierbare feste Schicht ist also nicht mehr vorhanden; alles lässt sich jetzt leicht deformieren. Aber da die Schmelzmengen innerhalb der vier Lagen noch sehr unterschiedlich sind (von 25% bis 60%), muss das Verhalten gegenüber mechanischer Deformation noch recht verschieden sein. Bei weiterer geringer Temperaturerhöhung, wenn die Schmelzmenge 50% in jeder Lage übersteigt, wird wohl eine mechanische Durchmischung unter Verwischung der Bänderlagen und Textur erfolgen können.

Der hier geschilderte Gedankengang ist wegen der leichten Übersichtlichkeit allein am Beispiel unterschiedlicher Grauwacken entwickelt worden. Durch Berücksichtigung von Ton-, Arkose-, Quarzsand- und Tufflagen im sedimentären Komplex würde sich der Vorgang der Anatexis prinzipiell nicht verändern; denn bei einer gleichen Temperatur werden einige Lagen noch keine Schmelzphase, andere dagegen unterschiedliche Schmelzmengen aufweisen, so dass das mechanische Verhalten der Lagen zueinander unterschiedlich sein muss. Ob bei höherer Temperatur eine Durchmischung und Verwischung der Lagengrenzen erfolgen kann, hängt jedoch von der mineralogischen Zusammensetzung des aus dem jeweiligen Sedimentpaket entstandenen Metamorphits ab, insbesondere davon, ob Quarz, Alkalifeldspat und An-ärmerer Plagioklas in genügender Menge vorhanden sind, damit ein ausreichender Schmelzanteil entstehen kann.

Auf diese Weise, also unter *massgeblicher Beteiligung einer anatektischen Schmelzphase*, möchten wir die *Bildung von Migmatiten*, den in der Natur häufig beobachteten Übergang von Bändergneisen in Migmatite, und ihre verschiedenartigen strukturellen Ausbildungen bis zu den Nebuliten und homogenen Anatexiten erklären.

Unsere Vorstellung ist in bester Übereinstimmung mit der Geländebeobachtung. Denn READ (1957, S. 38, 39, 34) stellt fest: "One of the most firmly established facts of metamorphic geology is the close association in the field of high-grade metamorphic rocks and migmatites". "It is clear, that WEGMANN, with many others, considers the domain of regional metamorphism to be transitional to and genetically connected with the domain of migmatisation." "When we follow rocks into higher metamorphic grades we finally end in a granitic core. This cannot be accidental, the association of metamorphites, migmatites and granites must mean something."

Nachdem diese Geländebeobachtungen vorliegen und wir aus den Experimenten über Metamorphose wissen, dass Temperaturen über 650°C zur Bildung höchstgradiger Metamorphite notwendig sind, ist nicht einzusehen, warum die sich unmittelbar anschliessende Anatexis nicht auch grossräumig in der Natur stattgefunden hat. Dann aber muss man die Konzequenz ziehen und den entstehenden granitischen (im weitesten Sinn) *Schmelzen* ihre petrogenetische Bedeutung zuweisen, die bei den bisherigen Hypothesen über "Granitisation und Migmatitbildung" nicht beachtet worden ist und auch nicht erkannt werden konnte, weil sie erst durch die Experimente offenbar geworden ist.

Anerkennung—Die Deutsche Forschungsgemeinschaft, Bad Godesberg, hat unsere Arbeiten apparativ und personell unterstützt und ihr dadurch eine dankbar anerkannte Förderung zuteil werden lassen.

REFERENCES

MATTIAT B. (1960) Beitrag zur Petrographie der Oberharzer Kulmgrauwacke. *Beitr. Mineral. Petrogr.* **7**, 242–280.

NOCKOLDS S. R. (1954) Average chemical compositions of some igneous rocks. *Bull. Geol. Soc. Amer.* **66**, 1007–1032.

READ H. H. (1957) *The Granite Controversy*. Interscience, New York.

TUTTLE O. F. and BOWEN N. L. (1958) Origin of granite in the light of experimental studies in the system $NaAlSi_3O_8$–$KAlSi_3O_8$–SiO_2–H_2O. *Geol. Soc. Amer. Mem.* 74.

WASHINGTON H. S. (1917) Chemical analyses of igneous rocks. *U.S. Geol. Survey Prof. Paper* 99.

WINKLER H. G. F. (1957) Experimentelle Gesteinsmetamorphose—I. Hydrothermale Metamorphose karbonatfreier Tone. *Geochim. et Cosmochim. Acta* **13**, 42–69.

WINKLER H. G. F. und VON PLATEN H. (1958) Experimentelle Gesteinsmetamorphose—II. Bildung von anatektischen granitischen Schmelzen bei der Metamorphose von NaCl-führenden kalkfreien Tonen. *Geochim. et Cosmochim. Acta* **15**, 91–111.

WINKLER H. G. F. und VON PLATEN H. (1960) Experimentelle Gesteinsmetamorphose—III. Anatektische Ultrametamorphose kalkhaltiger Tone. *Geochim. et Cosmochim. Acta* **18**, 294–316.

WINKLER H. G. F. und VON PLATEN H. (1961) Experimentelle Gesteinsmetamorphose—IV. Bildung anatektischer Schmelzen aus metamorphisierten Grauwacken. *Geochim. et Cosmochim. Acta.* **24**, 48–69.

Geochimica et Cosmochimica Acta, 1961, Vol. 24, pp. 260 to 265. Pergamon Press Ltd. Printed in Northern Ireland

Chemical and mineralogical studies of fossil red clays from Timor

S. K. El Wakeel* and J. P. Riley
Department of Oceanography, The University, Liverpool

(*Received* 31 *October* 1960)

Abstract—Chemical analyses are presented for two Cretaceous clays from Noil Tobee, Timor. Mineralogical examination has shown that they consist principally of quartz, feldspar, illite and chlorite, together with minor amounts of montmorillonite. Both chemically and mineralogically the clays are very similar to the recent argillaceous deep-sea sediments of the Pacific and Indian Oceans, which confirms Molengraaff's theory (1921) that they are of deep-sea origin. Further confirmation of this theory is provided by comparison of the composition of micromanganese nodules, separated from one of these clays, with that of manganese nodules from the Pacific Ocean.

Molengraaff (1921) has drawn attention to the similarity in chemical compositions and appearance of deep-sea red clays to the red clays of Noil Tobee in Dutch Timor. Certain strata of the latter also contain large manganese nodules, partly dissolved fish teeth, remains of elasmobranchs, and other debris of marine origin. He concluded that these sediments are true deep-sea deposits, of Mesozoic, probably Cretaceous, age. These findings have been endorsed by Kuenen (1942), who added that the Mesozoic geosyncline of Timor also contains other rocks indicating deposition at great depth, such as cephalopod limestones and silicified Halobia limestones both covered with manganese crusts.

A chemical and mineralogical examination has been carried out on two samples of these red clays; which had been collected near the Noil Tobee river by Professor H. G. Jonker in 1916.

(1) Sample B.R.C. was taken from near the bottom of the exposure and was brown in colour.

(2) Sample L.R.C. originated in an upper stratum and was of a light red colour. It contained a number of small manganese nodules averaging about 2–3 mm in diameter, which were separated from the sample by hand picking.

Chemical Examination of Samples

The samples were finely ground, washed thoroughly and dried at 110°. Analyses were made as described by El Wakeel and Riley (1961). The results of the analyses for major constituents are shown in Table 1, together with an analysis by H. T. Meulen of another Mesozoic clay from Noil Tobee (Molengraaff, 1921), and the average composition of twelve Pacific and Indian Ocean argillaceous sediments calculated from analyses by El Wakeel and Riley (1961). Corresponding spectrographic analyses for trace elements are presented in Table 2.

The general similarity between the two Timor clays and recent marine sediments both as regards their major and minor elements, is very striking and provides strong confirmation of Molengraaff's theory that they are of deep-sea origin. The only noteworthy differences between them are the absence of ferrous iron in the fossil clays, and their considerable content of potassium. Much of the latter has

* Present address: Dept. of Oceanography, University of Alexandria, Egypt.

presumably been taken up by the clay minerals from the ground water by ion exchange with sodium and perhaps magnesium.

The Niggli al values of the Timor clays (33·7 for B.R.C. and 38·5 for L.R.C.) lie below 40 and are typical of values found for recent Pacific and Indian Ocean sediments (El Wakeel and Riley, 1961).

Table 1. Percentage compositions of Timor clays and of recent Pacific and Indian Ocean sediments (dried at 110°C)

	Present work		Timor (Noil Tobee) (Molengraaff, 1921)	Pacific argillaceous sediments (El Wakeel and Riley, 1961)
	B–R–C	L–R–C*		
SiO_2	58·98	59·52	61·3	55·51 ± 1·84
TiO_2	0·84	0·74	0·7	0·85 ± 0·12
Al_2O_3	14·34	16·24	20·4	17·04 ± 1·87
Fe_2O_3	8·63	6·83	7·6	6·80 ± 1·13
FeO	0·00	0·05	—	1·25 ± 0·67
MnO	1·38	0·77	tr.	0·48 ± 0·27
CaO	0·39	0·57	1·3	1·19 ± 0·47
MgO	2·44	1·96	1·5	3·56 ± 0·49
Na_2O	1·05	0·94	2·5	1·64 ± 1·29
K_2O	4·90	7·00	tr.	3·24 ± 0·80
P_2O_5	0·24	0·20	tr.	0·15 ± 0·13
$H_2O(+110°)$	5·63	4·12	4·3	6·44 ± 0·82
$CaCO_3$	0·66	0·54	—	0·74 ± 0·21
$MgCO_3$	0·55	0·42	—	0·85 ± 0·30
Org. C	0·25	0·27	—	0·26 ± 0·13
	100·28	100·17	98·60	100·00

* Manganese nodules removed before analysis.

Mineralogical Examination of Clay Samples

A mineralogical examination was carried out on washed samples which had been dried in air at room temperature to avoid alteration of the clay minerals. Under the petrological microscope the samples showed the presence of some quartz, but owing to its very fine state of division the remainder of the sample could not be identified.

Using a combination of X-ray diffraction and differential thermal analysis techniques (El Wakeel and Riley, 1961), quartz, feldspar, illite, chlorite and some montmorillonite were detected in both samples. These are the commonest minerals present in recent pelagic sediments. Comparison of the X-ray diffraction patterns and differential thermal analysis curves (Fig. 1) with those of recent Pacific and Indian Ocean sediments, suggests that little alteration of the clay minerals has occurred.

Composition of micronodules separated from Timor clay L.R.C.

About 100 mg of the dark-brown micronodules were separated from 5 g of Timor clay L.R.C. by hand picking. They were crushed, dried at 110° and analysed

Table 2. Trace elements in Timor clays and recent Pacific and Indian Ocean sediments (in ppm)

	Sr	Ba	Cu	Pb	Co	Ni	Ga	La	Sn	Zr
L.R.C.*	620	1050	750	120	220	350	15	220	10	200
B.R.C.	1200	500	600	140	95	380	17	110	—	120
Average Pacific and Indian Ocean red clays**	450 ± 230	2900 ± 2000	400 ± 130	175 ± 70	100 ± 34	300 ± 76	20 ± 4	90 ± 60	20 ± 9	130 ± 50

	V	Cr	Mo
L.R.C.*	420	60	17
B.R.C.	360	40	—
Average Pacific and Indian Ocean red clays**	390 ± 170	55 ± 20	17 ± 9

** Manganese nodules removed before analysis.
** El Wakeel and Riley, 1961.

as described by Riley and Sinhaseni (1958). The fraction (39·73 per cent) insoluble in 2 N hydrochloric acid was isolated, and after ignition at 800°, was analysed by the micromethods of Riley and Williams (1959).

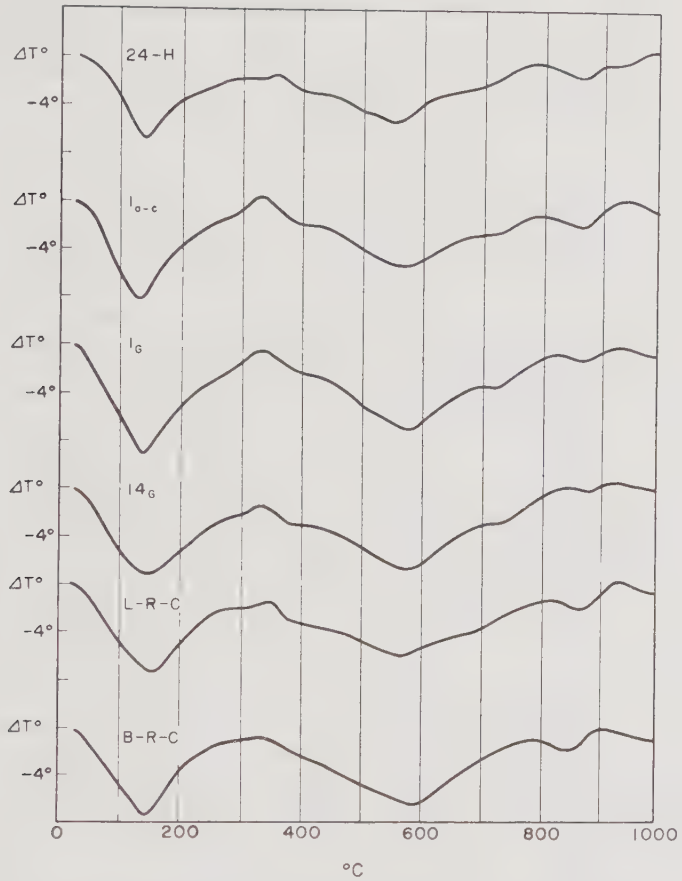

Fig. 1. Differential thermal analysis of Timor clays and Pacific argillaceous deep-sea sediments. B.R.C., Noil Tobee, Timor clay; L.R.C., Noil Tobee, Timor clay; 24 H., chocolate coloured clay* 16° 44′S., 161° 22′W., depth 4685 m; Ia-c., brown clay* 29° 24′N., 153° 06′W., depth 3460 m; I G., red clay* 31° 05′N., 135° 24′W., depth 4940 m; 14 G., tan clay* 43° 49′N., 143° 07′W., depth 4270 m.

* Samples supplied by Dr. G. O. S. Arrhenius of Scripps Institute of Oceanography; for analyses of samples see El Wakeel and Riley (1961).

The results of the analyses of the micronodules (including the insoluble fraction) are shown in Table 3. For comparison, analyses by Meulen of spherical nodules (type 1) and plates of manganese minerals (type 2) from Timor clays (Molengraaff 1921) are also shown, together with the average analyses of three manganese nodules (less nucleii) from recent Pacific sediments (Riley and Sinhaseni, 1958). There is good qualitative agreement between compositions of the micronodules and the recent nodules, particularly as regards their characteristic minor components,

Table 3. Composition of manganese nodules from Timor and Pacific Ocean (expressed as a percentage of the nodules dried at 110°C)

Oxide	Timor nodules			Average of 3 Pacific Ocean nodules* (Riley and Sinhaseni, 1958)
		Molengraaff (1921)		
	L.R.C.	Type 1	Type 2	
Al_2O_3	12·25	10·6	†	6·15
BaO	0·13	0·35	11·7	0·36
CaO	10·20	1·63	5·6	1·93
CoO	0·24	0·17	0·3	0·15
CuO	0·20	0·13	—	0·39
Ga_2O_3	0·0006	—	—	0·0018
Fe_2O_3	17·75	27·7	2·3‡	17·35
PbO	0·10	—	—	0·22
MgO	0·00	0·37	—	0·44
MnO	7·32	14·9	57·6	22·01
MoO_3	0·016	—	—	0·045
NiO	0·43	0·30	—	0·40
P_2O_5	0·43	—	—	0·29
K_2O	2·08	0·16	—	1·49
SiO_2	33·25	26·5	2·09	22·04
Na_2O	1·43	1·59	1·1	2·62
SrO	0·018	—	—	0·076
SnO_2	0·017	—	—	0·028
TiO_2	1·55	—	—	0·72
V_2O_5	0·060	—	—	0·062
ZnO	0·31	—	—	0·44
ZrO_2	0·010	—	—	0·030
Cl	—	0·65	—	—
Available O	1·48	3·4	10·6	4·53
H_2O	6·63	11·1	~15·3	17·07
CO_2	4·52	—	—	1·13
Total	100·40	99·55	~106·6	99·98

* Including acid-insoluble part, but excluding nucleii.
† Included in Fe_2O_3.
‡ Including Al_2O_3.

Table 4. Composition of hydrochloric acid insoluble fraction of micronodules (ignited at 800°)

	%
SiO_2	83·70
TiO_2	2·61
Al_2O_3	5·16
Fe_2O_3	0·25
MnO	0·061
CaO	4·30
MgO	0·00
Na_2O	0·60
K_2O	3·28
P_2O_5	0·31
Total	100·27

viz. nickel, cobalt, copper, lead, zinc and molybdenum. The micronodules are rather deficient in manganese, which is quite a variable constituent in recent nodules. The nucleii of the micronodules were not removed before analysis, and since these consist of fish debris containing apatite and calcium carbonate, this probably accounts for the comparatively large amounts of calcium, carbon dioxide, and phosphate found.

The acid-insoluble matter, the composition of which is shown in Table 4, consisted mainly of quartz, feldspar and clay minerals, together with some apatite. Iron and manganese, both of which are major constituents of the soluble part of the nodules are virtually absent from the insoluble fraction.

Acknowledgements—The authors wish to thank Dr. J. C. Ubaghs of the Mineralogisch Geologisch Museum, Technische Hogeschool, Delft, for the gift of the two samples of Timor clay, and Professor Hollingworth of University College, London, for providing facilities for differential thermal analysis.

References

Kuenen P. H. (1942) *The Snellius-Expedition*, Vol. V. *Geological Results*, pt. 3. Bottom samples. Section 1. Collection of the samples and some general aspects, pp. 24–5.

Molengraaff G. A. F. (1921) Mangan Knollen in Mesozische Deipzee af Zettingen van Nederlandsch-Kimor. *Verlag. K. Akad., Amsterdam*, **29**, p. 677.

Riley J. P. and Sinhaseni P. (1960) The chemical composition of three manganese nodules from the Pacific Ocean *J. Mar. Res.* In press.

Riley J. P. and Williams H. (1959) The microanalysis of silicate and carbonate minerals—III. Determination of silica, phosphorus pentoxide and metallic oxides. *Microchim. Acta* 804–24.

El Wakeel S. K. and Riley J. P. (1961) Chemical and mineralogical studies of deep-sea sediments. *Geochim. et Cosmochim. Acta*, in press.

Geochimica et Cosmochimica Acta, 1961, Vol. 24, pp. 266 to 276. Pergamon Press Ltd. Printed in Northern Ireland

High sensitivity detection of naturally occurring radiocarbon—I

Chemistry of the counting sample

M. A. Tamers*, J. J. Stipp† and J. Collier‡
Department of Chemistry, University of Texas, Austin, Texas

(*Received* 22 *November* 1960)

Abstract—The production of C^{14} on the earth by cosmic rays has received wide attention as a means of determining the ages of archeological and geological samples. However, the low activities that must be measured necessitate devising special sensitive counting arrangements. This is particularly true if it is desired to extend the usefulness of the technique to materials several tens of thousands of years old or at the other end of the time scale, for samples only a few hundred years old.

The most promising method of increasing the sensitivity of radiocarbon dating is the use of radiation detection techniques that are capable of counting large quantities of carbon. The liquid scintillation spectrometer is an instrument that has been applied in several cases to increase the efficiency of C^{14} dating. This paper presents a means by which the entire counting solution (not including the small amounts of phosphors) can be synthesized from the sample to be dated. The solvent used is benzene, which is one of the most suitable materials for liquid scintillation counting since it contains 92 per cent carbon and shows no scintillation quenching properties.

The chemistry involved in the complete synthesis of benzene is described in detail. The sample to be dated is burned and carbon dioxide collected in ammonium hydroxide solution. Strontium carbonate is precipitated upon the addition of strontium chloride. The dried carbonate is mixed with magnesium powder and strontium carbide is produced by ignition of the mixture in an evacuated stainless steel tube. Reaction of the carbide with water generates acetylene which is led into a circuit containing dry ice-cooled traps and a pyrolysis tube at 600°C. The acetylene polymerizes to benzene. This is collected in the cooled traps and then purified by distillation. The overall yield in the synthesis is 30 per cent. The chemical steps involve no special equipment or training. A 20-ml sample can be produced by two man-days of work and the entire procedure completed in less than a week.

I. Introduction

Since the observation of C^{14} activity in nature and the realization that this phenomenon could be used to determine the age of organic materials many thousands of years old (Anderson and Libby, 1947), much effort has been expended to make the radiocarbon dating method more accurate and to extend the maximum age for which information could be obtained. The sensitivity of the technique depends upon the precision of the radioactivity determinations that are made on various materials. The main difficulty lies in the fact that the C^{14} content of contemporary specimens is low and that efficient detection methods and prolonged counting must be used in order to decrease the errors resulting only from the statistical nature of the radioactivity process. Furthermore, extensive investigations have been carried out to improve the counting statistics by finding the most efficient ways of reducing the background counting rate, which must be subtracted from the total observed activity. At present, approximately forty institutions throughout the world are operating or setting up radiocarbon dating laboratories working on these problems.

In low level radioactivity counting investigations, a figure of merit that is

* Present address: Centre d'Etudes Nucléaires de Saclay, Service d'Electronique Physique, Gif-sur-Yvette, France.
† Present address: Radiocarbon Dating Laboratory, Anthropology Department, University of Texas.
‡ Present address: Texas Eastman Chemical Co., Longview, Texas.

generally agreed upon is N^2/B, where N is the net counting rate of a contemporary sample as observed in a particular detection arrangement, and B is the background counting rate of the same detector. It may be seen, therefore, that improvements in the sensitivity of C^{14} dating will be relatively more effective if they cause an increase in net sample counting rate rather than if the same absolute percentage change in background reduction is achieved. For this reason, the work in this laboratory has so far been to develop a radiocarbon detection system that promises higher net counting rates than obtained in the laboratories now in operation. The subject of this paper is the detailed method involved in synthesizing benzene, a carbon-containing compound that is particularly suited for radioactivity measurements. The fundamental procedure used has been reported previously (Tamers, 1960).

II. C^{14} dating

A. *Solid and gas samples*

The original radiocarbon dating method counted the sample in the form of solid elemental carbon. This technique had the advantage of a simple chemical procedure and a counter that could be switched to background measurements without removing the sample (Libby, 1952). Unfortunately, the low-energy β-particles coming from C^{14} decay resulted in a high degree of self-absorption; the overall efficiency of the detection system was only 5 per cent. Another disadvantage was that the carbon was not easily purified and with the advent of nuclear weapons testing, fission product contamination became very troublesome. Although several hundred radiocarbon dates were obtained by this method, the disadvantages mentioned above are so serious that almost all laboratories have now switched to gas counting.

A more efficient method of radiocarbon dating than solid counting is to convert the sample of interest into a suitable gas and completely fill a Geiger or proportional counting tube with the material. In this way the self-absorption effect, so predominant in the solid sample method, is eliminated and the gaseous compounds may be easily purified from fission product contamination. The more promising methods now in operation use carbon dioxide (DeVries and Barendsen, 1953; Brannon *et al.*, 1955; Fergusson, 1955), methane (Burke and Meinshein, 1955; Diethorn, 1956), and acetylene (Crathorn, 1953; Suess, 1954). These three compounds are simple enough so that the chemical preparations involved are minor problems. The main disadvantage to gas counting is that the low density of gases permits only small amounts of material to be counted in reasonable sized detectors. Compressing the gases has led to some improvement, but the amount of carbon that can be counted in any of the existing systems is still less than 1 mole. This means that low activities have to be tolerated, which require long counting times and extensive measures to lower the background as much as possible. However, the simplicity and stability of gas counting has caused it to be the most common method used for C^{14} dating (Kulp, 1954).

B. *Liquid samples*

Liquids containing C^{14} are now conveniently counted with the liquid scintillation spectrometer. This new detection method has been developed to such an

extent that every carbon-containing material can effectively be introduced into an organic liquid scintillator system (Bell and Hayes, 1958). This type of counting has distinct advantages over both solid and gas counting for radiocarbon. The relatively dense liquid phase means that much larger quantities can be submitted to counting than in the gas systems. Then, too, liquid scintillation samples may be easily purified from extraneous radioactive materials and do not exhibit the property of radiation self-absorption. The compact liquid samples are counted in inexpensive glass containers and may be stored indefinitely for possible later recounting. The disadvantage of liquid scintillation counting lies in the fact that for the best results, the chemical procedures are more difficult than for gas or solid counting.

Soon after the discovery of the principle of liquid scintillation counting, it was suggested that the method be applied to the technique of C^{14} dating (Hayes *et al.*, 1953). The main problem is the conversion of the samples' carbon into materials suitable for liquid scintillation counting. Due to the peculiarities of this detection method only certain classes of compounds can be considered. The compounds should be colourless and either soluble in the scintillation counter solvent systems or capable of becoming the solvent itself by dissolving small amounts of scintillator compounds. Then too, a large number of common organic materials cause varying degrees of scintillation light quenching and are therefore not suitable (Hayes *et al.*, 1955b). Despite these essential requirements, several successful procedures were devised for converting sample carbon into forms suitable for liquid scintillation counting.

Most of the methods employed involve the dilution of a standard solvent system with a particular compound synthesized from the sample to be dated. Both methyl and ethyl alcohols have been effectively produced and used as diluents in various solvent systems (Arnold, 1954; Pringle *et al.*, 1955; Delaney and McAulay, 1959). These simple molecules may be relatively easily synthesized from carbon dioxide and are thus especially applicable to routine dating. However, both of the alcohols have scintillation quenching properties and may be used only in moderate amounts as diluents in the regular solvent systems. For this reason, it turns out that counting systems using alcohols offer no special advantages in sensitivity over the gas counting methods.

Two procedures have been suggested whereby the sample carbon is converted into a gaseous compound which is subsequently dissolved in a toluene solvent system. It was found that acetylene, an easily obtainable gas, would dissolve in large quantities in toluene containing 2 per cent ethanol cooled to dry ice temperatures (Audric and Long, 1954). Carbon dioxide, which is the simplest gas to produce from all forms of organic material, was used as a diluent in a toluene solvent (Barendsen, 1957). It was found that up to 30 per cent by weight could be introduced. Apparently, however, difficulties involved in these methods have prevented their being applied in a routine C^{14} dating laboratory.

Trimethyl borate has been synthesized with little more difficulty than methyl alcohol and used as a diluent in a benzene–naphthalene solvent system (Pringle *et al.*, 1957). Dates obtained by this method have been reported, but the counting characteristics still do not seem to offer any advantages over ordinary gas dating systems.

The two most successful liquid scintillation counter dating systems use hexane–octane (Arnold, 1954) and paraldehyde (Leger and Pichat, 1957) as diluents. The former method utilizes a fairly difficult chemical procedure that produces a mixture of hexane and octane. This material is an excellent diluent and may be added in large quantities to the solvent system. However, the ratio of hexane and octane varies and the mixtures must be analysed each time for carbon content. The paraldehyde method likewise requires an involved synthesis. It is also an excellent diluent and may be added in even larger quantities to the solvent system. These two methods both hold promise for increasing the sensitivity of radiocarbon dating.

One method has been reported that permits the sample carbon to be incorporated as part of the solvent itself (Pringle *et al.*, 1955). In this procedure carbon dioxide from the sample to be dated is attached to benzene by a Grignard reaction and an involved reduction produces toluene. This organic liquid is one of the best scintillation solvents. However, only one of the seven carbon atoms of the toluene molecule comes from the sample to be dated and the chemical procedure is lengthy and difficult. This method does not seem readily adaptable for routine C^{14} dating.

In this paper we will describe a procedure that permits a complete synthesis of the solvent from the sample carbon. The solvent used, benzene, is one of the best scintillation counter solvents and contains a high percentage of carbon. The chemical procedure is at least as simple as that of the other liquid methods. The benzene system, therefore, is at present the only liquid C^{14} dating procedure for which virtually all the solvent carbon atoms originate from the sample being dated (those of the scintillator compounds are less than 1 per cent of the total).

III. Chemical Procedure

A. *Objectives and general procedure*

The use of benzene in the counting vial was chosen because it is felt that this liquid offers the most favourable conditions for increasing the sensitivity of radiocarbon dating. It is anticipated that the large proportion of carbon in the molecule, combined with excellent counting properties in the liquid scintillation spectrometer, will permit optimum utilization of the phenomenon of the natural occurrence of C^{14} on the earth. Since archeological and geological materials to be dated sometimes consist of very large samples, it is important that methods be developed to count larger amounts of carbon and thus give better precision to dates obtained when sufficient sample quantities are available. We believe that the benzene method offers promise in those cases where the highest possible sensitivity is required.

The effectiveness of methods for radiocarbon dating depends on the system being simple enough so that it can be handled without highly specialized training or elaborate chemical equipment. With this in mind we have decided to sacrifice, to some extent, elegance and efficiency for simplicity, safety, and the saving of time for the procedure. The most obvious instance is in our pyrolysis of acetylene. Several competent papers in the literature suggest various catalysts for this reaction (Zelinsky, 1924; Fisher *et al.*, 1929; Pungs and Krägeloh, 1933;

Taylor and van Hook, 1935; Reppe and Schweckendick, 1949; Pichat and Baret, 1957; Shapiro and Weiss, 1957). However, the procedure presented here does not use any catalyst for this conversion. The conditions previously suggested for the reaction either require such high pressures of acetylene as to be unsafe for all but very small quantities or use special catalysts whose preparations are so difficult as to be entirely unfeasible without large expenditures of time and equipment. Those procedures using ordinary catalysts do not seem to promise better yields than experienced in our system and were, therefore, not investigated.

The general procedure employed for the synthesis of benzene is given by the following steps:

(1) $\text{Sample} + O_2 \rightarrow CO_2$.

(2) $CO_2 + 2NH_4OH \rightarrow (NH_4)_2CO_3 + H_2O$.

(3) $(NH_4)_2CO_3 + SrCl_2 \rightarrow SrCO_3 + 2NH_4Cl$.

(4) $2SrCO_3 + 5Mg \rightarrow SrC_2 + SrO + 5MgO$.

(5) $SrC_2 + H_2O \rightarrow C_2H_2 + SrOH_2$.

(6) $3C_2H_2 \rightarrow C_6H_6$.

The first step is standard practice in C^{14} dating systems and merely involves converting all forms of samples to a common starting material, carbon dioxide. Carbonate materials are reacted with acid whereas all other samples are burned in an oxygen stream. The carbon dioxide is collected by bubbling it through a tube containing ammonium hydroxide solution. The resultant carbonate is precipitated by the addition of a strontium chloride solution. In the previous description of the process, barium chloride was used in this step. It was decided to switch to the strontium salt because it was our experience that the yield in step (4) was generally slightly higher when the lighter alkaline earth metal was used. The chemical yield of steps (1) to (3) is 100 per cent.

The conversion of carbonate to carbide, step (4), utilizes essentially the same procedure as worked out at the U.S. Geological Survey Laboratory (Suess, 1954). It was decided to carry out the solid-state reaction in an enclosed tube rather than in an open one under a helium stream as reported previously (Tamers, 1960), in order to increase the yield, which is now consistently 90 per cent. Since the reaction proceeds very exothermally and we are reacting much larger quantities than Suess and Rubin, the reactions were carried out in an enclosed hood and various precautions, to be described in a later section, were taken. Despite this, the reaction occasionally got out of hand in the early experiments. However, our safety devices have prevented any injury from those occurrences.

Strontium carbide is completely converted to acetylene by controlled addition of the products obtained in step (4) into distilled water in an evacuated system. The gaseous acetylene is collected in a trap cooled by liquid nitrogen and the accompanying hydrogen is pumped off. The acetylene is then released into a circuit that passes through a Vycor tube heated to 600°C. The benzene and other hydrocarbon pyrolysis products are removed by two traps cooled with dry ice

that are located in the circuit. The acetylene gas is circulated by a positive displacement pump. The yield of benzene from acetylene in this step is approximately 40 per cent.

Benzene is the major product of the yellow-brown liquid obtained and is extracted by a simple distillation. It was found that our vigreux column, 16 in. long and 20 mm inside diameter, with an evacuated silvered jacket, was sufficient for this separation. The hold-up volume was 1 ml. The overall yield in the carbon dioxide to purified benzene synthesis is 30 per cent. The details of this chemical process are presented in the following sections.

B. *Conversion to carbonate*

Samples to be dated that are of a non-carbonate nature are first washed with successive portions of distilled water, dilute NaOH solution, water, dilute HCl, and again water. The sample is finally visually inspected for any extraneous materials such as rootlets. These are removed manually. All water used in this method has been freed of dissolved carbon dioxide by distillation and then continuous bubbling of nitrogen through the water. After washing, the sample is dried in an oven and then packed into a Vycor combustion tube. When the oxygen stream has swept out all air from the system, the ignition is started with a bunsen burner. The gas coming out of the combustion tube passes over a heated tube containing CuO which oxidizes any carbon monoxide that may be formed.

The combustion gases are bubbled through a room-temperature 10 per cent NH_4OH solution which collects all the carbon dioxide. $SrCO_3$ is then precipitated with $SrCl_2$ solution and the precipitate is allowed to settle after a short digestion. The supernatant liquid is removed and replaced with CO_2-free distilled water, the suspension is agitated, and again permitted to settle. This type of washing is repeated from two to five more times depending on the approximate age of the sample and done in such a manner that the solution does not come into contact with the air. Removing the excess NH_4OH in this way minimizes contamination from contemporary carbon dioxide. The $SrCO_3$ suspension is filtered, still out of contact with the air, on a medium-porosity Buchner funnel, washed with distilled water, and dried in an oven at 120°C.

C. *Carbonate to carbide*

The reaction of Mg powder with $SrCO_3$ is a pure solid state reaction and proceeds with some difficulty. The yield has been increased to at least 90 per cent by carefully experimenting with different conditions. The basic procedure used here was suggested by M. Rubin (Rubin, 1960) from his experience at the U.S. Geological Survey Laboratory.

The dried strontium carbonate was ground very fine. One hundred grammes were blended with 117 g of 40-mesh Mallinckrodt no. 5894 Mg powder,* and this mixed as well as possible by grinding the two powders together. Further drying of this mixture at 120°C was found desirable. The containing vessels used in the conversion to carbide were fabricated in our shop from stainless steel tubing of 35 mm inside diameter and 1·5 mm wall thickness. The tubes were 19 in. in length and one end was sealed with a stainless steel plate silver soldered vacuum tight. The $SrCO_3$–Mg mixture was placed in the upright tube and packed to only a moderate extent by tapping. The filled reaction tube was clamped into place in an enclosed hood. In practice, three tubes were filled and reacted individually. It was decided against going to larger tubes and batches in order to lessen the loss and danger if one of the reactions got out of control. Each of the tubes was connected to 1-l. side arm vacuum flasks that provided ballast for the small amount of gas that comes off during the reactions.

The ignition and maintainence of the solid-state reaction was found to be a particularly critical step. The procedure finally adopted was to clamp off the vacuum pump and to heat

* A large proportion of the metallic magnesium sold is produced by the reduction of magnesium salts by carbon. This method leaves significant amounts of unreacted carbon in with the magnesium powder and, therefore, makes it unsuitable for use in radiocarbon dating. The brand of magnesium used here has been shown to be free from this type of contamination.

gently the whole tube with two gas–oxygen torches having cool flames. After a minute or two intense heat was applied to the tube at the location of the top of the mixture to be reacted. A small amount of gas comes off and is observed by the manometer deflection. This gas was analysed in a mass spectrograph and found to have the composition of air. The carbide reaction tubes were connected to a manometer and vacuum pump placed outside the hood. The mixture should be evacuated for at least 2 hr. The Mg–$SrCO_3$ reaction is highly exothermic and causes the tube to glow bright red at the location of the heating. To force the reaction to proceed down the tube the two torches are gradually lowered to points just below the location of the red glow. With the torches slowly being moved down the tube, the entire reaction goes smoothly in less than 5 min. The small amount of gas present helps to carry the heat to the material in the centre of the tube and, therefore, is not pumped off during the reaction.

Several safety measures were taken for this operation. Foremost was the presence of an assistant who watched the manometer during the reaction and quickly opened the system to the pump if the pressure inside the tube approached atmospheric. The torches were extended by 14-in. handles and heavy asbestos gloves were always worn. These practices and the use of a partially enclosed hood prevented any injuries the several times that the hot mixture burst out of the top of the containing tube. It was found that the mishaps mainly occurred due to insufficient drying and/or pumping.

After the reacted tubes had cooled, the mixture was removed. Fair amounts adhered to the walls and had to be scraped off to obtain the high yields desired. If the original mixture was packed tightly, the reacted material was very difficult to remove and had to be drilled out with large wood-working drills, but this usually did not produce a smaller yield.

D. *Carbide to benzene*

The grey carbide mixture was placed in a 2-l. vacuum flask attached to a 4-l. vacuum flask containing about 2 l. of distilled water. After the system was thoroughly evacuated the carbide material was allowed to sift into the water, producing acetylene, as shown in reaction step (5). The connexion between these two flasks was a short length of flexible plastic tubing. The transference of the carbide to the water was controlled at this point by a pinch clamp. Along with the acetylene came varying amounts of hydrogen, which is produced when unreacted Mg or Sr metal present were oxidized by the water. The combined gases were let into the left side of the vacuum rack, as seen in Fig. 1. Traps *A* and *C* were cooled continuously by dry ice–acetone baths and were intended to remove all H_2O from the gas. With the stopcock connecting to the acetylene generator turned off, acetylene was frozen out in trap *B* by liquid nitrogen. H_2 was not collected. It was pumped out, and a new batch of gas admitted, the acetylene collected, and the H_2 again pumped out. It is not really essential to remove H_2 as it has been shown that this does not have a significant effect on the benzene yield (Coats and Anderson, 1959). However, the pyrolysis of acetylene to benzene proceeds much faster if H_2 is not present and for this reason it was removed at this point.

After approximately $\frac{1}{4}$ mole of acetylene had been collected in trap *B* by several batches of gas being let in from the acetylene generator, the liquid nitrogen is withdrawn and the solid acetylene allowed to vaporize into one of the three 5·4-l. gas storage bulbs connected to the vacuum line. After a bulb is filled to 1 atm with pure acetylene gas, it is shut off and a second bulb then opened to the line. It can be seen from the diagram that any of the storage bulbs may be filled without interfering with the operation of the right side of the vacuum rack. This permits the process of acetylene generation, purification, and storage to be carried out while manipulations with the pyrolysis reaction on the other side are performed simultaneously. It was found that this results in a considerable saving of time.

As soon as the pressure in one of the bulbs reached 1 atm it was opened to the pyrolysis circuit. This consists of a Vycor tube surrounded by an induction heater and maintained at 600°C, two dry ice–acetone cooled traps, *D* and *E*, and a positive displacement pump which keeps the gas moving in the circuit. The pyrolysis tube is heated through a length of 12 in. and has an inside diameter of 25 mm. The cyclic polymerization of acetylene to benzene took place here and the latter material was removed soon after it was formed by the traps. The unreacted acetylene was passed into the pyrolysis tube continuously. The large volume of gas in the

connected storage bulb does not mix with the moving acetylene in the circuit, but merely adds its gas to replenish the acetylene which has reacted, and as the other storage bulbs were filled to 1 atm with acetylene, they were also opened to the circuit, lowering the rate at which the pressure decreased due to the reaction of acetylene.

The usual procedure was to arrange for as many storage bulbs as possible to be open to the circuit and the pressure to be close to 1 atm at the end of the day. The reaction goes overnight and uses up most of the gas present in the system. The next morning either more acetylene was generated from the carbide or the small amount of acetylene left in the line was collected in the

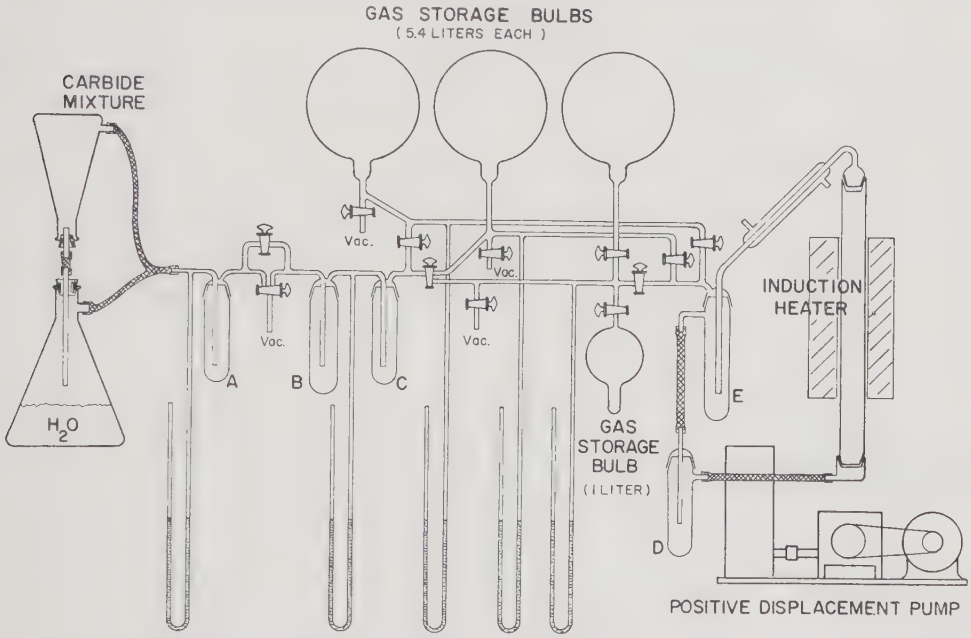

Fig. 1. Schematic diagram of C_2H_2 generator and pyrolysis system.

1-l. storage bulb (which is equipped with a cold finger for this purpose) and only this bulb opened to the pyrolysis circuit. The last amount of acetylene was then reacted in the first part of the morning. In practice, about one mole of acetylene can be reacted per day.

Our observations are in agreement with previous reports of the acetylene polymerization to benzene having a bimolecular homogeneous rate determining step (Pease, 1929; Taylor and van Hook, 1935). We found that packing the pyrolysis tube with glass wool definitely decreased the benzene yield. The total reaction rate was increased by this step or by raising the temperature, but this caused large amounts of acetylene to be reduced to carbon or high molecular weight hydrocarbon chains and resulted in lower relative amounts of benzene. The optimum conditions were found to be around 600°C, no packing in the pyrolysis tube, and the acetylene pressure close to 1 atm. Higher pressures were not attempted due to the danger of explosion.

The liquid collected in traps *D* and *E* was dark brown, immiscible with water, and had a density of 0·9 g/ml. A distillation separated the benzene which composed 50 per cent of the original liquid. The higher boiling materials were shown by vapour phase chromatography to be toluene and various hydrocarbon chains. The distillation step is a standard organic chemistry technique and no special arrangement was needed for this work.

E. *Counting sample preparation*

The benzene produced by the preceding steps was added to a low-potassium glass vial. If a limited amount of sample was available and only a small quantity of benzene produced, the vial

was brought up to volume with ordinary commercial benzene, which is obtained from coal tars and therefore shows no C^{14} activity. Primary and secondary scintillators were added to the liquid to give solutions having concentrations of 3 g/l. PPO and 0·1 g/l. POPOP. These are materials commonly used in liquid scintillation counting (Hayes *et al.*, 1955a, 1956). The solutions were finally relieved of oxygen quenching by bubbling helium through them for 10 min and filling the top air space with helium (Pringle *et al.*, 1953). The cap of the vial was secured, and after thorough mixing to dissolve the scintillator, the sample was ready for counting.

IV. Discussion

The procedure for the total synthesis of benzene is now being carried out on a routine basis in this laboratory. A 20-ml counting sample requires approximately two man-days of chemistry work; a sample can be converted to benzene and

Table 1. Comparison of liquid scintillation dating systems

System	Reference	% by weight of the counting solution that is carbon originating from the sample being dated
Ethanol	Arnold (1954)	20
Aliphatic hydrocarbons	Arnold (1954)	64
Acetylene	Audric and Long (1954)	11
Carbon dioxide	Barendsen (1957)	8
Methanol	Delaney and McAulay (1959)	7
Paraldehyde	Leger and Pichat (1957)	38
Methanol	Pringle *et al.* (1955)	11
Toluene	Pringle *et al.* (1955)	15
Benzene	This work	92

counted in 1 week. The chemistry used in the benzene method employs only two more steps than that used for the acetylene method, which is one of the standard gas counting C^{14} dating procedures.

Comparison of the effectiveness of benzene as a liquid scintillation counter dating material with other systems described in the literature is given in Table 1. In addition to this very high carbon content, benzene may now be obtained with a relatively trouble-free synthesis. The aliphatic hydrocarbons method (Arnold, 1954) comes closest in competing with sample carbon content of the counting solution, but suffers from the disadvantages that a carbon content analysis must be made for each sample, and the chemical method appears dangerous and more lengthy than with benzene. The paraldehyde method (Leger and Pichat, 1957) has an even lower carbon content and also a more difficult chemical preparation.

Of the other methods listed in Table 1, none give promise of providing more sensitive systems than the present gas-counting methods have achieved. Since the gas procedures are much simpler and employ intrinsically more stable counting instruments, it is doubtful that they will be superseded by liquid scintillation counting if higher sensitivity is not obtained. The chemical yield in the benzene synthesis is the same as that for the liquid hydrocarbon and paraldehyde methods.

It is less than the other liquid scintillation methods, but, as explained previously, these procedures do not offer any special advantages over the standard gas-counting systems and, therefore, cannot really be considered to be competing. The 30 per cent yield in the benzene process necessitates concern over an isotope effect producing changed C^{14}–C^{12} ratios from the original ratio. In order to minimize this error, we hope to increase the yield as much as possible and to correct for it in each case by measuring C^{13}–C^{12} ratios mass spectrometrically (Broecker and Olsen, 1959). In any case, our experience with the present procedure for the synthesis of benzene shows that the yield is approximately constant. If this situation can be maintained, the isotope effect will also be constant between our standard and samples and, therefore, the effect will to a large extent cancel out in the age calculations.

The aliphatic hydrocarbons, paraldehyde and benzene methods are capable of increasing the range of radiocarbon dating by allowing much greater amounts of carbon to be counted than is feasible using gas counters. Due to its high carbon content, and no requirement of a diluting solvent, the use of benzene in the liquid scintillation counter presents, at this time, the best probability for extending the sensitivity of present methods used in the detection of naturally occurring radiocarbon.

Various types of samples are now being run in our laboratory. Work is in progress to reduce the background of our liquid scintillation counter by putting it into a large shield. In addition, different size counting vials are being investigated and, finally, optimum voltage and window setting will be determined. The results of these counter characteristics studies will be presented in a later paper.

Acknowledgements—Dr. E. M. Davis of the Anthropology Department, The University of Texas, was exceptionally helpful and encouraging throughout the progress of this work. Dr. E. F. Gloyna of the Civil Engineering Department graciously loaned us an uncontaminated laboratory. The Robert A. Welch Foundation of Houston, Texas provided funds for the liquid scintillation counter used in the project.

References

Anderson E. C. and Libby W. F. (1947) Radiocarbon from cosmic radiation. *Science* **105,** 576.

Arnold J. R. (1954) Scintillation counting of natural radiocarbon—I. The counting method. *Science* **119,** 115.

Audric B. N. and Long J. V. P. (1954) Use of dissolved acetylene in liquid scintillation counter for the measurement of C^{14} of low specific activity. *Nature, Lond.* **173,** 992.

Barendsen G. W. (1957) Radiocarbon dating with liquid CO_2 as diluent in a scintillation counter. *Rev. Sci. Instrum.* **28,** 430.

Bell C. G. and Hayes F. N. (1958) *Liquid Scintillation Counting.* Pergamon Press, New York.

Brannon H. R. and Taggart M. S. (1955) Proportional counting of carbon dioxide for radiocarbon dating. *Rev. Sci. Instrum.* **26,** 269.

Broecker W. S. and Olson E. A. (1959) Lamont radiocarbon measurements—VI. *Amer. J. Sci.*, Radiocarbon Suppl. **1,** 111.

Burke W. H. and Meinshein W. G. (1955) C^{14} dating with a methane proportional counter. *Rev. Sci. Instrum.* **26,** 1137.

Coats F. H. and Anderson R. C. (1959) Mass spectrometric studies of thermal reactions in acetylene-deuterium and acetylene-d_2-hydrogen mixtures. *J. Phys. Chem.* **63,** 1340.

Crathorn A. R. (1953) Use of an acetylene-filled counter for natural radiocarbon. *Nature, Lond.* **172,** 631.

Delaney C. F. G. and McAulay I. R. (1959) A radiocarbon dating system using scintillation techniques. *Sci. Proc. Roy. Dublin Soc.* **1,** 1.

DeVries H. and Barendsen G. W. (1953) Radio-carbon dating by a proportional counter filled with carbon dioxide. *Physica* **19,** 987.

Diethorn W. (1956) *A Methane Proportional Counter System for Natural Radiocarbon Measurements.* U.S. Atomic Energy Commission Report NYO–6628.

Fischer F., Baugert F. and Pichler H. (1929) Über die Bildung flüssiger Kohlenwasserstoffe aus Acetylen. *Brennstoff-Chem.* **10,** 279.

Fergusson G. J. (1955) Radiocarbon dating system. *Nucleonics* **13,** No. 1, 18.

Hayes F. N., Ott D. G., Kerr V. N. and Rogers B. S. (1955a). Liquid Scintillators—I. Pulse height comparison of primary solutes. *Nucleonics* **13,** No. 12, 38.

Hayes F. N., Ott D. G., and Kerr V. N. (1956) Liquid scintillators.—II. Relative pulse height comparisons of secondary solutes. *Nucleonics* **14,** No. 1, 42.

Hayes F. N., Rogers B. S. and Sanders P. C. (1955b) Importance of solvent in liquid scintillators. *Nucleonics* **13,** No. 1, 46.

Hayes F. N., Williams D. L. and Rogers B. (1953) Liquid scintillation counting of natural C^{14}. *Phys. Rev.* **92,** 512.

Kulp J. L. (1954) Advances in radiocarbon dating. *Nucleonics* **12,** No. 12, 19.

Leger C. and Pichat L. (1957) Utilisation du paraldehyde pour incorporer de grandes quantites de carbone marque dans un scintillateur liquide. *C.R. Acad. Sci., Paris* **244,** 190.

Libby W. F. (1952) *Radiocarbon Dating,* University of Chicago Press, Chicago.

Pease R. N. (1929) The kinetics of the polymerization of acetylene. *J. Amer. Chem. Soc.* **51,** 3470.

Pichat L. and Baret C. (1957) Une methode simple de synthese de benzene $^{14}C_6$ et strolene $^{14}C_8$. *Tetrahedron* **1,** 269.

Pringle R. W., Black L. D., Funt B. L. and Sobering S. (1953) A new quenching effect in liquid scintillators. *Phys. Rev.* **92,** 1582.

Pringle R. W., Turchinetz W. and Funt B. L. (1955) Liquid scintillation techniques for radiocarbon dating. *Rev. Sci. Instrum.* **26,** 859.

Pringle R. W., Turchinétz W., Funt B. L. and Danyluk S. S. (1957) Radiocarbon age estimates obtained by an improved liquid scintillation technique. *Science* **125,** 69.

Pungs W. and Krägeloh F. (1933) Verfahren zur herstellung aromatischer Kohlenwasserstoffe. *D.P.* 547080.

Reppe W. and Schweckendick W. J. (1949) Cycliesierende polymerisation von Acetylen. *Chem. Ber.* **560,** 104.

Rubin M. (1960) Private communication.

Shapiro I. and Weiss H. G. (1957) Cyclization of acetylene d_2 to benzene d_6. *J. Amer. Chem. Soc.* **79,** 3294.

Suess H. E. (1954) Natural radiocarbon measurements by acetylene counting. *Science* **120,** 5.

Tamers M. A. (1960) C^{14} dating with the liquid scintillation counter: A total synthesis of the benzene solvent. *Science* **132,** 668.

Taylor H. A. and van Hook A. (1935) The polymerization and hydrogenation of acetylene. *J. Phys. Chem.* **39,** 811.

Zelinsky N. (1924) Über die kontakt-kondensation des Acetylens. *Ber. deut. chem. Ges.* **57,** 264.

Geochimica et Cosmochimica Acta, 1961, Vol. 24, pp. 277 to 298. Pergamon Press Ltd. Printed in Northern Ireland

The concentration and isotopic abundances of carbon dioxide in rural and marine air

Charles D. Keeling*
Division of Geological Sciences, California Institute of Technology

(*Received* 11 *July* 1960)

Abstract—An earlier study of the concentration and isotopic abundances of C^{13} and O^{18} of carbon dioxide in rural air (Keeling, 1958) has been extended by reporting the analysis of 106 additional samples of rural air and thirteen samples of air collected over tropical waters of the eastern Pacific Ocean. At locations far removed from terrestrial plants and the influence of cities, the concentration and C^{13} abundance of carbon dioxide in the air are found to be nearly constant; but the O^{18} abundance of carbon dioxide, under various circumstances, appears to show a systematic variation with air temperature, ocean water temperature, or season. Extreme values are, concentration: from 0·0303 to 0·0320 volume per cent of original air; C^{13}/C^{12} ratio: from −6·7 to −7·4 per mil; O^{18}/O^{16} ratio: +0·8 to −0·6 per mil. A correlation between C^{13} abundance and concentration of carbon dioxide previously observed for forest air is again observed. On the basis of this correlation, the C^{13}/C^{12} ratio of the carbon dioxide released by the forest plants has been computed and is found to vary for different stations between −21 and −26 per mil. The O^{18} abundance of carbon dioxide in forest air is observed to be variable but shows no simple relationship with other measured quantities.

Introduction

The molar concentration and C^{13}/C^{12} ratio of carbon dioxide have been found to vary proportionately in the air of forests and grassland near the Pacific coast of the United States (Keeling, 1958). The manner of mutual variation suggests a simple process of mixing together two species of carbon dioxide with distinctly different isotopic ratios, one species characteristic of the general atmosphere, the other a product of the respiration of plants and soil. From the magnitude of the shift in isotopic ratio with molar concentration during a 24 hr period of sampling, the carbon isotope ratio of the carbon dioxide respired by the plants and soil was computed and found to have a value within the range previously reported for carbon of terrestrial plants (Wickman, 1952; Craig, 1954). Minimum concentrations and associated carbon isotope ratios, found during the afternoon, were nearly the same at all locations, and agreed with values for air collected in mountain and coastal areas far removed from terrestrial plants. This agreement was attributed not to any special effect produced by the plants, but to meteorological conditions, i.e. the air of the forest during the afternoon of each sampling period mixed so completely with air from beyond the zone of influence of the plants and soil that their metabolic activity had no observable effect on the air.

Although the data at all stations tended to support these conclusions, the scope of the study was limited to seven stations all near the west coast of the United States during a single season. The maximum length of sampling period at any one station was 36 hr. In order further to test the generality of the observations, additional samples have been collected at five new stations in forest and grassland representing a greater coverage than before; near two of the earlier stations in forests one year later to observe the reproducibility of sampling in different years;

* Present address, Scripps Institution of Oceanography, University of California, La Jolla, California.

and at two stations in desert areas where attempts were made, unsuccessfully, to detect the respiration of desert plants. In order to obtain a better understanding of the composition of atmospheric carbon dioxide in areas far from the influence of vegetation, additional samples were collected at one high altitude station over barren ground during 6 days of variable weather, near beaches and over water along the California coast, and over waters of the tropical Pacific Ocean both north and south of the equator. The present paper describes the results of these additional analyses. As in the previous paper, oxygen isotope ratios of atmospheric carbon dioxide are also reported and discussed.

Experimental

Air samples were collected and processed as described previously (Keeling, 1958): the carbon dioxide from 5 l. of air was isolated by condensation in a liquid nitrogen trap and afterwards sublimed at the temperature of dry ice to separate it from condensed water vapour; the concentration of the carbon dioxide was determined manometrically; and the mass ratios were measured by a double collector mass spectrometer as described by McKinney *et al.* (1950).

Isotopic ratios are again reported relative to carbon dioxide gas prepared from a standard sample of carbonate (standard "PDB-1"). Per mil differences in isotopic ratio from this standard are given by the function:

$$\delta = \left(\frac{R_{\text{sample}}}{R_{\text{standard}}} - 1 \right) 10^3$$

where R is the absolute ratio of two isotopes being compared. Carbon isotope ratios are reported as δC^{13} for which $R = C^{13}O^{16}O^{16}/C^{12}O^{16}O^{16}$, oxygen ratios by δO^{18} for which $R = C^{12}O^{16}O^{18}/C^{12}O^{16}O^{16}$. The determinations of δC^{13} and δO^{18} from the mass ratios measured by the mass spectrometer have been described by Craig (1957). Carbon dioxide concentrations are reported in parts per million (p.p.m.) of original air by volume (μ_{CO_2}), water vapour concentrations as volume per cent of original air (μ_{H_2O}). Carbon dioxide concentrations in parts per million of dry air are also reported for samples where humidity data are available. Carbon dioxide concentrations are considered to be accurate to $\pm 1{\cdot}0$ p.p.m., isotopic measurements to $\pm 0{\cdot}2‰$. Relative errors are smaller; experimental departures from predicted values indicate that the reproducibility for samples analysed within a short time interval approaches $\pm 0{\cdot}5$ p.p.m. for gas concentration and $\pm 0{\cdot}05‰$ for isotopic ratio.

Analysis of Data

Data for air collected at rural stations in the United States are presented in Table 1*; data for marine air in Table 2. Graphs of gas concentrations and isotopic ratios vs. time have been prepared (Figs. 1 to 10)* to illustrate the data. As previously observed, carbon dioxide concentration and carbon isotope ratios for air in forest areas again obey the relationship:

$$\delta C^{13} = I(C^{13}) + M(1/\mu_{CO_2}) \qquad (1)$$

where $I(C^{13})$ and M are empirical constants; δC^{13}, the carbon isotope ratio in per mil; μ_{CO_2}, the concentration of carbon dioxide in parts per million of original air. Values of $I(C^{13})$ and M were derived by the method of least squares (Worthing, 1943), taking the data of each station separately. Observed maximum and minimum concentrations and carbon isotope ratios associated with minimum concentrations are given in Table 3 together with several quantities based on equation (1). Values for stations reported earlier are included for comparison. Minimum

* Figures 1–11 and Tables 1–4 are set out at the end of this paper. Please see pp. 127–140.

concentrations and associated carbon isotope ratios fall in a narrow range except for one station in California (Canyon near Big Sur River), where the minimum concentration is distinctly higher and the carbon isotope ratio correspondingly shifted towards the value of carbon dioxide derived from vegetation; and one station in Indiana, where the reverse is observed. Excluding these two stations, the average minimum concentration is 314 p.p.m., the range ± 8 p.p.m. Carbon isotope ratios corresponding to this average concentration are reported in Table 3 as $\delta(C^{13})$. These were calculated by equation (1) using the values of $I(C^{13})$ and M determined separately for each station. Values of $I(C^{13})$ and average experimental deviations in $\delta(C^{13})$ from the least square relationship are also quoted. Experimental deviations are less than $\pm 0{\cdot}10‰$ for all stations during 1956, the average of all the analyses being $\pm 0{\cdot}05‰$. Values of $\delta_0(C^{13})$ for 1956 are within an interval of $\pm 0{\cdot}11‰$ (from $-6{\cdot}98$ to $-7{\cdot}20$, average: $-7{\cdot}06‰$) with an average deviation from average value of $\pm 0{\cdot}07‰$. Thus the carbon isotope ratio of carbon dioxide, predicted by the least square relationship for a concentration of 314 p.p.m., is the same at every station within the reproducibility of individual isotopic measurements. All but one of the $\delta_0(C^{13})$ values for 1955 also fall in this range. Carbon dioxide concentrations and carbon isotope ratios for air at mountain and desert stations and from over the Pacific Ocean near the coast of the United States fall within rather narrow ranges (from 309 to 320 p.p.m., from $-6{\cdot}85$ to $-7{\cdot}58‰$). Maximum and minimum concentrations, and average values of concentration and isotopic ratios are presented in Table 4. Analyses of air collected over equatorial waters (Table 2) fall in nearly the same ranges (from 303 to 317 p.p.m., from $-6{\cdot}70$ to $-7{\cdot}31‰$).

In spite of the close correlation between carbon isotope ratio and concentration at forest stations, oxygen isotope ratios at the stations show no simple relationship with concentration (see Figs. 1 to 10). A possible correlation between this ratio and barometric pressure, previously noted in data at a high altitude station (Inyo Mountains) on 8 and 9 July 1955, does not exist in the new data for the same station, from 9 to 14 March 1956 (Fig. 2). However, for two desert stations, on occasions when samples were collected over ground exposed to the sky during inferred nocturnal temperature inversions, the ratio showed a shift to higher O^{18}/O^{16} values roughly proportional to the decrease in temperature during the night (Figs. 1 and 4). Otherwise, the data reveal no systematic variation in ratio, except that a comparison of average values for air collected at mountain and desert stations and from over the Pacific Ocean near the United States indicates a seasonal trend (see Fig. 11).

Discussion

In almost all of the forest and grassland areas where samples of air have been analysed, a close proportionality is found between variations in carbon isotopic abundance and concentration of carbon dioxide. Observed minimum concentrations and associated isotopic abundances for most of these same areas agree with the nearly constant values found for barren areas near the Pacific coast of the United States. Unlike the earlier published results (Keeling, 1958) the new data, however, include some exceptions to these generalizations. The observed minimum concentration for Asseteague Island, near the Atlantic coast of the United States,

is slightly higher than minima generally observed near the Pacific coast; the minimum for a canyon near the Big Sur River is considerably higher. For a grassland station in Indiana, observed variations in carbon isotopic abundance and concentration are not proportional and the minimum concentration is significantly lower than elsewhere.

For both of the stations with high minima, the proportionality between variations in concentration and carbon isotope ratio is clearly evident; and the observed relationship between isotopic ratio and molar concentration, when extrapolated to the average observed minimum concentration for all forest stations (314 p.p.m.), yields a value of the carbon isotope ratio, $\delta_0(C^{13})$, which agrees closely with values found elsewhere.

Of several effects which might account for this agreement, one possibility is that no sample happens to have been collected at a time when the normal minimum concentration occurred. At neither station, however, is this possibility likely. In the case of Asseteague Island, air was collected over barren ground, a few kilometres from the forest, less than 2 hr after the air was collected in the forest which gave the lowest concentration. The compositions of the two samples agree closely (324 p.p.m., $-7{\cdot}52‰$; 322 p.p.m., $-7{\cdot}47‰$, resp.). Nearly the same composition was found for a sample of forest air collected during the afternoon of the previous day (323 p.p.m., $-7{\cdot}50‰$). In all likelihood, the composition of these three samples was characteristic of the general atmosphere in the vicinity of the station during the period of sampling. The agreement in value for $\delta_0(C^{13})$, computed for an appreciably lower concentration, implies that the carbon isotope ratio of carbon dioxide of the general atmosphere in the vicinity of Asseteague Island varies from the value found on the Pacific coast according to the same relationship as forest air.

On the other hand, for the station in a canyon near the Big Sur River the high minimum concentration was probably produced locally, since air collected at this station near noontime on 6 June showed a high concentration, while less than 2 km away air collected at Big Sur State Park showed the normal minimum value. This fact, and also the high concentration observed for the afternoon of the following day, suggests that a high minimum concentration occurs generally at this station. It is not immediately obvious, then, why the value of $\delta_0(C^{13})$ for this station should agree with that for stations where the normal minimum is observed. Conditions which might lead to such agreement are considered in a separate article which follows (Keeling, 1961).

At the grassland station in Indiana* the observed minimum concentration was lower than at any other station, the associated C^{13}/C^{12} ratio higher, a result which suggests a subtraction from the air of carbon dioxide with the isotopic ratio of plant carbon, relative to the normal minimum quantity. For the same station the observed maximum concentration was considerably higher than for any other station. Here it would seem that the metabolic activity of the plants influenced the local air so strongly that even the minimum concentration was affected. The data are too few, however, to attempt to explain the observed isotopic relationship for that station.

* The forest station in Indiana will not be discussed because only two samples were analysed.

Although the proportionality between variations in the carbon isotopic abundance and concentration of carbon dioxide is clearly evident at all stations except as just discussed, the deviations of individual measurements from proportionality appear, for a few stations, to lie outside the limits of experimental error. Therefore the isotopic abundance of the carbon dioxide added to the air was not equally homogeneous at all stations.

As sampling stations, areas of virgin timber or grassland were considered the most desirable. In such environments the growth and decay of the plants should be undisturbed to the greatest possible degree, and therefore the respiration and assimilation of carbon dioxide by the plants and soil should have the best possible opportunity to reach a state of balance. Except for the grassland station in Indiana which was in a field of alfalfa, clover and native grasses which had been harvested only 3 weeks before the period of sampling, all stations were representative of virgin conditions. The stations at Big Sur State Park, Hart's Pass, and Olympic National Park, however, were near or in areas open to public recreation where carbon dioxide released by dwellings, motor vehicles, or camp fires may have been included in some of the air samples. From Table 3 it may be seen that these stations exhibit the largest average deviations in δC^{13} from equation (1) (range 0·07 to 0·13‰).

Elsewhere local combustion was absent and evident disturbances to the plants were small. The station in Yosemite National Park was near a small public camp ground in a permanently preserved tract of virgin timber. Samples were collected in the spring before the public was permitted to enter the area. The station in a canyon near the Big Sur River was in an uninhabited ravine, unsuitable for grazing and showing little evidence of trespassers. Stations at Howard Pocket, Telephone Hill, and Asseteague Island were in uninhabited tracts of virgin timber which had been grazed by domestic stock but were otherwise undisturbed. The station near Rock Lake was in a sparsely settled farmland in a field of native grasses with no grazed or cultivated fields close by. The average deviation in δC^{13} for these latter stations lies within the range of precision of the mass spectrometer.

Thus under natural conditions the carbon isotope ratio of the carbon dioxide released to the air by plants and soil at a given location appears to be nearly constant. How then are we to account for the differences in ratio from station to station? Although the values reported in Table 3 as the quantity $I(C^{13})$ are extrapolations which are considerably less accurate than individual analyses or direct averages, their experimental uncertainty cannot greatly exceed $\pm 0{\cdot}5‰$. (In the single instance when two sets of samples were taken on different occasions at precisely the same location, the values for $I(C^{13})$ agree to $\pm 0{\cdot}3‰$). The values listed in Table 3 for different stations cover a range of 5‰. Moreover, they show a systematic relationship between isotopic ratio and concentration of carbon dioxide: least negative values, which represent least enrichment in C^{12} relative to atmospheric carbon dioxide, are found for stations with lowest observed average and maximum concentrations; most negative values, where the highest average and maximum concentrations were observed. Such a correlation accords with an hypothesis of Wickman (1952) which predicts that the enrichment of terrestrial plants should depend on the extent to which the plants are exposed to carbon

dioxide released to the local air supply by respiration of the plants and soils. This corroboration of Wickman's hypothesis is of special interest because of a denial by Craig (1954) that cyclic enrichment can be produced by plants under normal circumstances. In an article which follows (Keeling, 1961) this topic will be considered in detail.

For air over barren ground, variations in the composition of carbon dioxide were found to be small compared with air of forests or grassland. The samples collected at White Mountain Research station in the Inyo mountains were taken at an elevation of 3800 m above sea level, in an area devoid of vegetation, during strong winds. The data exhibit variations which scarcely exceed the range of experimental uncertainty. No diurnal variation in concentration or isotopic ratio is evident. There are no correlations with barometric pressure, air temperature or humidity, although these factors varied considerably and systematically during the 5 day period of the observations (see Fig. 2). Average values of the concentration and carbon isotope ratio agree closely with the average minimum concentration at forest stations and with the carbon isotope ratio corresponding to that concentration as determined from the least square relationship:

Inyo Mountain Station: $\mu_{CO_2} = 317$ p.p.m., $\delta C^{13} = -7{\cdot}13‰$.
Average of Forest Stations: $\mu_{CO_2} = 314$ p.p.m., $\delta_0(C^{13}) = -7{\cdot}06‰$.

The concentration and carbon isotope ratio for air collected at other stations over barren ground or from over the Pacific ocean near the United States, agree closely with the values for the Inyo Mountains. Average values taken from Table 4 are plotted in Fig. 11. (Data reported during 1955 (Keeling, 1958) are included for comparison). It may be seen that the concentration and carbon isotope ratio for nearly a year show no significant variation, with the possible exception of the data for Olympic National Park in September 1955.

Average oxygen isotope ratios, on the other hand, show a variation with season. From June to December 1955, the average ratios indicate progressively more negative values; during the early part of 1956, the reverse. The variation considerably exceeds the limits of experimental error and the progression of values is remarkably uniform.

Air collected over the eastern Pacific ocean in tropical latitudes yielded a somewhat more variable composition than was found for stations near the Pacific coast, but the data are too limited to establish significant ranges. Average values for concentration and carbon isotope ratio are close to those at the Inyo Mountain station:

5°S latitude: $\mu_{CO_2} = 310$ p.p.m., $\delta C^{13} = -6{\cdot}98‰$.
1°N latitude: $\mu_{CO_2} = 307$ p.p.m., $\delta C^{13} = -6{\cdot}92‰$.

The average oxygen isotope ratios differ considerably for each latitude, the difference being in the direction predicted for equilibrium with mean ocean water at the observed surface temperatures, as shown in Table 5.

The equatorial data suggest that carbon dioxide may equilibrate directly with adjacent ocean water. It seems justified to investigate whether this process also provides a reasonable explanation for the seasonal trend in oxygen isotope ratio indicated in Fig. 11.

If the temperature relationship is used which accords approximately with the equatorial data, the ocean water temperatures required to yield the oxygen isotope ratios of Table 4 are in a range between 20 and 30°C, with the maximum temperature occurring near the winter solstice. These temperature values are too high, and the maximum is too late in the season, to be due to a rapid equilibration of atmospheric carbon dioxide with ocean water having the mean isotopic abundance reported by EPSTEIN and MAYEDA (1953). Although it is reasonable to

Table 5. Predicted and observed δO^{18} for carbon dioxide of marine air

	Average temperature observed (°C)	δO^{18}, predicted* (‰)	δO^{18}, observed (‰)
5°S latitude	19·8	+0·9	+0·63
1°N latitude	25·9	−0·2	−0·30

* Based on the values of UREY (1947) for the fractionation factor of the isotopic reaction: $H_2O^{16} + CO^{16}O^{18} = H_2O^{18} + CO^{16}O^{16}$ at 0 and 25°C, and the value of EPSTEIN and MAYEDA (1953) as corrected by CRAIG (1957) for the δO^{18} value of mean ocean water.

suppose a delay of several months in the time for mixing ocean-equilibrated carbon dioxide with carbon dioxide of the general atmosphere, thus accounting for the late maximum, the computed equilibration temperatures are altogether too high for surface ocean water in the middle latitudes of the north Pacific Ocean (M. K. ROBINSON, private communication). Only if the value of EPSTEIN and MAYEDA for δO^{18} of mean ocean water were more negative by at least 1‰ than the value for surface ocean water in the vicinity of the air trajectories, could this discrepancy be readily accounted for. However, in view of the narrow range of isotopic abundances of normal surface ocean water according to EPSTEIN and MAYEDA, this does not appear likely, and an adequate explanation for the seasonal trend probably must await further data.

At desert stations the composition of air agrees with that observed at the Inyo Mountain station except for samples collected near the ground during inferred temperature inversions (Borrego valley, night of 1–2 February; Organ Pipe Cactus National Monument, night of 21–22 April). During both periods of temperature inversion, the oxygen isotope ratio shifted to significantly more positive values (increase in O^{18}/O^{16} ratio) than were observed during the day. The manner in which the shift occurred is made evident by the data for the latter station (Fig. 4). A change in δO^{18} approximately proportional to the change in air temperature occurred in a gully free of vegetation but was suppressed within dense brush which lined both sides of the gully. The suppression was greatest in the densest foliage (see Table 1). Apparently no more than relatively dry air near bare ground was responsible for the effect. If changes in oxygen isotope ratio can occur under such circumstances, similar changes might be expected to occur quite generally, although in vegetated areas they might be obscured by changes in the ratio brought about

by the addition during the same period of carbon dioxide with a different isotopic ratio derived from plants. For the forest stations departures from proportionality with gas concentration show a tendency towards shifts to more positive δO^{18} values during periods of inferred temperature inversion, but the data are not sufficiently consistent to offer proof of a similar process.

Acknowledgements—Through the courtesy and generous assistance of members of the United States National Forest and National Park services, the author was able to locate several sampling stations in areas not normally accessible to the public for overnight camping. For this privilege he would like to thank the park ranger at Organ Pipe Cactus National Monument, rangers K. A. Keeney and Jay H. Cravens of the Coconino and Kaibab National Forest, and John C. Preston and his staff of Yosemite National Park. The author also is grateful to Mr. Paul Manis and Mr. William Roche of White Mountain Research station for their generous sacrifice of time on his behalf, and to his associates at the California Institute of Technology and Scripps Institution of Oceanography: especially Dr. Norris W. Rakestraw who collected samples over the equatorial Pacific ocean, Mr. Charles McKinney who collected samples in Indiana, Mrs. Margaret K. Robinson for data on ocean water temperatures, and Mrs. Barbara Jones and Mrs. Ruth Pulkinghorn who performed some of the mass spectrometer analyses.

The author is particularly indebted to Dr. Harrison Brown and Dr. Samuel Epstein of the California Institute of Technology, whose interest in the geochemistry of carbon and oxygen was an important factor in directing him to a study of atmospheric carbon dioxide.

This work was supported by the Atomic Energy Commission Contract AT(11–1)–208.

References

Craig H. (1954) Carbon-13 in plants and the relationship between carbon-13 and carbon-14 variations in nature. *J. Geol.* **62,** 115–149.

Craig H. (1957) Isotopic standards for carbon and oxygen and correction factors for mass-spectrometric analysis of carbon dioxide. *Geochim. et Cosmochim. Acta* **12,** 133–149.

Epstein S. and Mayeda T. (1953) Variations of O^{18} content of waters from natural sources. *Geochim. et Cosmochim. Acta* **4,** 213–224.

Keeling C. D. (1958) The concentration and isotopic abundances of carbon dioxide in rural areas. *Geochim. et Cosmochim. Acta* **13,** 322–334.

Keeling C. D. (1961) A mechanism for cyclic enrichment of carbon-12 by terrestrial plants. *Geochim. et Cosmochim. Acta.* **24,** 299–313.

McKinney C. R., McCrea J. M., Epstein S., Allen H. A. and Urey H. C. (1950) Improvements in mass spectrometers for the measurement of small differences in isotope abundance ratios. *Rev. Sci. Instrum.* **21,** 724–730.

Urey H. C. (1947) The thermodynamic properties of isotopic substances. *J. Chem. Soc.* 562–581.

Wickman F. E. (1952) Variations in the relative abundance of the carbon isotopes in plants, *Geochim. et Cosmochim. Acta* **2,** 243–254.

Worthing A. G. (1943) *Treatment of Experimental Data.* John Wiley, New York.

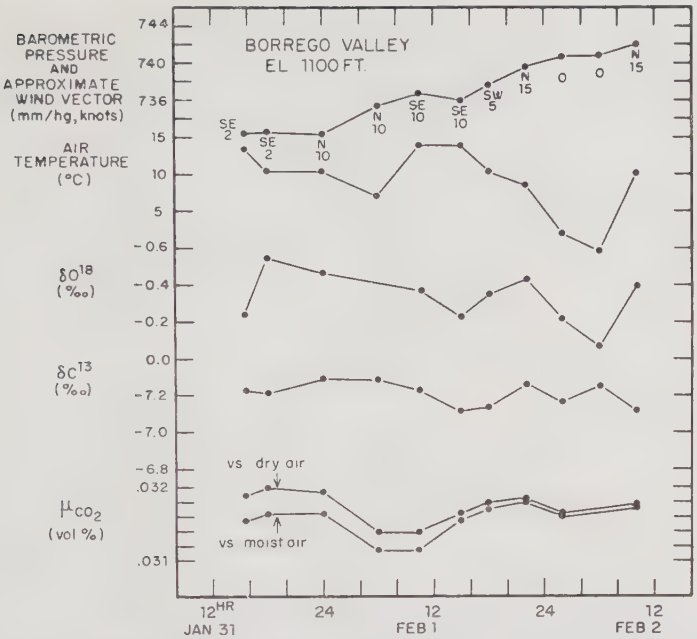

Fig. 1. Variation in the concentration and isotope ratios of atmospheric carbon dioxide, and in barometric pressure, wind vector and air temperature, over barren ground near desert vegetation, Borrego Valley, California.

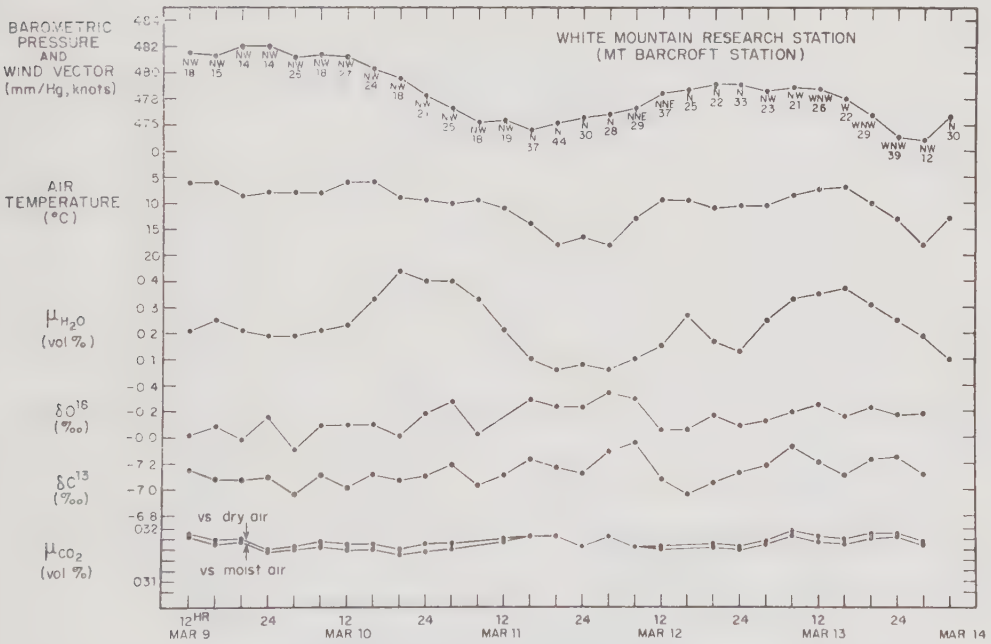

Fig. 2. Variation in the concentration and isotope ratios of atmospheric carbon dioxide, and in barometric pressure, wind vector, air temperature and water vapour concentration, over barren ground near White Mountain Research Station in the Inyo Mountains of California.

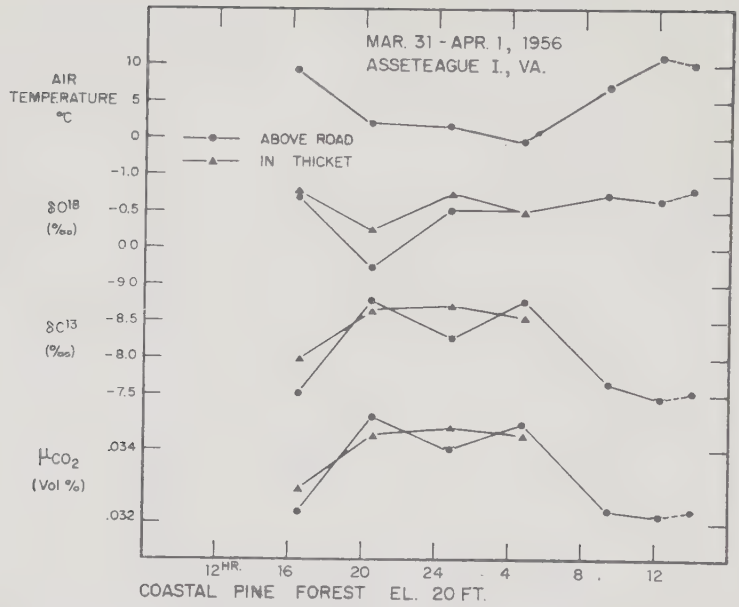

Fig. 3. Diurnal variation in the concentration and isotope ratios of atmospheric carbon dioxide in a coastal pine forest, Asseteague Island, Virginia.

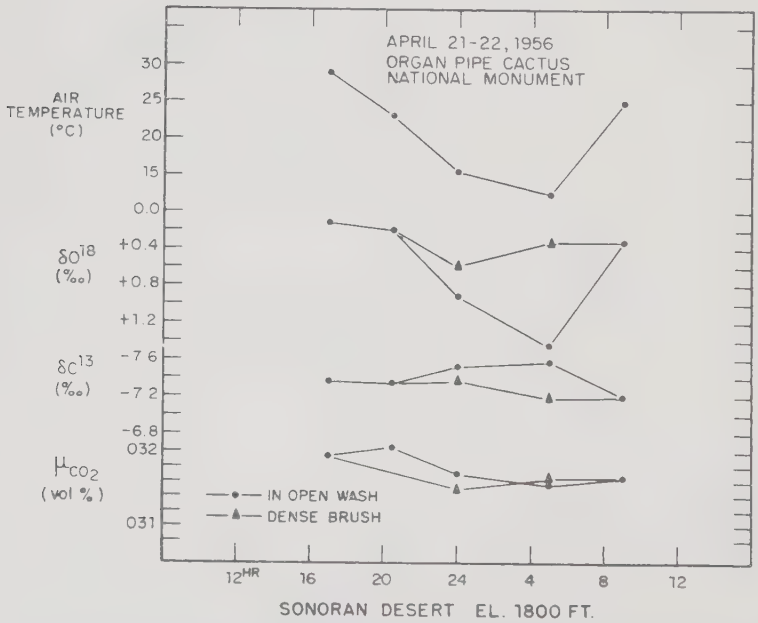

Fig. 4. Variation in the concentration and isotope ratios of atmospheric carbon dioxide, and in air temperature, over barren ground near desert vegetation and within dense desert vegetation, Upper Sonoran Desert, Arizona.

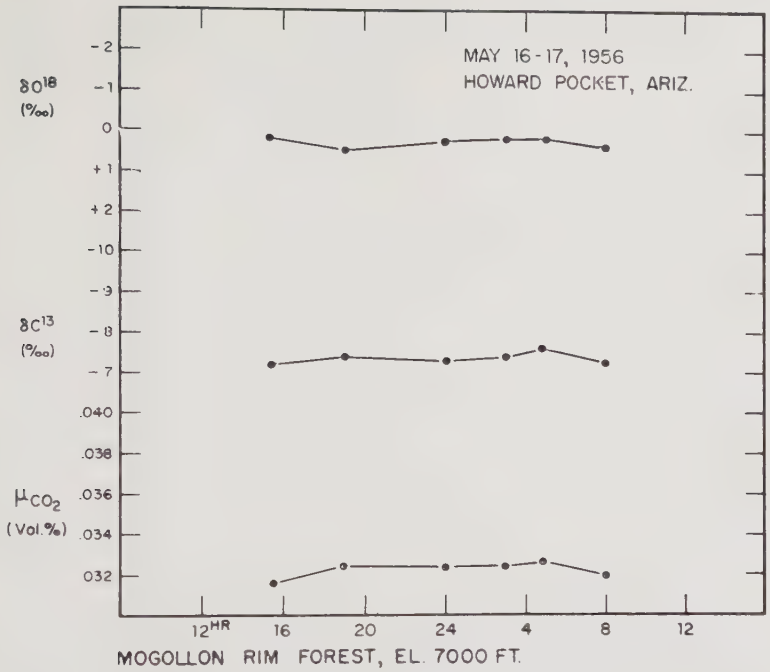

Fig. 5. Diurnal variation in the concentration and isotope ratios of atmospheric carbon dioxide in a conifer forest near the Mogollon Rim, Arizona.

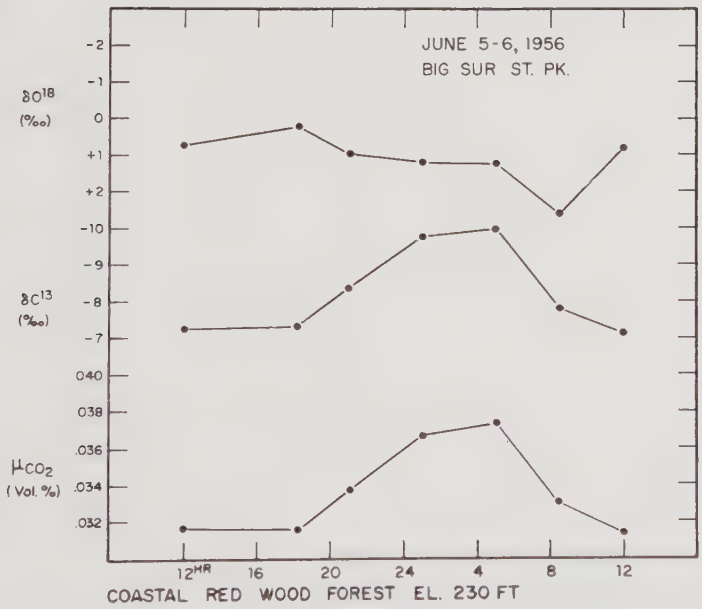

Fig. 6. Diurnal variation in the concentration and isotope ratios of atmospheric carbon dioxide in a coastal redwood forest of California.

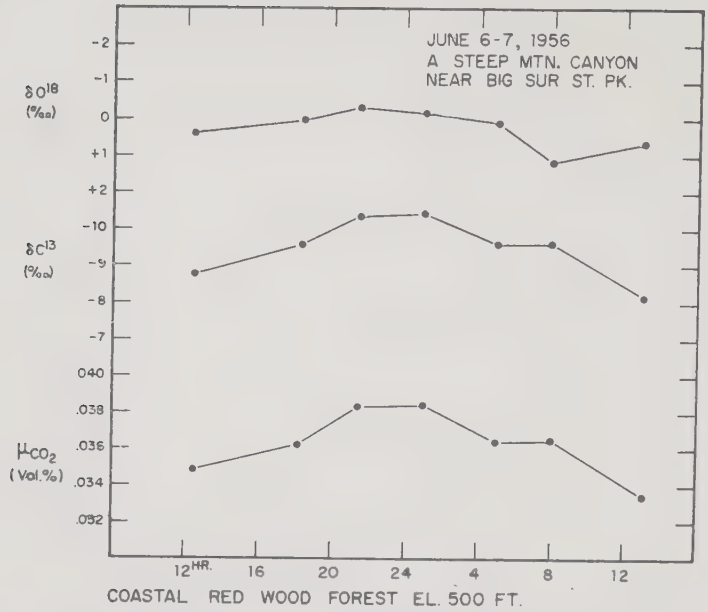

Fig. 7. Diurnal variation in the concentration and isotope ratios of atmospheric carbon dioxide in a grove of redwood trees within a steep coastal canyon, California.

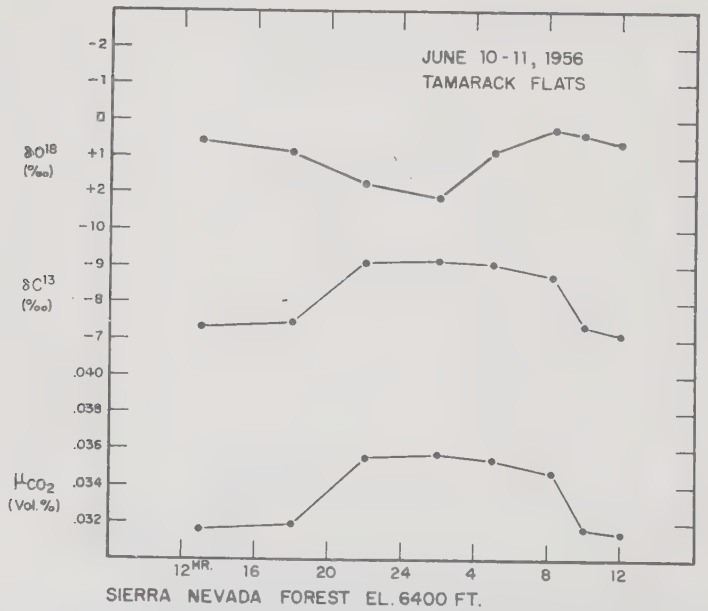

Fig. 8. Diurnal variation in the concentration and isotope ratios of atmospheric carbon dioxide in a forest of the Sierra Nevada, California.

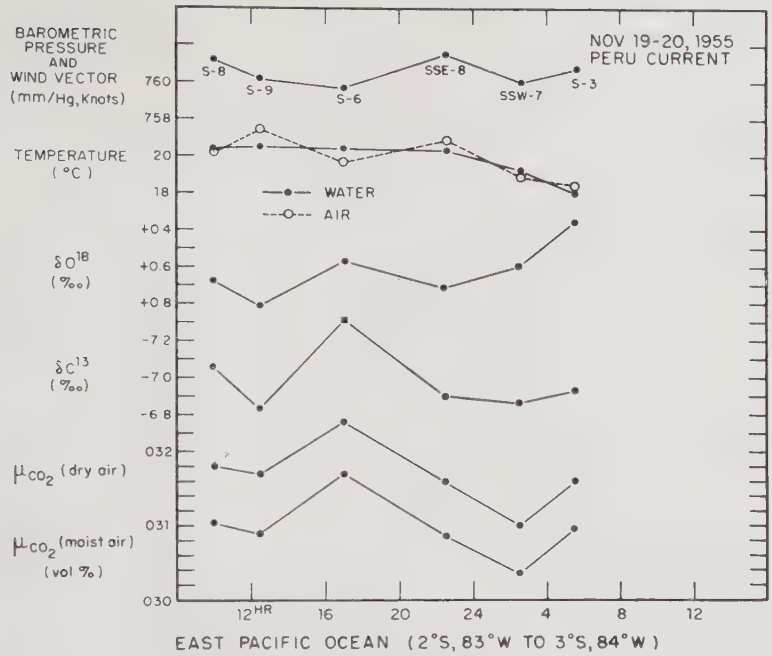

Fig. 9. Variation in the concentration and isotope ratios of atmospheric carbon dioxide over waters of the east Pacific ocean within the Peru Current.

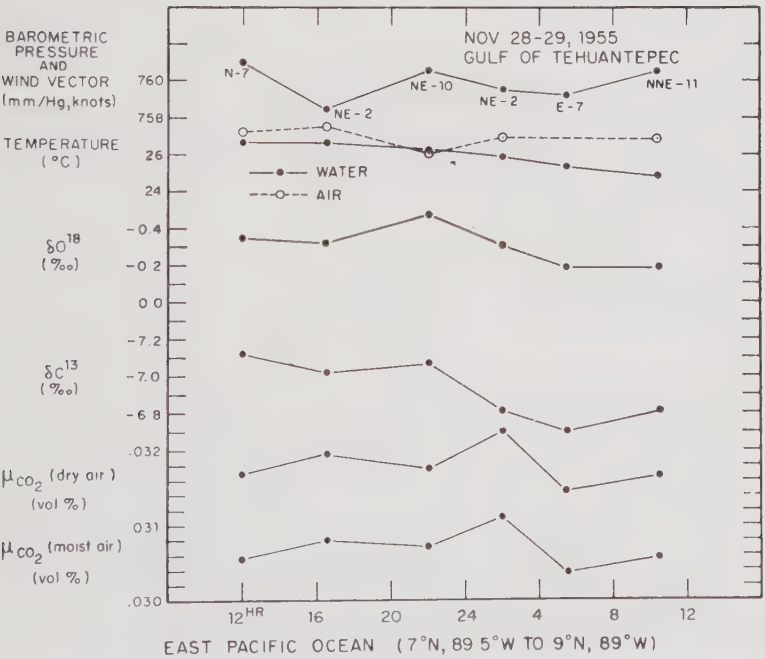

Fig. 10. Variations in the concentration and isotope ratios of atmospheric carbon dioxide over waters of the east Pacific ocean near the Gulf of Tehuantepec.

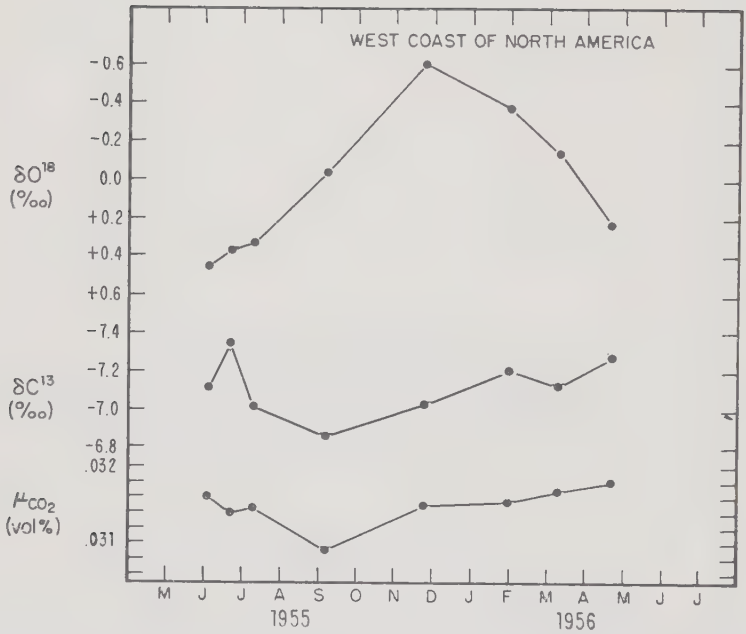

Fig. 11. Annual variation in the average concentration and isotope ratios of atmospheric carbon dioxide over barren ground and over the Pacific Ocean near the west coast of North America.

Table 1. Carbon dioxide composition and meteorological data for rural air*

Station descriptions	Local time (hr:min)	Air temp. (°C)	Wet bulb temp. (°C)	Rel. hum. (%)	μ_{H_2O} (vol. %)	Bar. press. (mm/Hg)	Wind (speed and direction (knots)	Cloud (fraction and type)	μ_{CO_2} (moist) (p.p.m.)	μ_{CO_2} (dry) (p.p.m.)	δC^{13} (‰)	δO^{18} (‰)
Otter Creek Township, Indiana Elevation 200 m (grassland, 3 km north of Terre Haute, a city with a population of 75,000; within 1 × 1 km flat open area of clover, alfalfa, and native grasses, cut and harvested 3 weeks previously; samples taken 1 m above ground, 25 August 1955)	4:45	10	—	—	—	—	E 8–12	—	506·3	—	−12·83	−0·81
	7:15	16	—	—	—	—	ESE 5–10	—	341·4	—	−8·28	−0·28
	11:30	26	—	—	—	—	SE 8–12	—	299·4	—	−6·57	−0·38
Otter Creek Township, Indiana Elevation 200 m (forest, 1 km south south-west of grassland site, in grove of native hardwood trees; samples taken 1 m above ground, 25 August 1955)	5:00	13	—	—	—	—	E 3–6	—	353·6	—	−9·00	−0·59
	7:00	16	—	—	—	—	ESE 3–6	—	378·3	—	−9·12	−0·67
	11:00	22	—	—	—	—	SE 3–6	—	—	—	—	—
Borrego Valley, California Elevation 340 m (desert valley with mountains 1500 m high to west, north, and east; 1 km downstream from Santa Catarina Spring in low wash with bushes on banks; samples taken 30 cm above ground near bank, 31 January–2 February 1956)	15:30	13·3	9·7	63	1·04	732·4	SE 1–3	1·0 Cu	315·4	318·8	−7·23	−0·24
	18:00	10·6	9·4	87	1·20	732·6	SE 1–3	0·8 Cu	316·3	320·2	−7·22	−0·55
	0:00	10·3	7·5	67	0·92	732·4	N 5–10	clear	316·4	319·4	−7·29	−0·47
	6:00	7·2	5·0	71	0·78	735·4	N 5–10	clear	311·7	314·2	−7·29	—
	10:30	13·9	8·6	49	0·84	736·8	SE 5–15	0·1 Cu	311·5	314·1	−7·23	−0·37
	15:00	13·9	5·0	18	0·30	736·0	SE 5–15	0·1 Cu	315·7	316·6	−7·12	−0·23
	18:00	10·6	2·8	18	0·24	737·5	SW 2–10	clear	317·0	317·8	−7·14	−0·35
	22:00	8·3	0·3	9	0·12	739·5	N 10–30	clear	318·0	318·3	−7·26	−0·43
	2:00	2·2	−3·9	14	0·12	740·5	calm	clear	316·3	316·6	−7·17	−0·22
	6:00	−0·6	−4·4	37	0·23	740·7	calm	clear	—	—	−7·25	−0·07
	10:00	10·0	1·7	11	0·15	742·0	SE 10–20	clear	317·3	317·8	−7·12	−0·39

* *Otter Creek Township* stations: air temperature by mercury thermometer to ±1°C, *Borrego Valley:* barometric pressure by special mercury manometer with mercury level read by cathotometer to ± 0·2 mm/Hg. *Inyo Mountains:* air temperature by mercury thermometer to ±0·5°F. (±0·3°C); relative humidity by recording hydrothermograph of unknown accuracy, barometric pressure by mercury barometer to ±0·1 mm/Hg; wind vector by recording cup-anemometer and wind vane. *Organ Pipe Cactus National Monument:* barometric pressure estimated from Palin altimeter readings to approximately ±0·5 mm/Hg. *Howard Pocket, Telephone Hill, Big Sur State Park, Canyon Near Big Sur River* and *Yosemite National Park:* mean barometric pressure for station estimated from altitude by an approximate barometric formula, value used in determining relative humidity. At all stations except Otter Creek Township stations and Inyo Mountains: air temperature and wet bulb temperature by sling psychrometer to ±0·5°F (±0·3°C). At all stations except Inyo Mountains: wind vector estimated visually. Cloud estimated visually at all stations: Ci = cirrus, Ac = altocumulus, As = altostratus, Cu = cumulus, Cb = cumulonimbus. m = metre, km = kilometre.

Table 1—(contd.)

Station descriptions	Local time (hr:min)	Air temp. (°C)	Wet bulb temp. (°C)	Rel. hum. (%)	μ_{H_2O} (vol. %)	Bar. press. (mm/Hg)	Wind (speed and direction) (knots)	Cloud (fraction and type)	μ_{CO_2} (moist) (p.p.m.)	μ_{CO_2} (dry) (p.p.m.)	δC^{13} (‰)	δO^{18} (‰)
Inyo Mountains, California	12:15	−6·1	—	35	0·21	481·5	NW 18	clear	318·5	319·1	−7·15	−0·02
Mt. Barcroft Station, elevation	16:00	6·1	—	40	0·25	481·3	NW 15	clear	317·1	317·9	−7·08	−0·08
3800 m (bare ground and snow,	20:00	−8·3	—	40	0·21	482·0	NW 14	clear	317·4	318·1	−7·07	+0·02
50–100 m north of building;	24:00	−7·8	—	35	0·19	482·0	NW 14	clear	315·7	316·3	−7·09	−0·16
samples taken 1 m above snow,	3:45	−8·0	—	35	0·19	481·2	NW 26	clear	315·9	316·5	−6·96	+0·10
9–14 March 1956)	8:00	−7·8	—	40	0·21	481·4	NW 18	clear	316·7	317·4	−7·11	−0·09
	12:15	−5·9	—	40	0·23	481·2	NW 27	0·2 Ci	316·0	316·8	−7·01	−0·09
	16:15	−6·1	—	55	0·33	480·3	NW 24	0·3 Ci	316·0	317·0	−7·11	−0·09
	20:00	−8·9	—	90	0·44	479·5	NW 18	—	314·8	316·2	−7·07	−0·01
	24:00	−9·4	—	85	0·40	478·2	NW 21	clear	315·7	317·0	−7·10	−0·18
	3:45	−10·0	—	90	0·40	477·2	NW 25	clear	315·9	317·2	−7·19	−0·27
	8:15	−9·4	—	70	0·33	476·2	NW 18	0·5 Ci	—	—	−7·03	−0·02
	11:45	−11·1	—	50	0·21	476·3	NW 19	0·1 Ci	317·5	318·2	−7·11	—
	15:30	−14·1	—	35	0·10	475·6	N 37	clear	318·3	318·7	−7·23	−0·29
	20:00	−17·8	—	30	0·06	476·1	N 44	—	318·5	318·7	−7·17	−0·23
	23:45	−16·4	—	30	0·08	476·6	N 30	clear	316·5	316·7	−7·12	−0·23
	3:45	−17·8	—	30	0·06	476·8	N 28	v. clear	318·3	318·5	−7·29	−0·34
	8:15	−13·0	—	30	0·10	477·3	NNE 29	clear	316·3	316·5	−7·36	−0·29
	12:00	−9·6	—	30	0·15	478·4	NNE 37	clear	315·8	316·3	−7·08	−0·06
	16:15	−9·6	—	60	0·27	478·7	N 25	clear	—	—	−6·96	−0·06
	19:45	−10·9	—	40	0·17	479·1	N 22	clear	316·7	317·2	−7·05	−0·14
	23:45	−10·6	—	30	0·13	479·1	N 33	clear	316·0	316·4	−7·13	−0·09
	4:30	−10·3	—	55	0·25	478·6	NW 23	—	316·9	317·7	−7·18	−0·13
	7:45	−8·3	—	65	0·33	478·9	NW 21	0·8 Ci	318·3	319·4	−7·33	−0·19
	12:00	−7·5	—	65	0·35	478·7	WNW 26	—	317·5	318·7	−7·21	−0·25
	16:00	−7·0	—	65	0·37	478·0	W 22	clear	316·8	318·0	−7·11	−0·16
	20:00	−10·0	—	70	0·31	476·7	WNW 29	clear	318·2	319·2	−7·23	−0·23
	23:45	−12·8	—	75	0·25	475·0	WNW 39	clear	318·5	319·2	−7·25	−0·17
	4:00	−17·8	—	100	0·19	474·8	NW 12	fog	317·1	317·7	−7·12	−0·18
	9:45	−13·0	—	30	0·10	476·6	N 30	clear	—	—	—	—
Assateague Island, Virginia	16:30	9·2	4·2	41	0·47	--	W 20–25	clear	323·0	324·5	−7·50	−0·69
Elevation 5 m (open area in	20:30	2·2	0·8	77	0·54	—	calm	clear	348·8	350·6	−8·77	+0·27
virgin pine forest, alternately	0:45	1·7	−0·3	67	0·46	—	calm	clear	339·7	341·4	−8·27	−0·51
swampy low land and dry sand	4:45	−0·3	−1·4	78	0·46	—	calm	clear	347·0	348·7	−8·75	−0·50
ridges; samples taken 30 cm	9:30	7·2	2·8	44	0·45	—	NW 1–3	clear	323·7	325·2	−7·63	−0·73
above dry road, moderately large	12:15	11·1	5·6	40	0·53	—	E 10	clear	322·2	323·9	−7·47	−0·65
trees on either side, 31 March–1												
April 1956)												

Asseteague Island, Virginia†	16:30								329·2	330·8	−7·98	−0·76
Elevation 2 m (dense thicket of	20:30								343·8	345·6	−8·67	−0·23
virgin pine forest, 50 m north of	0:45								345·9	347·6	−8·72	−0·73
open area site, near swamp;	4:45								344·1	345·7	−8·58	−0·45
samples taken 30 cm above ground in dense growth of low plants, beneath large pine tree, 31 March–1 April 1956)												
Chincoteague Island, Virginia	14:00	10·0	5·8	52	0·63	—	SW 12–18	—	323·5	325·6	−7·52	−0·79
Elevation 5 m (bare ground, 5 km fetch of open water to southwest; samples taken 2 m above ground, 1 April 1956)												
Organ Pipe Cactus National Monument,	17:00	28·9	13·6	15	0·62	714·8	NW 3–6	0·2 Ci	319·7	321·7	−7·37	+0·12
Arizona, elevation 550 m (open	20:30	23·3	12·2	24	0·73	715·5	calm	0·2 Ci	320·4	322·7	−7·34	+0·19
wash in desert, mountains 800 m	24:00	15·6	8·0	33	0·63	716·3	calm	0·2 Ci	317·0	319·0	−7·53	+0·91
high to north; thick bushes on	5:00	12·4	6·1	37	0·56	715·2	calm	0·2 Ci	315·7	317·5	−7·58	+1·44
south bank of wash; samples	9:15	24·7	12·2	20	0·64	715·2	NE 2–5	0·2 Ci	316·7	318·7	−7·19	+0·33
taken 1 m above gravel covered ground, 4 m from any vegetation, 21–22 April 1956)												
Organ Pipe Cactus National Monument,†	24:00								314·1	316·1	−7·45	+0·74
Arizona, elevation 550 m	5:00								316·2	318·0	−7·48	+0·74
(moderately dense desert brush, 10 m from open wash site, on top of south bank; samples taken 1 m above ground below branches of Palo Verde Bush, 21–22 April 1956)												
Organ Pipe Cactus National Monument,†	24:00								315·3	317·3	−7·48	+0·64
Arizona, elevation 550 m	5:00								315·6	317·4	−7·26	+0·74
(moderately dense desert brush, 5 m from site in Palo Verde bush, on top of bank; samples taken 1 m above ground, below branches of Mesquite bush, 21–22 April 1956)												

† For meteorological data see station above.

Table 1—(contd.)

Station descriptions	Local time (hr:min)	Air temp. (°C)	Wet bulb temp. (°C)	Rel. hum. (%)	μ_{H_2O} (vol. %)	Bar. press. (mm/Hg)	Wind (speed and direction) (knots)	Cloud (fraction and type)	μ_{CO_2} (moist) (p.p.m.)	μ_{CO_2} (dry) (p.p.m.)	δC^{13} (‰)	δO^{18} (‰)
Organ Pipe Cactus National Monument,†												
Arizona, elevation 550 m (very dense desert brush, 30 m west of site in Palo Verde bush, on top of bank; samples taken 1 m above ground within dense foliage of Iron wood tree, 21–22 April 1956)	24:00								315·0	317·0	−7·39	+0·58
	5:00								316·5	318·3	−7·18	+0·31
Howard Pocket, Arizona	15:30	23·9	8·9	12	0·44	—	2–3	clear	316·0	317·4	−7·21	+0·14
Elevation 2100 m (Mogollon Rim virgin pine and fir forest, near edge of extensive plateau; ground slopes gently down towards rim, a cliff with a vertical drop of 300–500 m; samples taken 1 m above limey soil covered with pine needles, limestone bedrock, in dense grove of small pines, near trunk of tree, 16–17 May 1956)	19:00	18·1	6·1	15	0·39	—	0–1	clear	323·4	324·6	−7·41	+0·46
	24:00	13·3	2·8	14	0·24	—	0–2	clear	323·2	323·9	−7·29	+0·25
	3:00	11·7	2·0	15	0·25	—	1–2	clear	324·0	324·8	−7·43	+0·22
	4:45	10·6	1·7	17	0·29	—	1–2	clear	325·9	326·8	−7·57	+0·18
	8:15	19·1	6·7	14	0·40	—	0–3	0·2 Ci	319·1	320·4	−7·26	+0·35
Telephone Hill, Arizona	15:00	18·3	8·0	26	0·71	—	0–2	1·0 Ac	317·7	320·0	−7·16	+0·31
18 May 1956 (see below for description of station)												
Telephone Hill, Arizona	20:45	8·1	7·0	87	1·24	—	calm	0·9 As	327·3	331·4	−7·76	+0·35
Elevation 2600 m (Kaibab plateau virgin pine and fir forest, ground slopes gently to north, 100 m from ridge top, in dense grove of medium sized trees; samples taken 1 m above limey soil covered with pine needles, 19–20 May 1956)	23:00	4·7	4·2	92	1·05	—	calm	0·2 Ac	335·7	339·2	−8·11	+0·57
	2:00	4·2	3·6	92	1·03	—	0–1	clear	358·5	362·3	—	+0·37
	4:45	4·2	3·9	92	1·03	—	0–1	clear	337·7	341·2	−8·36	+0·25
	7:45	10·6	6·7	61	1·03	—	0–1	0·5 Ac	336·7	340·2	−8·48	−0·22
	11:00	13·0	7·4	49	0·96	—	2–5	0·8 Cu + Cb	—	—	—	—

Big Sur State Park, California	12:00	19·4	14·4	58	1·30	754·0	1–3	clear	317·2	321·4	−7·23	+0·75
Elevation 70 m (virgin redwood	18:15	16·4	13·1	68	1·26	—	1–3	clear	315·8	319·8	−7·34	+0·23
forest in moderately steep-sided	21:00	12·2	10·8	85	1·21	—	0–2	clear	336·8	340·9	−8·34	+0·98
valley with mountains 1500 m	1:00	8·3	8·1	96	1·05	—	0–1	clear	366·7	370·6	−9·77	+1·20
high to east; 60 m upstream	5:00	8·0	7·8	96	1·02	—	0–1	clear	373·5	377·4	−9·95	+1·25
(south) from footbridge where	8:30	14·7	12·8	70	1·17	—	0–1	clear	329·8	333·7	−7·78	+2·61
samples were collected in 1955;	12:00	23·6	15·8	43	1·25	—	0· 3	clear	314·4	318·4	−7·08	+ 0·79
river lined with sycamore, maple, alder and willow trees, a few large redwood trees on west bank; samples taken 1 m above river on gravel bar, 3 m from dense growth of ferns and clover on west bank, near a large redwood tree, 5–6 June 1956)												
Canyon Near Big Sur River, California	12:30	20·6	14·4	51	1·23	754·0	1–2	clear	348·7	353·1	−8·78	+0·40
Elevation 150 m (virgin redwood	18:15	19·2	14·2	57	1·26	—	0–1	clear	362·9	367·5	−9·60	+0·07
forest, 5 km south of Big Sur	21:30	17·0	13·1	64	1·23	—	0–2	clear	383·4	388·2	−10·36	−0·28
River valley; narrow steep-	1:00	16·4	11·9	58	1·07	—	1–2	clear	383·8	388·0	−10·43	−0·16
walled coastal canyon on west	5:00	16·1	11·1	54	0·98	—	2–3	clear	364·2	367·8	−9·62	+0·11
slope of mountain, 1000 m high;	8:00	16·1	11·9	60	1·09	—	2–3	clear	365·0	369·0	−9·58	+1·16
large redwoods on sides of canyon	13:00	19·4	14·4	58	1·30	—	4–6	clear	334·7	339·1	−8·16	+0·64
with numerous projecting roots, dense lower growth of ferns, dense vegetation extends about 1 km up canyon from site; samples taken 2 m above stream, 2 m from nearest vegetation, 6–7 June 1956)												
Yosemite National Park, California	13:00	18·3	11·1	44	1·16	606·0	0–5	0·1 Ac	316·0	319·7	−7·34	+0·58
Tamarack Flats, elevation 1950	18:00	15·6	10·6	57	1·24	—	0–3	0·1 Ac	318·6	322·6	−7·46	+ 0·87
m (virgin pine and fir forest,	22:00	7·8	6·7	87	1·14	—	0–1	clear	354·9	359·0	−9·12	+1·73
west slope of Sierra Nevada	2:00	4·2	4·2	100	1·02	—	0–1	clear	357·0	360·7	−9·16	+2·10
mountain range; in gently slop-	5:00	2·0	2·0	100	0·87	—	0–1	clear	354·1	357·2	−9·06	+ 0·95
ing tributary valley, moderately	8:15	7·8	5·8	79	1·02	—	0–1	clear	347·2	350·8	−8·74	+0·25
dense trees near stream, samples	10:00	16·7	7·8	30	0·71	—	1–3	clear	316·8	319·1	−7·39	+0·39
taken 1 m above Tamarack Creek	12:00	19·6	9·6	28	0·81	—	1–5	clear	313·8	316·4	−7·11	+0·65
on footbridge, 10–11 June 1956)												

† For meteorological data see station above.

Table 2. Carbon dioxide composition and meteorological data for marine air*

Station descriptions	Local time (hr:min)	Air temp. (°C)	Water temp. (°C)	Wet bulb temp. (°C)	Rel. hum. (%)	μ_{H_2O} (vol. %)	Bar. press. (mm/Hg)	Wind (speed and direction) (knots)	Cloud (fraction and type)	μ_{CO_2} (moist) (p.p.m.)	μ_{CO_2} (dry) (p.p.m.)	δC^{13} (‰)	δO^{18} (‰)
Huntington Beach, California Elevation 2 m (bare ground, 0·5 km north-east of beach, open water to west; samples taken 1 m above ground, 22 June 1955)	14:40	23	—	—	—	—	—	W 15–25	clear	314·7	—	−7·40	+ 0·43
Corona del Mar, California Elevation 10 m (bare concrete, 0·3 km from beach, open water to west, 15 km south-east of Huntington beach site; samples taken 1 m above roof of building, 22 June 1955)	15:30	23	—	—	—	—	—	W 15–25	clear	313·4	—	−7·30	+0·30
Southern California Coast Elevation 910 m (from airship over ocean water, 10 km west of shore, 80 km south of Los Angeles, 25 Nov. 1955)	13:40	15	—	—	—	—	—	—	0·9 As	315·4	—	−6·94	−0·65
Southern California Coast Elevation 460 m (same location as above, 25 Nov. 1955)	13:45	15	—	—	—	—	—	—	0·9 As	315·0	—	−7·22	−0·62
	14:20	15	—	—	—	—	—	—	0·9 As	314·6	—	−6·93	−0·55
Eastropic Cruise Elevation 10 m (from bow of ship underway between 1° 50′ South, 83° 07′ West; and 2° 48′ South, 84° 12′ West, 19–20 Nov. 1955)	10:00	20·2	20·4	18·9	86	2·34	761·2	S 8	0·7	310·8	318·2	−7·06	+ 0·68
	12:30	21·4	20·5	19·7	83	2·51	760·2	S 9	1·0	309·1	317·1	−6·83	+0·81
	17:00	19·7	20·4	18·9	91	2·26	759·7	S 6	1·0	316·9	324·2	−7·31	+0·57
	22:30	20·8	20·3	18·9	81	2·42	761·5	SSE 8	1·0	308·4	316·0	−6·90	+0·73
	2:15	18·9	19·2	18·1	92	2·16	760·0	SSW 7	1·0	303·4	310·1	− 6·86	+ 0·60
	5:30	18·3	18·0	17·8	94	2·08	760·7	S 3	1·0	309·7	316·2	- 6·93	+0·36
Eastropic Cruise Elevation 10 m (from bow of ship underway near 4° 00′ North, 90° 30′ West, 29 Nov. 1955)	6:00	23·9	25·7	22·8	89	2·92	760·0	SW 8	0·7	306·7	316·0	- 7·38	+ 0·07
Eastropic Cruise Elevation 10 m (from bow of ship underway between 7° 00′ North, 89° 30′ West; and 9° 10′ North, 89° 00′ West, 30 Nov.–Dec. 1955)	12:00	27·2	26·6	25·8	90	3·57	761·0	N 7	0·7	305·4	316·9	−7·15	−0·35
	16:30	27·5	26·6	26·1	90	3·62	758·4	NE 12	0·7	307·9	319·5	−7·02	−0·32
	22:00	26·0	26·2	25·0	92	3·32	760·5	NE 10	—	307·2	317·7	−7·07	−0·46
	2:00	26·9	25·8	25·0	86	3·50	759·5	NE 2	0·9	311·2	322·5	−6·81	−0·30
	5:30	—	25·3	—	—	3·49	759·2	E 7	0·9	303·4	314·4	−6·70	−0·18
	10:30	26·8	24·8	25·3	89	3·47	760·5	NNE 11	0·1	305·7	316·7	−6·81	−0·18

* *Eastropic Cruise:* air temperature and wet bulb temperature by sling psychrometer to ±0·5°F (±0·3°C) water temperature by mercurial thermometer to ±0·1°C, barometric pressure to ±0·02 in/Hg (±0·5 mm/Hg) wind vector by indicating anemometer, cloud cover estimated visually. *Huntington Beach and Corona del Mar:* wind vector estimated visually. Cloud estimated visually at all stations: As = altostratus, m = metre, km = kilometre, etc.

Table 3. Characteristic composition of forest and grassland air

Station	Geographic location	Elevation (m)	Date	Minimum μ_{CO_2} (p.p.m.)	Maximum μ_{CO_2} (p.p.m.)	δC^{13} at minimum μ_{CO_2} (‰)	$\delta_0(C^{13})$ (‰)	$I(C^{13})$ (‰)	Av. dev. in δC^{13} (‰)	No. of analyses
			1955							
Big Sur State Park*	California	70	18–19 May	316	389	−7·41	−7·11	−24·1	0·098	9
Yosemite National Park*	California	1950	2–3 Jun.	313	364	−7·06	−7·07	−23·1	0·076	7
Otter Cr. Tp.—Grass†	Indiana	200	25 Aug.	299	506	−6·57	—	—	—	3
Otter Cr. Tp.—Forest†	Indiana	200	25 Aug.	—	—	—	—	—	—	2
Hart's Pass*	Washington	1900	31 Aug.–1 Sept.	307	321	−6·84	−7·20	−21·0	0·120	5
Olympic National Park*	Washington	170	6–7 Sept.	308	404	−6·66	−6·87	−24·2	0·134	7
Rock Lake*	Washington	600	10–11 Sept.	309	336	−6·83	−7·10	−25·0	0·046	7
			1956							
Asseteague Is.—Road	Virginia	5	31 Mar.–1 Apr.	322	349	−7·47	−7·04	−24·5	0·039	7
Asseteague Is.—Thicket†	Virginia	2	31 Mar.–1 Apr.	—	347	—	−7·06	−25·2	0·050	4
Howard Pocket	Arizona	2100	16–17 May	316	326	−7·21	−7·00	−20·9	0·040	5
Telephone Hill	Arizona	2600	18–20 May	318	358	—	—	—	—	6
Big Sur State Park	California	70	5–6 Jun.	314	374	−7·08	−7·09	−25·3	0·074	7
Canyon near Big Sur R.	California	150	6–7 Jun.	335	384	−8·16	−6·98	−25·9	0·044	7
Yosemite National Park	California	1950	10–11 Jun.	314	357	−7·11	−7·20	−23·6	0·030	8

* For original data see KEELING (1958).

† Missing entries are due to insufficient data.

Table 4. Characteristic composition of mountain, desert and marine air near the Pacific Coast of the United States

Station	Geographic location	Elevation (m)	Date	Minimum μCO_2 (p.p.m.)	Maximum μCO_2 (p.p.m.)	Average μCO_2 (p.p.m.)	Average δC^{13} (‰)	Average δO^{18} (‰)	No. of analyses
			1955						
Yosemite National Park*	California	2500–3000	3 Jun.	314	318	316·1	−7·12	+0·45	2
Huntington Beach and Corona del Mar	California	2–10	22 Jun.	313	315	314·1	−7·35	+0·37	2
Inyo Mountains*	California	3800–4300	8–9 Jul.	312	319	314·7	−7·02	+0·33	11
Olympic National Park*	Washington	0	6–7 Sept.	309	310	309·2	−6·86	−0·04	2
Southern California Coast	California	460–910	25 Nov.	315	315	315·0	−7·03	−0·61	3
			1956						
Borrego Valley†	California	340	31 Jan.–2 Feb.	312	318	315·5	−7·21	−0·38	10
Inyo Mountains	California	3800	9–14 Mar.	315	318	316·9	−7·13	−0·14	29
Organ Pipe Cactus Nat. Mon.†	Arizona	500	21–22 Apr.	317	320	318·2	−7·28	+0·23	2

* For original data see KEELING (1958).

† Data for air during temperature inversions are excluded.

Geochimica et Cosmochimica Acta, 1961, Vol. 24, pp. 299 to 313. Pergamon Press Ltd. Printed in Northern Ireland

A mechanism for cyclic enrichment of carbon-12 by terrestrial plants

Charles D. Keeling*
Division of Geological Sciences, California Institute of Technology

(*Received* 11 *July* 1960)

Abstract—A model is described which predicts that variations in the relative abundance of C^{12} and C^{13} in terrestrial plants may be due in part to varying degrees of local cycling of carbon dioxide gas. The model emphasizes the effectiveness of transient departures from a steady state in achieving cyclic enrichment, and predicts that cyclic enrichment should be limited by the maximum concentration of carbon dioxide occurring near the plants during their diurnal cycle. Experimental data are discussed which support the model.

Introduction

Two hypotheses have been advanced to explain why the C^{13}/C^{12} ratio of terrestrial plants is variable. One hypothesis emphasizes the role of the local environment; the other, the role of the plants themselves. Wickman (1952) proposed that ecological differences, especially variations in the local supply of air, were a major cause of variations in the C^{13}/C^{12} ratio, after observing that the ratio for plants from a herbarium of the Riksmuseum in Stockholm showed a dependence on environment; e.g. plants from windy locations showed higher ratios than plants which had grown where the air circulation was restricted. Craig (1954a) from data on plants, many of which he collected himself, found no similar correlation and, indeed, observed that different parts of the same plant could have different C^{13}/C^{12} ratios—a result which seemed to deny any ecological correlation. He further showed that Wickman's hypothesis cannot be fulfilled if carbon dioxide continuously enters and leaves a plant community at a steady state. He therefore concluded (Craig, 1954a, p. 119) that "there is no 'cyclical' mechanism which can operate to produce an enrichment in the plants greater than that performed by the plants themselves", and that variations in isotopic ratio must result from metabolic processes which occur within the plants themselves.

Nevertheless, Craig's basis for denying cyclic enrichment can be shown to depend on an unnecessary assumption that plants absorb carbon dioxide under *uninterrupted* steady state conditions. Furthermore, measurements by the author of atmospheric carbon dioxide near plants indicate a relationship which agrees with Wickman's hypothesis (Keeling, 1961). It therefore seems desirable to reopen the subject. It will be shown that the possibility should exist for both metabolic and ecological factors to influence the isotopic composition of plants.

A Model for Cyclic Enrichment

The degree to which the reabsorption by plants of carbon dioxide derived from the same plants might lead to isotopic enrichment greater than that performed by the plants themselves will be investigated by considering the model illustrated by

* Present address, Scripps Institution of Oceanography, University of California, La Jolla, California.

Fig. 1. An absorber, emitter and local air reservoir constitute a local system within which carbon dioxide can cycle in a closed path or can exchange with a much larger outside source of atmospheric carbon dioxide. The absorber which represents a local community of plants as an acceptor of carbon dioxide is assumed to obtain carbon dioxide from the local air reservoir by some unspecified process such that:

$$R_{\Delta a} = \alpha R \tag{1}$$

where R denotes the C^{13}/C^{12} ratio of the carbon dioxide in the local air reservoir at any selected moment, $R_{\Delta a}$ denotes the C^{13}/C^{12} ratio of carbon dioxide taken up by the absorber at the same selected moment, and α is a factor whose value depends only on intrinsic properties of the absorber.* To agree with experimental data to be discussed below, α will be assumed to be less than unity.

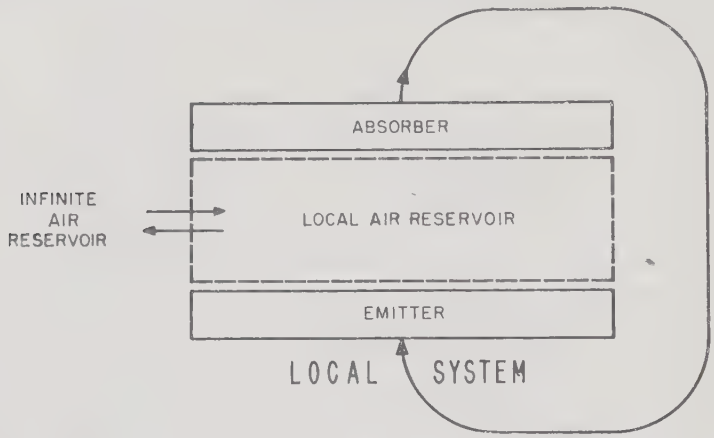

Fig. 1. Model for cyclic isotopic enrichment with a single absorber and emitter.

The emitter, which represents the same local community of plants (including soils) as a source of respired carbon dioxide is assumed to derive its supply of carbon from the absorber after some delay, and to release carbon dioxide to the local air reservoir, both transfers taking place without isotopic fractionation. The process of transforming the carbon of the absorber into carbon dioxide in the emitter is not specified.

The air of the local air reservoir which represents the air near the plants, may mix with air from an infinite air reservoir representing the regional atmosphere of the earth or be shut off from it. The infinite air reservoir is assumed to furnish the sole original source of carbon for the local system, and to have a composition independent of the local system.

For simplicity it will be assumed that no gradients in concentration or in isotopic abundance exist within the local air reservoir, and that the amount of carbon dioxide there is small compared to the quantity of carbon in the absorber

* In the development which follows R, $R_{\Delta a}$, R_a, R_e, R_s and R_I will be treated as variable, $R_.$, R_0, R_1, R_2, etc., as fixed values of the isotopic ratio. Enrichment will always signify enrichment of carbon 12, but ratios will be defined as C^{13}/C^{12} to conform with the practice of expressing data as the difference in per mil of this ratio.

and emitter. The isotopic composition of the local system as a whole, therefore, can be taken as the average of that of the absorber and emitter alone.

As an initial step in creating a supply of carbon in the local system, the absorber (and hence the emitter) will be allowed to build up a supply of carbon by direct absorption from the infinite air reservoir, i.e. without cyclic enrichment. This will lead to:

$$R_a = R_e = \alpha R_0 \tag{2}$$

where R_a is the isotopic ratio of the absorber (here equal to $R_{\Delta a}$), R_e and R_0 the isotopic ratios of the emitter and infinite air reservoir, respectively.

In considering the behaviour of this model three situations may be distinguished: (1) the local air reservoir remains completely mixed with the infinite air reservoir; (2) the local air reservoir is always shut off from the infinite air reservoir; (3) the local air reservoir sometimes mixes with the infinite air reservoir but at other times is shut off.

The first situation is equivalent to the representation of Craig (1954a, p. 117); the second can exist only temporarily under the assumption that the local system ultimately derives its carbon from the infinite air reservoir; the third is equivalent to Wickman's mechanism: "An essential point in this type of cyclic enrichment is that the local carbon dioxide cycle should not be quite complete, but that there should . . . . . be an exchange with the bulk of the atmosphere" (Wickman, 1952, p. 253).

That this third situation may lead to cyclic enrichment will now be shown by considering the following cycle:

(1) The emitter operates alone so that the concentration of the local air reservoir rises by a factor F_1 from μ_0, the concentration of the infinite air reservoir, to μ_1.

(2) The absorber operates alone so that the concentration of the local air reservoir is reduced again to μ_0.

(3) The local air reservoir mixes completely with the infinite air reservoir.

Calculating: The isotopic ratio, $\bar{R}$, of a mixture of components with isotopic ratios, $R_1, R_2, \ldots R_i$, and concentrations, $\mu_1, \mu_2, \ldots \mu_i$, is very nearly the geometric average:

$$\bar{R} = \frac{\sum_i R_i \mu_i}{\sum_i \mu_i} \tag{3}$$

For step (1) substitute for the first component in equation (3) the initial composition of the local air reservoir, μ_0, R_0; for the second component, the addition to the local air reservoir from the emitter, $\mu_1 - \mu_0$, R_e:

$$R_1 = \frac{R_0}{F_1} + \frac{R_e}{F_1}(F_1 - 1) \tag{4}$$

where μ_1, R_1 refer to the average composition of the local air reservoir at the completion of step (1) and

$$F_1 = \frac{\mu_1}{\mu_0}$$

For step (2) consider initially any infinitesimal subtraction of carbon dioxide from the local air reservoir. The composition will change from μ, R, to $\mu - d\mu$, $R - dR$, by removal of an increment, $d\mu$, having the isotopic ratio αR. Substituting these quantities in equation (3) leads to:

$$\mu\, dR = (\alpha - 1)R\, d\mu \tag{5}$$

For a finite subtraction equation (5) is integrated between the limits R_1 and R, μ_1 and μ. Solving for R:

$$R = R_1\left(\frac{\mu}{\mu_1}\right)^{\alpha-1} \tag{6}$$

At the completion of step (2):

$$R_2 = \frac{R_1}{F_1^{\alpha-1}} \tag{7}$$

where R_2 represents the isotopic ratio of the local air reservoir at the completion of the step. With the aid of equation (2) it can be shown that:

$$\text{If} \qquad \alpha - 1 \leqslant 0, \qquad R_2 \geqslant R_0$$

The average isotopic ratio of the carbon added to the absorber during step (2) is given by:

$$\bar{R}_{\Delta\alpha} = \int_{\mu_1}^{\mu_0} \frac{R_{\Delta\alpha} d\mu}{\mu_0 - \mu_1} \tag{8a}$$

$$= \int_{\mu_1}^{\mu_0} \frac{\alpha R\, d\mu}{\mu_0 - \mu_1} \tag{8b}$$

employing equation (3) in integral form, and then substituting αR for $R_{\Delta\alpha}$ according to equation (1). Substituting for R from equation (6) and integrating:

$$\bar{R}_{\Delta\alpha} = R_1\left(\frac{F_1 - F_1^{1-\alpha}}{F_1 - 1}\right) \tag{9a}$$

$$= R_2\left(\frac{F_1^{\alpha} - 1}{F_1 - 1}\right) \tag{9b}$$

where the second form of writing comes from the relationship between R_1 and R_2 given by equation (7). It can be shown that:

$$\text{If} \qquad \alpha - 1 \leqslant 0, \qquad \bar{R}_{\Delta\alpha} \leqslant \alpha R_0$$

Although performing steps (1) and (2) leaves the same amount of carbon dioxide in the local air reservoir, the absorber has taken up carbon dioxide which is enriched in carbon-12 with respect to the local air reservoir by a factor which differs from unity by an amount greater than $\alpha - 1$. The local air reservoir, on the other hand, has been depleted in carbon-12 with respect to the infinite air reservoir. The situation in the local air reservoir is illustrated by Fig. 2: the greater enrichment of the absorber during step (1) is compensated for by the departure of R_2 from R_0 at the end of step (2).

A closed loop in the R, μ plane is produced by step (3) in which the local air reservoir is caused to mix completely with the infinite air reservoir. During this step, the concentration of carbon dioxide in both air reservoirs is the same (μ_0), and, therefore, no net transfer of carbon dioxide takes place. An isotopic transfer occurs, however, since the depleted carbon of the local air reservoir is removed from the local system by exchange with the infinite air reservoir. Thus, the cycle of steps, (1) through (3), is not a steady state.

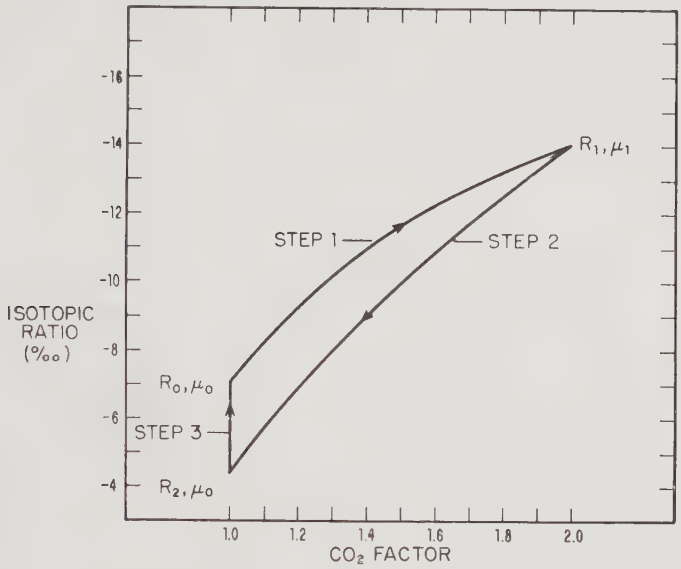

Fig. 2. Variations in composition of the local air reservoir during an initial stage of cyclic enrichment. The composition during steps (1) and (2) are described by equations (4) and (6), respectively. It is assumed that $R_s = \alpha R_0$, $F_1 = 2$, $\alpha = 0{\cdot}986$. The isotopic ratio is expressed as the per mil variation from a value chosen to agree with that of the isotopic standard used by KEELING (1958, 1961).

Sufficient repetition of the above cycle can bring the average isotopic composition of the absorber, R_a, close to the value of $\bar{R}_{\Delta a}$ given by equations (9). A steady state still does not result, however, because the isotopic ratio of the emitter, initially equal to αR_0 by equation (2) must approach that of the absorber according to the assumption that the emitter derives its supply of carbon from the absorber. If the emitter, thus enriched in carbon-12, participates further in the cycle, the enrichment of the local system may increase until:

$$R_2 = R_0 \tag{10}$$

This equation is associated with an isotopic steady state, for substituting R_0 for R_2 in equations (7) and (9b) leads to:

$$R_1 = R_0 F_1^{\alpha-1} \tag{11}$$

and

$$R_a = R_0\left(\frac{F_1^{\alpha} - 1}{F_1 - 1}\right) \tag{12}$$

where $\bar{R}_{\Delta a}$ can be replaced by R_a, the average isotopic ratio of the absorber.* When this new expression for R_1, derived from a consideration of isotopic relationships during step (2) and (3), is substituted in equation (4), which refers to step (1), the resulting expression for R_e is:

$$R_e = R_0\left(\frac{F_1^{\alpha} - 1}{F_1 - 1}\right) \tag{13}$$

Thus, if equation (10) is fulfilled, the isotopic ratio of the absorber and emitter are equal, and isotopic steady state exists both between the absorber and emitter and between the local air reservoir and the infinite air reservoir. The situation is illustrated by Fig. 3. A combination of steps (1) and (2) alone is now sufficient for

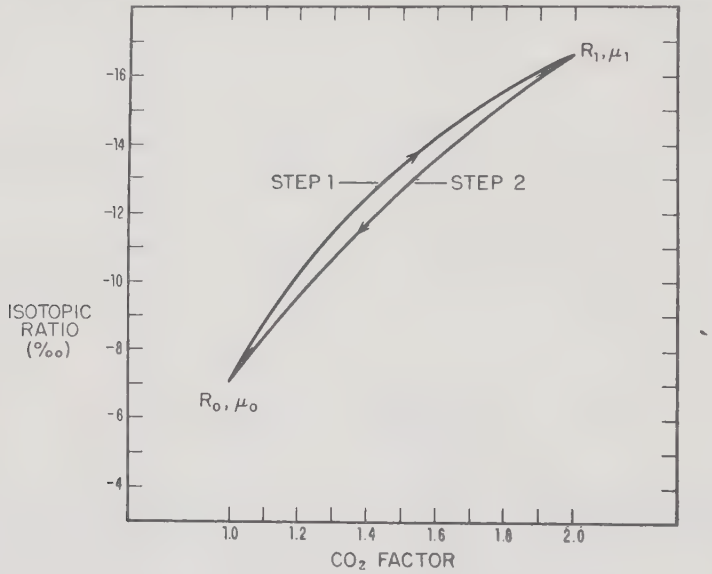

Fig. 3. Variations in composition of local air reservoir during steady state cyclic enrichment. The same isotopic units and values for F_1 and α, are assumed as for Fig. 2.

a closed loop in the R, μ, plane. At the completion of step (2) the local air reservoir has the same composition as the infinite air reservoir, so that mixing during step (3) cannot cause any change in the local system.

The average isotopic ratio of the local system, R_s, is equal to that given separately for the absorber and emitter by equations (12) and (13). This ratio is a function of α, the fractionation factor, and F_1. Adopting a term of plant physiology (LUNDEGÅRDH, 1954), F_1 may be called the maximum "CO_2 factor", a factor which describes the "intensity" of the local cycle of carbon dioxide. If F_1 is unity (no local cycle):

$$R_s = \operatorname*{Lim}_{F_1 \to 1} R_0\left(\frac{F_1^{\alpha} - 1}{F_1 - 1}\right) = \alpha R_0 \tag{14}$$

identical with situation (1). As F_1 increases, R_s decreases without limit, i.e. the enrichment of carbon-12 increases without limit.

* Equations equivalent to (11) and (12) have been derived by BROWN *et al.* (1957) in connexion with the uptake of gases on metal surfaces.

This result is consistent with the hypothesis of WICKMAN (1952, pp. 252–253): "The enrichment will be smallest where . . . . . the 'local atmosphere' for some reason or other does not develop, i.e. in a desert or at a constantly windy place. The largest isotopic effect will be observed where the cyclic process is most intense, e.g. a tropical rain forest."

The above mechanism illustrates how cyclic enrichment could occur under conditions of steady state which require that the amount and isotopic ratio of carbon dioxide entering a local system must equal that leaving the system, but which allow intermittent inequalities of concentration to exist between the local system and the outside. As an aid to calculation, the absorber and emitter were assumed to operate separately. Clearly, different relative rates of absorption and emission, by increasing or decreasing the tendency of the local system to cycle carbon dioxide during periods of high accumulation in the local air reservoir, should result in different degrees of cyclic enrichment for the same maximum CO_2 factor, F_1.

For example, if reductions in concentration in the local air reservoir result from the *simultaneous* operation of the absorber and emitter, one can show that the maximum enrichment for a given value of F_1 diminishes as the rate of emission approaches the rate of absorption. But if the emitter and absorber operate simultaneously at the same rate during part of the cycle, so that the concentration in the local air reservoir then remains steady, the enrichment increases as the proportion of absorption at high accumulation increases, reaching an upper limit when all but an infinitesimal portion of the absorption takes place while the local accumulation is maximum. This limiting situation could not, of course, be easily realized in nature, but it does not violate the condition of a steady state. Moreover, a calculation demonstrates that a moderate proportion of turnover at maximum accumulation results in an enrichment which closely approaches that for infinite turnover.* The theoretically greatest enrichment is, therefore, of interest as fixing an upper limit for any mechanism involving only one absorber and emitter. It can be calculated as follows:

(1) From the last paragraph it follows that the maximum enrichment attainable during periods when the concentration in the local air reservoir is decreasing, occurs when the absorber operates alone. The isotopic ratio of the local air reservoir at maximum accumulation corresponding to this situation is given by equation (11).

(2) If the absorber and emitter operate at equal rates during a period of maximum accumulation, the composition of the local air reservoir will approach a value differing by a factor α from the isotopic ratio of the emitter and absorber, that is:

$$R_a = R_e = \alpha R_1 \tag{15}$$

following a mechanism described by LANE and DOLE (1956) to explain the Dole effect (DOLE, 1952). Substituting for R_1 from equation (11) and writing R_s, the average isotopic ratio of the local system, for $R_a = R_e$:

$$R_s = \alpha R_0 F_1^{\alpha-1} \tag{16}$$

* For example, if the concentration of carbon dioxide in the local air reservoir at maximum accumulation is twice the concentration in the infinite air reservoir ($F_1 = 2$), and if an additional amount of carbon dioxide equal to the amount of accumulation is turned over while the accumulation remains maximum, the enrichment is increased above equation (13) by 75% of the increase for infinite turnover. For $F_1 = 1{\cdot}5$ the increase is 69%.

In Table 1 the isotopic enrichment of the local system, R_s as predicted by equation (12) (setting $R_a = R_s$) and equation (16) is given for various values of the maximum CO_2 factor, F_1, assuming values of α and R_0 which agree approximately with experimental data discussed below.

Table 1.* Isotopic enrichment (in per mil) predicted by equations (12) and (16)

F_1	$R_s = R_0\left(\frac{F_1^{\alpha} - 1}{F_1 - 1}\right)$ (‰)	$R_s = \alpha R_0 F_1^{\alpha-1}$ (‰)
1·0	−20·96	−20·96
1·1	−21·63	−22·27
1·2	−22·25	−23·46
1·3	−22·84	−24·55
1·4	−23·39	−25·56
1·5	−23·92	−26·50
1·6	−24·43	−27·38
1·7	−24·91	−28·21
1·8	−25·37	−28·98
1·9	−25·81	−29·72
2·0	−26·24	−30·42

* Isotopic ratios are expressed as per mil differences from an arbitrary value chosen so that the isotopic ratio of the infinite air reservoir has a value of −7·06‰. The fractionation factor, α, is assumed to be 0·986. These quantities are chosen to conform with some experimental data discussed below (pp. 308–309).

Extension of the Model to Stratified Local Systems

According to CRAIG (1954a), in a plant community where low and high growing plants share a common soil there exists the possibility of a steady state effect in which the rate of mixing of the local and general atmosphere affects the enrichment of the plants near the ground, because the lower plants have available a steady state excess of carbon dioxide derived in part from the higher plants. This possibility would be of greater interest if, as CRAIG believed, cyclic enrichment were not possible where the local air supply has a spacially uniform concentration of carbon dioxide. But one may still ask whether the presence of higher concentrations of carbon dioxide near the lower plants might produce *greater* cyclic enrichment for a given CO_2 factor than can be produced where the air supply is uniform.

To investigate this the author has considered a model, depicted by Fig. 4, which is assumed to have properties similar to the single stage model previously considered except that two absorber–emitter couples are joined in cascade. The inner couple, which represents the lower plants, has a separate local air reservoir which is joined to the local air reservoir belonging to the outer couple through a connexion which allows transfer of carbon dioxide either by mixing or by transport predominately in the outward direction. The outer air reservoir is allowed also to mix with an infinite air reservoir which represents, as before, the regional atmosphere of the earth.

If the inner and outer system interact by complete mixing of their respective local air reservoirs during some part of their cycles, it can be seen from a consideration of the possible paths in the R, μ, plane which represents the compositions of the respective local air reservoirs, that for steady state, these paths must have some point in common, and therefore the maximum enrichment for a given CO_2 factor for the inner system cannot significantly exceed that for a single stage model.

Of greater interest is the other limiting possibility: that all of the transport between the local air reservoirs is by forward diffusion from the inner air reservoir to the outer. Although this situation would never be precisely realized, it can be approached if some transport takes place by molecular diffusion. In this case, for steady state, the transfer from the inner air reservoir to the outer must be balanced by an equal transfer from the outer absorber to the inner emitter.

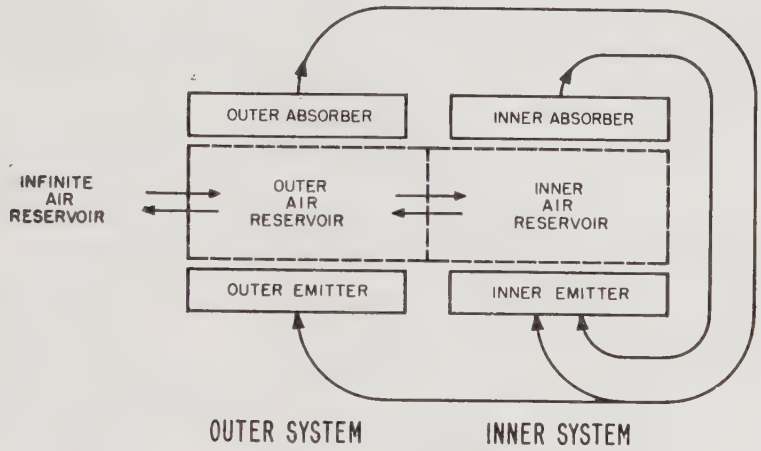

Fig. 4. Model for cyclic isotopic enrichment with two absorber emitter couples in cascade.

The maximum possible enrichment is fixed by the fact that the carbon transferred out of the inner system through its local air reservoir cannot be more enriched than that transferred in from the outer absorber. This leads to a limiting expression:

$$R_I = \alpha^2 R_0 F_I^{\alpha-1} F_O^{\alpha-1} \tag{17}$$

where R_I is the isotopic ratio of the inner system at maximum enrichment, F_I and F_O, the maximum CO_2 factors of the inner and outer air reservoirs, respectively.*

Although actual enrichments in nature ought to be considerably less than this upper limit, it far exceeds, at moderate CO_2 factors, the enrichment given by equation (16) for a uniform local air supply. Thus cyclic enrichment greater than single stage should be attainable for low growing plants under natural conditions such as Lundegårdh (1924) and Fuller (1948) have described.

Experimental Evidence for Cyclic Enrichment

Experimental data which may be directly compared with the foregoing models are available in the author's study of forest air (Keeling, 1958, 1961). The data are particularly suited for testing the model because they reflect average isotopic enrichments between the atmosphere and the organic phases within a plant community, without regard for variations which may occur within the plants after absorption. In agreement with the model, the concentration of carbon dioxide in the air near the plants fluctuated periodically, variations in the C^{13}/C^{12} ratio and in the concentration of this carbon dioxide were very nearly proportional, and minimum concentrations and associated isotopic ratios at all locations, except one, agreed with the value found for air representative of the general atmosphere.

* Craig (1954a) has calculated that the binary molecular diffusion coefficient ratio for $C^{12}O_2/C^{13}O_2$ is approximately 1·004. Since this figure is close to unity compared with α as deduced below, the counteracting effect of diffusion on the isotopic enrichment, R_I should be small and has been neglected in equation (17).

The proportionality between variations in concentration, μ, and relative isotopic ratios, δ, could be expressed by the relationship:

$$\delta = I + \frac{M}{\mu} \tag{18}$$

where δ is the per mil variation in the isotopic ratio, R, from a standard value, $R_\bullet$, i.e.:

$$\delta = \left(\frac{R - R_\bullet}{R_\bullet}\right) 10^3$$

and I and M are constants determined empirically for each station. It can be shown that equation (18) is equivalent to equation (4) if:

$$I = \delta_e$$

$$M = (\delta_0 - \delta_e)\, \mu_0$$

where

$$\delta_e = \left(\frac{R_e - R_\bullet}{R_\bullet}\right) 10^3$$

and

$$\delta_0 = \left(\frac{R_0 - R_\bullet}{R_\bullet}\right) 10^3$$

Thus from the empirical relationship at each station it is possible to deduce the value of R_e, the isotopic ratio of the carbon dioxide released to the air by the organic phases, and R_0, the isotopic ratio corresponding to the minimum concentration, μ_0.

Values of δ_e and δ_0, corresponding to R_e and R_0, respectively, are given in Table 2 together with the observed maximum and minimum concentrations and computed CO_2 factors for each station.*

To test quantitatively the relationship between the data and enrichment predicted by the model, the fractionation factor, α, has been estimated from the difference between δ_0 and δ_e at the two stations with such low observed CO_2 factors that the conditions leading to cyclic enrichment should have been nearly absent.

Howard Pocket: $F_1 = 1{\cdot}03$ $\qquad \alpha - 1 \cong \delta_e - \delta_0 = -13{\cdot}9‰$

Hart's Pass: $F_1 = 1{\cdot}05$ $\qquad \delta_e - \delta_0 = -13{\cdot}8‰$

These values indicate that α differs from unity by approximately $-14‰$ ($\alpha = 0{\cdot}986$). Assuming this value and a hypothetical infinite air reservoir with a

* The data are adapted from Table 3 of KEELING (1961). Descriptions of stations will be found there and in KEELING (1958). Two stations (Otter Creek and Telephone Hill) are excluded from Table 2 because of insufficient data; two others (Asseteague Island, Road and Thicket) because sampling occurred too early in the season (1 April) for the CO_2 factors to be even remotely representative.

composition equal to the average of δ_0 and μ_0 for all forest stations (KEELING, 1961), i.e.:

$$\delta_0 = -7{\cdot}06‰$$

$$\mu_0 = 314 \text{ p.p.m. (parts per million of air)}$$

the enrichment predicted by equations (12) and (16) is as appears in Table 1. The maximum enrichment as given by equation (16), is plotted in Fig. 5, where:

$$\mu_{max} = F_1\mu_0 = F_1 \times 314 \text{ p.p.m.}$$

Within the limits of uncertainty of the calculations and of the experimental results (indicated, for example, by the variance between the two points for Big Sur)

Table 2. Composition of forest and grassland air

Station, elevation (m), and date	CO_2 factor (F_1)	Minimum μ_{CO_2} (p.p.m.)	Maximum μ_{CO_2} (p.p.m.)	$\delta_0(C^{13})$ (‰)	$\delta_e(C^{13})$ (‰)
Canyon Near Big Sur River (Pacific Coast Redwood Forest) 150 m, 6–7 June 1956	—	335	384	−7·0	−25·9
Olympic National Park (Pacific Coast Rain Forest) 170 m, 6–7 Sept. 1955	1·31	308	404	−6·9	−24·2
Big Sur State Park (Pacific Coast Redwood Forest) 70 m, 18–19 May 1955	1·23	316	389	−7·1	−24·1
Ditto, 5–6 June 1956	1·19	314	374	−7·1	−25·3
Yosemite National Park (Sierra Nevada Pine and Fir Forest) 1950 m, 2–3 June 1955	1·16	313	364	−7·1	−23·1
Ditto, 10–11 June 1956	1·14	314	357	−7·2	−23·6
Hart's Pass, Washington (Cascade Mountain Crest Alpine Forest) 1900 m, 31 Aug.–1 Sept. 1955	1·05	307	321	−7·2	−21·0
Howard Pocket, Arizona (Mogollon Rim Pine and Fir Forest) 2100 m, 16–17 May 1956	1·03	316	326	−7·0	−20·9

the experimental enrichment and predicted maximum enrichment are in good agreement, except for a canyon near the Big Sur river, the point for which is omitted from the figure. This station was near the base of a very steep gorge within a few metres of dense low plants and the exposed roots of trees. A gentle downdraft of air persisted throughout the period of sampling. Unlike any other station, measurements indicated a continuous excess of carbon dioxide derived

from vegetation. This fact and a value of δ_e considerably more negative than that predicted by equation (16) suggest a stratified system where the enrichment of the lower plants is affected by diffusion.

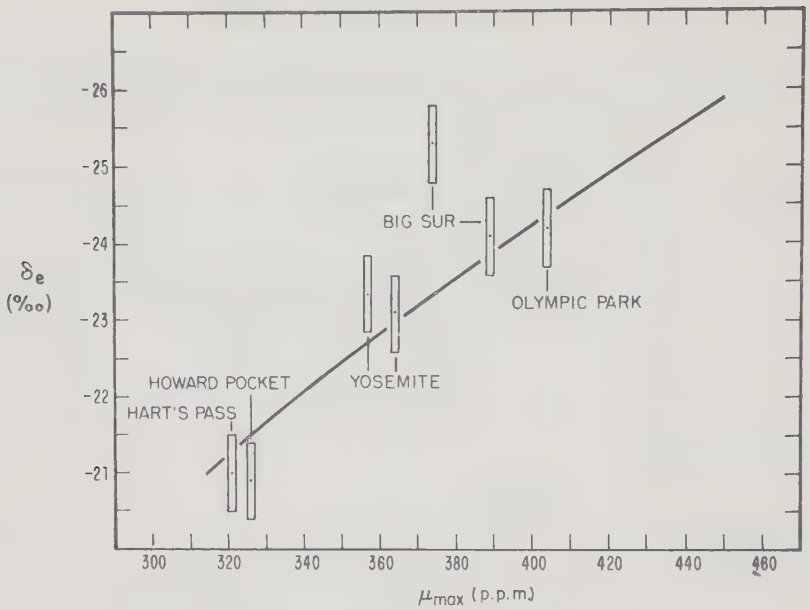

Fig. 5. Per mil variation in the isotopic ratio of carbon dioxide added to forest air, δ_e, as a function of μ_{max}, the observed maximum concentration of carbon dioxide in the air. The experimental data are plotted within rectangles. The smooth curve is a plot of the predicted maximum single stage enrichment employing values of α and R_0 which give the best correspondence with the experimental data.

Discussion

The hypothesis of cyclic enrichment does not rule out the possibility of isotopic variations in plants produced by metabolic factors, but its usefulness will depend on whether the fractionation factor, α, which was assumed to be constant in order to test the model, is in fact sufficiently invariant to allow useful ecological comparisons. Direct measurements of α by Weigl *et al.* (1951), Baertschi (1953), and Park and Epstein (1960) vary greatly for plants grown in laboratories. The fractionation factor reported by Baertschi (1952) and Craig (1953) for the absorption of carbon dioxide by aqueous hydroxide solution agrees with the author's value deduced from measurements of forest air, but whether the inorganic and organic mechanisms of absorption are the same has not been established. No direct determinations of α in nature have been reported; to produce the curve of Fig. 5, α was chosen simply to give the best fit with the experimental data. The consistency of this fit is the principal argument against supposing that the observed enrichments are not due to a fortuitous averaging of variable, perhaps even highly variable, fractionations by different plants as proposed, for example, by Lane and Dole (1956) for the absorption of oxygen. Since the fit is not perfect and the points are few, more measurements in the field are needed before the model is in any sense verified.

On the other hand, plants very likely undergo some cyclic enrichment even if the principal cause for variations in the C^{13}/C^{12} ratio lies within the plants. A periodic variation in concentration of carbon dioxide, a primary feature of the mechanism of cyclic enrichment, was unfailingly observed at forest stations by the author. Minimum concentrations occurred in the afternoon, maximum concentrations at night. This behaviour of the air near plants, known since the time of Saussure (1830), and shown by Hüber (1953) to persist throughout a growing season, is a consequence of the photosynthetic cycle (see, for example, Lundegårdh, 1954), and should occur to some extent in the vicinity of all plants. An additional feature of the mechanism is the requirement of concentrations equal to or higher than that of the general atmosphere. Also found at all stations, this is a likely result of the alternation of still air at night and turbulent air during the day. Alternations in turbulence occur whenever the prevailing wind is not so strong as to maintain turbulence throughout the night and the sunshine during the day is sufficient to heat the ground (Geiger, 1950). Turbulence is normally greatest in the afternoon, the same period in which the plants are most likely to have withdrawn more carbon dioxide from the air than could be returned by respiration. In virgin forests, such as the author has studied, assimilation and respiration of carbon dioxide should be nearly in balance so that the turbulence during the day will prevent a reduction of carbon dioxide relative to the general atmosphere under most conditions.

Conclusions

A full appraisal of the hypothesis of cyclic enrichment awaits more extensive measurements of air near plants. The general conclusion that higher local concentrations of carbon dioxide are associated with greater isotopic enrichment is explicit to the hypothesis, however, and leads to a number of predictions related to plant ecology which may also be used to test the hypothesis.

(1) On the average, the concentration of carbon dioxide in air diminishes from ground to the tops of the higher plants (Hüber, 1953). If the cyclic hypothesis holds, lower plants and branches of the same plant should show greater enrichment than taller plants and branches, as a plant grows taller relative to nearby plants its average enrichment should decline, etc.

(2) Areas exposed to the wind or with sufficient slope to limit temperature inversions of the air at night (Geiger, 1950) are less favourable for the accumulation of carbon dioxide than sheltered areas. If the cyclic hypothesis is obeyed, plants in topographic basins should, in general, be enriched with respect to those on slopes, the latter with respect to those on ridges or summits; plants in the lee of prevailing winds with respect to those in windward locations; etc.

(3) The concentration of carbon dioxide in air may show a dependence on rainfall, temperature or season (Lundegårdh, 1924, pp. 238 and 254) which would be reflected in the isotopic ratio.

(4) Except where the local production of carbon dioxide by carbonates in the soil leads to special effect (Craig, 1954a), the fractionation factor, α, ought to set a lower limit for the enrichment between plants and air. The C^{13}/C^{12} ratio of plants should reflect this lower limit unless depletion of carbon-12 occurs within the plants after they have absorbed carbon dioxide from the air.

Several of these predictions find experimental support.

An isotopic effect, possibly related to diminishing concentration of carbon dioxide with height, has been observed in tree rings, the very early rings of a Sequoia tree being enriched in carbon-12 with respect to succeeding rings (Craig, 1954b).

Direct evidence of an isotopic effect associated with height above ground is furnished by some recent measurements of Münnich and Vogel (1959), who found a steady decrease in carbon-12 from ground level to 20 m height for a tree in a forest in Upper Bavaria. The total variation in C^{13}/C^{12} ratio was 4‰.

The author's study of forest air shows a striking correlation of enrichment with topography. Least enrichment occurred for stations on a mountain saddle (Hart's Pass) and near a steep cliff (Howard Pocket), where the local air was continually in motion during the night. The values of δ_e for these stations ($-20{\cdot}9$ and $-21{\cdot}0$‰) agree with the C^{13}/C^{12} ratios of Wickman (1952) for plants grown in "notoriously windy places" ($-20{\cdot}8$ and $-21{\cdot}1$‰).* The author's station at Yosemite National Park with intermediate values of δ_e ($-23{\cdot}1$ and $-23{\cdot}6$‰) was in a gently sloping tributary valley, while the stations with more negative values of δ_e (Big Sur State Park and Olympic National Park, $-24{\cdot}1$ to $-25{\cdot}3$‰ respectively) were in nearly flat bottomed basins.

With respect to the author's value for carbon dioxide of the general atmosphere, the minimum enrichments of non-desert terrestrial plants reported by Wickman (1952) and Craig (1954a), $-12{\cdot}9$ and $-14{\cdot}5$‰, respectively, are close to the minimum fractionation indicated by the study of forest air (-14‰).

Acknowledgements—I wish to thank my associates at the California Institute of Technology and Scripps Institution of Oceanography, especially Drs. Harrison Brown, Harmon Craig, Samuel Epstein, Edward Goldberg and Devendra Lal, for helpful advice; Drs. Michael Rochester of the University of Toronto and Bert Bolin of the International Institute of Meteorology at Stockholm, to whom I am indebted for critical reading of the manuscript; and Drs. J. C. Vogel and K. O. Münnich for permission to quote unpublished results of their study of isotopic variation in plants.

References

Baertschi P. (1952) Die Fractionierung der Kohlenstoffisotopen bei der Absorption von Kohlendioxyd. *Helv. Chim. Acta* **35,** 1030–1036.

Baertschi P. (1953) Die Fractionierung der natürlichen Kohlenstoffisotopen im Kohlendioxydstoffwechsel grüner Pflanzen. *Helv. Chim. Acta* **36,** 773–781.

Brown J. B., Dole M. and Lane G. A. (1957) Fractionation of oxygen isotopes in the formation of oxide films on copper. *J. Chem. Phys.* **27,** 251–258.

Craig H. (1953) The geochemistry of the stable carbon isotopes, *Geochim. et Cosmochim. Acta.* **3,** 53–92.

Craig H. (1954a) Carbon 13 in plants and the relationships between carbon 13 and carbon 14 variations in nature. *J. Geol.* **62,** 115–149.

Craig H. (1954b) Carbon-13 variations in sequoia rings and the atmosphere. *Science* **119,** 141–143.

Dole M. (1952) The chemistry of the isotopes of oxygen. *Chem. Rev.* **51,** 263–300.

Fuller H. J. (1948) Carbon dioxide concentration of the atmosphere above Illinois forest and grassland. *Amer. Midland Naturalist* **39,** 247–249.

* Wickman's values have been converted to per mil using Wickman's determination of Craig's standard, as described by Craig (1954a).

Geiger R. (1950) *The Climate Near the Ground.* Harvard University Press, Cambridge, Mass.
Hüber B. (1953) Der Einfluss der Vegetation auf die Schwankungen des CO_2-Gehaltes der Atmosphäre, *Arch. Meteorol. Geophys. Bioklimat.* B **4,** 154–167.
Keeling C. D. (1958) The concentration and isotopic abundances of atmospheric carbon dioxide in rural areas. *Geochim. et Cosmochim. Acta* **13,** 322–334.
Keeling C. D. (1961) The concentration and isotopic abundances of carbon dioxide in rural and marine air. *Geochim. et Cosmochim. Acta.* **24,** 277–298.
Lane G. A. and Dole M. (1956) Fractionation of oxygen isotopes during respiration. *Science* **123,** 574–576.
Lundegårdh H. G. (1924) *Der Kreislauf der Kohlensäure in der Natur.* Gustav Fischer, Jena.
Lundegårdh H. G. (1954) *Klima und Boden in ihrer Wirkung auf das Pflanzenleben.* Gustav Fischer, Jena.
Münnich K. O., Vogel J. C. (1959) Variations in C^{14} content during the past years. Paper presented at the International C^{14} Symposium, Groningen, Sept. 1959.
Park R. and Epstein S. (1960) Carbon isotope fractionation during photosynthesis. *Geochim. et Cosmochim. Acta.* **21,** 110–126.
Saussure T. de (1830) Memoire sur les variations de l'acide carbonique atmospherique. *Ann. chim. phys.* **44,** 5–45.
Weigl J. W., Warrington P. M. and Calvin M. (1951) The relation of photosynthesis to respiration. *J. Amer. Chem. Soc.* **73,** 5058–5063.
Wickman F. (1952) Variations in the relative abundance of the carbon isotopes in plants. *Geochim. et Cosmochim. Acta* **2,** 243–254.

Geochimica et Cosmochimica Acta, 1961, Vol. 24, pp. 314 to 316 Pergamon Press Ltd., Printed in Northern Ireland

GEOCHEMICAL NOTES

A short note on the relative abundance of rubidium and strontium in vitrain ashes from coals in Nova Scotia

THE Sr content found in Nova Scotia coals (HAWLEY, 1955) suggested that the Rb–Sr content might be utilized in determining the absolute age of coals. The problem of the detrital origin of Rb and Sr arose, but was believed eliminated by using vitrain, which is believed to form only from organic debris. The vitrain samples were taken from the Sydney coalfield, Nova Scotia.

The vitrain samples were ashed in an electric furnace at 450°C. Ashing time varied from 18 to 30 hrs. The Rb and Sr contents of the vitrain ashes were determined by stable isotope dilution techniques on a solid source mass-spectrometer. Additional Rb determinations were made by spectrochemical analysis using standard operational procedures for the determination of an alkali metal by the addition method (AHRENS, 1950). The standard for Rb, using a three point working curve, was prepared by CANNEY (1952). The Sr content of the vitrains was not determined by spectrochemical analysis because a suitable standard was not available.

Two vitrains were analysed for Rb and Sr by isotope dilution. The results are presented in Table 1.

Table 1. Isotope dilution analyses of Rb and Sr contents in vitrain ashes

Name of sample*	Rb (p.p.m.)	Sr (p.p.m.)
Vitrain SRI	33	808
Vitrain IV6	46	437

* The sample numbers (Tables 1 and 2) refer to various coal seams in the Sydney coalfield.

Six vitrains were analysed for Rb for emission spectrography. The results are presented in Table 2.

Table 2. Spectrochemical analysis for Rb content in vitrain ashes

Name of sample	Rb (p.p.m.)
Vitrain SRI	35 ± 10
Vitrain IV 25	30 ± 10
Vitrain V 25-IB	55 ± 15
Vitrain IV 6	65 ± 20
Vitrain IV 3a8	100 ± 30
Vitrain Hb. no. 26	250 ± 75

Determinations by isotope dilution and by emission spectrography for Rb in vitrain SRI have essentially identical results. Such close agreement was not obtained for vitrain IV 6. The isotope dilution analysis is the more reliable of the two techniques (HERZOG and PINSON, 1955).

For Rb–Sr age determinations the Sr/Rb ratio should not exceed 2:1 for young Palaeozoic samples. If this ratio is exceeded the error is approximately equivalent to the age. This ratio is exceeded by vitrains SRI and IV 6 and these samples are therefore unfavourable for the determination of ages. Although the Sr content in four of the vitrains is not known, HAWLEY found an average content of 560 p.p.m. Sr in a suite of Sydney coals, not all of which were vitrains. This value agrees with our two analyses. Thus, the relatively low Rb content (Table 2) suggests that the Sr/Rb ratios will be unfavourably high and of no value for age determinations. A possible exception is vitrain Hb. no. 26. These ratios support the belief that the Sr/Rb ratio in the crust is approximately 6:1 (HERZOG and PINSON, 1956).

Acknowledgements—This research program was sponsored in part by the Nova Scotia Research Foundation, and by the Research Division, United States Atomic Energy Commission. The experimental work was carried out in the Department of Geology and Geophysics, M.I.T. We acknowledge the assistance of W. H. PINSON, W. H. DENNEN and W. L. WHITEHEAD. The coal samples were provided by L. H. KING of the Coal Research Laboratory, Department of Mines and Technical Surveys.

W. M. TUPPER*
and
D. H. LORING†

* Department of Geology, Carleton University, Ottawa, formerly at M.I.T.
† Department of Geology, Manchester University.

REFERENCES

AHRENS L. H. (1950) *Spectrochemical Analysis*. Addison Wesley Press, Cambridge, Mass.

CANNEY F. C. (1952) Some aspects of the geochemistry of potassium, cesium, and tellium in sediments. Unpublished Ph.D. thesis, M.I.T.

HAWLEY J. E. (1955) Spectrographic study of some Nova Scotia coals, *Trans. Canad. Inst. Min. Met.* **58,** 412–426.

HERZOG L. F. and PINSON W. H. (1955) The Sr and Rb contents of the granite G–1 and the diabase W–1. *Geochim. et Cosmochim. Acta* **8,** 295–298.

HERZOG L. F. and PINSON W. H. (1956) Rb/Sr age, elemental and isotopic abundance studies of stoney meteorites. *Amer. J. Sci.* **254,** 555–566.

The analysis of metallic spheroids from Meteor Crater, Arizona

AN X-RAY examination of metallic spheroids from Arizona's meteorite crater indicates that these particles were formed from terrestrial as well as meteoritic matter.

A careful investigation of the terrain around Arizona's meteorite crater has resulted in the discovery of a large number of rounded particles, principally from 0·1 to 0·2 mm in diameter, asymmetrically distributed around the crater (NININGER, 1956). These particles have been called metallic spheroids; they consist of a metallic core and an outer crust containing oxidized matter. Chemical analysis of the metallic spheroids has shown that they contain higher percentages of Ni and Co than the larger meteorite fragments found around the crater; this indicates that these particles represent altered meteoritic material, and it has been postulated that they are a condensation product from a metallic vapour cloud that formed after impact of the original meteorite. One-sixth of the total sample of whole spheroids used in the chemical analysis was unidentified and classified as "insoluble residue". In addition, the ratio Ni:Fe in the metallic cores was found to be greater than this ratio in the whole spheroids (NININGER, 1956).

In order to add to the description of these particles, we have obtained X-ray diffraction

photographs of several metallic spheroid samples with a powder camera having a 57·3 mm radius. Iron radiation was used on samples numbered 1 to 4 and Mo radiation on samples 5 and 6. Samples 1, 2 and 3 were whole spheroids, samples 4 and 5 were metallic cores mechanically freed of crust material and sample 6 comprised outer crust material obtained from nine spheroids. Positive mineral identifications are as follows: kamacite in samples 1, 2, 4 and 5; taenite in samples 5 and 6; quartz (α-quartz, hexagonal) in samples 1, 2, 3 and 4; magnetite in sample 6. Numerous lines on the sample 3 pattern were not identified, and the subsequent crushing of this whole spheroid indicated an exceedingly small shiny center. It should be noted that substances having intense reflections with large d-spacings, such as α-quartz, are very difficult to identify with Mo radiation because of poor resolution of the powder lines. The spheroids were obtained from Dr. Nininger.

The powder pattern lines show that single crystals having solid grain size of from 10^{-3} to 10^{-5} cm are found within the spheroids. It is apparent that there is a large variation in chemical composition within the spheroid group, and the presence of taenite in sample 6 indicates that 1:1 correspondence between core and outer crust, and non-oxidized and oxidized material does not exist. In view of this it is possibly surprising that the chemical analysis showed a higher Ni:Fe ratio in the metallic cores than in the whole spheroids, since the crust material is enriched with taenite fragments; however, a rapid leaching of oxidized Ni from the spheroid outer crusts during weathering would work in opposition to this effect.

The occurrence of SiO_2 in the samples is significant since quartz has not been reported present in the larger meteorite fragments from Meteor Crater. This accounts for the "insoluble residue" of the chemical analysis. Undoubtedly the source of SiO_2 is the Coconino sandstone which is found at the crater. The existence of quartz in the spheroids is not inconsistent with a metallic vapour cloud if the presence of a dispersed, quartz dust due to pulverization of the sandstone upon impact of the meteorite is allowed.

Department of Chemistry
Arizona State University
Tempe, Arizona

B. Zaslow and L. M. Kellogg

Reference

Nininger H. H. (1956) *Arizona's Meteorite Crater*. World Press, Denver.

Geochimica et Cosmochimca Acta, 1961, Vol. 24, p. 317, Pergamon Press Ltd., London

LETTER TO THE EDITOR

Beryllium in river water

In their interesting paper, Merrill *et al.* (1960) noticed amongst others the occurrence of excess quantities of non-dissolved beryllium in the river Lehigh. A short discussion about the origin of that excess excludes the possibility of industrial pollution, "although this river passes through an area of coal and steel industry", as stated by the authors.

There is a point which is worth raising: the source of the observed contamination could be the ashes of coal. This is of no great interest for the discussion and does not bring any modification to the conclusions of the article. However, as is fairly well known today, coal ashes sometimes contain relatively high amounts of beryllium as well as other rare elements (Jedwab, 1960) and the dumping or elimination conditions of industrial wastes are particularly favourable to the specific introduction of the finer particles enriched with beryllium into the hydrographic net.

J. Jedwab

Université Libre de Bruxelles

References

Jedwab J. (1960) Le charbon comme source de beryllium. *Bull. d. Soc. belge Géol., Paléontol. et Hydrol.* **69**, 67–77.

Merrill J. R., Lyden E. F. X., Hondia M. and Arnold J. R. (1960) The sedimentary geochemistry of the beryllium isotopes. *Geochim. et Cosmochim. Acta* **18**, 108–129.

Geochimica et Cosmochimica Acta, 1961, Vol. 24, p. 318. Pergamon Press Ltd. Printed in Northern Ireland

BOOK REVIEW

A. P. VINOGRADOV: **The Geochemistry of Rare and Dispersed Chemical Elements in Soils.** Second Edition, revised and enlarged. Consultants Bureau, New York, 1959. x + 209 pp., $9.50.

THIS book contains results of analyses of more than twenty complete soil profiles from the different soil zones of the Eastern European Plain. The profile distribution of forty-three trace elements is discussed together with the rare earths and radioactive elements.

Methods of determination are briefly reported. There then follows an interesting chapter dealing with geochemical regularities in the distribution of certain elements in soils. Much useful information on the physicochemical factors (parent material, weathering, water relations, ionic potential, oxidation–reduction systems, soil pH, and biological processes) which govern the behaviour of trace elements in soils is discussed.

After a brief description of the soils of the Eastern European Plain an admirable attempt is made to examine the behaviour of related groups of elements rather than individuals and much use is made of variations in element ratios, e.g. B/Cl, Ba/Sr, Ni/Co and Th/U in drawing conclusions on the processes of soil formation and development. Trace element analyses of soils from other parts of the world are presented separately and these results discussed in relation to Russian findings. The importance of certain elements in biological processes is briefly considered and the concept of "biogeochemical provinces" is evolved.

The chapter on boron is full and detailed. The reason for the high boron content of some salinized southern Russian soils appears to be due primarily to ancient volcanism together with marine accumulation of boron. The results presented agree well with American findings in studies on the boron-rich soils of the western U.S.A. Such groups as the halogens, alkali metals, alkaline earths and others are then discussed, the analytical data being presented in a similar pattern throughout. The need for further research particularly on the structure and properties of organometal complexes in soils is stressed throughout the volume.

Difficulties in translation have in places disturbed the flow of the text and in others led to confusion. Eluvial and illuvial horizons are confused (pp. 136, 149) while in Table 123, dolomite appears as diorite. Statements such as "the presence of MnO_2 makes iron unavailable," thus accounting for infertility in manganese-rich soils, have to be interpreted with caution. Fig. 7 (p. 12), Fig. 1 (p. 40) and Table 107 (p. 154) are wrongly referred to, while pages 169 and 170 have become reversed.

Most chapters end with a summary of the conclusions drawn and the final summary concludes with a plea for the production of soil maps according to trace element content. The bibliography, which is not complete, consists of a list of 560 scientific works.

M. L. BERROW

INFORMATION FOR CONTRIBUTORS

I. GENERAL

1. Papers on *geochemistry* should be submitted to the appropriate Executive Editor—Prof. L. R. WAGER for papers from the United Kingdom and British Commonwealth and for papers in English from Europe; PROF. C. W. CORRENS for papers in German or French; Prof. E. INGERSON for papers from the American continents. Papers submitted for publication will naturally be judged from the standpoint of scientific originality and novelty. Technical details of apparatus used in scientific investigation can, however, be presented in brief notes. Critical comments or preliminary results requiring early publication should be submitted as letters to the editors. Where possible, letters should be confined to 500 words. The preparation of progress reports and review articles will be invited by the editors from time to time. The journal appears as independent and complete numbers, which are combined into volumes of about 300 pages.

2. Only papers which have not been previously published can be accepted. Authors must agree not to publish elsewhere a paper submitted to and accepted by *Geochimica et Cosmochimica Acta*.

3. Fifty reprints of each paper are provided free. Additional copies can be purchased if ordered at the time the first proofs are returned. A reprint order form will accompany first proofs.

II. SCRIPT REQUIREMENTS

1. Scripts must be written in one of the three official languages—English, French or German.

2. The script should be typed (not a carbon copy). The text must be ready for printing and should be carefully checked for errors. Authors will receive proofs for correction. The original script plus two copies will assist in expediting publication.

3. Illustrations should accompany the script mounted on separate sheets. Line diagrams that require to be redrawn should include all relevant details. Half-tone illustrations should be restricted to the minimum necessary. Photographs should be enlarged sufficiently to permit their clear reproduction and if words or numbers appear on them, two copies should be sent, one clearly printed and the other without inscription. All illustrations should be provided with descriptive legends, which should be given on a separate sheet. Any lettering on diagrams—other than Greek letters, symbols, etc.—should be stencilled and should be sufficiently large and bold to permit reproduction when the diagram has been reduced to a size suitable for inclusion in the journal.

4. References in the text should be given by quoting the authors name and year of publication, i.e. AHRENS (1952). *Full references should be listed at the end of each paper, in alphabetical order, in the following manner*

AHRENS, L. H. (1952). The use of ionization potentials—I. Ionic radii of the elements. *Geochim. et Cosmochim. Acta* **2**, 155–169.

and should include the full title of the article, standard abbreviated title of the journal, year, volume number and inclusive page numbers.

5. The text of articles submitted should be concise and in a readily understandable style. The technical description of the methods used should only be given in detail when such methods are new. The essential contents of each paper should be briefly recapitulated in an abstract in English. Such an abstract may, however, be submitted by the author in the language of the original typescript for translation into English by the editorial staff.

6. To conserve space, authors are requested to mark less important portions of the paper (such as description of methods, record of experimental results, etc.) for printing in smaller type.

7. Indices of refraction should be denoted by the symbols α, β, γ, ω, ε, n, and vibration directions by X, Y, Z, O and E.

Pergamon Press are also publishers of the following Journals.

JOURNAL OF NUCLEAR ENERGY (*including* THE SOVIET JOURNAL OF ATOMIC ENERGY*). PART A: REACTOR SCIENCE; PART B: REACTOR TECHNOLOGY; PART C: PLASMA PHYSICS — ACCELERATORS — THERMONUCLEAR REACTORS
HEALTH PHYSICS (*The Official Journal of the Health Physics Society*)
JOURNAL OF INORGANIC AND NUCLEAR CHEMISTRY
TETRAHEDRON (*The International Journal of Organic Chemistry*)
TALANTA (*An International Journal of Analytical Chemistry*)
INTERNATIONAL JOURNAL OF APPLIED RADIATION AND ISOTOPES
BIOCHEMICAL PHARMACOLOGY
ARCHIVES OF ORAL BIOLOGY
* BIOPHYSICS
* JOURNAL OF MICROBIOLOGY, EPIDEMIOLOGY AND IMMUNO-BIOLOGY
* PROBLEMS OF HEMATOLOGY AND BLOOD TRANSFUSION
* PROBLEMS OF VIROLOGY
* PROBLEMS OF ONCOLOGY
* SECHENOV PHYSIOLOGICAL JOURNAL OF THE U.S.S.R.
* PAVLOV JOURNAL OF HIGHER NERVOUS ACTIVITY
* ELECTRIC TECHNOLOGY, U.S.S.R.
* RADIO ENGINEERING
* RADIO ENGINEERING AND ELECTRONICS
* TELECOMMUNICATIONS
* PHYSICS OF METALS AND METALLOGRAPHY
* THE ABSTRACTS JOURNAL OF METALLURGY
* APPLIED MATHEMATICS AND MECHANICS
CHEMICAL ENGINEERING SCIENCE
JOURNAL OF ATMOSPHERIC AND TERRESTRIAL PHYSICS
PLANETARY AND SPACE SCIENCE
ANNALS OF THE INTERNATIONAL GEOPHYSICAL YEAR
SPECTROCHIMICA ACTA
JOURNAL OF THE MECHANICS AND PHYSICS OF SOLIDS
ACTA METALLURGICA (*for the Board of Governors of Acta Metallurgica*)
INTERNATIONAL JOURNAL OF THE PHYSICS AND CHEMISTRY OF SOLIDS
DEEP-SEA RESEARCH
JOURNAL OF NEUROCHEMISTRY
JOURNAL OF PSYCHOSOMATIC RESEARCH
JOURNAL OF INSECT PHYSIOLOGY
INTERNATIONAL JOURNAL OF AIR AND WATER POLLUTION
INTERNATIONAL ABSTRACTS OF BIOLOGICAL SCIENCES (*for Biological and Medical Abstracts Ltd.*)
RHEOLOGY ABSTRACTS
VACUUM
OPERATIONAL RESEARCH QUARTERLY
ANNALS OF OCCUPATIONAL HYGIENE
ELECTROCHIMICA ACTA
JOURNAL OF CHILD PSYCHOLOGY AND PSYCHIATRY
JOURNAL OF SMALL ANIMAL PRACTICE
SOLID-STATE ELECTRONICS
INTERNATIONAL JOURNAL OF MECHANICAL SCIENCES

* *Translations of Russian journals published on behalf of the Pergamon Institute, a division of Pergamon International Corporation*

Leaflets giving further details and subscription rates of each of these journals are available on request

IN STACKS
12 Sep'61R

THE GEOCHEMICAL SOCIETY

OFFICERS

Tom F. W. Barth, President
Harold C. Urey, Vice-President
Konrad B. Krauskopf, Secretary
George T. Faust, Treasurer

COUNCILLORS

E. F. Osborn, 1958–1960
H. G. Thode, 1958–1960
Albert E. J. Engel, 1959–1961
Friedrich G. Houtermans, 1959–1961
Ralph Cannon, 1960–1962
Th. G. Sahama, 1960–1962

REGIONAL VICE-PRESIDENTS

Louis H. Ahrens
Rui Ribeiro Franco
Ing. Georges Ordoñez
C. W. Correns
J. F. Lovering
Ken Sugawara

COMMITTEES

Auditing Committee:
Joseph J. Tregoning, Chairman
William L. Hill
C. R. Nasser

Constitution and By-Laws Committee:
Michael Fleischer, Chairman
Julian R. Goldsmith
Denis M. Shaw

Education Committee:
H. D. Holland, Chairman
J. A. S. Adams
D. M. Henderson
Kurt E. Lowe
G. D. Nicholls
Hans P. Eugster

Membership Committee:
R. M. Garrels, Chairman
Harvey C. Diehl
Chester B. Slawson
James E. Slosson
Irving Breger

Nominating Committee:
Wm. Pecora, Chairman
Th. G. Sahama
C. E. Tilley
G. Tunell

Programme Committee:
H. T. Evans, Chairman
Gordon J. F. MacDonald
H. E. Lowenstam

Publications Committee:
E. W. Heinrich, Chairman
Julian R. Goldsmith
John C. Maxwell
N. W. Rakestraw
S. C. Robinson
L. R. Wager
Earl Ingerson

Research Committee:
C. G. Dodd, Chairman
W. F. Bradley
R. A. Rowland
T. G. Thompson

Russian Translations Committee:
Earl Ingerson

Standards Committee:
Alvin Van Valkenverg, Chairman
Michael Fleischer
Loren Stieff
George Switzer
George Tilton

Tellers Committee:
Charles Meyer, Chairman
Henry R. Cornwall
Colin O. Hutton